Ecomorphology and biomechanics of cetacean backbone in an evolutionary context

Amandine Gillet

Thesis submitted to obtain the degree of Doctor in Sciences (Biology)

Academic year 2019-2020

Université de Liège
Faculté des Sciences
Unité de Recherche FOCUS
Laboratoire de Morphologie Fonctionnelle et Evolutive
Prof. Eric Parmentier

Ecomorphology and biomechanics of cetacean backbone in an evolutionary context

Amandine Gillet

Thesis submitted to obtain the degree of Doctor in Sciences (Biology)

Academic year 2019-2020

Jury composition:

Prof. **Patrick Dauby**, president (ULiège)

Dr. **Bruno Frédérich**, secretary (ULiège)

Dr. **Anthony Herrel** (MNHN)

Dr. **Olivier Lambert** (RBINS)

Dr. **Krishna Das** (ULiège)

Dr. **Thierry Jauniaux** (ULiège)

Prof. **Eric Parmentier**, supervisor (ULiège)

Université de Liège

Faculté des Sciences

Unité de Recherche FOCUS

Laboratoire de Morphologie Fonctionnelle et Evolutive

Prof. Eric Parmentier

Cover picture: Common dolphin (*Delphinus delphis*), New South Wales, Australia (© A. Gillet)
Chapters cover picture: Spinner dolphin (*Stenella longirostris*), Tañon Strait, Philippines (photo: A. Gillet, DCEP 2015, photo editing: C. Ninane)

Abstract

Cetaceans (whales, dolphins, and porpoises) represent the most speciose taxon of extant marine mammals and exhibit a tremendous ecological disparity. Although all cetaceans possess a streamlined and hydrodynamic body adapted to their aquatic environment, they also have a wide phenotypic variability at the level of body size, body shape and fin shape. Moreover, the different species exhibit extraordinary disparity in the shape of their vertebral column. As whales and dolphins swim with dorso-ventral oscillations of their backbone, modifications of their vertebral morphology should impact their ability to swim in different kinds of habitats. However, relationships between the vertebral morphology, swimming performances, ecology, and evolutionary history of cetaceans remain uncertain.

This thesis aims at providing concrete elements regarding the causes and consequences of the large morphological variability of the cetacean backbone. To this purpose, we computed the largest database of cetacean vertebral morphology ever created by quantifying the vertebral shape of 73 species (i.e., 80 % of extant diversity). These morphological data were combined to backbone biomechanics and swimming kinematics data and were analysed in both evolutionary and ecological contexts.

Our results demonstrate that both ecological and phylogenetic factors are associated to vertebral shape. We identified two distinct phenotypic evolutionary patterns: non-delphinoids and delphinoids.

Non-delphinoids are a paraphyletic group comprising several cetacean clades: mysticetes, sperm whales, beaked whales, and 'river dolphins'. They are all characterised by a low number of elongated vertebrae, resulting in relatively flexible backbones. In this clade, inshore species retained a small body size while offshore species evolved towards an increased body size accompanied by a slightly increased vertebral count (pleomerism). The small size of riverine species ensures manoeuvrability in complex environments while gigantism of offshore species provides adaptation to deep diving, long distance migrations, and bulk-feeding.

Delphinoids form a monophyletic group comprising three families: Monodontidae (narwhals and belugas), Phocoenidae (porpoises) and Delphinidae (oceanic dolphins), the most

species-rich cetacean family. They all possess an extremely modified vertebral morphology, unique among mammals, by having an extraordinary high number of disk-shaped vertebrae while retaining a small body size. In this clade, inshore species have a lower vertebral count than offshore species. Within delphinoids, the closely related porpoises (Phocoenidae) and oceanic dolphins (Delphinidae) have clearly distinct vertebral morphology and follow slightly different phenotypic trajectories along the habitat gradient, probably reflecting parallel evolution with similar responses to same constraints. Furthermore, similar morphological adaptations are found between coastal and offshore ecotypes in the common bottlenose dolphin (*Tursiops truncatus*) suggesting that similar constraints act both at the micro- and macroevolutionary levels.

The extreme vertebral count increase and associated vertebral shortening observed in offshore delphinoids increases the stiffness of their backbone. These modifications provide enhanced body stability and allow delphinoids to use higher tailbeat frequencies in an energetic efficient manner, resulting in higher swimming speed. These new functional abilities allowed small delphinoids to exploit scattered oceanic resources in a new way and can be considered as key innovations that supported their explosive radiation and ecological success.

Résumé

Les cétacés (baleines, dauphins et marsouins) représentent le groupe de mammifères marins actuels contenant le plus d'espèces et possèdent également une grande variabilité écologique. Bien qu'ils possèdent tous un corps fuselé adapté à leur environnement aquatique, leur morphologie externe, telle que la taille et la forme du corps ou la forme des nageoires, varie largement entre les espèces. Au-delà de ces variations de morphologie externe, ils arborent également une variabilité extraordinaire au niveau de la forme de leur colonne vertébrale. Etant donné que la nage est assurée par des oscillations dorso-ventrales de la colonne vertébrale chez les cétacés, des modifications de leur morphologie vertébrale devrait avoir un effet sur leurs capacités à se déplacer dans un habitat donnée. Cependant, les facteurs qui influencent les modifications vertébrales et l'impact de ces modifications sur les capacités de nage restent à déterminer.

Cette thèse a pour but de fournir des éléments concrets à propos des causes et conséquences de la grande variabilité morphologique observée dans la colonne vertébrale des cétacés. Pour cela, nous avons établi la plus grande base de données de morphologie de la colonne vertébrale de cétacés en quantifiant la forme vertébrale de 73 espèces, ce qui représente environ 80 % de la diversité actuelle. Ces données morphologiques ont ensuite été combinées à des données de biomécanique de la colonne et de cinématique de nage pour être analysées dans un contexte évolutif et écologique.

Nos résultats démontrent que la morphologie vertébrale est aussi bien associée à des facteurs écologiques qu'à des facteurs phylogénétiques et permettent d'identifier deux modèles d'évolution phénotypique distincts: celui des non-delphinoides et celui des delphinoides.

Les non-delphinoides forment un groupe paraphylétique comprenant différents clades: les mysticètes, les cachalots, les baleines à bec et les 'dauphins de rivières'. Tous les non-delphinoides possèdent un faible nombre de vertèbres allongées, fournissant une certaine flexibilité à la colonne. Dans ce groupe, les espèces de rivière ont conservé une petite taille tandis que les espèces de pleine mer ont évolué vers de plus grandes tailles. Cette augmentation de taille du corps est accompagnée par une légère augmentation du nombre de vertèbres (pléiomerisme). La petite taille des espèces de rivière assure leur manœuvrabilité dans des habitats structurellement complexes tandis que la

grande taille des espèces océaniques est adaptée pour les plongées profondes, les migrations sur de longues distances et l'engouffrement de nombreuses petites proies.

Le groupe des delphinoides est un groupe monophylétique comprenant trois familles: les Monodontidae (narval et béluga), les Phocoenidae (marsouins) et la famille de cétacés la plus diversifiée, les Delphinidae (dauphins océaniques). Tous les delphinoides ont une colonne vertébrale extrêmement modifiée et unique au sein de mammifères puisqu'ils possèdent un très grand nombre de courtes vertèbres tout en conservant un corps de petite taille. Dans ce clade, les espèces vivant proche des côtes ont moins de vertèbres que les espèces de pleine mer. Au sein de groupe, les marsouins (Phocoenidae) et dauphins océaniques (Delphinidae) possèdent une morphologie vertébrale distincte l'une de l'autre et possèdent des trajectoires phénotypiques légèrement différentes le long du gradient d'habitat rivières-côtes-pleine mer ce qui reflète probablement une évolution parallèle de ces deux familles apparentées. Par ailleurs, des adaptations morphologiques de la colonne vertébrale similaires sont présentes entre les écotypes côtiers et océaniques du grand dauphin (*Tursiops truncatus*), suggérant que des contraintes similaires agissent aussi bien au niveau microévolutif que macroévolutif.

L'augmentation exceptionnelle du nombre de vertèbres ainsi que leur raccourcissement observé chez les delphinoides ont pour effet d'augmenter la rigidité de la colonne vertébrale. Ces modifications fournissent une plus grande stabilité du corps mais permettent également aux delphinoides d'augmenter la fréquence d'oscillation de leur queue et pédoncule caudal de façon peu couteuse en énergie, leur permettant ainsi de nager à des vitesses plus élevées. Ces nouvelles capacités fonctionnelles ont permis à ces petits cétacés d'exploiter les ressources alimentaires océaniques d'une nouvelle façon et ont joué un rôle clef dans leur succès écologique et leur rapide diversification.

Acknowledgements / Remerciements

De nombreuses personnes ont participé d'une façon ou d'une autre à l'aboutissement de ce travail et je souhaite toutes les remercier sincèrement.

Tout d'abord je veux bien sûr remercier mon promoteur, le ***Prof. Eric Parmentier****, de m'avoir proposé de poursuivre ce sujet d'étude, quelque peu éloigné des poissons, en tant que doctorante au sein de son laboratoire. Merci pour ton aide, tes pistes de réflexion et pour ta disponibilité presque permanente malgré un emploi du temps bien chargé. Mais surtout, merci pour la liberté que tu m'as laissée pour mener ce projet et de m'avoir permis de concilier mon travail avec mes allers-retours à l'étranger. Je pense avoir eu beaucoup de chance de pouvoir faire cette thèse sous ta supervision.*

Je souhaite remercier sincèrement le ***Dr. Bruno Frédérich****, également membre du Laboratoire de Morphologie Fonctionnelle et Evolutive, de s'être intéressé et impliqué dans ce projet. Merci pour tes nombreux conseils particulièrement pertinents. Merci aussi d'avoir pris le temps de m'initier à l'utilisation de R ainsi que de m'avoir appris les nombreuses techniques de phylogénie comparée et de morphométrie géométrique. Cette thèse ne serait qu'elle est aujourd'hui sans ton aide.*

Je remercie aussi le ***Prof. Patrick Dauby****, le* ***Dr. Anthony Herrel****, le* ***Dr. Olivier Lambert****, la* ***Dr. Krishna Das*** *et le* ***Dr. Bruno Frédérich*** *d'avoir accepté de faire partie de mon jury de thèse. Merci aussi aux membres de mon comité de thèse, la* ***Dr. Liesbet Geris*** *et le* ***Dr. Thierry Jauniaux*** *qui a également accepté d'être membre du jury, m'a permis de collecter des données sur les animaux échoués et m'a aidée pour la collaboration avec certains delphinariums et zoo.*

Un très grand merci au ***Prof. Olivier Brüls*** *et à* ***Romain Van Hulle*** *de la Faculté des Sciences Appliquées de l'ULiège d'avoir pris le temps d'expliquer des concepts de physique et de modélisation biomécanique à la biologiste que je suis et de m'avoir aidée dans le développement du modèle mathématique de la biomécanique de la colonne vertébrale. Merci également au* ***Dr. Christophe Becco*** *du Département de Physique de l'ULiège de m'avoir donné l'idée de la méthodologie pour l'extraction de la ligne médiane du corps des animaux pour l'analyse des vidéos.*

This thesis would not have been possible without the data collected in several Museums of Natural History so I wish to thank all the museum curators and staff that granted me access to their

collections and helped me with the logistical aspects of data sampling: ***Dr. Daniela Kalthoff****,* ***Dr. Julia Stigenberg****,* ***Peter Mortensen****,* ***Peter Nilsson****, and* ***Dr. Thomas Mörs*** *from the Naturhistoriska Riksmuseet in Stockholm for their especially warm welcome and kindness during my stay,* ***John Ososky****,* ***Paula Bohaska****, and* ***Darrin Lunde*** *from the Smithsonian's National Museum of Natural History in Washington DC,* ***Neil Duncan****,* ***Marisa Surovy****,* ***Eleanor Hoeger****, and* ***Sara Ketelsen*** *from the American Museum of Natural History in New York,* ***Dr. Greg Hofmeyr****,* ***Gill Watson****, and* ***Vanessa Isaacs*** *from the Bayworld Museum in Port Elizabeth,* ***Denise Hamerton****,* ***Jofred Opperman****, and* ***Noel Fouten*** *from the Iziko South African Museum in Cape Town,* ***Dr. Stefan Merker*** *and* ***Carsten Leidenroth*** *from the Staatliches Museum für Naturkunde in Stuttgart,* ***Heather Janetzki*** *from the Queensland Museum in Brisbane,* ***Luc Vives*** *from the Museum National d'Histoire Naturelle in Paris,* ***Dr. Tom Geerinckx****,* ***Dr. Annelise Folie****,* ***Sébastien Bruaux****, and* ***Terry Walschaerts*** *from the Royal Belgian Institute of Natural Sciences in Brussels, and* ***Dr. Christian Michel*** *and* ***Marie Bournonville*** *from the Aquarium-Museum in Liège.*

Similarly, kinematic analyses would not have been possible without the video recorded on living animals. All my thanks to the five facilities and their animal care teams that accepted to collaborate with me, let me share their daily routine and allowed me to work with their animals: ***Yann Panheleux****,* ***Salvatore Mura****,* ***Vairupe Doucet****, et toute* ***l'équipe du Moorea Dolphin Center*** *pour leur accueil et leur enthousiasme,* ***Maris Muzzy****,* ***Steven Aibel****,* ***Dr. Chuck Knapp****,* ***Susan Allen****,* ***Tim Ward*** *and the whole* ***marine mammal team at the Shedd Aquarium*** *in Chicago,* ***Sander van der Heul****,* ***Dr. Piet De Laender****, and all the* ***animal trainers at the Boudewijn Seapark*** *in Brugge,* ***Anneke Schrama****,* ***Mariëtte Smit****,* ***José Kemper****,* ***Lisanne Duursma****, and the* ***animal care team of Ecomare*** *in Texel, and* ***Dr. Kerstin Ternes*** *and the* ***animal care team of Duisburg Zoo****.*

Je souhaite également remercier la ***Dr. Géraldine Bolen****,* ***Laurie Van Bossuyt****, et le* ***Dr. Thierry Jauniaux*** *de la Faculté de Médecine Vétérinaire de l'ULiège ainsi que la* ***Dr. Krishna Das*** *et ses collaborateurs du projet européen* ***Marine Mammals Science Education*** *qui m'ont permis de réaliser des CT-scans de plusieurs animaux échoués. Tous mes remerciements également à toutes les autres personnes qui ont pris part à notre séance de découpage de marsouin pour reconstruire la musculature en 3 dimensions:* ***Marion Grimaud****, qui a réalisé un excellent travail durant son mémoire au laboratoire,* ***Etienne Lévy*** *pour la réalisation des photos,* ***Steven Braine****,* ***Michel Jansen****,*

Jacky Karpouzopoulos *et les membres de la LPA de Calais,* ***Dr. Géraldine Lacave****,* ***Dr. France Damseaux****,* ***Krystel Hillaire****,* ***Marianthi Ioannidis****,* ***Fanny Dessard*** *et* ***Alicia Quiévy****.*

Merci aussi au ***Dr. David Lecchini*** *et aux* ***membres du CRIOBE*** *de m'avoir accueillie durant mon séjour à Moorea, au* ***Dr. Thibaut Bouveroux*** *de m'avoir aidée pour la collaboration avec les musées sud-africains, to* ***Prof. Rui Diogo*** *and* ***Prof. Alejandra Hurtado de Mendoza*** *for hosting me in Washington DC, and to* ***Dr. Pierre Gallego, Calum Murie, members of the Marine Megafauna Foundation,*** *and* ***Peri Peri divers*** *for their collaboration during data collection in Mozambique.*

Je remercie sincèrement tous mes collègues, actuels et passés, du laboratoire de morphologie pour leur bonne humeur, leurs conseils et les nombreuses discussions scientifiques et surtout moins scientifiques qui ont contribué à la bonne ambiance générale au sein du labo. Mes remerciements vont donc à ***Alessia Huby****, ma comparse de thèse, workshop et congrès durant ces quatre (presque cinq) années, au* ***Dr. Loïc Kéver****, toujours prêt à nous faire rire et à supporter mes nombreuses discussions sans fin sur le modèle biomécanique de nage (promis j'arrête!), à* ***Mélanie Dussenne*** *avec qui j'aurai partagé les hauts et les bas des derniers mois de thèse (et beaucoup trop de vidéos de chiens et chats!), au* ***Dr. Frédéric Bertucci*** *sans qui je ne serais jamais allée en vac… euh… travailler à Moorea, au* ***Dr. Geoffrey Mélotte****, toujours partant pour se réunir autour d'un verre et élargir mes (piètres) connaissances cinématographiques, à* ***Steven Braine*** *pour ses supers modèles 3D de marsouins, son enthousiasme et pour avoir toujours été prêt à me donner un coup de main, à* ***Marine Banse*** *pour sa bonne humeur constante et communicative, à la* ***Dr. Marta Bolgan*** *pour son grain de folie, son soutien et sa philosophie positive durant les moments plus difficiles, à* ***Xavier Raick****, pour nos échanges scientifiques toujours intéressants, à* ***Séverine Henry****, ma voisine de bureau pendant plusieurs années, à la* ***Dr. Laura Gajdzik*** *pour ses conseils en statistiques et informations sur les bourses de voyage, ainsi qu'au* ***Dr. Orphal Colleye****, au* ***Dr. Damien Olivier*** *et à la* ***Dr. France Collard*** *et aux "Morphos du 3ème ", le* ***Dr. Philippe Compère****,* ***Yann Delaunois*** *et* ***Sarah Smeets****. Merci aussi à nos voisins de palier, les "Océanos", en particulier le* ***Dr. François Remy*** *(dit Licorne), la* ***Dr. France Damseaux****, et* ***Marianna Pinzone*** *qui savent aussi bien que moi que les mammifères marins sont les animaux les plus cool qui existent! Enfin, merci à nos super secrétaires* ***Mariella Lunetta*** *et* ***Françoise Bruls*** *pour leur aide dans les aspects administratifs.*

Je ne serais sans aucun doute jamais arrivée jusqu'ici sans ***mon père***, ***ma mère*** *et* ***mon beau-père****. Merci de m'avoir donné l'occasion de poursuivre des études et de me soutenir dans la poursuite de ma passion même si certains aspects de ma recherche et les méandres du monde académique restent encore un peu flous à leurs yeux. Merci aussi d'avoir joué les dog sitters durant mes séjours répétés à l'étranger. Merci aussi à* ***ma sœur***, ***ma marraine***, ***mes grands-mères*** *et* ***mes beaux-parents*** *pour leurs encouragements et leur intérêt.*

Cette thèse aurait été beaucoup plus difficile sans le soutien inconditionnel de mon partenaire à la vie comme à la science, ***Arnaud****. Merci pour tes encouragements, ton écoute permanente et ta compréhension. Merci pour ton intérêt et ton implication dans un domaine de recherche bien différent du tien, que ce soit pour des discussions, des relectures ou l'assistance dans la collecte de données (je n'aurais jamais réussi à porter ces vertèbres de baleine toute seule!). Merci de m'épauler dans les moments difficiles depuis le début. Merci de m'inciter à donner le meilleur de moi-même et de m'encourager à poursuivre ma passion jusqu'au bout. Tout simplement, merci d'être là.*

Merci à mes amis biologistes: ***Anaïs***, ***David,*** *Super-****Cat(h)*** *et l'unique* ***Kéké****(nodon) pour leur présence, leur aide, leurs avis et réflexions scientifiques, mais surtout pour les bonnes tranches de rire depuis de nombreuses années. Merci aussi à* ***Emlyn*** *ainsi qu'à* ***Sophie***, ***Poney***, ***JJ***, ***Marie, Mercédes, Mehdi, Bambi, Emilie*** *et tous les autres* ***membres du Zoo*** *(sans rapport avec le parc animalier, quoi que…) pour leur amitié, les nombreuses soirées et les courses d'orientation dans les bois qui permettent de se vider l'esprit.*

Merci au ***Fond de la Recherche Scientifique F.R.S.-FNRS*** *qui m'a accordé la bourse d'Aspirant qui a financé les quatre années de ce projet ainsi que plusieurs séjours à l'étranger. Merci aussi aux autres subsides et organismes ayant financé mes missions à l'étranger: le patrimoine de* ***l'Université de Liège***, *le concours bourse de voyage de la* ***Fédération Wallonie-Bruxelles***, *l'association luxembourgeoise* ***Odyssea***, *and the Synthesys grant from the* ***European Union's Seventh Framework Programme*** *(grant no. SE-TAF-6278).*

Table of contents

Chapter 3 : Evolutionary patterns of delphinoid backbone morphology at inter- and intraspecific levels

Chapter 4 : Linking vertebral morphology to backbone biomechanics and swimming kinematics

Chapter 1 :
General introduction

1. Ecomorphology and adaptation

Identifying factors supporting the extraordinary variability of forms and shapes of living organisms is a central biological question to comprehend the tremendous diversity of life. Variation in shape results in differences in functional abilities and, consequently, in the ecological fitness of organisms. In this framework, the field of ecomorphology aims at understanding how organisms are shaped (morphology) according to various environmental constraints (ecology) (Arnold, 1983; Bock, 1990; Wainwright, 1991; Wainwright and Reilly, 1994). Ecomorphological studies rely on two main aspects: (1) testing the relationship between morphology and function (i.e., the performance gradient), and (2) evaluating the interaction between function and ecology (i.e., the fitness gradient) (Arnold, 1983) (Figure 1.1). Hence, the integration of morphological, functional and ecological data allows inferring the link between the shape of an organism and its way of life. In other words, it should be possible to deduce the lifestyle of an organism, or at least its functional performances in a given habitat, by analysing its phenotypic characteristics. The ecomorphological patterns found in Caribbean *Anolis* lizards is a typical textbook example. Their morphological variation related to ecological diversity led Williams (1972) to categorize *Anolis* species in various ecomorphs (e.g., grass-bush, crown-giant, trunk-crown, twig, and trunk-ground) which were defined as groups of '*species with the same structural habitat/niche, similar in morphology and behaviour, but not necessarily close phyletically*' (Williams, 1972: p. 82). For instance, species living in open habitats such as trunk-ground ecomorphs tend to be stocky and have long limbs allowing them to run faster and jump farther between distant and broad trunks. On the other hand, twig ecomorphs that live on higher perches are smaller and have shorter legs implying that these species are slower but their morphology provide them a greater agility necessary to walk on narrower branches (e.g., Herrel *et al.*, 2008; Irschick and Losos, 1998; Losos, 1990b, 1990a; Moermond, 1979).

Ecomorphological concept is of peculiar interest for paleontological studies that can use ecomorphological trends of extant species to infer the life of fossil organisms (Foote, 1997; Van Valkenburgh, 1994). It relies on the principle that phenotypic adaptation to similar environmental constraints should be identical, resulting in evolutionary convergences. This approach has been applied to numerous vertebrate groups such as birds, mammals, fishes or reptiles (e.g., Bell and Chiappe, 2011; Bellwood, 2003; Chen and Wilson, 2014; Mcguire and Dudley, 2011). For instance,

morphological investigations of extinct aquatic vertebrates have proposed differences in swimming abilities among ichthyosaurs. Early Triassic ichthyosaurs had elongated body, caudal fluke and vertebral centra similar to bottom-dwelling catsharks (Scyliorhinidae) suggesting that they were anguilliform swimmers, whereas Late Triassic and Cretaceous parvipelvian ichthyosaurs probably had a more thunniform swimming style given some morphological similarities with pelagic sharks (e.g., Lamnidae) (Buchholtz, 2001a; Motani, 2005; Motani *et al.*, 1996).

Albeit morphology, function and ecology are often tightly interrelated, shapes can also be affected by other factors such as developmental and/or phylogenetic constraints. Organism ecomorphology is indeed inherently linked to their evolutionary history given that phylogenetically close organisms can inherit similar traits from their common ancestors. Integrating phylogenetic information to ecomorphological studies is crucial as it allows to distinguish if a peculiar morphology is present in several organisms due shared ancestry or if it was independently acquired multiple times in accordance with their ecology (Losos, 1990a; Losos and Miles, 1994).

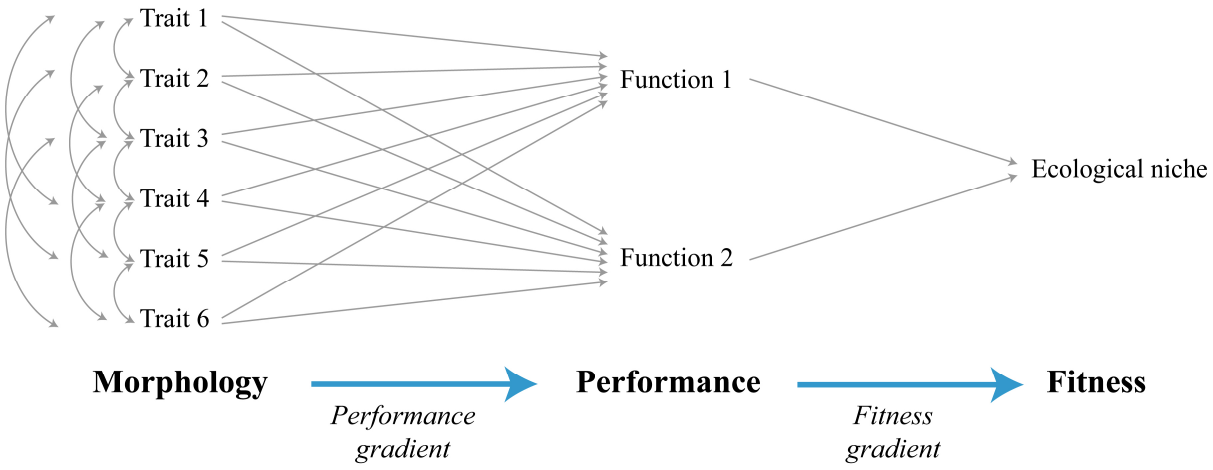

Figure 1.1. Schematic representation of ecomorphological principles. Morphology can be quantified through measurement of several phenotypic traits while performance is measured through functional abilities. Some morphological traits might be interrelated and covary (represented by curved arrows). Each phenotypic trait (e.g., body size, limb length, mandible shape) has an effect on one or several functions (e.g., running speed, bite force) which define the ability of an organism to occupy a peculiar ecological niche (e.g., feeding on large elusive preys). Figure redrawn and adapted from Arnold (1983) and Garland and Losos (1994).

Investigating links between morphology, function and ecology in a phylogenetic context also provide a powerful tool to test evolutionary hypotheses and identify which factors promote or hinder diversity. Specifically, adaptive radiation processes correspond to a rapid diversification of a monophyletic taxa into a variety of new forms and in the exploitation of new ecological niches (Grant, 2013; Schluter, 2000). Diversification of Darwin's finches on the Galápagos Islands through diet specialization and associated beak morphology modifications is a typical example of adaptive radiation (Grant and Grant, 2008).

These rapid radiations would be due to the availability of newly accessible ecological resources (i.e., ecological opportunity) supporting the specialization of diversification of organisms in a new adaptive zone; an adaptive zone being defined as a set of closely related ecological niches (Parmentier *et al.*, 2016; Schluter, 2000; Stroud and Losos, 2016; Yoder *et al.*, 2010). Three to four distinct phenomena, acting separately or in combination, are commonly recognized as sources of ecological opportunity (Figure 1.2) (Losos, 2010; Simpson, 1953; Stroud and Losos, 2016; Yoder *et al.*, 2010).

1) The first process that can generate ecological opportunity is through the appearance of new resources such as new dietary resources. For instance, higher diversity of angiosperms (combined to intrinsic factors) are thought to have supported the increased diversification of herbivorous weevils beetles (Curculionoidea) (McKenna *et al.*, 2009).

2) The colonization of a new geographic area can also promote adaptive radiation through the availability of ecological niches and/or the potential absence of predators and competitors. Several empirical examples of radiation following the colonization of islands have been described in birds including Darwin's finches and Hawaiian honeycreepers (Grant and Grant, 2008; Lerner *et al.*, 2011; Lovette *et al.*, 2002).

3) Emergence of ecological opportunity can also be due to the disappearance of an antagonist species (i.e., competitor or predator) such as the rise of mammals and birds following the extinction of non-avian dinosaurs at the Cretaceous-Paleogene boundary (Meredith *et al.*, 2011; Smith *et al.*, 2010) although this idea has been challenged by another study which identified a delayed diversification of mammals (Bininda-Emonds *et al.*, 2007).

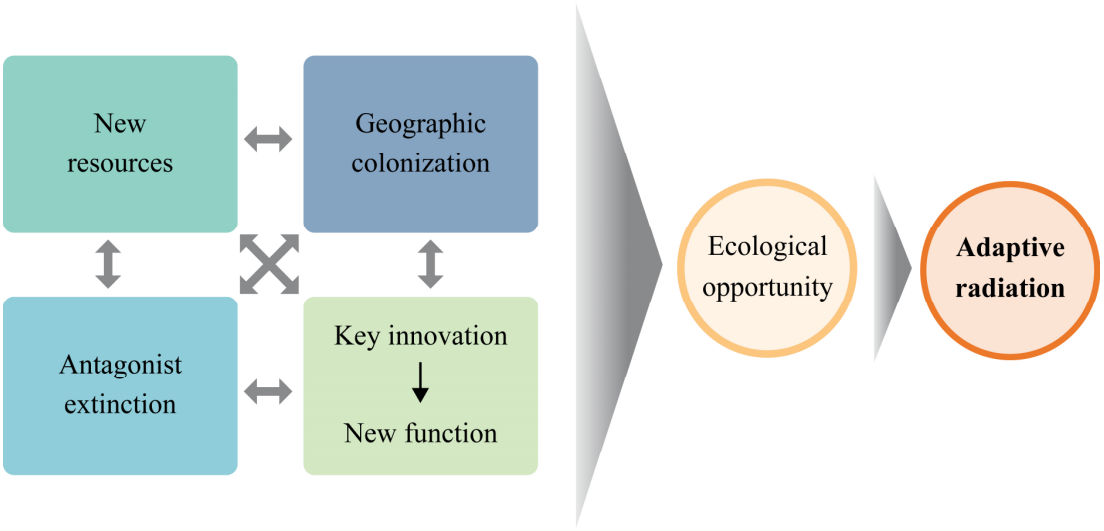

Figure 1.2. Schematic representation of processes spurring adaptive radiation. Four factors can create ecological opportunity: the emergence of new resources, the colonization of a new geographic area, the extinction of a predator or competitor and the acquisition of a key novelty supporting new functional abilities. These factors can act separately or in combination. The resulting ecological opportunity supports the occupation of a newly available adaptive zone and the subsequent specialization and diversification of organisms through adaptive radiation. Figure adapted from Yoder *et al.* (2010)

4) Acquisition of a new morphological or physiological trait can support new functional abilities and provide access to previously unavailable resources. These so-called key innovations hence provide an ecological opportunity and support the subsequent specialisation of organisms into the newly available adaptive zone (Alfaro, 2013; Heard and Hauser, 1995; Miller, 1949; Yoder *et al.*, 2010). For instance, the specialized morphology of the pharyngeal jaws, termed pharyngognathy, of some Percomorph fishes (Cichlidae, Pomacentridae, Labridae, etc.) permitted more efficient food processing and is usually considered as a key innovation associated with the high species richness of some of these clades (Liem, 1973; Mabuchi *et al.*, 2007; Wainwright *et al.*, 2012).

The concept of key innovation has been of peculiar interest for ecomorphological studies, yet its definition remains ambiguous and debated (Hunter, 1998; Rabosky, 2017; Wainwright and Price, 2016). A key innovation could be defined as a newly acquired trait supporting new functional abilities which allow interaction with the environment in a novel way, hence, providing access to new adaptive zones (e.g., Hunter, 1998; Miller, 1949; Stroud and Losos, 2016). This novelty might correspond to the acquisition of a single trait but will often result from the gradual accumulation of functionally related traits (Alfaro, 2013; Rabosky, 2017). For instance, the acquisition of wings (new trait) in birds allowed

them to fly (new functional ability) and to access a new set of ecological niches (Mayr, 1963). However, flying ability results from the acquisition of several successive new traits (feathers, elongation of digits, etc.) rather than a single one (Cracraft, 1990, 1986). As the acquisition of a key innovation provides access to a new adaptive zone, it is often considered that it should trigger adaptive radiation and that a change in the tempo (rate) of species diversification should be detectable (Figure 1.3*a*) (Alfaro, 2013; Drummond *et al.*, 2012; Hodges and Arnold, 1995; Sanderson and Donoghue, 1994). For instance, the acquisition of antifreeze glycoproteins (AFGPs) in notothenioid fishes allowed them to invade ice-cold waters in Antarctica and has been linked to their adaptive radiation (Matschiner *et al.*, 2011). However, key innovations might not always result in changes in the tempo of diversification as speciation and extinction processes also depend on other extrinsic and intrinsic factors such as niche unavailability (e.g., presence of a competing species or unfavourable environmental conditions) or simply due to the inability of the lineage to diversify in various

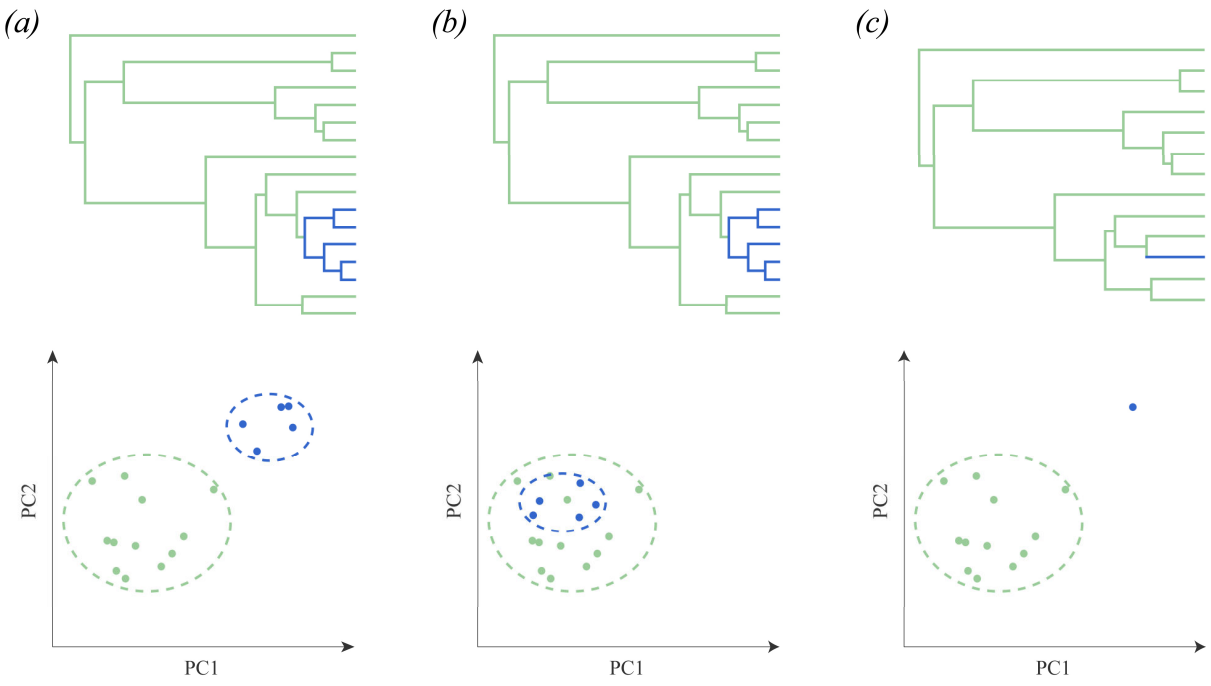

Figure 1.3. Theoretical patterns of species diversification and morphological/ecological disparification. *(a)* A subset of new species (blue) emerges after the acquisition of a novelty and significantly increases the diversity of the parent clade (green + blue). Moreover, new species experienced an ecological/morphological shift (bottom graph) compared to the ancestral clade (green). *(b)* The set of new species significantly increases the diversity of the parent clade but is not associated with the colonization of a new adaptive zone. *(c)* The acquisition of a novel trait results in a single highly specialized species which increases the clade disparity but not its diversity. Figure adapted from Rabosky (2017).

phenotypes (for instance, due to functional and/or developmental trade-offs) (Losos, 2010; Wainwright and Price, 2016). Increased diversification might also be delayed and occur once environmental conditions are appropriate (Alfaro, 2013; Wainwright and Price, 2016). Alternatively, changes in diversification rates in key innovation bearing clades might not be detectible anymore, especially in old clades, due to the natural species turnover (Rabosky, 2017). On the contrary, not all novel trait associated with a diversification rate increase can be considered as key innovations. Indeed, if the new trait does not allow the lineage to interact with its environment in a novel way and do not expand the ecological space of the entire clade, it should not be considered as a key innovation even if it led to an increased diversification rate (Figure 1.3*b*) (Rabosky, 2017; Stroud and Losos, 2016). Changes in diversification rate are therefore neither necessary nor sufficient to identify a key innovation. However the notion of increased diversity should be accounted in the definition otherwise the concept of key innovation could also be applied to single highly specialised species (Figure 1.3*c*) (Rabosky, 2017). However, different authors consider the apparition of a few specialized species should be included in the possible outcomes of key innovations (Wainwright and Price, 2016). Hence, it has been proposed that key innovations should rather be defined by an increase of species richness and/or ecological diversity (Alfaro, 2013; Rabosky, 2017). **In this work we consider that a key innovation is a trait or a set of functionally related trait that provided access to a new adaptive zone and contributed to the species richness of the lineage**, the detection of a diversification rate increase being only an additional argument supporting the key innovation hypothesis.

Overall, ecomorphological studies can highlight major macroevolutionary trends in a lineage and help to establish which factors promoted or hindered its diversification. Such studies require a comparative and a multidisciplinary approach combining morphological and/or physiological, functional, ecological and phylogenetic data on a wide variety of species.

2. Exploring the ecomorphology of cetaceans

Investigating ecomorphological and macroevolutionary patterns requires gathering data on a large sample of species that exhibit a variety of morphologies and ecologies and whose phylogenetic relationships are known in order to draw robust and reliable conclusions. Modern cetaceans (whales, dolphins and porpoises) represent the most speciose clade of extant marine mammals and are

considered as a highly successful taxon (Committee on Taxonomy, 2019; Thewissen, 1998). Their phylogenetic relationships have been extensively investigated. Albeit some uncertainty remains at shallow phylogenetic levels (especially in the recent group of oceanic dolphins), the phylogeny is considered as well-resolved at higher levels (i.e., family level) and several time-calibrated trees including most extant species have been published in the past few years (McGowen *et al.*, 2019, 2009; Slater *et al.*, 2010; Steeman *et al.*, 2009). Cetaceans are found in all oceans of the world and are encountered in a variety of environments. For instance, coastal areas are inhabited by numerous dolphins (Delphinidae) and porpoises (Phocoenidae), narwhals (*Monodon monoceros*) and belugas (*Delphinapterus leucas*) swim close to ice caps in polar regions, rivers possess a few specialized freshwater species, and sperm whales (*Physeter macrocephalus*) and beaked whales (Ziphiidae) prey on cephalopods in bathyal zones (Berta, 2015; Perrin *et al.*, 2009). Accordingly, they display a tremendous morphological diversity. Besides the large variation in body size which ranges from approximately 1.4 meters for the Hector's dolphin (*Cephalorhynchus hectori*) and the Vaquita (*Phocoena sinus*) to more than 25 meters for the blue whale (*Balaenoptera musculus*), cetaceans also show a wide variability in body shape such as the long rostrum of riverine dolphins, the exceptionally elongated pectoral fins of humpback whales, or the absence of dorsal fin in narwhals (Figure 1.5).

Previous works have highlighted links between some anatomical features and the ecology within this clade. For instance, pectoral fin shape is associated with swimming behaviour and ecology: slow-swimming species living in shallow waters and complex habitats (e.g., Amazon River dolphins, *Inia geoffrensis*, and grey whales, *Eschrichtius robustus*) have broad paddle-shaped fins adapted for precise manoeuvres at low speed whereas fast-swimming pelagic species have smaller and narrower pectoral fins enhancing body stability (Weber *et al.*, 2009; Woodward *et al.*, 2006). Cetacean body size is related to the type of prey they feed on; the largest cetaceans (mysticetes) rely on filter feeding techniques, medium size odontocetes feed mainly on cephalopods and small odontocetes prey on fishes (Slater *et al.*, 2010). Skull shape is also correlated to the feeding mechanism and prey size. Suction feeders (e.g., sperm whales, *P. macrocephalus*, beaked whales, *Mesoplodon* spp., and belugas, *D. leucas*) tend to feed only on small preys and have shorter and more robust head and mandibles than raptorial feeders (e.g., bottlenose dolphins, *Tursiops truncatus*, harbour porpoises, *Phocoena phocoena*, and Franciscana, *Pontoporia blainvillei*) that feed on a wider range of prey (Bloodworth and Marshall, 2007; MacLeod *et al.*, 2006; McCurry *et al.*, 2017; Werth, 2006). In the latter group, species

with more elongated mandibles, such as common dolphins (*Delphinus delphis*) or spinner dolphin (*Stenella longirostris*), can feed on proportionally smaller prey than brevirostrate species as porpoises (*Phocoena* spp.) or pygmy killer whales (*Feresa attenuata*) (McCurry *et al.*, 2017).

Besides the aforementioned examples of ecomorphological disparity, cetaceans also exhibit a wide variety of vertebral phenotypes (Figure 1.4) (e.g., Buchholtz, 2001b; Slijper, 1936; Van Beneden and Gervais, 1880). For instance the vertebral count varies from 40 in the Franciscana (*P. blainvillei*) to slightly less than 100 in the Dall's porpoise (*Phocoenoides dalli*) (Buchholtz, 2007). Buchholtz (2001b) thoroughly described the vertebral shape variation along the backbone of several modern cetaceans to infer their flexibility. By comparing these data to visual analysis of swimming movements of four different species she demonstrated that swimming patterns differed among species in accordance with their vertebral morphology (Buchholtz, 2001b). She identified three different morpho-functional groups. In the first group, all the vertebrae of the torso are uniform in shape, except in the tail stock, which result in undulations of the entire body length during swimming (e.g., humpback whales, *Megaptera novaeangliae*, blue whales, *B. musculus*, and sperm whales, *P. macrocephalus*). The second group differs from the first one by having elongated anterior torso vertebrae but shorter mid-torso vertebrae, producing severe curvature in the mid-torso (e.g., Amazon River dolphins, *I. geoffrensis*, narwhals, *M. monoceros*, and Cuvier's beaked whales, *Ziphius cavirostris*).The third group is characterised by a shortening of all torso vertebrae but an elongation of vertebrae in the tail stock, resulting in a oscillatory movement restricted to the posterior region of the body (e.g., harbour porpoises, *P. phocoena*, Altantic white-sided dolphins, *Lagenorhynchus acutus*, and killer whales, *Orcinus orca*). In addition, another study experimentally tested the vertebral stiffness at different points along the backbone of the common dolphin and showed that regions with more discoidal vertebrae (i.e., large diameter and short length) tended to be stiffer than regions with more elongated vertebrae (Long *et al.*, 1997). Based on these results, several works have suggested that low vertebral count and spool-shaped vertebrae would be an ancestral state typical of slow-swimming coastal cetaceans while high vertebral count and discoidal vertebrae would be a derived condition that correspond to fast-swimming pelagic dolphins but this hypothesis was not statistically tested (Buchholtz and Gee, 2017; Buchholtz and Schur, 2004; Marchesi *et al.*, 2019, 2018). Statistical investigation of these results in a phylogenetic context contradicted previous studies and concluded that vertebral morphology was only impacted by phylogenetic relationship, not by the habitat (Viglino

et al., 2014). Unfortunately, the analysis was run on a restricted number of species (seven) belonging only to two different families (Delphinidae and Pontoporiidae), questioning the statistical power of these results. Exact relationships between vertebral morphology, backbone biomechanics, swimming kinematics, ecology and the evolutionary history of cetacean remain therefore unclear and should be further investigated on a large number of species.

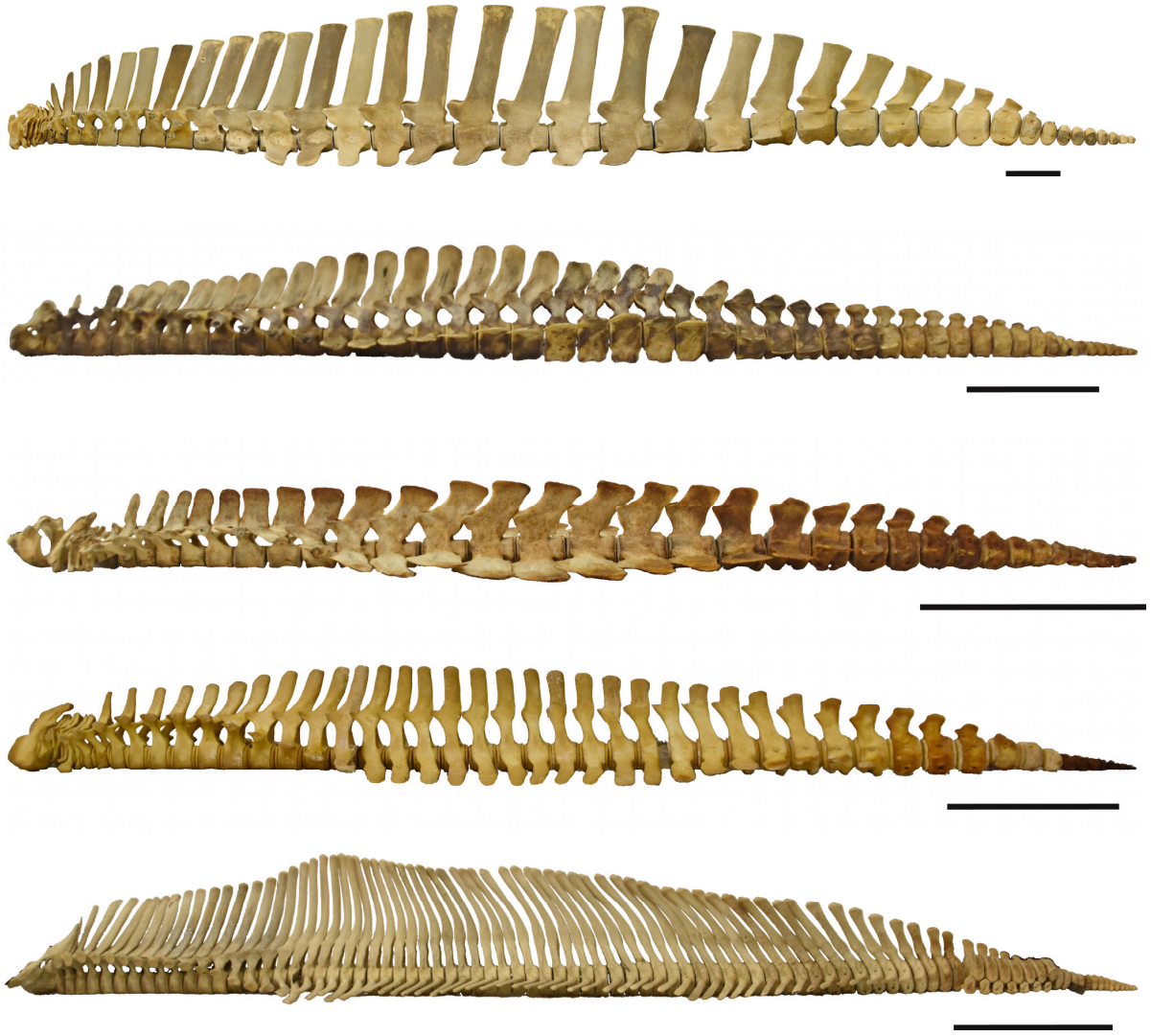

Figure 1.4. Cetacean vertebral disparity. Left lateral view of the vertebral column of four different cetacean species. From top to bottom: Hubb's beaked whale (*Mesoplodon carlhubbsi*) (USNM 396304), dwarf sperm whale (*Kogia sima*) (USNM 504221), Franciscana (*Pontoporia blainvillei*) (USNM 504920), Indian humpback dolphin (*Sousa plumbea*) (USNM 550939), Dall's porpoise (*Phocoenoides dalli*) (USNM 504128). Black bars correspond to 20 cm length. Chevron bones are not present on these pictures.

3. General aspects of cetacean biology

Investigating the ecomorphology of cetacean locomotion requires morphological, functional, ecological, and evolutionary dataset. Current knowledge about these various aspects is succinctly presented in this section.

3.1. Phylogeny and extant diversity

Cetaceans belong to the clade of Cetartiodactyla (even-toed ungulates and whales) which comprises approximately 330 species (Agnarsson and May-Collado, 2008; Hassanin *et al.*, 2012; Zurano *et al.*, 2019). Their closest terrestrial living relatives are hippopotamids and together they form the clade of Whippomorpha (also sometimes named Cetancodonta, but see Asher and Helgen (2010) for a note about this concern) (Geisler and Theodor, 2009; Uhen, 2010; Waddell *et al.*, 1999). However this classification has only been recently widely accepted (Marx *et al.*, 2016; Uhen, 2010). In 1883, Flower was the first to suggest a link with ungulates based on the anatomy of soft tissues (stomach, liver, respiratory and reproductive organs) but this hypothesis was not retained (Flower, 1883; Uhen, 2010). It was only during the second half of the 20th century that molecular-based phylogenies considered cetaceans as belonging to the clade of artiodactyls (e.g., Boyden and Gemeroy, 1950; Fitch and Beintema, 1990; Goodman *et al.*, 1985; Irwin *et al.*, 1991; reviewed in Gatesy, 1998). However, morphological and paleontological data were not sufficient to support nor reject these affinities until 2001 when several exceptionally well preserved fossils of early cetaceans (the pakicetids *Pakicetus* and *Ichthyolestes*, and the protocetids *Rodhocetus* and *Artiocetus*) were described (Gingerich *et al.*, 2001; Thewissen *et al.*, 2001). The morphology of the ankle bone (astragalus) of these specimens is similar to the unique and specialized morphology of artiodactyl ankle, hence reconciling molecular phylogenies with paleontological data. Further support for the close relatedness of cetaceans and hippopotamus was provided in 2007 with the description of the fossil artiodactyl *Indohyus* (Thewissen *et al.*, 2007). The morphology of its ear bone (tympanic bulla) placed it as a close relative of cetaceans and phylogenies combining molecular and morphological data placed them together as close relatives of hippopotamids (Geisler and Theodor, 2009; Spaulding *et al.*, 2009).

Modern cetaceans comprise 89 extant species from 14 families divided in two larger monophyletic taxa: mysticetes and odontocetes (Figure 1.5) (Committee on Taxonomy, 2019).

3.1.1. Mysticetes

The group of mysticetes, or baleen whales, is composed of 14 living species that are characterised by the absence of teeth in adults and the presence of keratinous plates extending from the palate, the baleen, also called whalebone (Rice, 2009). Baleen plates are associated with their specialized feeding strategy relying on filter-feeding of relatively small organisms (zooplankton or schooling fishes). Most mysticetes are large, ranging from the 6 meters long pygmy right whale (*Caperea marginata*) to the approximately 30 meters long blue whale (*B. musculus*), the largest animal that has ever existed (Berta, 2015; Marx *et al.*, 2016; Perrin *et al.*, 2009). Most species annually migrate between their feeding ground in cold and rich waters and their breeding ground in warmer waters (Bannister, 2009). Mysticetes are divided in 4 families.

The family of **Balaenidae**, commonly called right whales, groups 4 species from two genera: *Eubalaena*, sometimes called black whales, living in temperate waters of both hemispheres, and the monospecific *Balaena*, the Bowhead whale, living in Arctic waters. Right whales are notably characterized by extremely long baleen plates (up to 4 meters) hanging from their curved upper jaw. Right whales are skim-feeders: they swim with their mouth open, continually filtering water through their baleen plates. They are usually considered as slow steady swimmers. Externally, their body is robust, the large head corresponds to approximately a third of the body length, the dorsal fin is lacking, and flippers are large and broad (Kenney, 2009; Pivorunas, 1979; Rugh and Shelden, 2009; Woodward *et al.*, 2006).

Neobalaenidae comprises a single species, the pygmy right whale (*C. marginata*). This species is probably the only surviving species of the once diverse Cetotheriidae group (Fordyce and Marx, 2013). Sightings at sea are scarce and most aspects of the biology and ecology of this species remain enigmatic but observations have been recorded both in pelagic and coastal waters and seasonal migrations between these habitats might occur but it remains uncertain (Kemper, 2009; Ross *et al.*, 1975). Their skull and backbone also exhibit peculiar morphologies including the presence of numerous (17-18) flattened ribs and a lumbar region limited to a single vertebra (Buchholtz, 2011). Pygmy right whales are probably relatively slow swimmers and exhibit undulations of their entire body during swimming movements (Ross *et al.*, 1975).

Balaenopteridae, or rorquals, constitute the largest family of mysticetes with 8 species and are found in all oceans. Rorquals rely on bulk-feeding strategy which consists in gulping a large quantity of waters and filter it through baleen plates to retain preys. Accordingly, they possess multiple ventral grooves permitting the expansion of the buccal cavity during engulfment (Bannister, 2009; Pivorunas, 1979). Compared to right whales, rorquals have a slender body and small falcate pectoral fins (except the humpback whale). Rorquals have high aspect ratio flukes typical of fast swimmers and are able to reach high swimming speeds (Bannister, 2009; Woodward *et al.*, 2006).

Eschrichtiidae is a monospecific family formed by the gray whale (*Eschrichtius robustus*). Most phylogenies place it nested within the balaenopterid family indicating that it should rather be considered as a subfamily (Marx and Fordyce, 2015; McGowen *et al.*, 2019; Slater *et al.*, 2010). The gray whale is only encountered in the North Pacific although it used to be also present in the North Atlantic (Bisconti and Varola, 2006; Hufthammer *et al.*, 2018). They developed a peculiar feeding method: they roll on their side and filter the sediment to extract infauna (e.g., amphipods, polychaete, and bivalves) in shallow coastal waters. Alternatively, they can also use gulp-feeding and skim-feeding (Jones and Swartz, 2009; Pivorunas, 1979). Grey whales are considered as slow swimmers with high manoeuvrability; they lack external dorsal fin, and have large pectoral fins (Woodward *et al.*, 2006).

3.1.2. Odontocetes

Odontocetes, or toothed whales, regroup 75 species. Contrarily to mysticetes, modern odontocetes still possess teeth although dentition can be highly reduced or even absent in some species and/or sexes (especially in specialised suction feeders such as beaked whales) (MacLeod *et al.*, 2006; Uhen, 2009). Odontocetes are notably characterised by their ability to echolocate and the associated presence of a lipid-rich structure involved in sound guiding, the melon (Harper *et al.*, 2008; Hooker, 2009). Most odontocetes are small to medium-sized with only a few large species (e.g., sperm whale and giant beaked whales). Besides the giant sperm whale, odontocetes usually do not migrate over long distances such as mysticetes but some species show daily or seasonal changes in distribution (e.g., between inshore and offshore waters) (Hooker, 2009). There are 10 extant odontocete families.

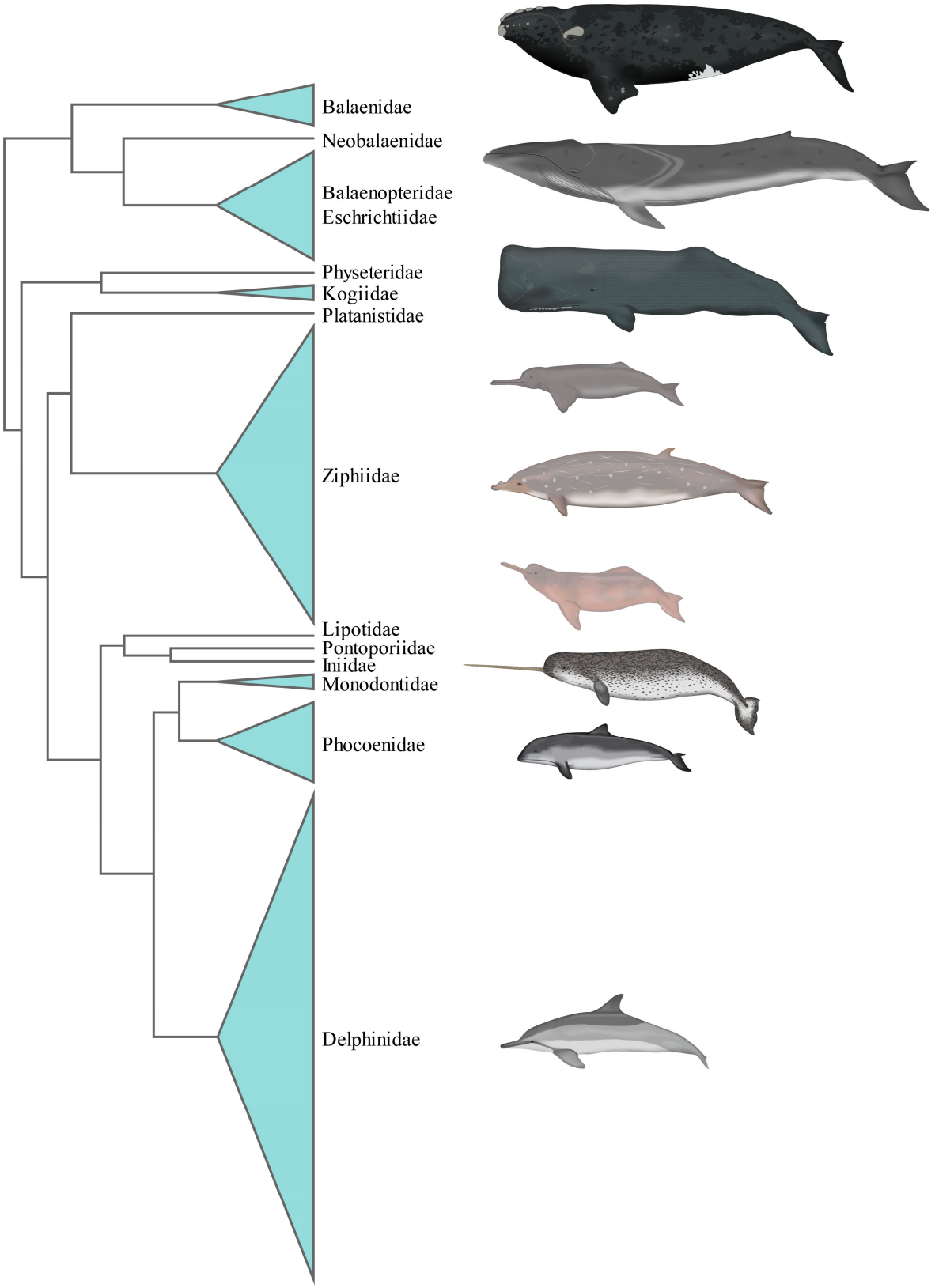

Figure 1.5. Phylogeny of extant cetaceans. The simplified time-calibrated tree of modern cetaceans shows their phylogenetic relationships, species richness, and morphological disparity. Representations from top to bottom: Southern right whale (*Eubalaena australis*), fin whale (*Balaenoptera physalus*), sperm whale (*Physeter macrocephalus*), South Asian river dolphin (*Platanista gangetica*), Blainville's beaked whale (*Mesoplodon densirostris*), Amazon River dolphin (*Inia geoffrensis*), narwhal (*Monodon monoceros*), harbour porpoise (*Phocoena phocoena*), and spinner dolphin (*Stenella longirostris*).

Physeteridae, sperm whale, and the closely related **Kogiidae**, dwarf and pygmy sperm whales, are deep-divers and suction feeders mainly preying on cephalopods. The three species owe their name to the presence of a wax filled organ in the head, the spermaceti. This organ is thought to be involved in sound focusing but buoyancy regulation has also been suggested for the sperm whale (Cranford, 1999; Schenkkan and Purves, 1973). While the sperm whale is the largest odontocetes (approximately 16 meters for males), pygmy and dwarf sperm whales are much smaller (up to 4 meters and 3 meters, respectively) (McAlpine, 2009; Whitehead, 2009).

Ziphiidae, or beaked whales, group 22 species and are the second most speciose cetacean clade. All beaked whales are specialized deep divers. The Cuvier's beaked whale (*Ziphius cavirostris*) holds indeed the record of the deepest dive ever recorded for cetaceans at 2992 meters deep (Schorr *et al.*, 2014). They primarily feeding on deep-sea cephalopods, fishes and, to a lesser extent, crustaceans (MacLeod *et al.*, 2003). Given their deep-diving behaviour, information about the ecology of most beaked whales remains scarce. Beaked whales are medium-sized cetaceans (from approximately 4 meters to 12 meters), they are characterised by their relatively long snout and an extreme reduction of the number of teeth, and possess small pectoral fins (Mead, 2009).

There are four monospecific families of so-called 'river dolphins': **Platanistidae** (South Asian river dolphin), **Iniidae** (Amazon river dolphin), **Pontoporiidae** (Franciscana), and **Lipotidae** (Yangtze river dolphin), the latter being considered as potentially extinct (Turvey *et al.*, 2007). The three last families are closely related and from a monophyletic group but Platanistidae are placed as the sister clade of the group formed by Ziphiidae, other river dolphin families, and Delphinoidea or, alternatively, as the sister taxon of Ziphiidae (Geisler *et al.*, 2011). Contrarily to the three other species which live in freshwaters, the Franciscana is encountered in estuaries and shallow coastal marine waters (up to 30 meters deep) (Crespo *et al.*, 2010; Zerbini *et al.*, 2010). These species share several morphological characteristics such as an extremely long rostrum (adapted for raptorial feeding), unfused cervical resulting in a flexible neck, and large and broad pectoral fins (Cassens *et al.*, 2000; Page and Cooper, 2017). They are considered as slow swimmers with high manoeuvring abilities which are necessary in their complex habitat (Fish, 1997).

The three remaining families (Monodontidae, Phocoenidae, and Delphinidae) belong to the clade of Delphinoidea which groups half of the modern cetacean species.

The clade of **Monodontidae** consists only of two species: the narwhal (*Monodon monoceros*) and the beluga (*Delphinapterus leucas*). Both species are medium-sized cetaceans living exclusively in Arctic and sub-Arctic waters. They are encountered in coastal and offshore waters where they can dive to depths of hundreds of meters (Laidre *et al.*, 2004; Richard *et al.*, 2001). Kinematic analyses of belugas show that it is a slow and manoeuvrable swimmer (Fish, 1997). Narwhals and belugas both lack a dorsal fin presumably linked to their ice-associated ecology. The flippers of belugas are large and broad whereas those of narwhals are smaller and relatively narrower.

The **Phocoenidae** family groups the 7 extant species of porpoises. All porpoises are small-sized and do not exceed 2.5 meters in length. Compared to most delphinids, porpoise have an extremely short snout and have spatulate-shaped teeth (Berta *et al.*, 2006). Osteological morphology suggests that porpoises are paedomorphic species (Barnes, 1985a; Galatius *et al.*, 2011). There is a relatively large ecological diversity among species as they are encountered in a variety of habitat: riverine, coastal or offshore waters. They have a stocky body shape and small flippers (Read, 2009).

Delphinidae represent the most species rich family of modern cetaceans with 37 species (40% of cetacean current diversity). They are often called 'oceanic dolphins' though some delphinids live in rivers and shallow near-shore waters (e.g,. tucuxi, *Sotalia fluviatilis*, humpback dolphins, *Sousa* spp., and Irrawaddy dolphins, *Orcaella brevirostris*). Most delphinids are small-sized (less than 5 meters) but a few reach larger body sizes (i.e., killer whales, *Orcinus orca*, pilot whales, *Globicephala* spp.). They exhibit wide variations in external morphology (snout length, fin shapes) that are most probably linked to their various feeding mode (suction, ram feeders), prey type (fishes, cephalopods, marine mammals) and habitats (rivers, estuaries, coasts, offshore waters) (LeDuc, 2009). As this family emerged recently and rapidly diversified, phylogenetic relationships within the family remain uncertain and debated (McGowen, 2011; Vollmer *et al.*, 2019).

3.2. Evolutionary history

Earliest cetaceans appeared approximately 53 million years ago (Ma) in the Indo-Pakistan region. Stem cetaceans, also known as archaeocetes, are the common ancestors of crown cetaceans, neocetes (living and extinct mysticetes and odontocetes), and their fossil record highlights the gradual steps of the land-to-sea transition (Uhen, 2010).

The oldest cetacean family is the Pakicetidae which groups three genus: *Pakicetus*, *Ichthyolestes*, and *Nalacetus* (Uhen, 2010). These medium dog-sized cetaceans are known from partial postcranial skeletons and several skulls. They conserved morphological features similar to terrestrial artiodactyls such as long and well-developed limbs with an ankle bone retaining the double-pulley morphology associated with running abilities of artiodactyls, long cervical vertebrae, and well developed sacrum suggesting a terrestrial mode of life (Thewissen *et al.*, 2001). However, their vertebral morphology suggests that they had a well-developed axial musculature and a robust tail that could have contributed to locomotion. Their phalanges possess lateral muscular crest that could be indicative of webbed-feet and their bones show characteristics of increased density which is detrimental for terrestrial running but act as stabilising ballast in aquatic environment (Madar, 2007). These morphological features associated to stable isotopes analyses indicate that pakicetids were mostly adapted to a freshwater environment where they walked on the bottom and could have also used quadrupedal paddling assisted by tail undulations (Clementz *et al.*, 2006; Madar, 2007).

Subsequent crownward archaeocetes exhibit morphological features reflecting a gradual increasing adaption to the aquatic environment. *Ambulocetus* which belong to the Ambulocetidae family exhibit a shortened femur, extremely elongated hands and feet, and possibly weak hindlimbs musculature suggesting they could still walk on land but not as well as pakicetids (Madar *et al.*, 2002; Thewissen *et al.*, 1994). Morphological features suggest that they might have used hindlimbs paddling in combination with pelvic dorso-ventral undulations (similar to sea otters) to swim (Fish, 2016; Thewissen and Fish, 1997; Thewissen *et al.*, 1994). While Ambulocetidea were mainly associated with brackish or freshwater, the more aquatic derived Remingtonocetidae and Protocetidae lived mainly in coastal marine habitats (Newsome *et al.*, 2010). Remingtonocetidae still had four fused sacral vertebrae and a relatively elongated neck but protocetids exhibited various degree of fusion among species and had shortened neck. Most species of both families retained well-developed hindlimbs and pelvis suggesting they were still able to walk on land (Gingerich *et al.*, 1995; Uhen, 2010). In water, they probably relied on pelvic paddling or on pelvic undulations for most crownward protocetids (Uhen, 2010).

The transition to a fully aquatic lifestyle took place approximately 40 Ma with the emergence of Basilosauridae. This species-rich family is a close relative of neocetes and they both belong to the clade

of Pelagiceti, i.e., exclusively aquatic cetaceans (Uhen, 2008). Their pelvis is completely detached of the backbone, hindlimbs are highly reduced and their forelimbs were probably already transformed into flippers (Uhen, 2010). Its vertebral morphology suggests the presence of a caudal tail stock and a caudal fin which indicates that it relied on dorso-ventral body undulations to swim (Buchholtz, 2001b). Although fully aquatic, stable isotope analyses suggest they mostly stayed in coastal areas (Clementz *et al.*, 2006).

Neocetes appeared in the late Eocene, probably around 37-39 Ma (Lambert *et al.*, 2017; McGowen *et al.*, 2019), and rapidly became the largest cetacean clade while archaeocetes became extinct (Marx *et al.*, 2016). The emergence and evolutionary success of neocetes might be related, at least in part, to the onset of the Antarctic Circumpolar Current (ACC) and subsequent increase in ocean productivity, notably the proliferation of diatoms (Marx and Uhen, 2010; Steeman *et al.*, 2009). Further, the acquisition of baleen in mysticetes and echolocation in odontocetes are often considered as key innovations that permitted enhanced feeding efficiency. Early neocetes might have rapidly diversified through an adaptive radiation process associated with early niche partitioning reflected by feeding strategies: filter-feeding, bottom-feeding, specialised cephalopod or fish predators (Marx and Fordyce, 2015; Slater *et al.*, 2010).

A key feature of neocetes is their immovable elbow joint associated with the transformation of forelimbs into paddles (Gatesy *et al.*, 2013). Mysticetes and odontocetes also notably share an important reorganization of their skull consisting in elongation of rostral and posterior displacement of caudal bones. Due to this rearrangement, termed telescoping, nasal openings are placed on the top of the head (Miller, 1923). Extant cetaceans share several other morphological characteristics including, but not limited to, the absence of external hindlimbs, the presence of caudal flukes, an increased number of phalanges in digits (hyperphalangy) to form the flipper, and the acquisition of a single set of permanent teeth during their life (monophyodonty), among others. While all the aforementioned features are shared by neocetes, some of these characteristics might also have been present in the most derived archaeocetes (Gatesy *et al.*, 2013; Geisler, 2018).

According to paleontological data, neocetes reached their peak diversity with approximately 200 species around 10-15 Ma and was followed by an important decrease in species richness dropping to the 89 extant species (Marx *et al.*, 2016; Morlon *et al.*, 2011). This species-richness decrease is

attributed to diversity decline or disappearance of several families of mysticetes and odontocetes, including extinction of numerous species in the Platanistoidea superfamily whose last living representative is the South Asian river dolphin (*Platanista gangetica*) (Fordyce and de Muizon, 2001; Morlon *et al.*, 2011). However Balaenopteridae, Ziphiidae, Phocoenidae and Delphinidae rather experienced a diversity increase at this period (Morlon *et al.*, 2011; Steeman *et al.*, 2009). Specifically, the sudden increase in diversification rate on one of the branches leading to delphinids is particularly pronounced and has been reported by several studies (Morlon *et al.*, 2011; Rabosky, 2014; Slater *et al.*, 2010; Steeman *et al.*, 2009). Ocean restructuring that occurred in the Late Miocene could have spurred the delphinid explosive diversification through a combination of vicariant events due to fluctuating sea-levels and adaptation to concentrated and distant food sources (Steeman *et al.*, 2009). Alternatively, the radiation of oceanic dolphins could be attributed to the acquisition of a key innovation that has not been identified yet (Rabosky, 2014). The high extant diversity of delphinids might have occurred through two diversification phases: the first diversity increase corresponds to the emergence of the family and its subsequent diversification in the Late Miocene resulting in the establishment of the major delphinid subfamilies, the second corresponds to the apparition of modern species in the Late Pliocene – Pleistocene (Bianucci, 2013).

3.3. Anatomy of the musculo-skeletal system

3.3.1. Postcranial axial skeleton

The vertebral column, or backbone, is a central feature of vertebrates. It provides support and rigidity to the body but it also gives the flexibility needed for body movements. The backbone is a segmented and regionalized structure. The number of vertebrae and the position of boundaries between vertebral regions are defined early during the embryonic development through somitogenesis processes and patterns of homeobox (*Hox*) genes expression along the body axis, respectively (Harima *et al.*, 2013; Kessel and Gruss, 1990; Wellik, 2007; Woltering, 2012). Five different regions are traditionally identified in terrestrial mammals: cervical, thoracic, lumbar, sacral, and caudal; with the thoracic region further subdivided in pectoral (on which shoulder muscles insert), anterior dorsal (bearing true ribs) and posterior dorsal (bearing false ribs) regions (Jones *et al.*, 2018b; Wellik, 2007).

At the level of the vertebral axis, morphological modifications during the land-to-water transition of cetacean were accompanied by the loss of a fully differentiated sacral region and

homogenisation of vertebral shape along the backbone compared to their terrestrial relatives (Buchholtz, 2001b; Buchholtz *et al.*, 2005). Nonetheless, several regions are still identified in the cetacean backbone (e.g., DeSmet, 1977; Slijper, 1936). Albeit alternative regionalisation patterns have been suggest for cetaceans (e.g., Buchholtz, 2007; Buchholtz and Schur, 2004), in this work, we use Rommel's description of the bottlenose dolphin (*Tursiops truncatus*) backbone in which the following regions were identified: cervical, thoracic, lumbar, caudal, and fluke (Rommel, 1990) (Figure 1.6*a*).

As in other mammals, cervical vertebrae are the seven first vertebrae and usually do not bear ribs. The cervical region is dramatically shortened compared to terrestrial mammals, this provides a more streamlined external body shape and help to stabilize the head (Buchholtz, 2001b). In addition, fusion (ankylosis) between two or more successive cervical vertebrae is present in most species but Monodontidae, Balaenopteridae, and 'river dolphins' (Buchholtz, 2001b; DeSmet, 1977).

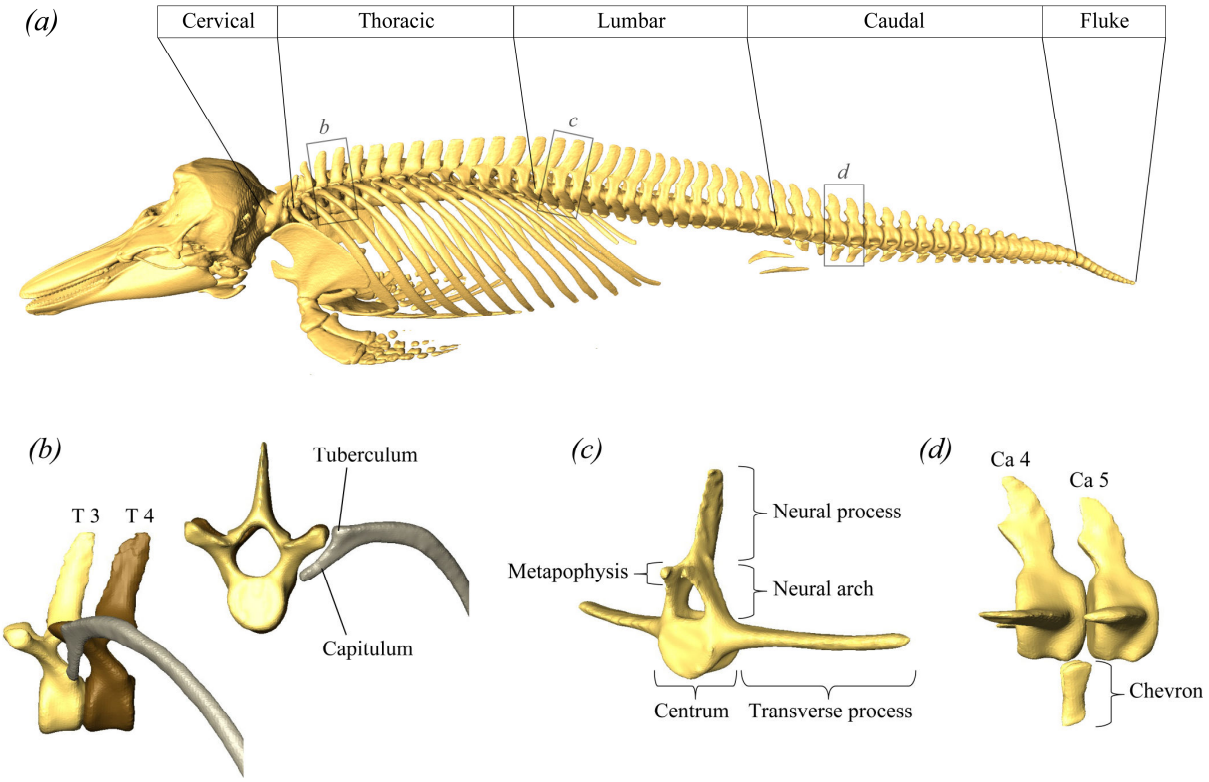

Figure 1.6. Anatomy of the cetacean postcranial skeleton. *(a)* 3D reconstruction of a harbour porpoise (*Phocoena phocoena*) skeleton and showing the five vertebral regions. Grey boxes show parts of the skeleton enlarged in the remaining panels. *(b)* Lateral (left) and cranial (right) view of the 4th rib (grey) which inserts on the 4th thoracic (brown) with its tuberculum and on the 3rd thoracic (beige) with its capitulum. *(c)* Cranio-lateral view of the 2nd lumbar vertebra showing the different vertebral apophyses. *(d)* Lateral view of 4th and 5th caudal vertebrae and the articulation of the 4th chevron on the ventro-posterior face of the 4th caudal vertebra.

Thoracic vertebrae are identified by the presence of ribs. Anterior ribs are in connected to the sternum but not the posterior ones. Unlike most terrestrial mammals, ribs connected to sternum are composed of two ossified structures attached to each other by a cartilaginous or fibrous flexible joint: the vertebral rib which is connected to the vertebra, and the sternal rib which is connected to the sternum (Flower, 1885; Rommel and Reynolds, 2009). According to the species, a variable number of anterior pairs of ribs are bicipital ribs, also, also sometimes called 'double-headed' ribs. Those ribs insert to the backbone through two articulations instead of one: a dorsal tuberculum inserting at the tip of the transverse process of the corresponding vertebra, and a ventro-rostral capitulum inserting on the posterolateral face of the vertebral centrum of the preceding vertebra (Figure 1.6*b*). The remaining ribs insert only on the vertebral transverse processes via the tuberculum (Rommel, 1990).

The lumbar region is characterised by vertebrae that do not have ribs or chevron bones (see caudal region) (Figure 1.6*c*). In accordance with their fully aquatic lifestyle and hindlimbs loss, cetaceans do not have a distinct sacral region. However, anatomical investigations of the nervous system as well as analyses of vertebral shape suggest that the few last lumbar vertebrae (42% of the lumbar length) could be homologous to the sacral region of terrestrial mammals (Buchholtz and Gee, 2017; Slijper, 1936).

The first caudal vertebra is identified by the presence of a chevron bone on the ventro-caudal face of its vertebral centrum. Chevron bones are ventral ossifications situated below the intervertebral disks and articulating with the two vertebrae surrounding the disk (Figure 1.6*d*). In some species, the posterior part of the caudal region is characterised by laterally-compressed vertebrae (i.e., vertebral centra higher than wide) corresponding to the tail stock (Buchholtz, 2001b; Buchholtz and Schur, 2004).

The few last caudal vertebrae, the fluke vertebrae, are dorso-ventrally compressed (i.e., vertebral centra wider than high). In general, these vertebrae do not have vertebral apophyses such as neural spines and arches or transverse processes, but the most anterior ones usually have small chevron bones. These vertebrae are situated in the medial region of the caudal fin up to the fluke notch. In most species, the vertebra at the transition between caudal and fluke regions, called the 'ball' vertebra, has a spherical shape with convex anterior and posterior face providing high flexibility at the region of

fluke insertion (Watson and Fordyce, 1993). In our analyses, we however did not distinguish this unique vertebra from other fluke vertebrae.

3.3.2. Axial musculature

The axial musculature of cetaceans has been previously described in a few species such as harbour porpoises (*P. phocoena*), bottlenose dolphins (*T. truncatus*), and common dolphins (*D. delphis*) (e.g., Pabst, 1990; Parry, 1949; Slijper, 1936; Smith *et al.*, 1976). Yet, given the complexity of the axial musculature, nomenclature and description vary widely among authors (see Pabst (1990) for a review of the nomenclature). In this work, we mostly follow the nomenclature proposed by Pabst (1990) for bottlenose dolphins (*T. truncatus*) but we do not distinguish the anterior (dorsal) and posterior (caudal) parts of muscles and thus use a single name for each muscle. For clarity purpose the description of the muscular anatomy is summarized and concerns here only the main sites of muscular origin and insertion (see Pabst (1990) and Slijper (1936) for a thorough description) (Figure 1.7).

The epaxial musculature is composed of five principal muscles.

1) The *m. iliocostalis* takes origin on the transverse processes of the atlas and axis and on the lateral faces of ribs. It inserts on the subdermal connective tissue sheath (SDS) surrounding the entire axial musculature up to the anterior lumbar region. Its suggested role is to move the rib cage caudally (Pabst, 1990).

2) The *m. intertransversarius caudae dorsalis* (ICD) is a small lateral muscle in the lumbar and caudal regions. It takes origin on the distal tip of the dorsal surface of transverse processes in the mid-lumbar and caudal regions, or, in the posterior caudal region, on the lateral face of vertebral centra. Each muscular fibre inserts a few vertebrae more posteriorly than its origin, on the distal tip of the transverse process in the lumbar and caudal regions, or on the lateral face of the vertebral centrum in the posterior caudal region. Although it might be slightly involved in dorsal extension of the backbone, its principal role is probably to flex the body laterally (Pabst, 1990; Parry, 1949).

3) The *m. semispinalis* is only present in the cervical and anterior thoracic region of the body and takes origin on the occipital region, on the supraoccipital bone) It inserts on

metapophyses and dorsal tips of neural spines in the anterior and mid thoracic region. Its role is to move and stabilize the head (Pabst, 1990; Slijper, 1936).

4) The last two epaxial muscles are the *m. longissimus* and the *m. multifidus* and are of peculiar interest for this work as they are the main muscles generating dorsal extension of the backbone. These muscles represent the largest part of the epaxial musculature and run along the body from the posterior face of the skull up to the posterior caudal region. The *m. multifidus* originates on the lateral surfaces of the neural spines, dorsally to the metapophyses, of cervical, thoracic, lumbar and caudal vertebrae. It inserts, via a series of long tendon fibres called the deep tendon, on the metapophyses of all vertebrae except those in the fluke (Pabst, 1990; Slijper, 1936; Smith *et al.*, 1976).

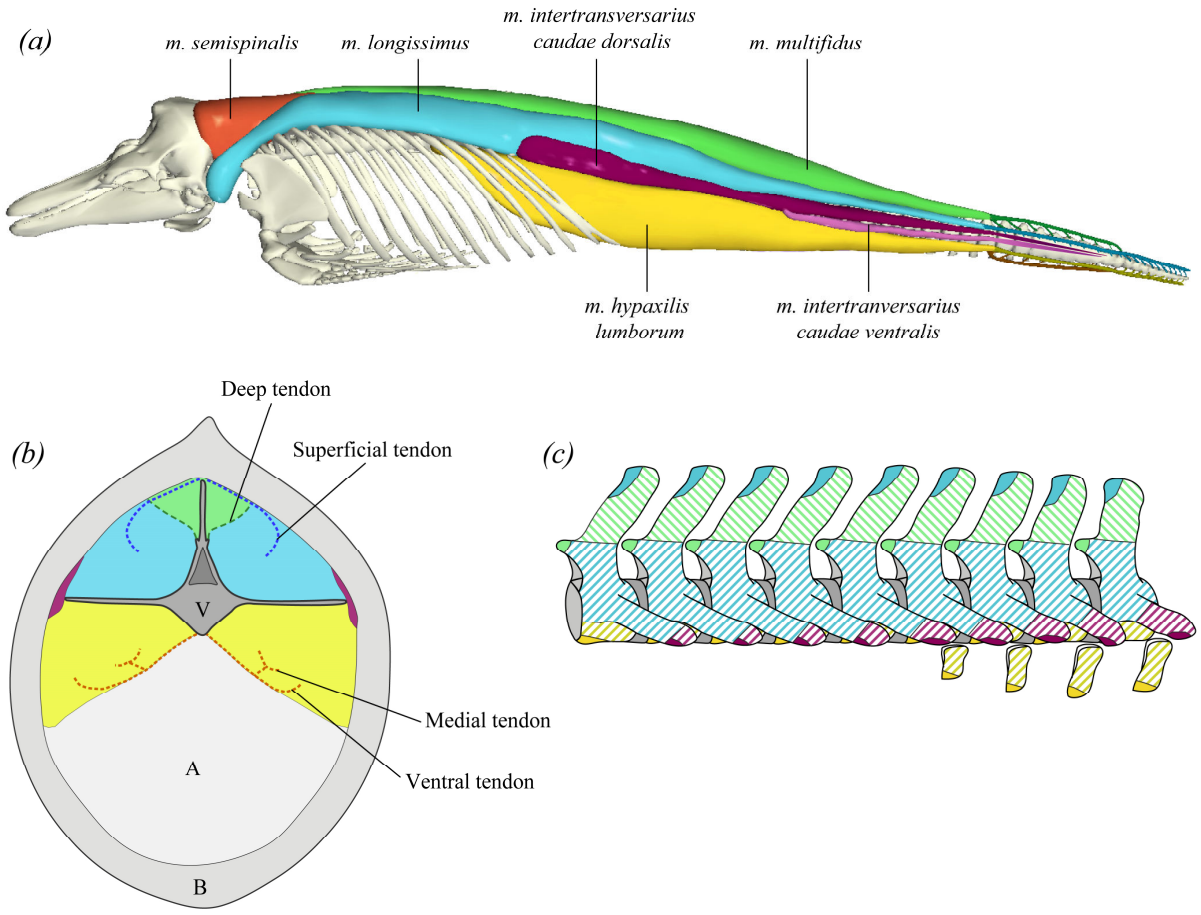

Figure 1.7. Cetacean axial musculature. (a) 3D model of harbour porpoise (*P. phocoena*) skeleton, axial muscles (except the *m. iliocostalis*), and terminal tendons. *(b)* Schematic cross-section in the mid-lumbar region showing muscles and tendons position. *V*: vertebra; *A*: abdominal cavity; *B*: blubber. *(c)* Areas of origin (hatched zones) and insertion (coloured zones) on vertebrae for each muscle. Muscle colour legend is the same in all panels. Panel *(c)* adapted from Slijper (1936). 3D model made by Marion Grimaud and Steven Braine.

5) The *m. longissimus* takes origin on the posterior face of the skull (exoccipital and squamosal) and on the dorsal faces of transverse processes and neural arches (below metapophyses) of cervical, thoracic, lumbar and caudal vertebrae. It inserts on dorsal tips of the neural spines posterior thoracic, lumbar and caudal vertebrae and on the dorsal face of the vertebral centrum in the fluke, via a series of tendons called the superficial tendon. This tendon emerges laterally from the muscle mass and covers the dorsolateral surface of the *m. multifidus* to insert on the dorsal tip of the neural spines (Pabst, 1990; Slijper, 1936; Smith *et al.*, 1976). The *m. multifidus* and the *m. longissimus* should act together to place in extension the lumbo-caudal region. In addition, the *m. longissimus* could control the orientation of the flukes in the horizontal plane (i.e., the angle of attack of the flukes) via its insertions on the fluke vertebrae (Pabst, 1990; Smith *et al.*, 1976).

The hypaxial complex is composed of two distinct muscles only.

1) The *m. intertransversarius caudae ventralis* is comparable to the ICD but is shorter as it only originates in the caudal region. It takes origin on the distal part of the ventral surfaces of transverse processes of caudal vertebrae. It inserts on the distal tip of the transverse processes and lateral faces of vertebral centra in the caudal region. Similar to the ICD, it could play a function in the lateral flexions of the backbone (Pabst, 1990).

2) The *m. hypaxialis lumborum* originates on the ventral surfaces of transverse processes and vertebral centra from the posterior thoracic region to the posterior caudal region, as well as on the lateral aspects of the chevron bones in the caudal region. It inserts via the ventral and medial tendons on the ventral surface of vertebral centra and on chevron bones of mid-lumbar, caudal and fluke vertebrae (Pabst, 1990). It is responsible of ventral flexion of the body and controls the flukes angle of attack (Pabst, 1990; Smith *et al.*, 1976).

3.4. Locomotion: swimming kinematics and efficiency

During their land-to-sea transition, cetacean locomotion evolved from quadrupedal or bipedal paddling to more efficient caudal and fluke oscillations (Fish, 2016). Given their fusiform body shape with a narrow peduncle and a crescent-shaped tail, and their swimming movements relying on dorsoventral oscillations of the posterior part of the body, i.e., the peduncle and the flukes, cetaceans

are usually considered as thunniform swimmers, or 'carangiform swimmers with semi-lunate tail' (Fish *et al.*, 2003; Webb, 1975). Although only a few studies investigated swimming movements of cetaceans, they clearly highlighted differences between the regions in which maximal bending occur among species (see section 2 of this chapter) (Buchholtz, 2001b; Curren *et al.*, 1994; Videler and Kamermans, 1985). This therefore suggests that not all cetaceans should be considered as thunniform swimmers or that a further classification level among thunniform swimmers is needed. The laterally compressed morphology of the peduncle results in a hydrodynamic shape in the vertical plane, allowing dorsoventral oscillations with low resistance and drag. On the contrary, the large horizontal surface of the flukes acts as an oscillating hydrofoil generating lift and associated thrust.

In addition to peduncle oscillations, fluke pitching is modified thorough the swimming cycle providing enhanced thrust generation. During up and down movements of the peduncle, the pitch angle of the flukes, which corresponds to the angle between the animal swimming direction and the median axis of the fluke, is different from zero. It increases at the beginning of the half stroke and decreases at the end, reaching its maximal value at a third of each half-cycle duration. At the transitions between up- and downstroke, the pitch angle is close to zero meaning that fluke axis is parallel to the animal's forward direction and ensuring low drag but not producing thrust either (Fish, 1993) (Figure 1.8).

At regular cruising speed, cetaceans increase their swimming speed by increasing fluke oscillation frequency rather than increasing amplitude, which is comparable to patterns observed in fishes (Bainbridge, 1958; Fish, 1998; Rohr and Fish, 2004; Steinhausen *et al.*, 2005). However, fluke amplitude increases with increasing speed at low swimming speeds. Oscillating frequency is also correlated with body size, with larger species naturally oscillating at lower frequencies (Rohr and Fish, 2004; Sato *et al.*, 2007). For example, baleen whales and sperm whales usually swim with oscillating frequencies between 0.20 and 0.25 Hz whereas small dolphins and porpoises use frequencies higher than 1 Hz (Gough *et al.*, 2019; Rohr and Fish, 2004; Sato *et al.*, 2007).

The generation of large forces by flukes in the posterior part of the body creates large recoil force on the anterior region of the animal. If not counteracted, recoil forces lead to increased dorsoventral oscillation of the head and increased drag, resulting in less efficient swimming movements. Yet, head vertical movements in delphinids is low (approximately 5% of body length)

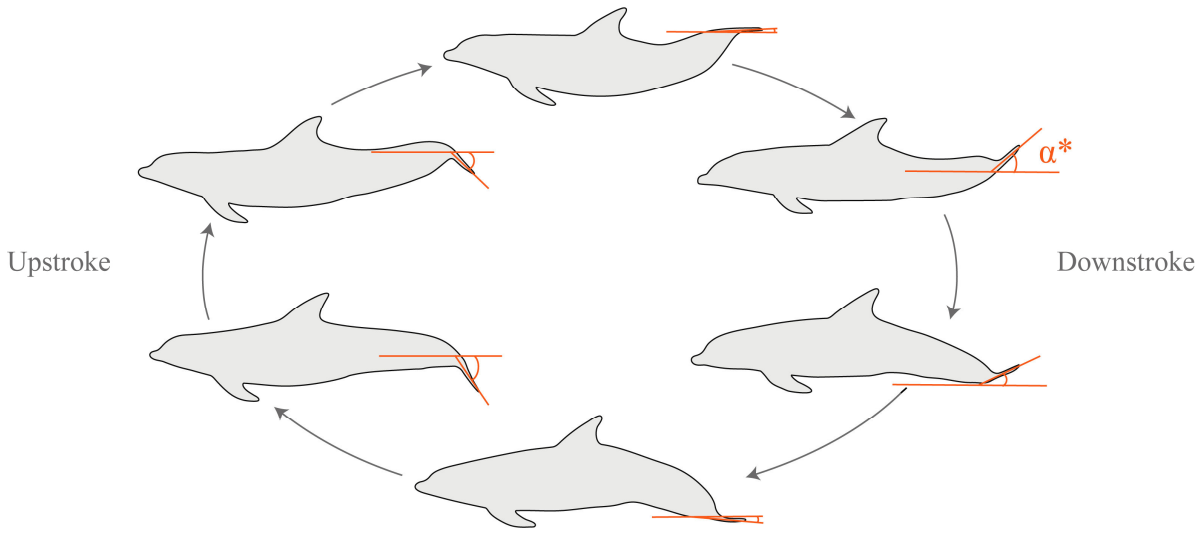

Figure 1.8. Dolphin swimming cycle and pitch angle. Decomposition of the swimming cycle of a bottlenose dolphin (*T. truncatus*), from left to right: maximal dorsal extension; downstroke, maximal ventral flexion, upstroke. The pitch angle (α*) corresponding to the angle between flukes and animal's swimming direction are indicated by orange lines. At maximal extension and flexion, the pitch angle is close to zero, limiting drag. During downstroke and upstroke, the pitch angle is large to maximise lift.

compared to fluke amplitude (between 15 and 30% body length) at cruising speeds (Fish *et al.*, 2003; Skrovan *et al.*, 1999). This suggests that recoil movements are counteracted passively through increased body and backbone stiffness in the anterior region and actively through muscular contraction and orientation of flippers to generate opposite forces and confer greater stability to the animal (Fish *et al.*, 2003).

Stability is an important feature of locomotion. In aquatic environment, body stability will provide more efficient swimming movements while instability will provide greater manoeuvrability, i.e., high turning performances. Stability is notably influenced by body stiffness, body size and the position, shape and mobility of fins. This implies that morphology will vary among species depending on their ecology and that there is a trade-off between high swimming speed and manoeuvrability (Fish, 1997; Weihs, 2002, 1993). Species using steady and fast swimming over long distance such as the Pacific white-sided dolphin (*Lagenorhynchus obliquidens*) and the Commerson's dolphin (*Cephalorhynchus commersonii*), have a morphology suited for stability (high body stiffness, highly swept fins with reduced mobility) and take large turn at high swimming speed. On the contrary, the Amazon River dolphin (*Inia geoffrensis*) and the beluga (*Delphinapterus leucas*) are able to take thigh

turns but at lower speed and possess a morphology enhanced for manoeuvrability (flexible body and neck, large and highly mobile pectoral fins, absent dorsal fin) (Fish, 1997; Fish and Rohr, 1999).

4. Thesis objectives

The vertebral morphology of cetaceans varies widely among species. Although, previous investigations have proposed that vertebral modifications result in different swimming movements, it has not been quantitatively tested in a comparative framework (Buchholtz, 2001b; Long *et al.*, 1997; Smith *et al.*, 1976; Smith and Burrows, 2010). Hence, the hypothesis of this thesis postulates that the vertebral morphology, swimming performances, ecology, and evolutionary history of cetaceans are related.

The present work aims at providing concrete elements concerning the causes and consequences of the tremendous morphological variability of the cetacean backbone. To this purpose, we statistically investigated the morphology and biomechanics of the cetacean backbone in an ecological and phylogenetic context. We quantified the variability of vertebral morphology for more than 70 cetacean species using specimens available in nine natural history museums worldwide. Cutting-edge phylogenetic comparative methods were then used to establish the impacts of the environment and evolutionary history on vertebral morphology in modern cetaceans. We also briefly compared our results with the vertebral morphology of some fossil species. Biomechanical properties of the vertebral column were mathematically modelled for several species based on morphological data. Finally, swimming kinematics of four species were quantitatively analysed based on videos recorded in aquariums.

5. Thesis outline

Besides this first chapter presenting the general background relative to evolutionary processes and the morphology and diversity of cetaceans, this work is composed of four additional chapters: two chapters investigate the ecological and evolutionary aspects of vertebral morphology and one chapter investigates the functional aspects.

The second chapter aims at identifying whether the vertebral morphology of modern cetaceans is related to their ecology or not and the consequences it had on the evolutionary history and diversity of the entire clade. This chapter also presents the detailed methods of vertebral measurements acquisition on museum specimens. A subset of this dataset was also used in chapters 3 and 4.

The third chapter is dedicated to a more detailed analysis of the vertebral morphology, ecological transitions and evolutionary processes in the Delphinoidea subclade (porpoises, oceanic dolphins, and narwhal and beluga) at inter- and intraspecific levels. It aims at establishing if macro- and microevolutionary patterns are similar in this clade.

The fourth chapter intend to investigate the link between vertebral morphology and swimming movements. The first part of this chapter focuses on the biomechanical aspects of the backbone while the second part is dedicated to the swimming kinematics of four different species: the Amazon River dolphin (*Inia geoffrensis*), the harbour porpoise (*Phocoena phocoena*), the common bottlenose dolphin (*Tursiops truncatus*) and the Pacific white-sided dolphin (*Lagenorhynchus obliquidens*).

Finally, the fifth chapter presents a general discussion of the ecomorphological and evolutionary patterns of the cetacean backbone and locomotion based on the combination of results obtained in preceding chapters.

Chapter 2 :
Vertebrae are the backbone of cetacean diversity: How morphological innovations sustained dolphin explosive radiation[1]

[1] Gillet A., Frédérich B., Parmentier E. (2019) Divergent evolutionary morphology of the axial skeleton as a potential key innovation in modern cetaceans. *Proceedings of the Royal Society B: Biological Sciences,* **286**(1916):20191771

Authors' contributions to the publication: A.G. and E.P. designed the project. A.G. collected and analysed the data. B.F. assisted in comparative analyses. A.G., B.F. and E.P. wrote the manuscript.

Abstract

Cetaceans represent the most diverse clade of extant marine tetrapods. Although restructuring of oceans could have contributed to their diversity, other factors might also be involved. Similar to ichthyosaurs and sharks, variation of morphological traits could have promoted the colonization of new ecological niches and supported their diversification. By combining morphological data describing the axial skeleton of 73 cetacean species with phylogenetic comparative methods, we demonstrate that the vertebral morphology of cetaceans is associated to their habitat. All riverine and coastal species possess a small body size, lengthened vertebrae and a low vertebral count compared to open ocean species. Extant cetaceans have followed two distinct evolutionary pathways relative to their ecology. Whereas most offshore species such as baleen whales evolved towards an increased body size while retaining a low vertebral count, small oceanic dolphins underwent deep modifications of their axial skeleton with an extremely high number of short vertebrae. Our comparative analyses provide evidence these vertebral modifications have potentially operated as key innovations. These novelties contributed to their explosive radiation, resulting in an efficient swimming style that provides energetic advantages to small-sized species.

1. Introduction

Morphological disparity often supports various functional abilities, promoting the occupation of new ecological niches. Although many ecomorphological studies focused on external body shape or skull morphology, some have demonstrated correlations between vertebral morphology and species ecology in several vertebrate lineages (Chen *et al.*, 2005; Granatosky *et al.*, 2014; Jones *et al.*, 2018a; Randau *et al.*, 2016). For example, scansorial felids and arboreal marsupials have wider and/or shorter vertebral centra than their terrestrial counterparts (Chen *et al.*, 2005; Randau *et al.*, 2016). In the aquatic ichthyosaurs and sharks, variation of body form and vertebral phenotypes has been linked to different lifestyles like the inhabitation of coastal or offshore habitats (Kim *et al.*, 2013; Motani *et al.*, 1996; Thorne *et al.*, 2011). For instance, the disparification of body shape in ichthyosaurs is assumed to be linked to their adaptive radiation, with transitions from coastal habitats to open seas (Motani *et al.*, 1996; Thorne *et al.*, 2011).

In terms of body shape, cetaceans exhibit a strong convergence with lamniform sharks and ichthyosaurs (Kelley and Pyenson, 2015; Motani, 2002). Cetaceans adapted to coastal or oceanic habitat differ in some phenotypic traits such as body proportions, fin shapes or inner ear morphology (Fish, 1998; Gutstein *et al.*, 2014; Woodward *et al.*, 2006). Slow swimming coastal species tend to have paddle-shaped fins and flukes and large bulbous heads compared to cruising species (Fish, 1998; Woodward *et al.*, 2006). Cetaceans also exhibit a wide variation in their vertebral morphology which could support different swimming abilities (Buchholtz, 2001b; Buchholtz and Gee, 2017; Buchholtz and Schur, 2004; Long *et al.*, 1997). Surprisingly, despite their large ecological diversity, no study has statistically the relationship between the axial skeleton and the various habitats of cetaceans at a large phylogenetic scale. Previous studies have suggested that low vertebral count and spool-shaped vertebrae would be a primitive state in extant cetaceans typical of slow-swimming coastal species. In contrast, high vertebral count and discoidal vertebrae would be a derived condition corresponding to fast-swimming pelagic dolphins (Buchholtz and Gee, 2017; Buchholtz and Schur, 2004; Marchesi *et al.*, 2018). On the other hand, Viglino and colleagues did not find a correlation between vertebral morphology and habitat when using phylogenetic comparative methods on seven dolphin species (Viglino *et al.*, 2014). This supports the need to further investigate the cetacean vertebral morphology

by studying a large number of species and by using recently developed comparative methods to understand how the cetacean backbone diversified.

With 89 species (Committee on Taxonomy, 2019), cetaceans are currently the most species-rich clade of extant marine tetrapods. In particular, 40% of cetacean species are Delphinidae, the family of oceanic dolphins. This high level of species diversity in Delphinidae results from increased rates of lineage diversification during the past 10 Ma (do Amaral *et al.*, 2016; Morlon *et al.*, 2011; Rabosky, 2014; Slater *et al.*, 2010; Steeman *et al.*, 2009). This explosive radiation might be due to a combination of vicariant events and adaptation to scattered production areas caused by the restructuring of oceans that occurred during the Middle-Late Miocene (do Amaral *et al.*, 2016; Steeman *et al.*, 2009; Whitmore, 1994). However, it was later suggested that this shift might also be driven by the appearance of an unidentified key innovation (Rabosky, 2014). As forward propulsion of cetaceans is achieved by oscillation of the backbone, the axial skeleton plays a central role in swimming and travelling capabilities. We might then expect that the disparity of the vertebral morphology in cetaceans to be linked to their ecological diversity (Buchholtz and Gee, 2017; Buchholtz and Schur, 2004; Marchesi *et al.*, 2018). Accordingly, variation of their axial skeleton could have acted as evolutionary innovations supporting their adaptive radiation.

In the present study, we hypothesize that the axial skeleton morphology of modern cetaceans is related to the species lifestyle and their diversification. We have thus compiled meristic and morphometric data on the axial skeleton of most cetacean species. Using various phylogenetic comparative methods, we demonstrate that the vertebral morphology is linked to the ecological diversity of cetaceans and that the explosive radiation of oceanic dolphins could be linked to sudden vertebral modifications that acted as key innovations.

2. Materials and methods

2.1. Data sampling

2.1.1. Extant cetaceans

Vertebral count and shape data were collected from 217 specimens, representing 73 extant species (specimen list in Table S 2.1). Specimens used come from nine different natural history

museums: the Royal Belgian Institute of Natural Sciences in Brussels (RBINS), the French National Museum of Natural History in Paris (MNHN), the State Museum of Natural History in Stuttgart (SMNS), the Swedish Royal Museum of Natural History in Stockholm (NRM), the Bayworld Port Elizabeth Museum in Port Elizabeth (PEM), the Iziko South African Museum in Cape Town (SAM), the Queensland Museum in Brisbane (QM), the National Museum of Natural History in Washington D.C. (USNM) and the American Museum of Natural History in New York (AMNH) (Table S 2.1). Every genus, except the monospecific *Indopacetus*, is represented in our dataset. We sampled at least two specimens per species although twelve species were represented by one specimen. Whenever possible, we measured specimens of different sex and/or from different populations. To estimate intraspecific variation, the morphological disparity was calculated for two species represented by numerous specimens (*Phocoena phocoena*: 17 specimens, *Tursiops truncatus*: 11 specimens) and was compared to the disparity level of the entire dataset. Morphological disparities were calculated using the function *morphol.disparity* from the *geomorph* R-package (v.3.0.7) (Adams *et al.*, 2018)).

Total vertebral count was taken only on complete specimens or on specimens missing up to three vertebrae and for which the number of missing vertebrae could be estimated. When specimens of the same species had different vertebral counts, we retained the highest count for the species. To quantify vertebral shape, two angular and 12 linear measurements were taken on each vertebra with a protractor, digital calipers, and rulers (Figure 2.1 *a, b, c, d*) (Buchholtz *et al.*, 2005). Shape data were collected on thoracic, lumbar, and caudal vertebrae allowing the inclusion of specimens missing most of their fluke vertebrae. The first caudal vertebra was defined as the first vertebra possessing an articular facet for a chevron bone on its posterior face (Rommel, 1990). The first fluke vertebra was identified as the first vertebrae for which the centrum height was at least 5% lower than the centrum width.

Prior to analysis, each species was classified into one of the following habitat categories based on synthetic bibliographic works; (*i*) rivers, bays, and estuaries; (*ii*) continental shelf; (*iii*) continental slope and offshore waters; and (*iv*) mixed lifestyle between continental shelf and offshore waters (Berta, 2015; IUCN, 2017; Perrin *et al.*, 2009). All phylogenetic analyses were based on the cetacean consensus time-tree published by Steeman (Steeman *et al.*, 2009). The topology and divergence time estimations of this tree are congruent with other recently published phylogenies (Geisler *et al.*, 2011;

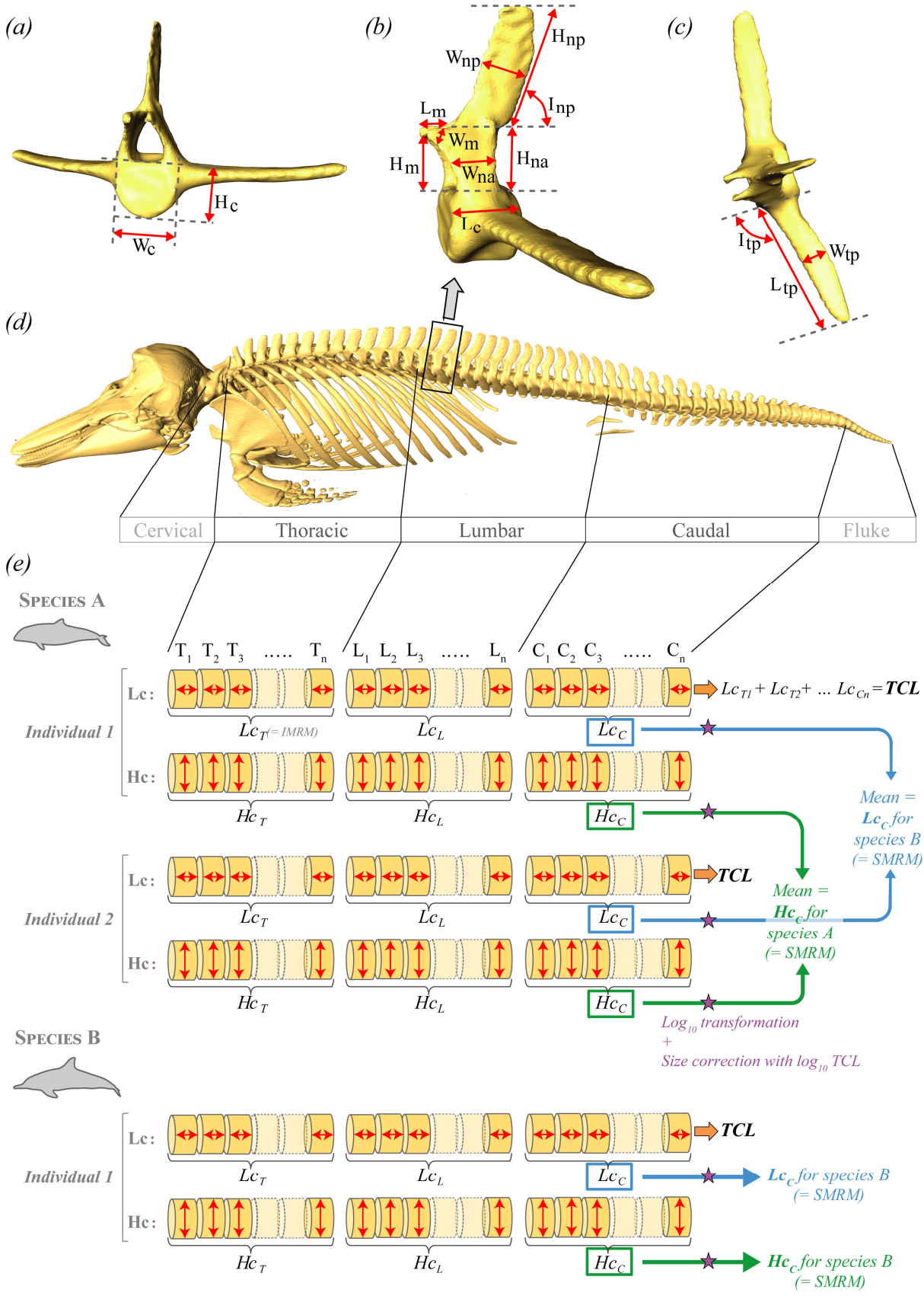
(a)
Hc
Wc
(b)
Hnp
Wnp
Inp
Lm
Wm
Hm
Hna
Wna
Lc
(c)
Itp
Wtp
Ltp
(d)
Cervical
Thoracic
Lumbar
Caudal
Fluke
(e)
SPECIES A
T1 T2 T3 ..... Tn
L1 L2 L3 ..... Ln
C1 C2 C3 ..... Cn
Lc:
Hc:
Individual 1
Individual 2
LcT (= IMRM)
LcL
LcC
HcT
HcL
HcC
Lc1 + Lc2 + ... LcCn = TCL
TCL
Mean = LcC for species B (= SMRM)
Mean = HcC for species A (= SMRM)
Log10 transformation + Size correction with log10 TCL
SPECIES B
LcC for species B (= SMRM)
HcC for species B (= SMRM)

McGowen *et al.*, 2009; Slater *et al.*, 2010; Zurano *et al.*, 2019). Although some uncertainties remain at shallow phylogenetic levels, relationships at the family levels are well established. Similarly to other recent comparative studies in cetaceans (Morlon *et al.*, 2011; Rabosky, 2014), we are confident that this phylogenetic uncertainty should not impair our results. Prior to analysis, *Orcaella heinsohni* which is not included in Steeman's tree was added to the tree (*add.species.to.genus* function, R-package *phytools* (v.0.6-44) (R Core Team, 2017; Revell, 2012)).

In order to highlight raw morphological variation without accounting for phylogenetic signal, all analyses described hereafter were repeated by using regular statistics (Appendix I in Supplementary materials).

2.1.2. Fossil cetaceans

The scarcity of undamaged fossilised backbones and phylogenetic uncertainties of some fossil taxa prevented us from reliably including extinct cetaceans in our analyses. However, length and height of vertebral centra of 13 fossil taxa were obtained from the literature. Only species that have previously been included in phylogenetic analyses were selected. Data were obtained for four stem cetaceans: *Basilosaurus cetoides* (Kellogg, 1936), *Dorudon atrox* (Uhen, 2004), *Zygorhiza kochii* (Kellogg, 1936) and *Cythiacetus peruvianus* (Martínez-Cáceres *et al.*, 2017). Two extinct mysticetes were also included: *Aetiocetus cotylalveus* (Emlong, 1966) and *Thinocetus arthritis* (Kellogg, 1969). Finally, data were also obtained for seven extinct odontocetes: *Zarhachis flagellator* (Kellogg, 1924), *Ninoziphius platyrostris* (de Muizon, 1984), *Kentriodon pernix* (Kellogg, 1927), *Pliopontos littoralis*

Figure 2.1 (Previous page). Schematic representation of vertebral shape data collection and standardisation. Twelve linear and two angular measurements (red double arrows) taken on each vertebra are shown on a vertebra in *(a)* frontal view, *(b)* lateral view and *(c)* dorsal view. *Wc*: centrum width, *Hc*: centrum height, *Lc*: centrum length, *Hnp*: neural spine height, *Wnp*: neural spine width, *Inp*: neural spine inclination, *Hna*: neural arch height, *Wna*: neural arch width, *Lm*: metapophysis length, *Wm*: metapophysis width, *Hm*: metapophysis height, *Ltp*: transverse process length, *Wtp*: transverse process height, *Itp*: transverse process inclination. *(d)* 3D model of a harbour porpoise (*Phocoena phocoena*) skeleton based on CT-scan. Measurements were taken only on vertebrae of three regions: thoracic, lumbar and caudal. *(e)* For each individual, the mean value of each measurement in each region was calculated (= IMRMs). The total centrum length (TCL) was calculated by summing centra lengths of the three regions. All IMRMs were then $\log_{10}$-transformed and size-corrected using $\log_{10}$-TCL as a proxy for body size. Species values of each measurement of each region (SMRM) were then calculated as the mean of IMRM of all individuals belonging to the species.

(de Muizon, 1984), *Atocetus iquensis* (de Muizon, 1988), *Albireo whistleri* (Barnes, 2008) and *Piscolithax longirostris* (de Muizon, 1984). Measurements were taken from data tables available in the original description of the specimens except for *Albireo whistleri*. For this later species, no raw measurements were available but ratios were obtained from pictures of the backbone available in the original publication. Phylogenetic relationships were synthetized from various recently published phylogenies (Aguirre-Fernández and Fordyce, 2014; Geisler *et al.*, 2011, 2012; McGowen *et al.*, 2009; Murakami *et al.*, 2014; Slater *et al.*, 2010; Steeman *et al.*, 2009).

Their mean length/height (L/H) ratios were compared to extant species. For extant species, L/H ratios were calculated for each vertebra of the thoracic, lumbar and caudal regions. The average ratio for the entire backbone was then calculated and used for the analysis. Densities for the violin plot were computed with the R-package *ggplot2* (Wickham, 2016). The number of vertebrae from which measurements were obtained for extinct specimens varied depending on the preservation state of each specimen but it generally consisted of several vertebrae from at least two different regions of the backbone (apart from the cervical region). Some specimens used were reconstructed from a composite of several specimens. Similar to extant species, the mean L/H ratio of each extinct species was then calculated and compared to extant species.

2.2. Vertebral count and body size

We first investigated variation in the number of vertebrae and tested its linear relationship with body length using a phylogenetically corrected generalized least squares regression (PGLS) in the *nlme* R-package (v.3.1-131) (Pinheiro *et al.*, 2017). For this analysis, the average body length of each species was obtained by calculating the mean value of the body size range provided by Berta (Berta, 2015). We also tested the effect of habitat on the vertebral count with a phylogenetic ANOVA (*aov.phylo* function, R-package *geiger* (v.2.0.6) (Pennell *et al.*, 2014)).

Due to an apparent difference in vertebral count among families (see Results), we tested whether Delphinidae and Phocoenidae (i.e., oceanic dolphins and porpoises) differ from other families in their vertebral count and body size by applying a phylogenetic MANOVA (*aov.phylo* function). According to the results from this MANOVA and those from evolutionary patterns analyses (see section 2.4, below), we repeated the analysis testing the effect of habitat (phylo-ANOVA)

and body size (PGLS) on four different subgroups of species: (*i*) Delphinidae and Phocoenidae; (*ii*) all species except Delphinidae and Phocoenidae; (*iii*) Delphinoidea; and (*iv*) non-Delphinoidea.

2.3. Morphospace of vertebrae

To compare vertebral shape among species with highly different vertebral counts, we calculated individual mean regional measurements (IMRMs) which correspond to the mean of each linear/angular measurement for each region of each individual (Figure 2.1 *e*). All linear IMRMs were log_{10}-tranformed and then phylogenetically size-corrected using the function *phyl.resid.intra* (López-Fernández *et al.*, 2014). Total centrum length (TCL) was calculated for each specimen by summing the length of the vertebral centrum of all measured vertebrae (Buchholtz *et al.*, 2005). It was log_{10}-transformed and used as a proxy of body length for IMRMs size-correction. Angular IMRMs were not correlated to body size and were thus transformed using a cosine function. Specimen residuals of each IMRM were then averaged for each species to obtain species mean regional measurements (SMRMs).

All SMRMs were implemented in a regular principal component analysis (PCA) based on the correlation matrix, using the *prcomp* function in R. Similarly to analyses on vertebral count, four additional PCAs were run separately for each species subgroup. According to the Jollife cut-off, only principal components (PCs) with an eigenvalue ≥ 0.7 were conserved. Thus the first eight PCs for the "all cetaceans" PCA and the first nine PCs for each subgroup PCA were used in the following analyses.

We first tested the effect of habitat on vertebral shape (PCs) for each PCA separately using phylogenetic MANOVAs. Then, we tested the effect of body size on vertebral shape with a multivariate phylogenetic linear regression (*procD.pgls* function, *geomorph* package). A multivariate PGLS was also used on the "all cetaceans" PCA to test the relationship between vertebral count and vertebral shape. Differences in vertebral shape between Delphinidae and Phocoenidae *versus* other species were tested with a phylogenetic MANOVA.

2.4. Evolutionary shifts of phenotypic traits

Analyses of vertebral count and morphospace point out to a marked divergence of oceanic dolphins and porpoises from other species (see Results). In order to test if this morphological divergence corresponds to evolutionary shifts, we applied two Bayesian statistical methods to our

phenotypic data. BAMM (v.2.5.0) (Rabosky, 2014) uses a Bayesian multi-rate approach and allows the detection of variations in the rate of morphological evolution. Bayou (v.2.1.1) (Uyeda and Harmon, 2014) is based on a Bayesian multi-regime Ornstein-Uhlenbeck approach and can identify changes in phenotypic optima over time. These two methods can identify the presence of one or several shifts without *a priori* information on the position of shifts along the phylogeny. Analyses were run independently for each PC of the "all cetaceans" PCA and on the $\log_{10}$-transformed vertebral count.

For BAMM, priors were automatically generated in the R-package *BAMMtools* (v.2.1.6) (Rabosky *et al.*, 2014). Analyses were run using a Metropolis-coupled Markov chain Monte Carlo (MCMC) with 5,000,000 generations for each univariate trait. Parameters were sampled every 1,000 iterations, with the first 10% deleted as burn-in.

For Bayou, several independent MCMC chains with different priors were run and their respective marginal likelihoods were computed to select the most appropriate ones. Priors retained for analyses were as follow: the density of the expected number of shifts had a conditional Poisson distribution with a total number of expected shifts (λ) of 3, only one shift was allowed to occur on the same branch and the probability of the location of the shift was uniform along the branch, the density of phenotypic optima followed a normal distribution with a mean value corresponding to the dataset mean and a standard deviation being twice the standard deviation of the data, finally, the density of the evolutionary rate (σ^2) and the constrain parameter (α) both possessed a half-Cauchy distribution. For each univariate dataset, five MCMC chains of 1,000,000 generations were run independently and the first 20% of each chain were deleted as burn-in. Chains convergence was assessed using Gelman and Rubin's *R* and the chains were then combined as a single chain from which results were computed.

2.5. Diversification and morphological evolutionary rates

Here, we explored the relationship between lineage diversification rate and phenotypic evolution rate to test the key innovation hypothesis. The linear relationship between speciation rate and the vertebral count and shape evolutionary rates were tested with the ES-sim test under a Brownian motion model (Harvey and Rabosky, 2018). Similar to BAMM and Bayou, ES-sim runs only on univariate data and continuous traits. We used the $\log_{10}$-transformed number of vertebrae for

vertebral count analysis and we ran the ES-sim test for each PC independently for vertebral shape analysis. Each analysis was run with 1,000 iterations. When a significant relationship was found between speciation and a trait, a regular linear model based on generalized least squares was applied to determine the slope of the regression using the *gls* function from the R-package *nlme*.

3. Results

Hereafter, we present the results of statistical analyses accounting for phylogenetic information. Results from regular statistics, which are congruent with phylogenetic comparative methods, are detailed in the Appendix I of the Supplementary materials. The morphological variance at the species level (*P. phocoena* and *T. truncatus*) is relatively low compared to the disparity of all cetaceans for vertebral shape and count (Table 2.1). Intraspecific variability should not impair our results.

3.1. Number of vertebrae, body size and ecology

While most mammals possess fewer than 70 vertebrae (Narita and Kuratani, 2005), the number of vertebrae constituting the axial skeleton of cetaceans greatly varies, ranging from 42 (*Caperea marginata* and *Inia geoffrensis*) to 97 units (*Phocoenoides dalli*) (Figure 2.2 *b*). Habitat has no significant effect on the number of vertebrae across all cetaceans (phylo-ANOVA: $p = 0.39$, $\eta^2 = 0.08$) but it has a significant effect in oceanic dolphins and porpoises (phylo-ANOVA: $p = 0.01$, $\eta^2 = 0.3$) (Figure 2.3 *a, b*).

Table 2.1. Comparison of intra- and interspecific morphological disparity. Disparity is reported for the entire cetacean clade for two species. The absolute disparity of each group is expressed as Procrustes variance in the first part of the table. The second part of the table shows the results of pairwise comparisons of disparity. Significant *p*-values are in bold. *Diff.*: absolute pairwise differences between variances.

	Vertebral count		**Vertebral shape**	
	Variance		**Variance**	
Cetacea	163.27		0.916	
P. phocoena	18.07		0.293	
T. truncatus	4.26		0.379	
	Diff.	***P*-value**	**Diff.**	***P*-value**
Cetacea *vs P. phocoena*	145.19	**0.009**	0.622	**0.005**
Cetacea *vs T. truncatus*	159.01	**0.023**	0.537	**0.017**
P. phocoena vs T. truncatus	13.81	0.863	0.086	0.731

When considering all cetaceans, species living in rivers, bays, or estuaries are small body sized and possess a relatively low vertebral count, similar to the range observed in terrestrial mammals (Figure 2.2 and Figure S2.1). On the other hand, species living on and off the continental shelf follow two distinct morphological patterns. The first pattern corresponds to large species with a low vertebral count (up to 65), while the second is made of small species (less than 4 meters) with an extremely high number of vertebrae.

All species following the second pattern belong to the closely related families of Delphinidae (oceanic dolphins) and Phocoenidae (porpoises) (Slater *et al.*, 2010; Steeman *et al.*, 2009), both of which significantly differ in body size and vertebral count from the remaining families

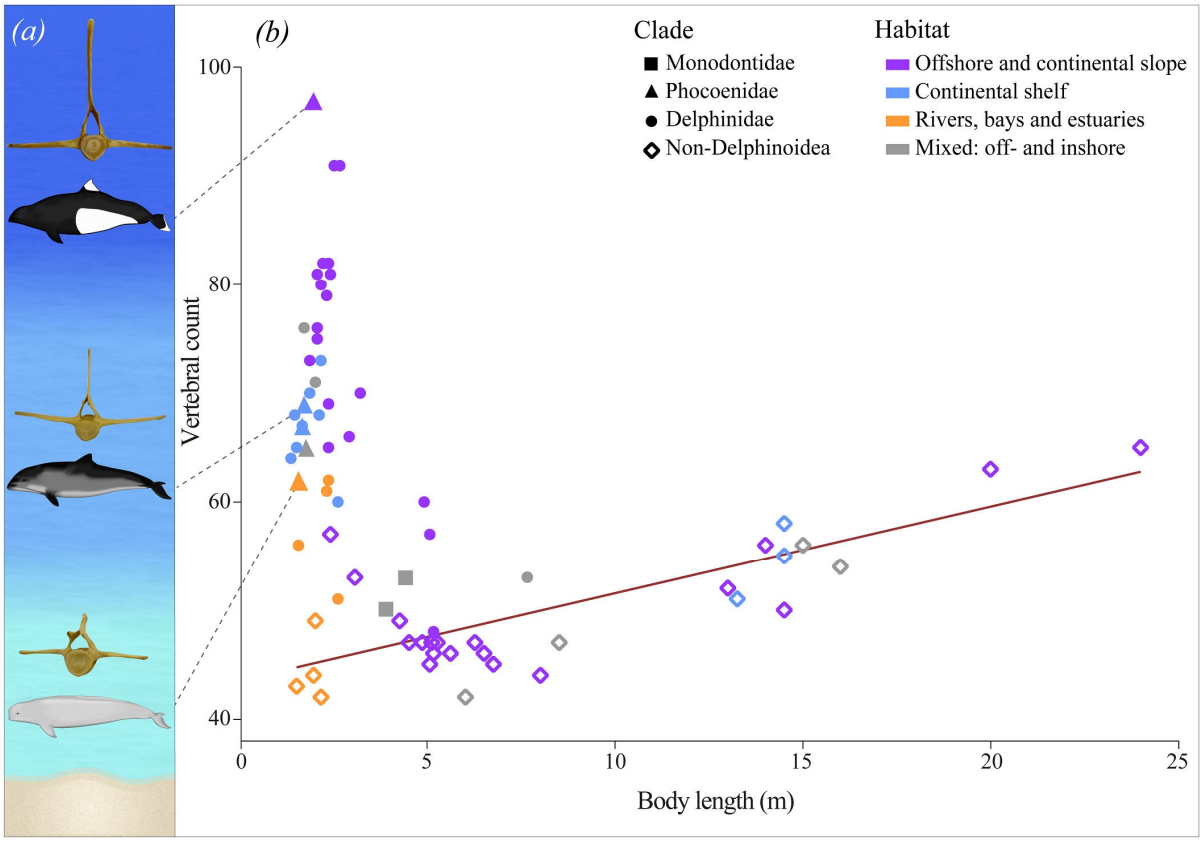

Figure 2.2. Relationship between vertebral count and body size according to habitat. *(a)* Correspondence between vertebral shape and count for three species of porpoises. From top to bottom: Dall's porpoise (*Phocoenoides dalli)*, harbour porpoise (*Phocoena phocoena),* finless porpoise (*Neophocaena phocaenoides*). Light shades of blue correspond to shallow water habitats and darker shades correspond to offshore habitats. *(b)* Vertebral count according to body length for all cetacean species. Symbol shapes correspond to different phylogenetic groups and colours correspond to different habitats. The statistically significant relationship between vertebral count and body length for non-Delphinoidea and Monodontidae based on phylogenetically-corrected linear regression (*pgls*) is represented by the solid grey line.

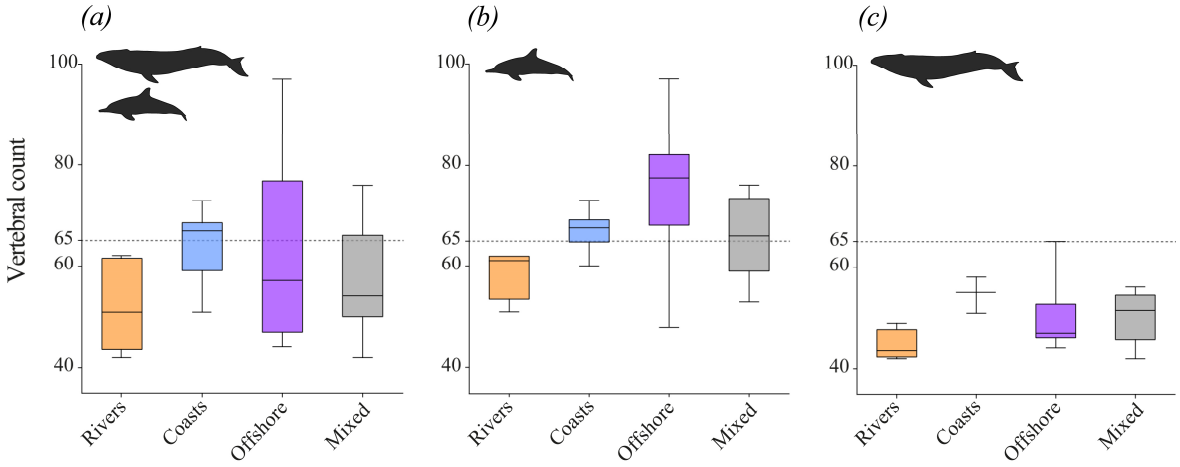

Figure 2.3. Relationship between vertebral count and habitat. Vertebral counts according to habitat for *(a)* all cetaceans, *(b)* Delphinidae and Phocoenidae and *(c)* other cetaceans. For each data set, horizontal line represents the median value, lower and upper limits of boxes represent the 25% and 75% quartiles respectively and lower and upper whiskers represent minimum and maximum values respectively. Non-delphinoids never have more than 65 vertebrae *(c)*.

(phylo-MANOVA: $p = 0.03$, $\eta^2 = 0.69$) (Figure 2.2). In this group, the vertebral count is weakly related to body size (PGLS: $p = 0.04$, $R^2 = 0.14$, slope ± *s.e.* = -4.36 ± 2.00) but is habitat-related. Offshore species have significantly more vertebrae than species living closer to shore (Figure 2.2, Figure 2.3 *b*, Table S2.2and Table S2.3). On the other hand, the vertebral count is not associated with habitat variation in the remaining families (phylo-ANOVA: $p = 0.52$, $\eta^2 = 0.17$), but it is correlated to body size, with approximately eight additional vertebrae per ten metres increase in body length (PGLS: $p < 0.001$, $R^2 = 0.56$, slope ± *s.e.* = 0.80 ± 0.18) (Figure 2.2, Figure 2.3 *c*, Table S2.2 and Table S2.3).

3.2. Morphospace of vertebrae and ecology

In the morphospace approach including all studied cetaceans PC1 accounts for 41% of the total variance. PC1 is mainly associated with the relative length of vertebral centra, width of vertebral processes, and inclination of neural spines (Figure 2.4). PC2 explains almost 21% of the variation and is primarily associated with the length of transverse processes and the height of vertebral centra (Figure 2.4 and Figure S2.2). When considering all cetaceans, vertebral shape is strongly associated with habitat (phylo-MANOVA: $p = 0.001$, $\eta^2 = 0.35$, Table S2.3) and the number of vertebrae (PGLS: $p = 0.001$, $R^2 = 0.31$, Figure 2.2 *a*) but not with body size (PGLS: $p = 0.06$, $R^2 = 0.11$, Table S2.2).

As shown in Figure 2.4, the vertebrae of Delphinidae and Phocoenidae differ in shape from those of other families (phylo-MANOVA: p = 0.02, η^2 = 0.87). Species from these families have shorter vertebral centra, narrower processes, and neural spines with an anterior inclination (Figure 2.4 and Figure S2.2). Based on PC scores of the "Delphinidae and Phocoenidae" PCA, vertebral shape is not correlated to body size (PGLS: p = 0.13, R^2 = 0.05, Table S2.2) but it is strongly associated with the habitat within this group (phylo-MANOVA: p = 0.001, η^2 = 0.46, Table S2.3). In addition to a higher vertebral count, offshore species have shorter vertebral centra and narrower processes than riverine and coastal species (Figure 2.5 *a*).

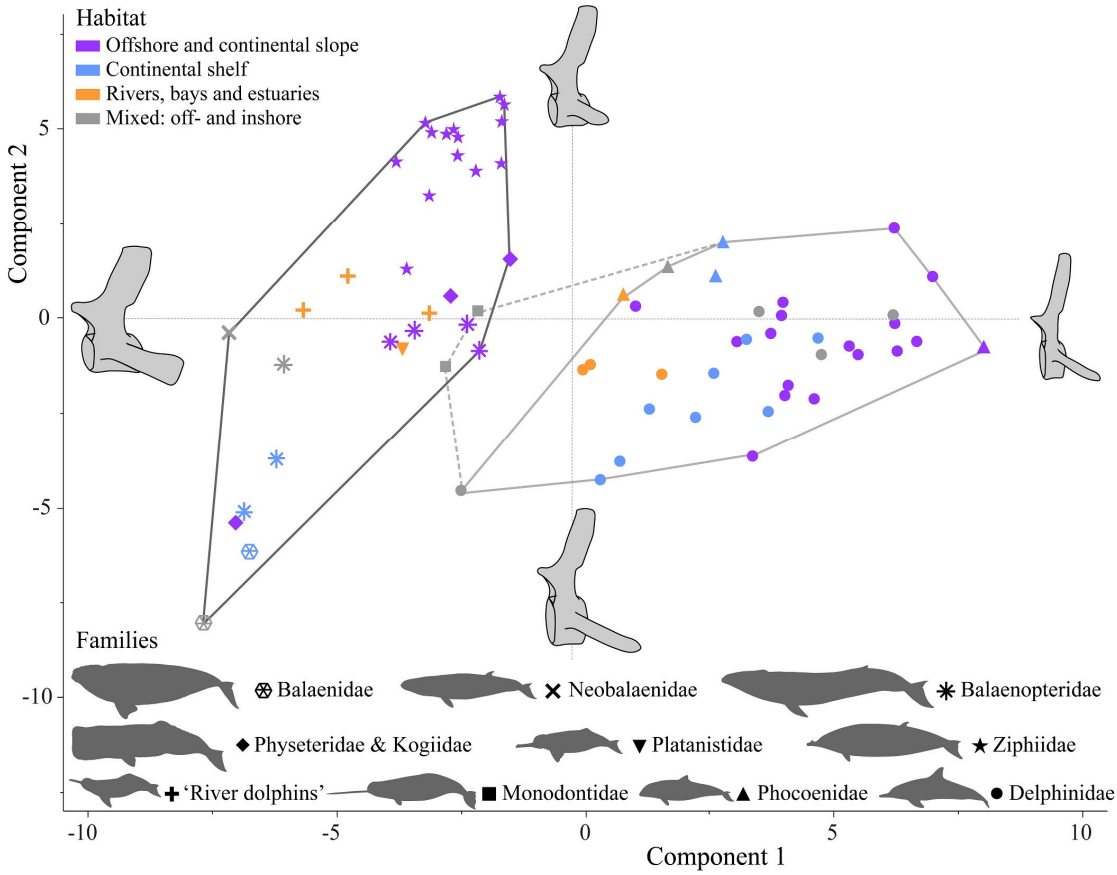

Figure 2.4. Effect of the habitat on the vertebral shape. Principal components analysis plot of PC1 *vs.* PC2 of the PCA calculated on all cetacean species. PC1 accounts for 41% of the total variance and is associated with the relative length of vertebral centra, width of vertebral processes, and inclination of neural spines. PC2 explains 21% of the variation and is primarily associated with the length of transverse processes and the height of vertebral centra. Typical vertebral shapes are shown on each extremity of the axes. Symbol shapes correspond to phylogenetic groups and symbol colours correspond to habitats. Convex hulls represent (1) Delphinidae and Phocoenidae (grey lines) and (2) non-delphinoidean cetaceans (black lines). Dotted grey lines show the inclusion of Monodontidae with Phocoenidae and Delphinidae.

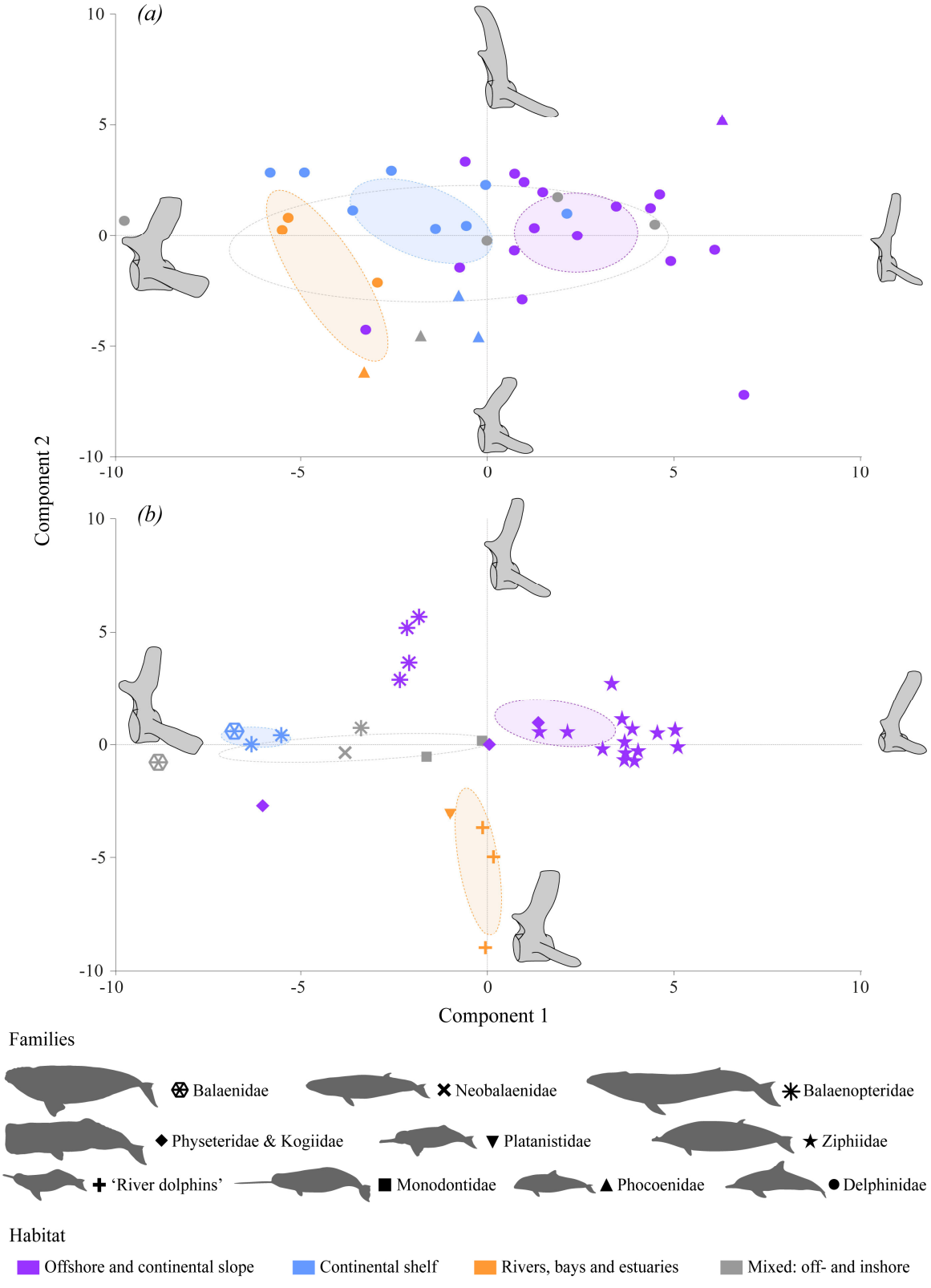

Figure 2.5. Effect of the habitat on vertebral shape. Principal components analysis plot of PC1 *vs.* PC2. Symbol shapes correspond to phylogenetic groups. Symbol colours correspond to different habitats. Dashed ellipses represent the 95% confidence intervals of the mean coordinates for each habitat category. *(a)* Delphinidae and Phocoenidae. PC1: 35% of variance, PC2: 19%. *(b)* All families excluding Delphinidae and Phocoenidae. PC1: 36%, PC2: 17%.

Based on the PCA on the remaining families (i.e., all cetaceans except Phocoenidae and Delphinidae), the vertebral shape of these families is related to the habitat (phylo-MANOVA: p = 0.001, η^2 = 0.62, Table S2.3) and is weakly related to body size (PGLS: p = 0.03, R^2 = 0.11, Table S2.2). However, their habitat-associated shape variation is different from the pattern seen in dolphins and porpoises. Whereas riverine species still differs from other species by having more elongated vertebrae, coastal and offshore species tend to have vertebrae of similar length. Coastal species differs from offshore ones by having higher and wider centra and larger metapophyses (Figure 2.5 *b*).

Concerning the analysis of L/H ratio of modern cetaceans, extant delphinoids have lower L/H ratio (mean ± S.D. = 0.73 ± 0.15), i.e., more discoidal centra, than non-delphinoid odontocetes (1.14 ± 0.18), although there is some overlap. Extant mysticetes cover a range of ratio (0.88 ± 0.20) overlapping with delphinoid and non-delphinoid odontocetes (Figure 2.6). Regarding fossil taxa, mysticetes and stem cetaceans, except *Basilosaurus cetoides,* have ratios between 0.92 and 1.05 and fall within the range of extant non-delphinoids. *Basilosaurus cetoides* has a ratio higher than any other cetacean (L/H = 1.72). Extinct non-delphinoid odontocetes have ratios extending from 1.08 to 1.38 and are similar to extant non-delphinoid odontocetes. *Kentriodon pernix* has a ratio of 1.13, similar to non-delphinoids. The stem delphinoid, *Atocetus iquensis* has a ratio (L/H = 0.88) similar to delphinoids such as the tucuxi (*Sotalia fluviatilis* L/H = 0.84) or the bottlenose dolphin (*Tursiops* spp. L/H = 0.83). The sperm whale (*Physeter macrocephalus,* L/H = 0.68) is the only non-delphinoid having a lower ratio than *Atocetus*. *Albireo whistleri* has a ratio (L/H = 0.63) equivalent to most delphinoids such as the stripped dolphin (*Stenella coeruleoalba* L/H = 0.62) or the Peale's dolphin (*Lagenorhynchus australis* L/H = 0.65).

3.3. Shifts during morphological evolution

The consistent segregation of oceanic dolphins and porpoises from other cetaceans suggests that they might follow a distinct evolutionary pattern. Evolutionary mode and tempo of vertebral count and shape were then investigated using Bayesian multi-rate (BAMM) and multi-regime (Bayou) approaches.

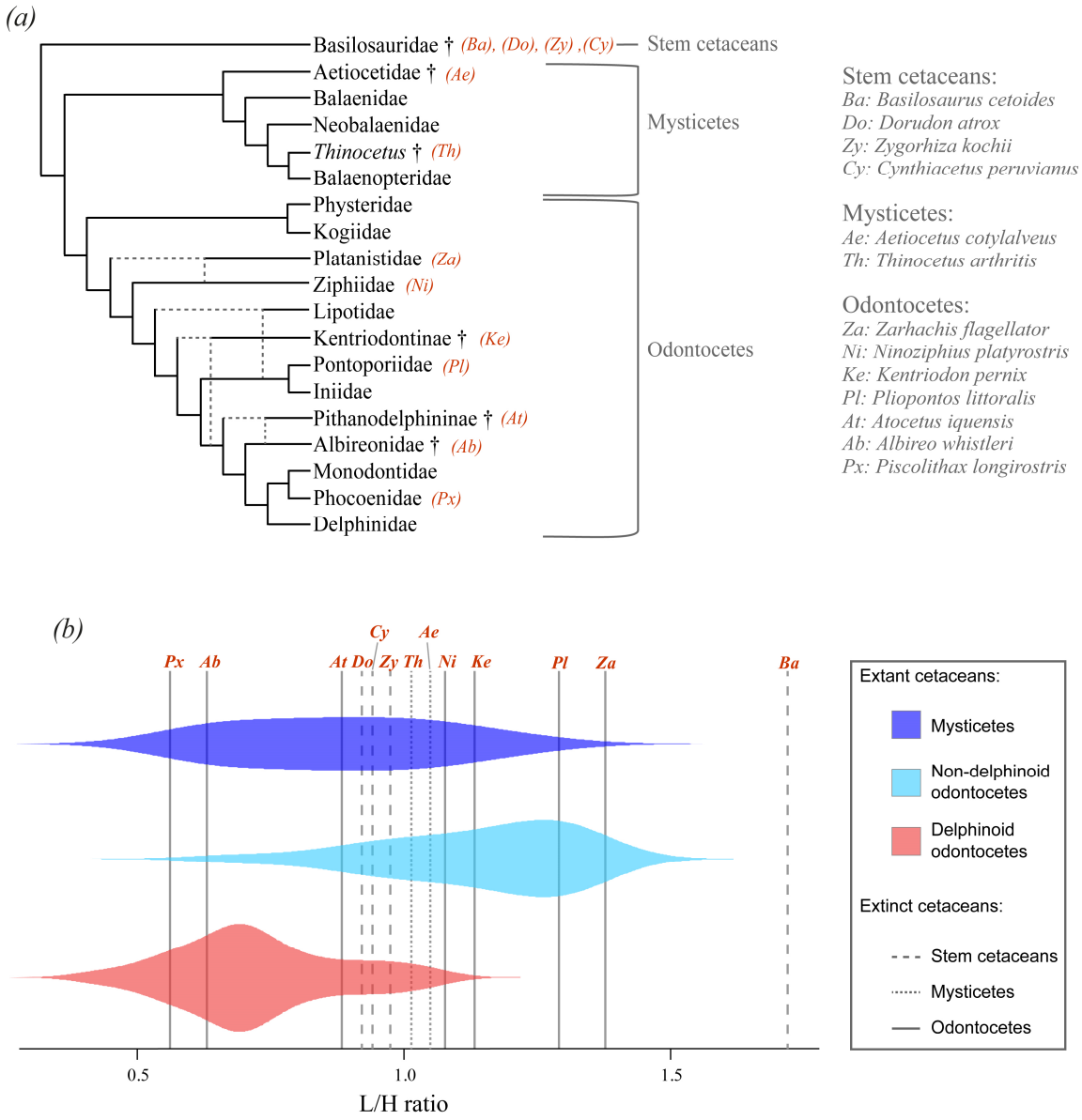

Figure 2.6. L/H ratios of extant and extinct cetaceans. *(a)* Simplified phylogenetic tree of cetaceans including some extinct families and genera (indicated by the dagger symbol) adapted from Marx *et al.* (2016). Dotted lines represent the phylogenetic uncertainty of some lineages. Fossil specimens included in the analysis are annotated in red beside their respective lineage. *(b)* Violin plot of L/H ratios of extant species. L/H ratios of extinct species are represented by vertical lines. The name of the species is annotated in red above its corresponding line. Lower ratios correspond to more discoidal vertebrae and higher ratios correspond to more spool-shaped vertebrae.

For the vertebral count, both BAMM and Bayou showed an evolutionary shift occurring on the branch leading to Delphinoidea, the clade grouping Delphinidae, Phocoenidae and Monodontidae (BAMM marginal shift probability = 0.95, Bayou posterior probability = 0.52) (Figure 2.7 *a, c*). BAMM showed a 10-fold increase of the evolutionary rate on this branch while Bayou found optima of 50 vertebrae for non-Delphinoidea and 67 vertebrae for Delphinoidea. Interestingly, the main shift detected by BAMM for the vertebral shape is on the same branch and correspond to a 5-fold rate increase (PC1: marginal shift probability = 0.68) (Figure 2.7 *b*, see Figure S2.3 for PC2 to PC8). Bayou detected the presence of two shifts rather than one for PC1 (Figure 2.7 *b, d*). One shift is on the branch leading to all Delphinidae except killer whales (*Orcinus orca*) (posterior probability = 0.73) while the second is on the branch supporting Phocoenidae (posterior probability = 0.63). Nonetheless, the respective optimum of Delphinidae and Phocoenidae fall in the same posterior distribution peak reflecting that the two families probably follow a similar evolutionary regime (Figure 2.7 *d*).

This supports the hypothesis that Delphinidae and Phocoenidae differ substantially from other cetaceans. They also suggest some similarities between Monodontidae, Delphinidae, and Phocoenidae, at least concerning their tempo of morphological diversification. Accordingly, we repeated our comparative analyses on the effect of habitat and body size on vertebral count and shape by including monodontids with delphinids and phocoenids (Figure S2.4). The inclusion of these two species did not alter previous statistical results (Table S2.2 and Table S2.3). Cetaceans could thus be divided into two groups in accordance with their distinct mode and tempo of morphological evolution: Delphinoidea and non-Delphinoidea.

Figure 2.7. (Next page). Evolutionary patterns of vertebral count and shape. *(a)* and *(b)* Phylogenetic tree of cetaceans showing tempo of phenotypic trait evolution. Branches are coloured according to the evolutionary rates of phenotypic traits calculated from a Bayesian multi-rate approach (BAMM): *(a)* $\log_{10}$-transformed vertebral count; *(b)* PC1 from the PCA on vertebral shape for all extant cetacean in our dataset. Higher PC1 values correspond to more discoidal vertebrae Red shades correspond to higher evolutionary rates than blue ones. *(c)* and *(d)* Traitgrams showing mode of phenotypic optimum evolution calculated from a Bayesian multi-regime Ornstein-Uhlenbeck approach (Bayou): *(c)* $\log_{10}$-transformed vertebral count; *(d)* PC1 from the PCA on vertebral shape of all cetaceans. Phylogenetic tree tips are plotted according to their phenotypic score and internal nodes according to their estimated state. Branches colours show clades with different evolutionary regimes and coloured arrows correspond to their respective phenotypic optima. Density curves show the posterior distribution of traits optima sampled from 4,000,000 simulations. Orange and blue circles in each panel indicate significant shifts of the evolutionary rate (BAMM) and the phenotypic optima (Bayou) respectively. Circles relative sizes correspond to the posterior probability of the shift. Probable positions of speciation rate increase identified by previous studies are shown by black arrows on *(a)*.

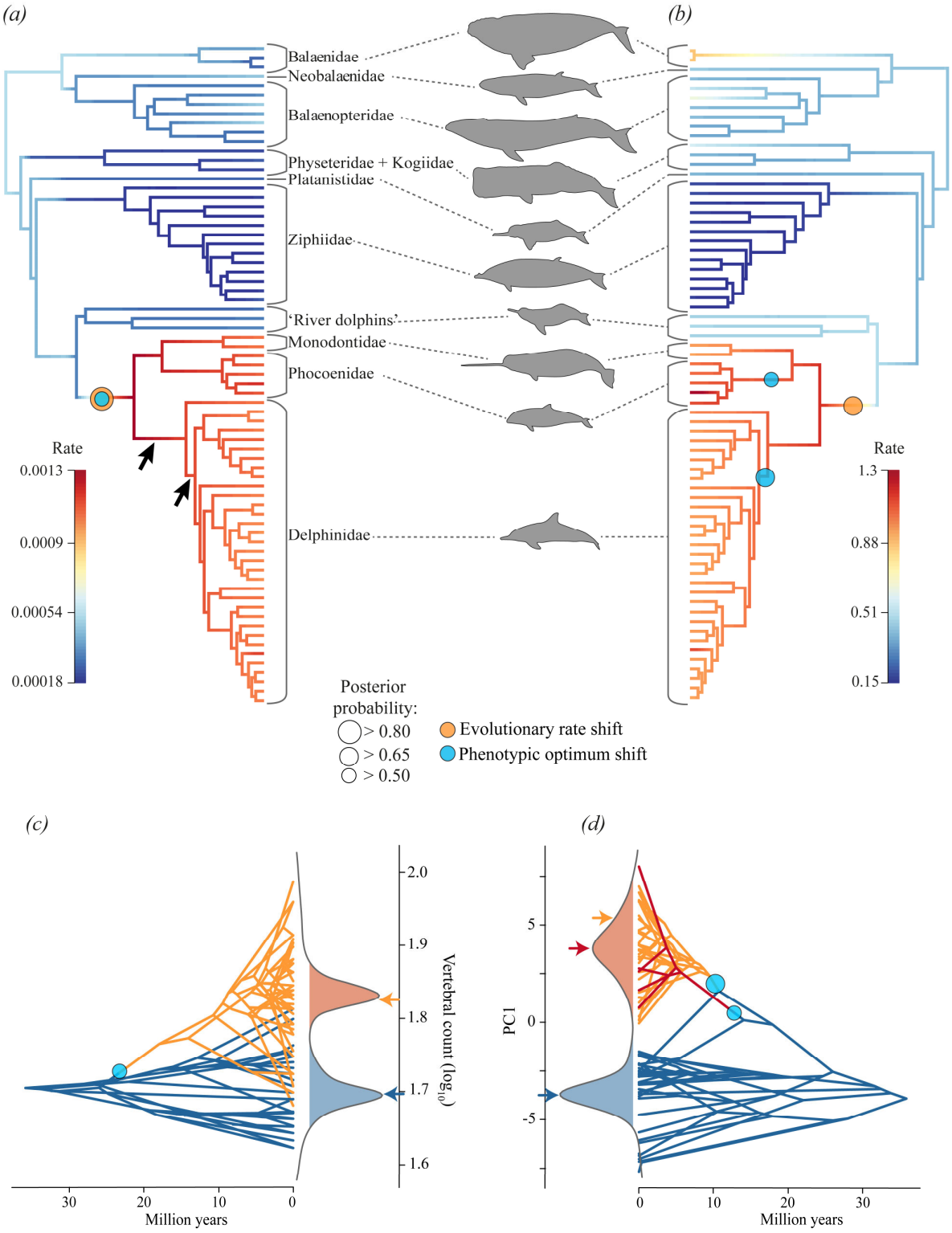
(a)
(b)
Balaenidae
Neobalaenidae
Balaenopteridae
Physeteridae + Kogiidae
Platanistidae
Ziphiidae
'River dolphins'
Monodontidae
Phocoenidae
Delphinidae
Rate
0.0013
0.0009
0.00054
0.00018
Rate
1.3
0.88
0.51
0.15
Posterior probability:
> 0.80
> 0.65
> 0.50
Evolutionary rate shift
Phenotypic optimum shift
(c)
(d)
Vertebral count (log10)
2.0
1.9
1.8
1.7
1.6
30
20
10
0
Million years
PC1
5
0
-5
0
10
20
30
Million years

3.4. Diversification and phenotypic evolutionary rates

The ES-Sim analyses found evidence for a correlation between the rate of lineage diversification and the rates of morphological evolution of the axial skeleton (Vertebral count: $p = 0.03$, $R^2 = 0.37$, slope ± s.e. = 5.02 ± 0.79; Vertebral shape: $p = 0.002$, $R^2 = 0.55$, slope ± s.e. = 0.14 ± 0.02) (Figure 2.8 and Table S2.4).

4. Discussion

Our results show the existence of two distinct evolutionary patterns in modern cetaceans: Delphinoidea and non-Delphinoidea. Vertebral shape varies with habitat in both groups but vertebral count is associated to habitat only in delphinoids. Non-delphinoids retained a low vertebral count similar to terrestrial mammals but exhibit large variation in body sizes, offshore species being larger than estuarine and riverine species (Figure 2.2) (Narita and Kuratani, 2005). On the other hand, Delphinoidea retained a small body size but coastal and offshore species have an extremely increased vertebral count associated with shortening of all vertebrae.

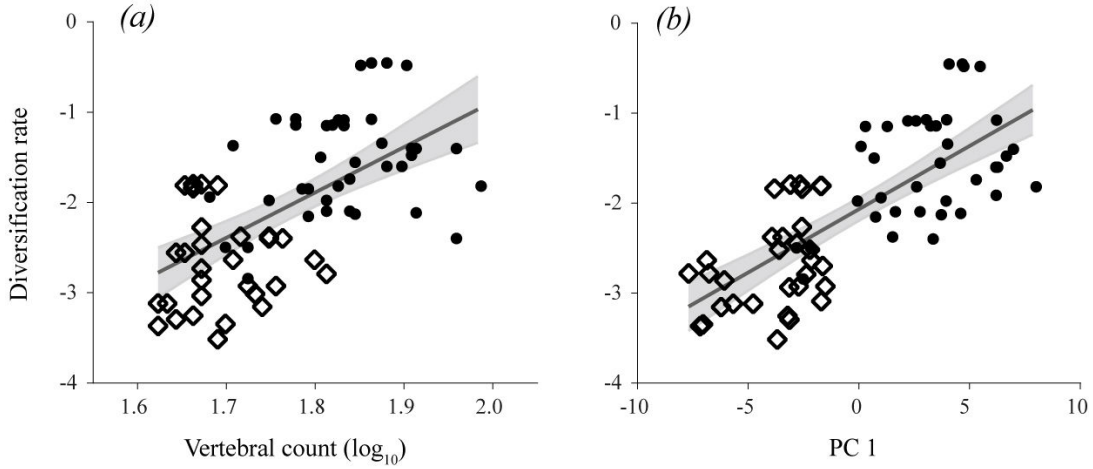

Figure 2.8. Relationship between diversification rate and phenotypic traits. *(a)* $\log_{10}$-transformed vertebral count. *(b)* PC1 scores from the 'all cetaceans' PCA'. Higher PC1 values correspond to more discoidal vertebrae while lower values correspond to more elongated vertebrae. Filled circles represent Delphinoidea while empty diamonds are for non-Delphinoidea. Diversification rates are the log-transformed speciation rates based on equal splits measure as described by Harvey and Rabosky (2018). For both traits, we found a significant correlation with diversification rates. Solid grey lines represent the linear best fit and grey-shaded areas correspond to the 95% confidence intervals.

4.1. Vertebral morphology and biomechanical advantages

Whilst the small body length of riverine non-Delphinoidea allows swimming in shallow and complex habitats, the large body size of their oceanic counterparts might provide various advantages in pelagic habitats (Clauset, 2013; Fish, 1997; Millar and Hickling, 1990; Noren and Williams, 2000; Slater *et al.*, 2010, 2017). For example, the large body size of mysticetes has been linked to higher feeding performances in scattered high density prey patches and better resistance to long travelling distances (Slater *et al.*, 2017). Large body size of sperm whales and beaked whales might also be an adaptation to their deep-diving behaviour (Noren and Williams, 2000). As the ancestor of crown cetaceans had an estimated body weight comparable to extant dolphins, small body size is likely the ancestral condition and gigantism is a derived state (Montgomery *et al.*, 2013). Within non-Delphinoidea, the number of vertebrae increases with body size (Figure 2.2). Although pleomerism has been reported in teleosts and snakes, body size is usually unrelated to vertebral count in mammals (Figure S2.1) (Lindell, 1994; Lindsey, 1975; Muller *et al.*, 2010). As baleen whales reach body sizes greater than any other terrestrial mammal, their pleomerism might reflect functional or developmental limits to vertebral elongation. From a biomechanical point of view, the addition of a few more vertebrae while increasing body length could improve the backbone flexibility needed for foraging, provided that vertebrae remain globally spool-shaped (Segre *et al.*, 2019). Stem cetaceans of the genus *Basilosaurus* reached body sizes comparable to extant mysticetes and possessed 58 to 67 extremely elongated vertebrae (Figure 2.6) (Buchholtz, 2001b; Gingerich *et al.*, 1990; Kellogg, 1936). Their vertebral morphology is clearly atypical among cetaceans and could reflect a specialised ecology.

Conversely, the axial skeleton of Delphinoidea has undergone deep modifications with an extreme increase of the vertebral count in offshore species (Figure 2.2) resulting in vertebrae with a discoidal shape (Figure 2.4 and Figure 2.5 *a*). Such a vertebral shortening provides a stiffer body and restricts swimming oscillations to the posterior third of the body whereas species possessing elongated vertebral centra display undulation of almost the entire body (Buchholtz, 2001b; Long *et al.*, 1997). Body rigidity enhances stability and swimming efficiency and is thus adapted for sustained high-speed swimming styles in opposition to a more flexible body providing higher manoeuvrability (Buchholtz and Gee, 2017; Fish, 2002, 1997; Motani *et al.*, 1996; Weihs, 1993). Vertebral modifications of small delphinoids provide energetic advantages allowing them to cover long distances between scattered

production areas in offshore environments (Bainbridge, 1957; Jacobs *et al.*, 2004). Manoeuvrability, i.e., turning performances, in marine mammals is not only dependent on body flexibility but also on body size and the use of control surfaces (Fish, 1997). Given their small size, offshore dolphins are more manoeuvrable than most large pelagic non-delphinoids likely allowing the exploitation of the same habitat in a different manner.

The pattern of axial skeleton disparity in small delphinoids could be paralleled to sharks and ichthyosaurs. Anguilliform sharks and Early Triassic ichthyosaurs have a slender body and spool-shaped vertebrae whereas thunniform sharks and more derived oceanic ichthyosaurs are deep-bodied and possess more discoidal vertebrae (Buchholtz, 2001a; Motani, 2002; Motani *et al.*, 1996; Thorne *et al.*, 2011). Beyond strong convergences in body and fin shapes (Kelley and Pyenson, 2015; Motani, 2002), cetaceans appear to follow similar vertebral modifications than sharks and ichthyosaurs in accordance with their ecology. Transitions between coastal and offshore waters are a recurrent evolutionary pattern that promoted diversification in various marine organisms such as fishes or cephalopods (e.g., Frédérich *et al.*, 2016; Kröger and Yun-Bai, 2009).

4.2. Key innovation and refining evolutionary shift with the fossil record

An increase of the lineage diversification rate characterizes the evolutionary history of Delphinidae and, to a lesser extent, Phocoenidae (do Amaral *et al.*, 2016; Morlon *et al.*, 2011; Rabosky, 2014; Slater *et al.*, 2010; Steeman *et al.*, 2009). Remarkably, we found that large changes in vertebral morphology also occurred in these clades (Figure 2.7). Moreover, evolutionary rates of these morphological traits are significantly related to diversification rates in cetaceans. Accordingly, we suggest that dolphin backbone modifications acted as a key innovation that allowed small species to occupy a new adaptive zone in offshore waters and thus supported their explosive radiation.

The results of both multi-rate and multi-regime Bayesian methods highly suggest the morphology of Delphinoidea evolved under a different rate of phenotypic diversification and/or through a different phenotypic optimum. However, some uncertainty remains in the position of the morphological evolutionary shift between these two methods. There might either be a single shift on the branch supporting the clade of Delphinoidea, or two distinct shifts occurring later with one on the

branch supporting Delphinidae (except *Orcinus orca*) and another on the branch of Phocoenidae (Figure 2.7).

The L/H ratios analysis shows that all extinct non-delphinoids have higher ratios (i.e., more spool-shaped centra) than most extant delphinoids (Figure 2.6). These data should be interpreted with caution as they rely on a limited number of mostly incomplete fossils and only capture a small portion of vertebral shape variation. Nevertheless, these results are in accordance with previous works that considered that stem cetaceans and extinct mysticetes had a vertebral morphology comparable to extant mysticetes (Buchholtz, 2001b). At equivalent body size, stem cetaceans appear to have more vertebrae than extant mysticetes (Gingerich *et al.*, 1990; Kellogg, 1936; Martínez-Cáceres *et al.*, 2017; Uhen, 2004). For example, *Dorudon atrox* had 65 vertebrae and had an estimated body length of 5.35 meters while most extant beaked whales (*Mesoplodon* spp.) have 45 to 49 vertebrae (Uhen, 2004). However, the vertebral count of stem cetaceans remains lower than 70 and support the hypothesis of a low vertebral count ancestral state for cetaceans.

Medium-sized extinct dolphins *Atocetus* and *Albireo* and the extinct porpoise *Piscolithax* possess a morphology comparable to modern delphinoids (Figure 2.6) (Barnes, 1985b; Buchholtz, 2001b; de Muizon, 1988). According to Barnes, the vertebral count and shape of *Atocetus nasalis* are comparable to those of the bottlenose dolphin (*Tursiops truncatus*) (Barnes, 1985b). Similarly, *Albireo whistleri* has discoidal vertebrae and possesses more pre-caudal vertebrae than most non-delphinoids (Barnes, 2008). Although there is still some uncertainty on the precise phylogenetic position of *Albireo* and *Atocetus*, most phylogenetic analyses identify them as stem delphinoids (Aguirre-Fernández and Fordyce, 2014; Geisler *et al.*, 2012; Murakami *et al.*, 2014). Their morphology and their phylogenetic relatedness with Delphinoidea hence support the hypothesis of a single morphological shift for all delphinoids.

The single shift hypothesis implies that Monodontidae also experienced the morphological shift albeit their backbone is more similar to non-Delphinoidea. Their morphology might be associated to their specialized arctic habitat requiring manoeuvrability or to their large body size. Indeed, larger Delphinidae such as pilot whales (*Globicephala* spp.), killer whales (*Orcinus orca*) and false killer whales (*Pseudorca crassidens*) possess vertebral count and shape more similar to non-Delphinoidea.

Thus, we cannot rule out the possibility that body size could affect the vertebral morphology in Delphinoidea.

Our results highlight the presence of phenotypic evolutionary shift concordant with an increase in the rate of diversification of extant delphinoids. Data from fossil taxa suggest that some stem delphinoids at least also experienced this phenotypic change. Investigating diversity and disparity through time at the family level using total evidence phylogeny could help to infer the precise timing of the evolutionary shift but current morphological and phylogenetic data on fossils prevent such analysis. For example, *Kentriodon pernix* is represented by a well-preserved skeleton composed of approximately 48 spool-shaped vertebrae (Kellogg, 1927) but, depending on the analyses, it is either considered as a stem Delphinida or a stem Delphinoidea (Aguirre-Fernández and Fordyce, 2014; Geisler *et al.*, 2011, 2012; Murakami *et al.*, 2014).

5. Conclusion

Our study reveals that the body size and morphology of the axial skeleton are linked to the ecology of cetaceans. While all species inhabiting rivers, bays, and estuaries are small body sized and have a low vertebral count, other species acquired a morphology adapted for open sea following two distinct evolutionary patterns. The evolution of most oceanic species tended towards an increased body size while retaining a low vertebral count. Conversely, small delphinoids experienced extreme modifications of their axial skeleton morphology. Such a variation in vertebral morphology has been linked to an increased stiffness of the backbone resulting in a more efficient swimming style and allowing small dolphins to maintain a high swimming speed over long distances in offshore waters (Buchholtz, 2001b; Fish, 2002; Long *et al.*, 1997). Our results support the hypothesis that the exceptionally high vertebral count and associated vertebral morphology of Delphinoidea operated as key morphological innovations helping for the adaptation of oceanic dolphins to coastal and offshore environments and leading to their explosive radiation.

Supplementary materials

Contents:

Appendix I: Comparative analyses without phylogenetic correction

1. Material and methods

In order to investigate the raw morphological variation across cetaceans, we repeated all the comparative analyses described in the main text without accounting for phylogenetic information. An identical structure was conserved but all phylogenetically informed analyses were replaced by regular statistics.

(a) Vertebral count and body size

The effect of habitat on the vertebral count was tested using a regular ANOVA with the function *aov* from the R-package *stats* (v.3.5.1) (R Core Team, 2017). We then tested whether Delphinidae and Phocoenidae (i.e., oceanic dolphins and porpoises) differ from the other species in their vertebral count and body size by applying a MANOVA with the *manova* function in R. This analysis was repeated to test such a habitat effect within: *(i)* Delphinidae and Phocoenidae; *(ii)* all species except Delphinidae and Phocoenidae; *(iii)* Delphinoidea; and *(iv)* non-Delphinoidea. The linear relationship between vertebral count and body length was tested for each group by using a generalized least squares regression (GLS analysis) with the *gls* function from the *nlme* package (v. 3.1-131) (Pinheiro *et al.*, 2017).

(b) Morphospace of vertebrae

All linear IMRMs were log10-tranformed and were then size-corrected with a generalised least square regression using the function *gls* (Figure 2.1 *e*). The $\log_{10}$ TCL was used as a proxy for body size for size-correction. Angular IMRMs (i.e., inclination of neural processes and inclination of transverse processes) were not correlated to body size and were thus transformed using a cosine function. Species mean regional measurements (SMRMs) for linear and angular values were then computed by calculating the mean value of residuals of each IMRM of all individuals belonging to the same species (Figure 2.1 *e*). In order to explore morphological variation of vertebrae, we performed a principal component analysis (PCA) on SMRMs of all cetacean species using the *prcomp* function in R. PCA was produced on the correlation matrix because the scales of the different morphological traits vary among them. Four distinct PCAs were also run separately for each group: *(i)* Delphinidae and

Phocoenidae; *(ii)* all species except Delphinidae and Phocoenidae; *(iii)* Delphinoidea; and *(iv)* non-Delphinoidea. According to the Jollife cut-off, only principal components (PCs) with an eigenvalue equal to or higher than 0.7 were conserved for further analysis. This corresponds to the first eight PCs for each PCA except the 'Delphinoidea' PCA for which the first nine PCs were conserved. Differences in vertebral morphology between the group of dolphins and porpoises and other species were tested by a MANOVA. A second MANOVA was used to test for a difference between Delphinoidea and non-Delphinoidea. We used a multivariate linear regression to test the correlation between vertebral count and vertebral shape (Joliffe cut-off PCs) for each PCA, using the *procD.lm* in the R-package *geomorph* (v. 3.0.6) (Adams *et al.*, 2018). For all cetaceans and for every group, we tested the effect of habitat on the variation of vertebral morphology using MANOVAs.

(c) Evolutionary shifts of phenotypic traits and relationships with the rate of diversification

BAMM and Bayou analyses, allowing the detection of evolutionary shifts, were performed on PCs 1 to 8 from the 'all cetacean' PCA that was calculated on non-phylogenetically corrected residuals. Parameters for these analyses were the same as those used for phylogenetically corrected data.

Similarly, the ES-Sim analyses, used to detect the correlation between speciation rate and phenotypic traits evolutionary rates, were performed on non-phylogenetically corrected PCs 1 to 8 with 1,000 iterations. When a significant relationship was found between speciation and a trait, a regular linear model based on generalized least squares was applied to determine the slope of the regression using the *gls* function from the R-package *nlme*.

2. Results

(a) Vertebral count and shape in relation to body size and ecology

Generally speaking, results obtained from non-phylogenetically corrected analyses regarding the relationship between vertebral morphology and body size and ecology were very similar to those obtained with phylogenetic comparative methods. The sole difference was that the correlation between the vertebral count and body size for all cetaceans was significant without the phylogenetic correction (GLS: $p = 0.01$, $R^2 = 0.09$) while it was not when accounting for the effect of phylogeny (pGLS: $p = 0.7$). However, the coefficient of determination was very low, reflecting that the linear regression did not fit well these data. Delphinidae and Phocoenidae differ in body size, vertebral count

and vertebral shape from the other families (MANOVAs: $p \leq 0.0001$). Similarly, Delphinoidea differ in vertebral shape from non-Delphinoidea (MANOVA on PCs1-8: $p \leq 0.0001$). Projections of the first two PCs for each PCA are in Figure S2.5 and Figure S2.6 and statistical results are listed in Table S2.5 and Table S2.6.

(b) Evolutionary patterns of phenotypic traits

When using uncorrected morphological data for phylogenetic information, BAMM found strong support for a shift occurring for the evolutionary rate of PC1 with 72% of simulated trees having one shift. The principal shift sampled in the posteriors was on the branch leading to beaked whales (Ziphiidae) (marginal shift probability: 0.50). However, a shift on one of the branches leading to Delphinoidea was still sampled but with a lower marginal shift probability (0.26) (Figure S2.7). Both these shifts are mutually exclusive meaning that they were never sampled together on the same simulated tree.

Bayou also found support for at least one evolutionary shift for PC1 although the effect was weaker than for phylogenetically-corrected data. Three branches with a posterior probability of having a shift greater than 0.12 (i.e., 15 times greater than the prior probability of 0.008) were sampled. The shift on the branch leading to all Delphinidae except the killer whale (*Orcinus orca*) was still sampled (posterior probability = 0.19) but the shift leading to porpoises (Phocoenidae) was not detected anymore. Only a shift on the terminal branch of the Dall's porpoise (*Phocoenoides dalli*) was sampled (posterior probability = 0.13). In addition, a shift on the branch supporting river dolphins (*Pontoporia, Inia* and *Lipotes* genera) was also detected (posterior probability = 0.16) (Figure S2.6). Results of both BAMM and Bayou for PC2 to 8 obtained from the 'all cetaceans' PCA on non-phylogenetically corrected residuals are shown in Figure S2.8.

The results of the ES-Sim test were very similar to those obtained on phylogenetically corrected data. PC1 scores were significantly correlated to the diversification rate ($p = 0.03$, $R^2 = 0.41$, slope ± *s.e.* = 0.13 ± 0.02) while scores on PCs 2 to 8 were not (see Table S2.7).

3. Discussion

Running analyses without accounting for the non-independence of species did not change the main results about the effect of body size and ecology on vertebral count and shape. Analyses on evolutionary patterns (BAMM, Bayou and ES-Sim) still found an evolutionary shift on one of the branches leading to Delphinoidea for PC1. However, the signal was weaker than for analyses on phylogenetically size-corrected data. This is undoubtedly due to the overlap of Delphinoidea and non-Delphinoidea on PC1 that weakens the observed morphological difference between the two groups. Moreover, both methods highlighted other shifts that were less frequently sampled with phylogenetically corrected data which probably also tend to reduce the signal for a shift of the branch leading to Delphinoidea. Nonetheless, the multivariate analysis of variance (MANOVA) ran on PCs 1 to 8 still returned a significant difference between these two groups. This demonstrates that the morphological difference between Delphinoidea and non-Delphinoidea is still present but might be less pronounced on PC1 when data are not phylogenetically corrected.

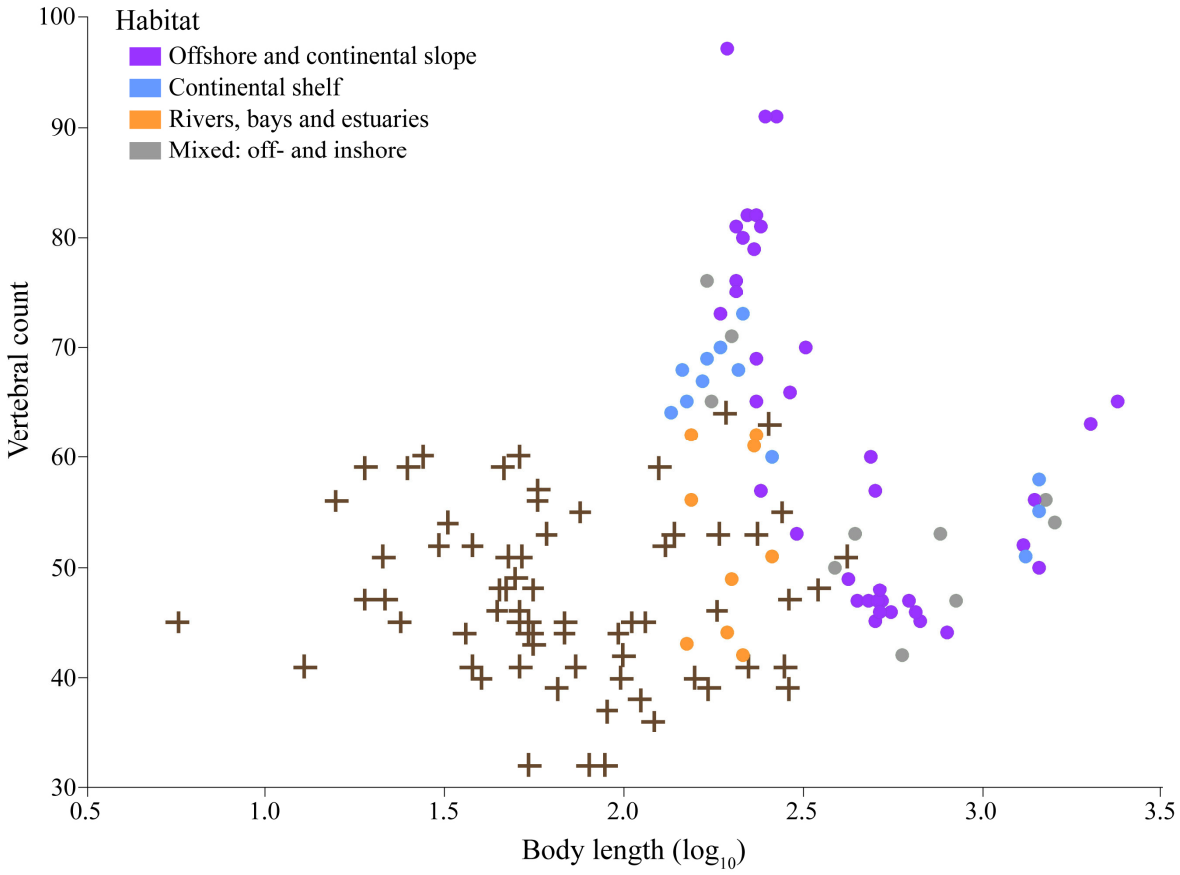

Figure S2.1. Vertebral counts for cetaceans compared to other mammalian lineages. Vertebral count according to body length in meters (log_{10}-tansformed). Filled circles represent cetaceans; 'plus' signs represent other mammals. For cetaceans, symbol colours correspond to different habitats: orange for rivers, bays and estuaries; light blue for continental shelf; purple for continental slope and offshore; and green for mixed off- and in- shore. For non-cetacean species, vertebral counts data are from Narita and Kuratani (2005) and body size data are from the panTHERIA database (Jones *et al.*, 2009).

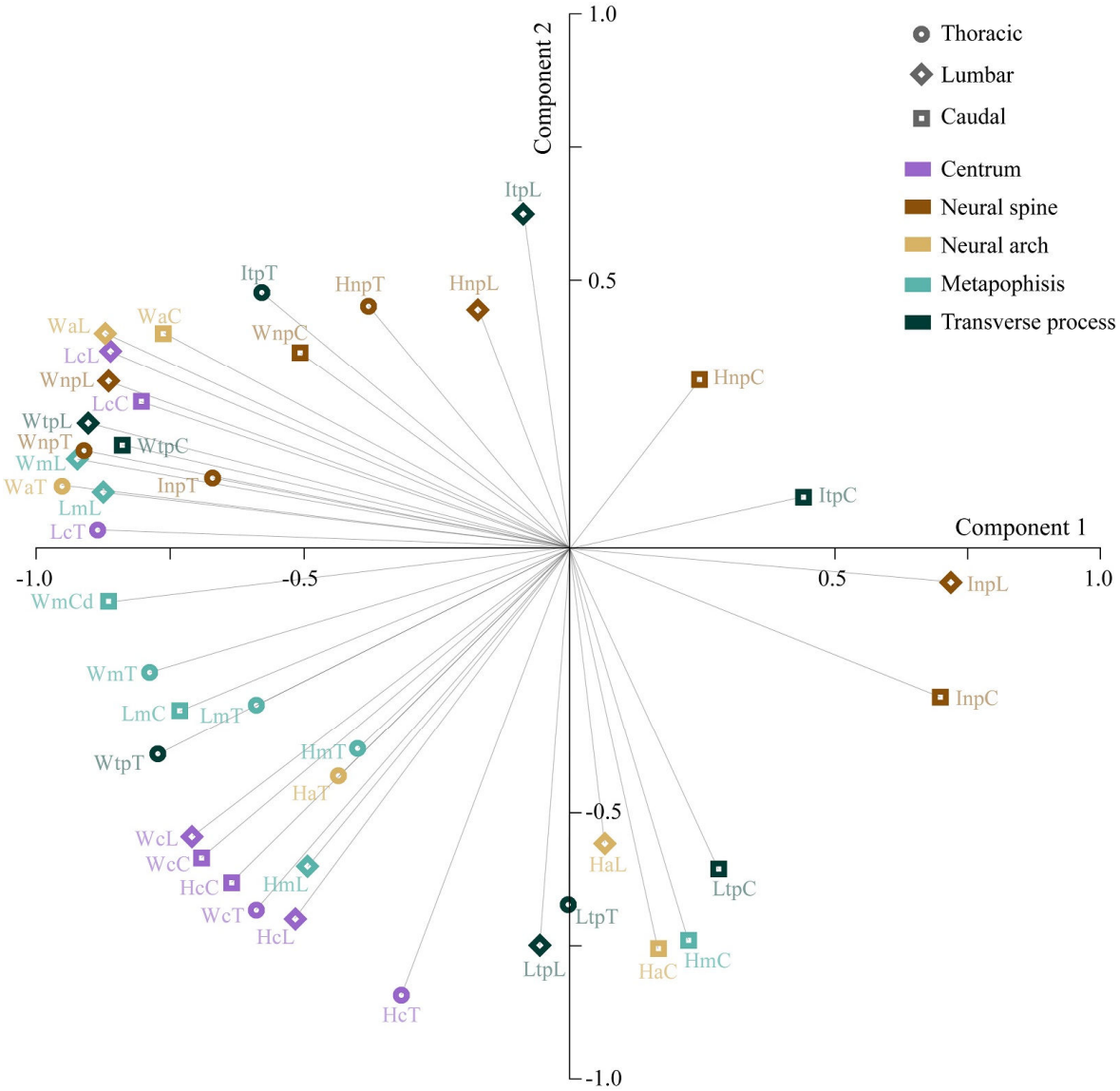

Figure S2.2. Biplot of the principal components analysis. Loadings of variables on PC1 and PC2 for the PCA calculated on all cetacean species (Figure 2.4). Symbol shapes correspond to the regions of the vertebral column. Each colour corresponds to a different part of the vertebra. Variables abbreviations are explained in Figure 2.1.

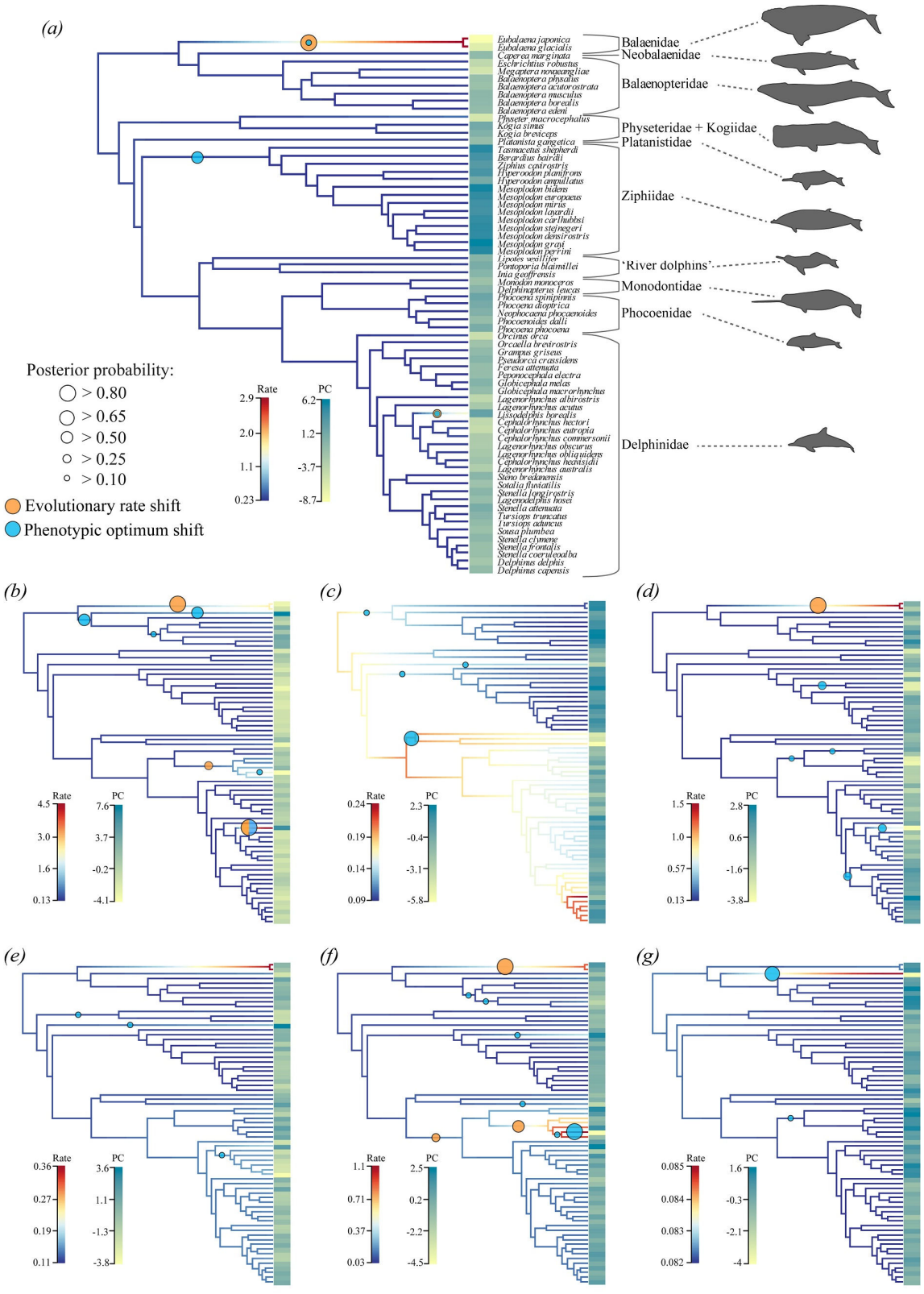

Figure S2.3. Evolutionary patterns of the vertebral shape (PC2 to PC8). Phylogenetic tree of cetaceans with branches coloured according to the evolutionary rates of each principal component from the 'all cetaceans' PCA based on phylogenetically corrected residuals. *(a)* PC2, *(b)* PC3, *(c)* PC4, *(d)* PC5, *(e)* PC6, *(f)* PC7 and *(g)* PC8. Coloured rectangles at trees tips represent species PC score. Orange circles show shifts in evolutionary rates and were calculated with BAMM. Blue circles represent shifts in phenotypic optima and were obtained with Bayou.

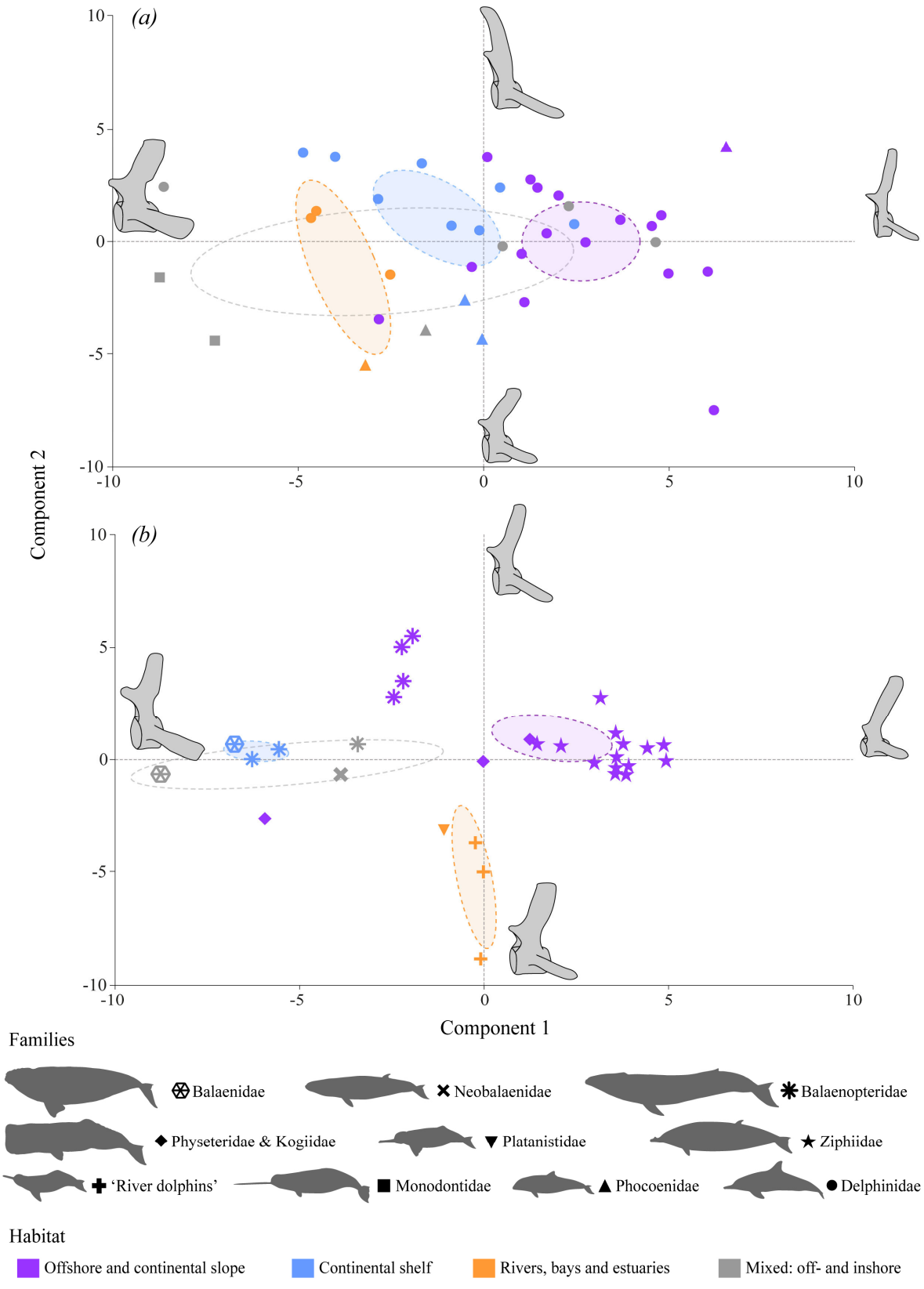

Figure S2.4. Effect of habitat on vertebral shape. Principal components analysis plot of PC1 *vs.* PC2. Symbol shapes correspond to phylogenetic groups. Symbol colours correspond to different habitats. Dashed ellipses represent the 95% confidence intervals of the mean coordinates for each habitat category. *(a)* Delphinoidea. PC1: 37% of variance, PC2: 19%. *(b)* Non-Delphinoidea. PC1: 37%, PC2: 18%.

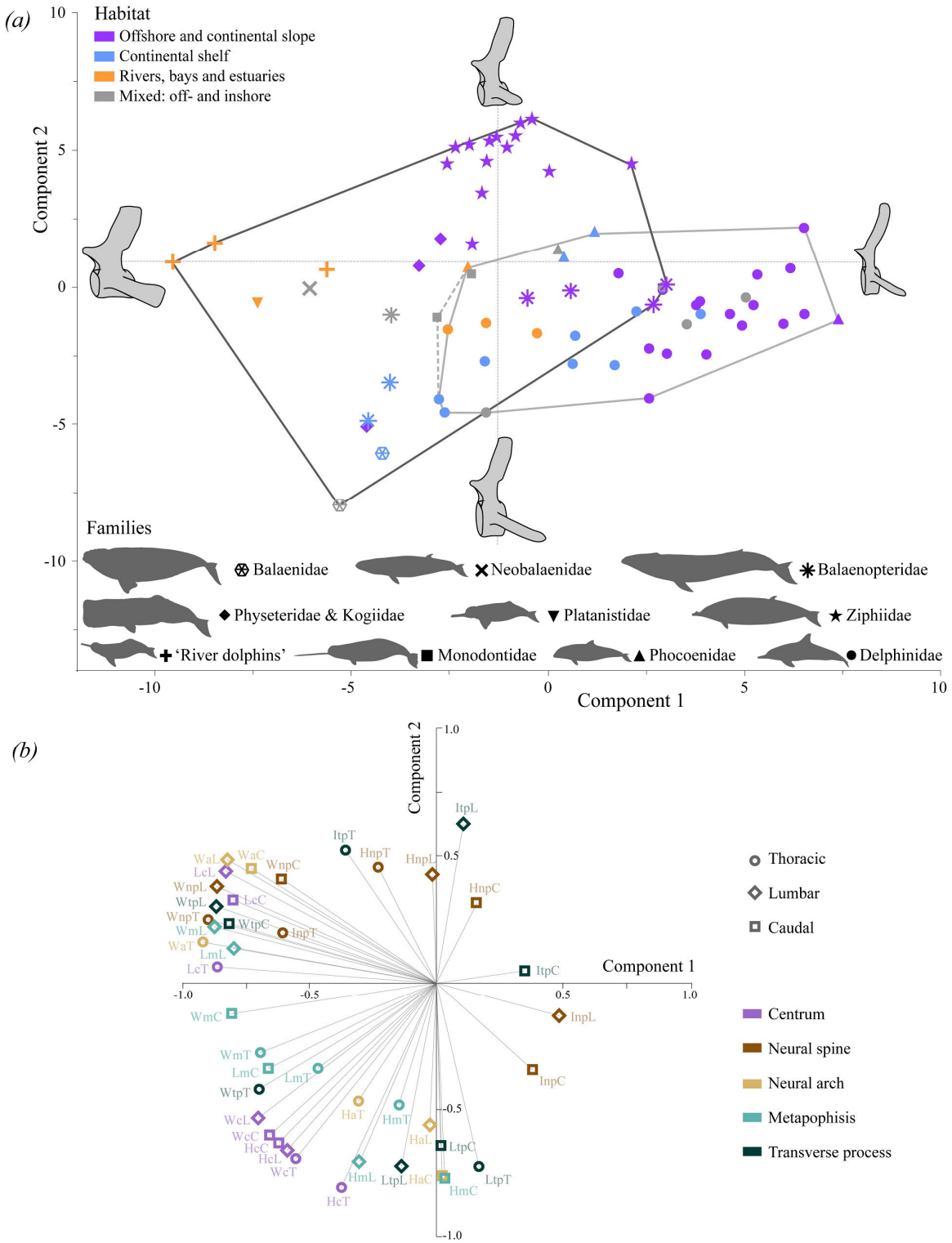

Figure S2.5. Effect of habitat on vertebral shape without phylogenetic correction. *(a)* Projection of species scores on PC1 *vs.* PC2 for the 'all cetaceans' PCA calculated from non-phylogenetically size-corrected residuals. PC1 represents 35% of the variance and PC2 23%. Typical vertebral shapes are shown at each extremity of the axes. Symbol shapes correspond to phylogenetic groups and colours correspond to habitats. Convex hulls represent (1) Delphinidae and Phocoenidae (light grey) and (2) non-delphinoidean cetaceans (dark grey). Dotted lines show the inclusion of Monodontidae with Phocoenidae and Delphinidae. *(b)* Projection of variable loadings on PC1 and PC2. Symbol shapes correspond to regions of the backbone and colours to different parts of the vertebrae.

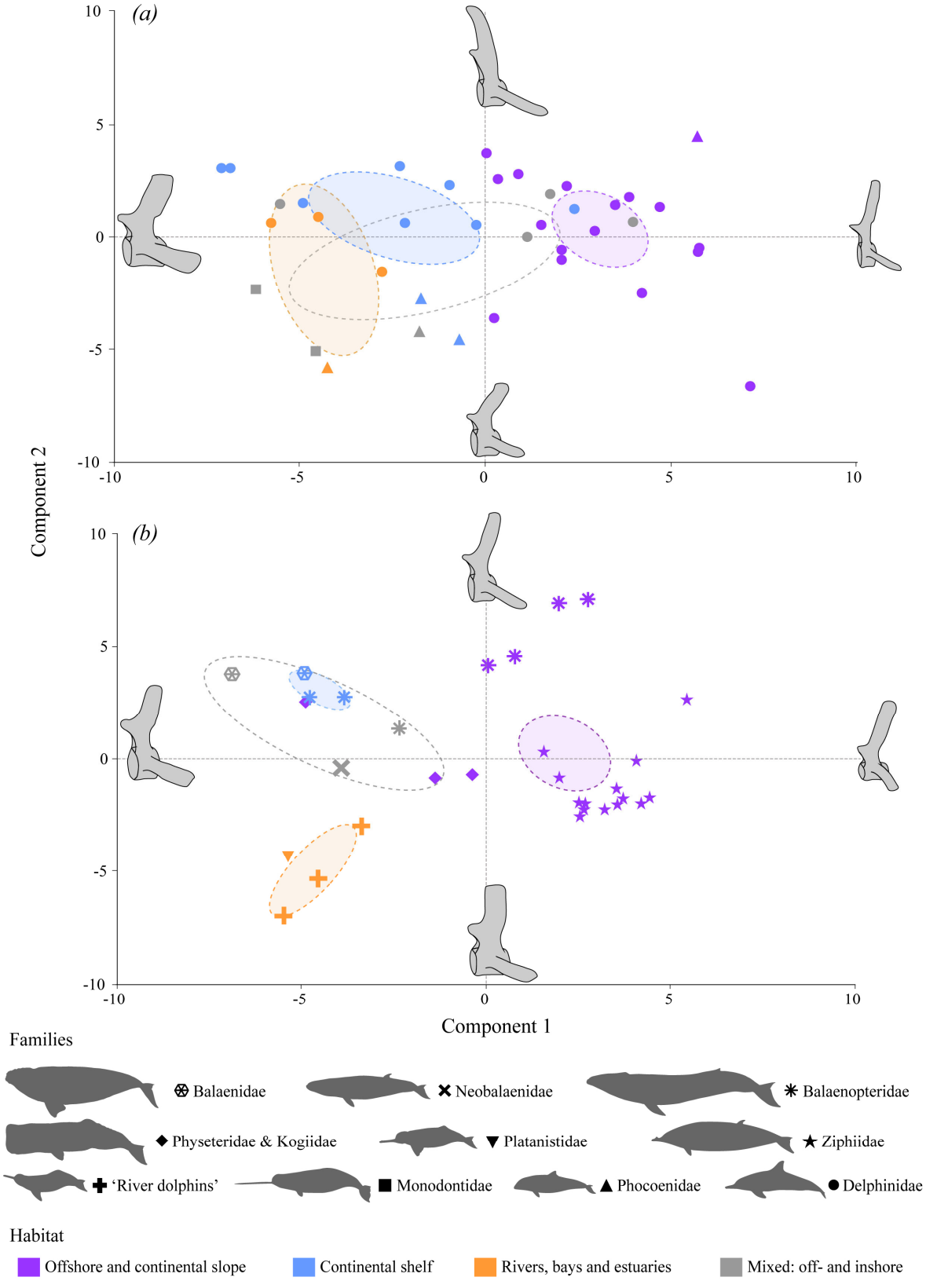

Figure S2.6. Effect of the habitat on vertebral shape without phylogenetic correction. Principal components analysis plot of PC1 *vs.* PC2. Symbol shapes correspond to phylogenetic groups and colours to habitats. Dashed ellipses represent the 95% confidence intervals of the mean coordinates for each habitat category. *(a)* Delphinoidea. PC1: 37% of variance, PC2: 18%, *(b)* non-Delphinoidea. PC1: 34%, PC2: 27%.

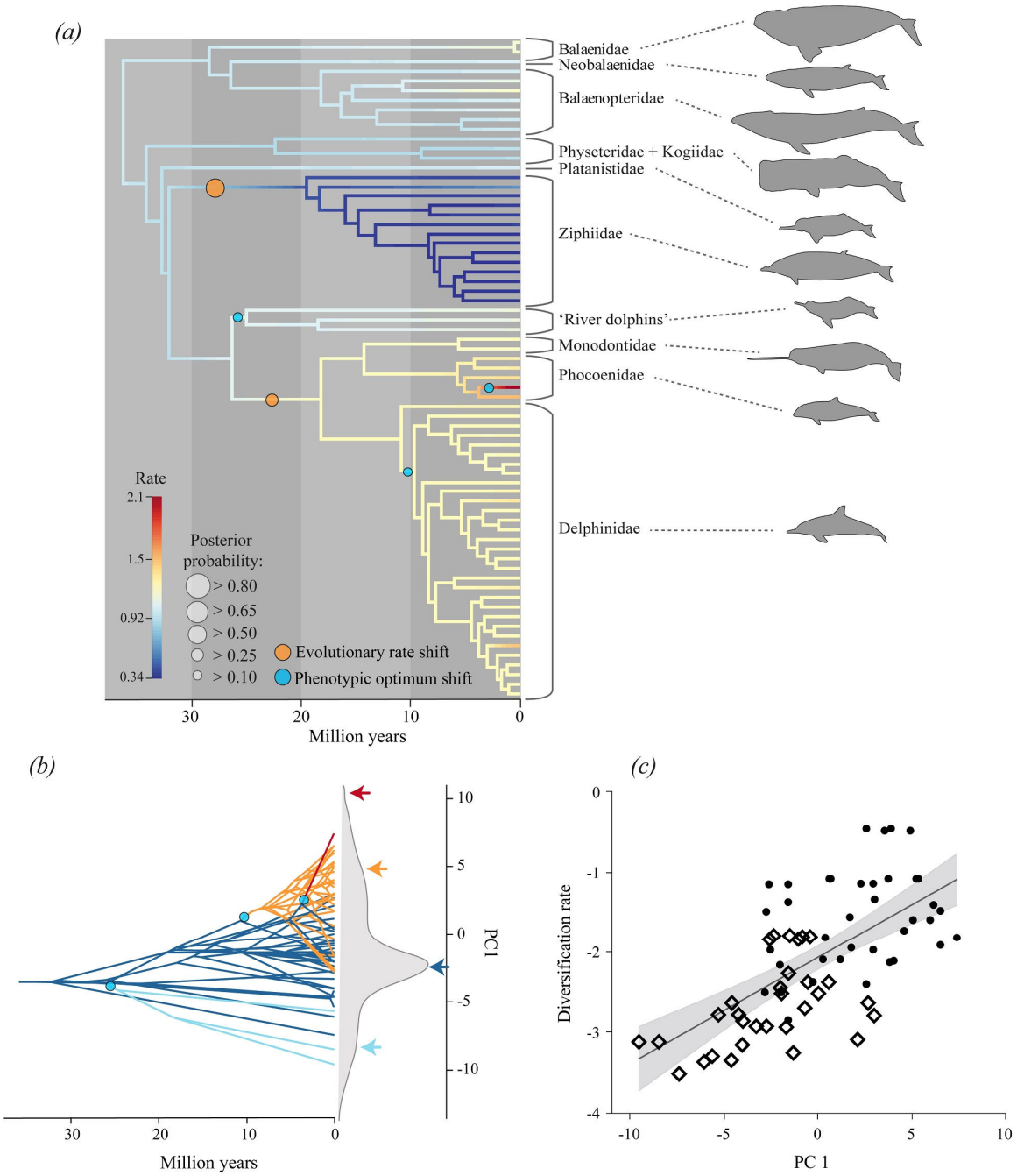

Figure S2.7. Evolutionary patterns of the vertebral shape (PC1) without phylogenetic correction. *(a)* Phylogenetic tree of cetaceans showing the evolutionary rates of PC1 from the 'all cetaceans' PCA on non-phylogenetically corrected residuals. Rates were obtained from a Bayesian multi-rate approach (BAMM). Red shades correspond to higher evolutionary rates. *(b)* Phenogram showing pattern of PC1 evolution calculated from a Bayesian multi-regime Ornstein-Uhlenbeck approach (Bayou). Phylogenetic tree tips are plotted according to their phenotypic score and internal nodes according to their estimated state. Branches colours show clades with different evolutionary regimes and coloured arrows correspond to their respective phenotypic optima. Posterior distribution of traits optima is represented by the grey shaded area. *(c)* Regression between PC1 and diversification rates obtained from the ES-Sim test. The solid grey line represents the linear best fit and the grey-shaded area to the 95% confidence intervals. Orange and blue circles in *(a)* and *(b)* show significant shifts of the evolutionary rate (BAMM) and the phenotypic optima (Bayou) respectively. Circles relative sizes correspond to the posterior probability of the shift. Both evolutionary rate shifts identified on *(a)* are mutually exclusive.

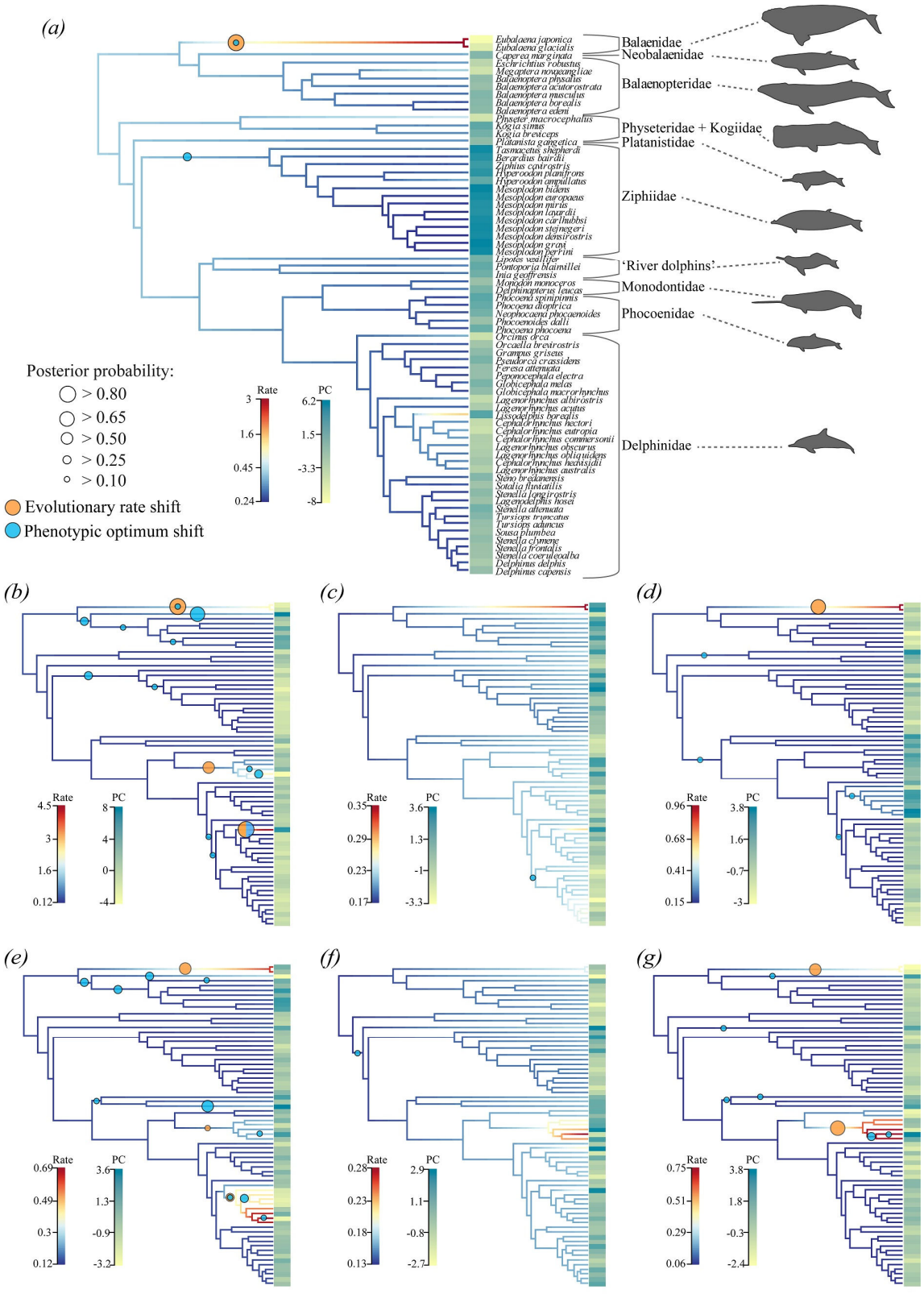

Figure S2.8. Evolutionary patterns of the vertebral shape (PC2 to PC8) without phylogenetic correction. Phylogenetic tree of cetaceans with branches coloured according to the evolutionary rates of each principal component from the 'all cetaceans' PCA based on non-phylogenetically corrected residuals. *(a)* PC2, *(b)* PC3, *(c)* PC4, *(d)* PC5, *(e)* PC6, *(f)* PC7 and *(g)* PC8. Coloured rectangles at trees tips represent species PC score. Orange circles show shifts in evolutionary rates and were calculated from a Bayesian multi-rate approach (BAMM). Blue circles represent shifts in phenotypic optima and were obtained from a Bayesian multi-regime Ornstein-Uhlenbeck approach (Bayou).

Table S 2.1. List of specimens used in this study. Collection numbers of specimens from nine different museums: the American Museum of Natural History, New York (AMNH); the French National Museum of Natural History, Paris (MNHN); the Swedish Royal Museum of Natural History, Stockholm (NRM); the Bayworld Port Elizabeth Museum, Port Elizabeth (PEM); the Queensland Museum, Brisbane (QM); the Royal Belgian Institute of Natural Sciences, Brussels (RBINS); the Iziko South African Museum, Cape Town (SAM); the State Museum of Natural History, Stuttgart (SMNS) and the National Museum of Natural History, Washington D.C. (USNM). For most specimens, both vertebral count and shape data were collected. Specimens on which only vertebral count was collected are marked with 'C', specimens on which only vertebral shape was collected are marked with 'S'.

Balaenidae	
Balaena mysticetus	NRM 558409 C
Eubalaena australis	PEM N0019 C
Eubalaena glacialis	NRM 558386 S
	NRM 558389
	USNM 593893
Eubalaena japonica	USNM 339990 S
Neobalaenidae	
Caperea marginata	RBINS 1536
Balaenopteridae	
Balaenoptera acutorostrata	NRM 558397 S
	USNM 49775
Balaenoptera borealis	NRM 558432
	USNM 236680
Balaenoptera edeni	NRM 558399
	SAM ZM12962 S
	USNM 572922
Balaenoptera musculus	NRM 558430 C
	USNM 124326
Balaenoptera physalus	NRM 558431
	NRM 558434
Eschrichtius robustus	NRM 558391 C
	USNM 593558 S
Megaptera novaeangliae	NRM 558433
	SAM ZM02288
Physeteridae	
Physeter macrocephalus	NRM 558211 S
	NRM 558400 C
	SMNS 26429
	USNM 301634
Kogiidae	
Kogia breviceps	PEM N1862
	PEM N989
	SMNS 7618 S
	USNM 504737
	USNM 572932
Kogia sima	PEM N1564
	PEM N3554
	USNM 504221
	USNM 593890
Platanistidae	
Platanista gangetica	MNHN A7945
	NRM 608417 C
	SMNS 45652 S
	SMNS 45648
	SMNS 45651 S
	SMNS 45653
Ziphiidae	
Berardius bairdii	USNM 49726 S
Hyperoodon ampullatus	NRM 558402
	RBINS 1503
Hyperoodon planifrons	NRM 558395
	SAM ZM41892
Mesoplodon bidens	MNHN A14519
	NRM 558398
	USNM 594220
Mesoplodon carlhubbsi	USNM 504128
Mesoplodon densirostris	USNM 504217
	USNM 550754
	USNM 550951
Mesoplodon europaeus	USNM 550824
	USNM 572952
	USNM 593439
Mesoplodon grayi	PEM N0021
Mesoplodon layardii	PEM N0020
	SAM ZM19931
Mesoplodon mirus	SAM ZM36844
	USNM 504612
	USNM 504724
Mesoplodon perrini	USNM 504260
Mesoplodon stejnegeri	USNM 504731 S
	USNM 550113
Tasmacetus shepherdii	SAM ZM40484
	USNM 484878
Ziphius cavirostris	RBINS 1504
	USNM 347645
	USNM 49599
'River dolphins'	
Inia geoffrensis	MNHN A61
	SMNS 45662
	USNM 395614
	USNM 49582

Lipotes vexillifer	AMNH 57333
Pontoporia blainvillei	SMNS 45597
	USNM 501168
	USNM 501179
	USNM 504920
Monodontidae	
Delphinapterus leucas	MNHN A3246 [S]
	NRM 558404
	RBINS 1508
	USNM 571021
Monodon monoceros	MNHN A3235 [S]
	NRM 558407
	USNM 594407
Phocoenidae	
Neophocaena phocaenoides	SMNS 45679
	SMNS 45680
	SMNS 45681
	USNM 240002
Phocoena dioptrica	USNM 571485
	USNM 571486 [S]
Phocoena phocoena	NRM 558322
	NRM 805026
	NRM 815072
	NRM 835011
	NRM 845002
	NRM 855083
	NRM 855196
	NRM 865039 [C]
	NRM 865044
	NRM 875045
	NRM 875216
	NRM 875358 [C]
	NRM 895156
	NRM 20065226
	RBINS 16233 [C]
	USNM 550312
	USNM 571709
Phocoena spinipinnis	USNM 395751
	USNM 550782
	USNM 550785 [S]
Phocoenoides dalli	USNM 396304
	USNM 504417
	USNM 504969
Delphinidae	
Cephalorhynchus commersonii	SAM ZM40555
	USNM 550154
	USNM 550156
Cephalorhynchus eutropia	NRM 616647
	USNM 395374
Cephalorhynchus heavisidii	SAM ZM 0014
	SAM ZM19943
	SAM ZM36717 [S]
Cephalorhynchus hectori	SAM ZM36182
	USNM 500864
Delphinus capensis	PEM N1649
	SMNS 45763 [S]
Delphinus delphis	NRM 805172
	RBINS 1519B
	USNM 500273
	USNM 593770
Feresa attenuata	PEM N4762 [S]
	PEM N4763
	SMNS 8841
	USNM 571268
Globicephala macrorhynchus	USNM 22561 [S]
	USNM 593641
Globicephala melas	NRM 558264
	USNM 21118
Grampus griseus	MNHN A3248
	NRM 558392 [C]
	PEM N117 [S]
	USNM 347613
	USNM 504328
Lagenodelphis hosei	PEM N395
	PEM N827 [S]
	USNM 571619
Lagenorhynchus acutus	USNM 504153
	USNM 504154
	USNM 504164
Lagenorhynchus albirostris	NRM 20065395
	SMNS 7591
	USNM 550208
Lagenorhynchus australis	USNM 395347
	USNM 395350
Lagenorhynchus obliquidens	USNM 504412 [S]
	USNM 504413
	USNM 504415
Lagenorhynchus obscurus	SAM ZM41890 [S]
	SAM ZM35681
Lissodelphis borealis	USNM 484929
	USNM 550026
Lissodelphis peronii	NRM 558419 [C]
Orcaella brevirostris	RBINS 1512
Orcaella heinsohni	QM JM511 [C]
Orcinus orca	MNHN A3231 [S]
	NRM 558250 [S]
	NRM 558251
	NRM 558401
Peponocephala electra	SAM ZM38245
	USNM 550399
	USNM 593799
	USNM 593941 [S]

Pseudorca crassidens	NRM 558271 [S]
	NRM 558405
	QM J14210
	SMNS 7617
Sotalia fluviatilis	RBINS 1516
	RBINS 20137
	USNM 571558
Sousa plumbea	PEM N1179
	PEM N1266
	PEM N1582 [S]
	PEM N1593
	USNM 550939
Stenella attenuata	USNM 395390
	USNM 396028
	USNM 500122
Stenella clymene	USNM 550501
	USNM 550511
	USNM 550532
Stenella coeruleoalba	PEM N289 [S]
	USNM 504350
	USNM 504384
Stenella frontalis	USNM 21915
	USNM 22017
	USNM 504321
Stenella longirostris	PEM N1278 [S]
	USNM 395414
	USNM 500017
Steno bredanensis	SAM ZM41124
	USNM 504462
	USNM 504468
Tursiops aduncus	SAM ZM38240
	SMNS 45711 [S]
Tursiops truncatus	SAM ZM35678 [S]
	USNM 484529
	USNM 504618
	USNM 504726 [S]
	USNM 504906 [S]
	USNM 550225
	USNM 550364
	USNM 550422
	USNM 550852
	USNM 571388
	USNM 572831

Table S2.2. Effect of body size on vertebral count and shape. The table shows the comparison of the effect of body size on vertebral count and shape when excluding or including Monodontidae with Delphinidae and Phocoenidae. Significant values are indicated in bold.

Test	n	*P*-value	R^2	Slope ± *s.e.*
Effect of body size on vertebral count (PGLS)				
All cetaceans	71	0.7	-0.35	-0.27 ± 0.69
Delphinidae and Phocoenidae	38	**0.04**	0.14	-4.36 ± 2.00
Other cetacean families	33	**< 0.001**	0.56	0.80 ± 0.18
Delphinoidea	40	**0.03**	0.19	-4.51 ± 1.93
Non-Delphinoidea	31	**< 0.001**	0.61	0.80 ± 0.17
Effect of body size on vertebral shape (multivariate PGLS)				
All cetaceans	71	0.06	0.11	/
Delphinidae and Phocoenidae	38	0.13	0.05	/
Other cetacean families	33	**0.03**	0.11	/
Delphinoidea	40	0.07	0.06	/
Non-Delphinoidea	31	**0.04**	0.11	/

Table S2.3. Effect of habitat on vertebral count and shape. The table shows the comparison of the analysis of variance tests when excluding or including Monodontidae with Delphinidae and Phocoenidae. Significant values are indicated in bold. *n*: number of species, *df*: degrees of freedom, *F*: F-value, *P*: *P*-value, η^2: effect size (eta-squared), ω^2: effect size (omega-squared).

Test	n	df	F	P	η^2	ω^2
Effect of habitat on vertebral count (pANOVA)						
All cetaceans	71	3,67	1.87	0.39	0.08	0.04
Delphinidae and Phocoenidae	38	3,34	4.86	**0.01**	0.30	0.24
Other cetacean families	33	3,29	2.05	0.52	0.17	0.09
Delphinoidea	40	3,36	5.8	**0.02**	0.33	0.27
Non-Delphinoidea	31	3,27	1.9	0.53	0.17	0.08
Effect of habitat on vertebral shape (pMANOVA)						
All cetaceans	69	3,65	4.96	**0.001**	0.35	/
Delphinidae and Phocoenidae	36	3,32	3.03	**0.001**	0.46	/
Other cetacean families	33	3,29	6.15	**0.001**	0.62	/
Delphinoidea	38	3,34	2.44	**0.009**	0.40	/
Non-Delphinoidea	31	3,27	6.99	**0.001**	0.62	/

Table S2.4. Correlations between diversification rate and morphological traits. The ES-sim test was run with 1,000 iterations on vertebral count and on each principal component (PC) of the PCA applied on all cetacean species. Significant values are indicated in bold. Slope was only calculated for significant correlations.

Variable	**n**	***P*-value**	**R^2**	**Slope ± *s.e.***
Vertebral count	71	**0.030**	0.367	5.02 ± 0.79
PC1	69	**0.002**	0.553	0.14 ± 0.02
PC2	69	0.923	0.002	/
PC3	69	0.675	0.033	/
PC4	69	0.701	0.026	/
PC5	69	0.697	0.043	/
PC6	69	0.777	0.019	/
PC7	69	0.813	0.016	/
PC8	69	0.999	0.0001	/

Table S2.5. Effect of body size on vertebral count without phylogenetic correction. The table shows the comparison of the effect of body size on vertebral count when excluding or including Monodontidae with Delphinidae and Phocoenidae. Significant values are indicated in bold.

Test	n	*P*-value	R^2	Slope ± *s.e.*
Correlation between vertebral count and body size (GLS)				
All cetaceans	71	**0.01**	0.09	-0.81 ± 0.32
Delphinidae and Phocoenidae	38	**0.01**	0.15	-3.47 ± 1.35
Other cetacean families	33	**< 0.0001**	0.57	0.75 ± 0.12
Delphinoidea	40	**0.003**	0.21	-4.08 ± 1.30
Non-Delphinoidea	31	**< 0.0001**	0.61	0.79 ± 0.12

Table S2.6. Effect of habitat on vertebral count and shape without phylogenetic correction. The table shows the comparison of the analysis of variance tests when excluding or including Monodontidae with Delphinidae and Phocoenidae. Significant values are indicated in bold. *n*: number of species, *df*: degrees of freedom, *F*: F-value, *P*: *P*-value, η^2: effect size (eta-squared), ω^2: effect size (omega-squared).

Test	n	df	F	*P*	η^2	ω^2
Effect of habitat on vertebral count (ANOVA)						
All cetaceans	71	3,67	1.87	0.143	0.08	0.04
Delphinidae and Phocoenidae	38	3,34	4.86	**0.006**	0.30	0.24
Other cetacean families	33	3,29	2.05	0.129	0.17	0.09
Delphinoidea	40	3,36	5.80	**0.002**	0.33	0.27
Non-Delphinoidea	31	3,27	1.90	0.153	0.17	0.08
Effect of habitat on vertebral shape (MANOVA)						
All cetaceans	69	3,65	4.52	**< 0.001**		/
Delphinidae and Phocoenidae	36	3,32	2.84	**< 0.001**		/
Other cetacean families	33	3,29	6.15	**< 0.001**		/
Delphinoidea	38	3,34	2.44	**0.002**		/
Non-Delphinoidea	31	3,27	6.99	**< 0.001**		/

Table S2.7. Correlations between diversification rate and morphological traits without phylogenetic correction. The ES-sim test was run with 1,000 iterations on each principal component (PC) of the 'all cetaceans' PCA applied on non-phylogenetically corrected residuals. Significant values are indicated in bold. Slope was only calculated for significant correlations.

Variable	n	*P*-value	R^2	Slope ± *s.e.*
PC1	69	**0.030**	0.408	0.13 ± 0.02
PC2	69	0.757	0.014	/
PC3	69	0.470	0.085	/
PC4	69	0.448	0.107	/
PC5	69	0.857	0.015	/
PC6	69	0.685	0.042	/
PC7	69	0.903	0.0002	/
PC8	69	0.929	0.001	/

Chapter 3 :
Evolutionary patterns of delphinoid backbone morphology at inter- and intraspecific levels

Abstract

Extant cetacean species possess different vertebral morphologies that are related to the occupation of different kinds of habitats (including riverine, coastal and offshore waters). Interestingly, the same kind of relationship between habitat and morphology seems also to take place at the intraspecific level. These apparent similar ecological specialisations within and between species provide an interesting framework to compare ecomorphological patterns at the macro- and microevolutionary levels. Do the morphotypes always undergo the same kind of modifications according to habitat? Can we consider that the ecomorphological variability within a species can prefigure the morphology of future new species? In this work we investigate the evolutionary history of the delphinoid clade to test whether habitat-related morphological modifications are similar between and within species and to assess the importance of ecological transitions during their evolution. To this purpose, we quantified and compared the vertebral morphology among Delphinidae (oceanic dolphins) and Phocoenidae (porpoises) to investigate the macroevolutionary level and we compare the morphology of coastal and offshore ecotypes of Northwest Atlantic Ocean bottlenose dolphins (*Tursiops truncatus*) to investigate the microevolutionary level. We also modelled and quantified the number of habitat shifts during delphinoid evolution to investigate its frequency. Our results demonstrate that Phocoenidae and Delphinidae experienced numerous ecological transitions during their evolutionary history. The vertebral modifications associated to these ecological transitions are so important that they can be used to predict the ecology of an unknown specimen or species. Oceanic dolphins and porpoises have clearly distinct vertebral morphologies and follow slightly different phenotypic trajectories along the river-coast-offshore ecological gradient which might be related to their different evolutionary histories. Interestingly, morphological modifications between coastal and offshore bottlenose dolphin ecotypes are similar in direction and magnitude to those observed in the entire delphinid family. This further supports the hypothesis that delphinoid ecotypes reflect ongoing ecological speciation processes and that ecological specialisation played a central role in delphinoid evolutionary history both below and above the species level.

1. Introduction

One of the major aims of evolutionary biology is to understand and identify factors underlying organismic diversity and disparity. Morphological variability can be studied both at the intraspecific and interspecific levels. However, the question whether diversification patterns observed at the species level can be explained by the variation observed at the intraspecific level is still debated (Arnold *et al.*, 2001; Grantham, 2007; Simons, 2002). In other words, can macroevolutionary patterns be predicted by microevolutionary patterns? Only a few empirical studies have focused on evolutionary processes at various levels but some of them highlighted that macroevolutionary patterns could be explained and predicted, at least in part, by microevolutionary processes (Hulsey *et al.*, 2006; Pointer and Mundy, 2008; Rolland *et al.*, 2018). For instance, comparisons of molecular, phenotypic and ecological traits of clownfishes (Pomacentridae) at the inter- and intraspecific levels using phylogenetic comparative methods have demonstrated that macroevolutionary patterns can be partially predicted from microevolutionary patterns showing selective pressures can act in the same way regardless of the taxa level (Rolland *et al.*, 2018).

At the intraspecific level, divergent ecological specialisation of populations can sometimes trigger the process of speciation, termed ecological speciation (Mayr, 1947; Schluter, 2001). Speciation is a continuous process ranging from uniform variation within a species to increasing phenotypic and genotypic divergence between populations, resulting in reproductive isolation between the newly formed sister species (e.g., Clausen, 1951; Nosil *et al.*, 2009; Schluter, 2000). In this framework, ecotypes correspond to populations differing from each other by variation of several traits in response to divergent environmental conditions and are considered as one of the stages that can result in speciation (Clausen, 1951; Dobzhansky, 1951; Lowry, 2012; Nosil *et al.*, 2009; Turesson, 1922). For instance, the stick insects *Timema cristinae* possess two ecotypes corresponding to two different host plants. The ecotypes differ in a suite of traits including colour, colour pattern, body size, and body shape. However, reproductive isolation between the *T. cristinae ecotypes* is incomplete implying that speciation has not occurred. The same series of morphological adaptations occur within *Timema podura* which is the allopatric, sister species of *T. cristinae*. Complete isolation between these two species was attained by combining differentiation of morphological and physiological traits adapted to their host plant. In other words, ecotypes of parent species most probably evolved from different

selection on niche dimension. Morphological ecotypes within each species are therefore considered as intermediate stages of speciation (Nosil, 2007; Nosil and Sandoval, 2008).

Cetaceans exhibit a wide variability in their backbone morphology which is linked to their ecology along a rivers-coasts-offshore habitat gradient (chapter 2; Gillet *et al.*, 2019). Shallow-waters species are characterised by a small body size and low count of elongated vertebrae while species living in deeper waters either retained a low vertebral count with a large body size (i.e., baleen whales, sperm whales, beaked whales) or retained a small body having an extremely high number of discoidal vertebrae (i.e., porpoises and oceanic dolphins). In addition to specific habitat specialisation, population partitioning related to ecological preferences has also been described for several cetaceans such as killer whales (*Orcinus orca*) (de Bruyn *et al.*, 2013; Dahlheim *et al.*, 2008), bottlenose dolphins (*Tursiops truncatus*) (Gaspari *et al.*, 2015; Mead and Potter, 1995), common dolphins (*Delphinus delphis*) (Amaral *et al.*, 2012; Segura-García *et al.*, 2016), spotted dolphins (*Stenella attenuata*) (Leslie and Morin, 2018), spinner dolphins (*Stenella longirostris*) (Andrews *et al.*, 2013; Perrin *et al.*, 1999), or harbour porpoises (*Phocoena phocoena*) (Fontaine *et al.*, 2014). In killer whales ecotypes are mainly related to the type of prey they feed on (fishes *vs.* marine mammals) (de Bruyn *et al.*, 2013; Dahlheim *et al.*, 2008). The East Atlantic, Iberian and Mauritian harbour porpoise populations (upwelling ecotype) rely on upwelling-driven food chains while the Northeast Atlantic population (continental shelf ecotype) lives and feeds on the continental shelf (Fontaine *et al.*, 2014). In the other aforementioned species, local coastal populations are genetically divergent from the more widely distributed offshore population and can also be morphologically distinct (e.g., coloration patterns, body size or skull shape) (e.g., Andrews *et al.*, 2013; Costa *et al.*, 2019, 2016; Leslie and Morin, 2018; Segura-García *et al.*, 2016).

Ecotypes have been especially studied for the common bottlenose dolphin (*Tursiops truncatus*) and they have been described in most of its geographical range. Ecotypes have been mainly identified based on genetic data but they also differ in morphology, feeding ecology, parasitic load and haemoglobin profile (Caballero *et al.*, 2012; Costa *et al.*, 2016; Gaspari *et al.*, 2015; Hersh and Duffield, 1990; Hoelzel *et al.*, 1998; Louis *et al.*, 2014b; Mead and Potter, 1995; Moura *et al.*, 2013; Natoli *et al.*, 2004; Perrin *et al.*, 2011; Segura-García *et al.*, 2018; Torres *et al.*, 2003; Walker, 1981). Genetic studies showed that coastal populations emerged from offshore animals that specialised in the exploitation of

resources in shallower habitats. The oldest segregation between coastal and offshore ecotypes was in the Northwest Atlantic Ocean (NWA) (Moura *et al.*, 2013). In this population, the monophyletic coastal ecotype is ecologically and morphologically differentiated from the offshore ecotype, suggesting that it could be an example of incipient speciation. Coastal NWA specimens are generally smaller, have larger flippers, possess proportionally longer snout and the diameter of their internal nares is smaller (Hersh and Duffield, 1990; Mead and Potter, 1995). One study has focused on the vertebral morphology in *Tursiops truncatus* in the Southeast Atlantic population and concluded that coastal individuals are bigger than offshore specimens and have fewer but more elongated vertebrae (Costa *et al.*, 2016).

As they exhibit ecological specialisation between coastal and offshore habitats below and above the species level, cetaceans appear as an appropriate clade to test whether patterns of morphological adaptation are similar at the macro- and microevolutionary levels. Our previous work has demonstrated that delphinoid and non-delphinoid cetaceans followed distinct evolutionary patterns (chapter 2; Gillet *et al.*, 2019). In this study we focus only on the delphinoid taxon to further investigate the evolutionary history of the entire clade. Delphinoids group three distinct families: Monodontidae only comprises two species (belugas, *Delphinapterus leucas*, and narwhals, *Monodon monoceros*) that live both in coastal and offshore waters while Phocoenidae (porpoises) and Delphinidae (oceanic dolphins) families possess numerous species that specialised in different habitats (rivers, continental shelf, and oceanic waters).

The aim of this work is to understand whether micro- and macroevolutionary processes can follow the same patterns. To this purpose, we seek whether habitat-related morphological adaptation patterns are similar between families and populations. We quantified the effect of habitat on vertebral morphology at three different taxonomic levels: 1) for the whole Delphinoid clade, 2) within Delphinidae and Phocoenidae, and 3) within the Northwest Atlantic Ocean bottlenose dolphin population. We identified the vertebral traits that are related to habitat transitions and compare the morphological trajectories of each group to test whether habitat-related morphological adaptations are similar among Delphinidae, Phocoenidae and bottlenose dolphin ecotypes. As ecological specialisation appears to trigger speciation processes in several extant dolphin and porpoise species, we also investigated whether ecological specialisation played a significant role in delphinoid

macroevolution by modelling and quantifying ecological transitions during their evolutionary history. We demonstrate that habitat has a significant effect on vertebral shape both above and below the species levels and that we could predict the morphology of the axial skeleton according to the habitat. We also show that habitat-related evolution of the vertebral column at the supra-specific level mirrors the modifications that are adopted by populations living in different habitats. However, vertebral modifications along the river-coast-offshore gradient differ between oceanic dolphins and porpoises.

2. Materials and methods

2.1. Data sampling

Specimens used in this research were the same as those presented in chapter 2 (see chapter 2 materials and methods) but solely delphinoid species were conserved, resulting in 126 specimens from 38 different species. This corresponds approximately to 80% of the total number of extant delphinoid species (see Table S 2.1 for specimen collection numbers). Most species were represented by 3 specimens. Whenever possible, specimens of different sex and/or from different populations were sampled. Eleven specimens of *Tursiops truncatus* were measured. Population and ecotype information for bottlenose dolphins was retrieved from the museum database. One specimen (SAM ZM35678) came from the Adriatic Sea and the remaining specimens came from the North-West Atlantic Ocean (NWA). The ecotypes of the Adriatic Sea specimen and one NWA specimen (USNM 572831) were not available and these specimens were then considered of unknown ecotype. For the remaining NWA specimens, three were from the coastal ecotype (1 male, 2 females), three from the offshore ecotype (2 males, 1 female) and three were considered as intermediate between coastal and offshore (1 male, 2 females).

The vertebral shape of each specimen was quantified by taking twelve linear and two angular measurements with digital calipers, rulers and a protractor on every vertebra of the thoracic, lumbar and caudal regions (see Figures 2.1*a, b, c, d*, Chapter 2). The mean value of each measurement was then calculated for each vertebral region. The total centrum length (TCL), i.e., the sum of the vertebral centrum of all vertebrae, was also calculated for each specimen. Specimens mean regional measurements were then $\log_{10}$-transformed and size-corrected using the R-function *phyl.resid.intra* (López-Fernández *et al.*, 2014; R Core Team, 2017). The $\log_{10}$-transformed TCL was used as a proxy

for body length for size-correction. The consensus time-tree published by Steeman was used for the phylogenetic size-correction (Steeman *et al.*, 2009).

Specimens were classified according to two factors: phylogenetic group and ecology. Phylogenetic groups correspond to the three families of delphinoids: Monodontidae (belugas and narwhals), Phocoenidae (porpoises) and Delphinidae (dolphins). However, to avoid duplicating common bottlenose dolphin specimens in two different groups and hence avoid pseudo-replication, these specimens were not included in the Delphinidae group but were instead considered as a fourth distinct group in order to establish the effect of habitat at the intraspecific level. Ecological data for each species were collected from synthetic bibliographic works (Berta, 2015; IUCN, 2017; Perrin *et al.*, 2009). Species were then classified in each of the following ecological categories: (*i*) rivers, bays, and estuaries; (*ii*) continental shelf; (*iii*) continental slope and offshore waters; and (*iv*) mixed lifestyle between continental shelf and offshore waters. The ecotype of each NWA common bottlenose dolphin specimen was retrieved from the museum database (Smithsonian National Museum of Natural History).

2.2. Correlation between vertebral shape and habitat

In order to assess the effect of habitat and family on the vertebral shape, size-corrected shape residuals of each specimen were implemented in a regular PCA based on the correlation matrix with the *prcomp* function in R and vertebral morphology variability was visually explored. Furthermore, the effect of habitat and family were quantitatively tested by using MANOVAs with a residual randomization permutation procedure (RRPP) were applied on specimens' size-corrected residuals with the *procD.lm* function from the *geomorph* package (Adams *et al.*, 2018). The effect of habitat within each phylogenetic group (Delphinidae, Phocoenidae and *Tursiops truncatus*) was also evaluated by applying a MANOVA with RRPP on each group. As both belugas and narwhals have a mixed ecology, this test was not run for the group of Monodontidae. For each MANOVA, data were centred and scaled prior to analysis (*scale* function in R) and significance tests were performed on 10,000 simulations.

2.3. Variables correlated to the ecology

To precisely identify which vertebral apophyses are mostly affected by ecological factors for the entire delphinoid group, a linear discriminant analysis (LDA) was applied to the specimens' size-corrected measurements with the *lda* function from the *MASS* R-package (Venables and Ripley, 2002). As the mixed habitat category comprises species with variable ecology, all specimens classified in this habitat category as well as common bottlenose dolphin specimens with an intermediate or unknown ecotype were excluded from the dataset for this analysis. Given that LDA are relevant only if groups are significantly different, pairwise Hotelling's T-squared tests were used prior to LDA to test for significant differences of distribution between each ecological category using the function *hotelling.test* from the R-package *Hotelling* (Curran, 2018). Afterwards, the Wilks' lambda (λ) criterion and the associated *P*-value of each variable were calculated using a stepwise forward procedure with the function *greedy.wilks* from the *klaR* package (Weihs *et al.*, 2005). At each step, the procedure retains the variables with the highest Wilks' lambda while accounting for the effect of variables already retained during previous steps. Variables are then returned by lambda decreasing order. The first variable of the list with *P*-value > 0.05 and all subsequent variables were not retained to build the LDA model. After building the discriminant model, its performance was assessed using a leave-one-out cross-validation procedure. Standardized function coefficients and structure coefficients (r) were calculated to evaluate the contribution of each variable to each discriminant function. The reliability of the model built on Wilks' lambda values was also evaluated. To assess the variables contribution of the entire set of variables, a second LDA based on all variables (without Wilks' lambda pre-selection) was performed.

The reliability of the selected model was further assessed by testing the impact of the number of variables retained and the number of specimens used. The impact of the number of variables was tested by iteratively retaining one to all variables and calculating the accuracy of each iterative model. Variables were ordered by decreasing Wilks' lambda values. Hence, the first model, based on one variable, uses the variable with the highest λ, the second model, based on two variables, uses the two variables with the highest λ, etc. The impact of the number of specimens used was assessed by building models on subsamples of individuals starting from 15 retained specimens to all of them (103 specimens). For each number of retained specimens, individuals were randomly sampled 50 times and a LDA model was built for each 50 random samples. The average accuracy of all the 50 random

sample models was then reported for each number of specimens retained. All models were constructed based on the 12 Wilks variables used for the main LDA. The LDA model constructed on Wilk's variables was then used to predict the habitat category of the two bottlenose dolphins of unknown ecotype.

2.4. Ecological transitions

Pattern and frequency of habitat transitions during delphinoid evolutionary history were investigated with models of discrete trait evolution and stochastic mapping to establish the importance and frequency of ecological transitions during delphinoid evolutionary history. Several macroevolutionary models were tested using the function *fitDiscrete* from the *geiger* R-package (Harmon *et al.*, 2008). The following models were tested: (*i*) an equal rates model (ER) where all transitions between habitats have the same rate, (*ii*) an all rates different (ARD) model where all habitat transition have different rates, (*iii*) an ordered model (ORD1) where only the following reciprocal transitions are possible and have different rates: rivers-coasts, coasts-mixed, mixed-offshore, (*iv*) a second ordered model (ORD2) similar to ORD1 but where the transitions between coasts and offshore are also possible. Patterns of the two ordered models postulate that transitions from offshore to river habitats, and conversely, are gradual and only occur through an intermediate state in coastal waters. The model with the highest weighted Akaike information criterion (AICc) was conserved for simulations during stochastic mapping. . This stochastic mapping was calculated using the *make.simmap* function from the *phytools* R-package (Revell, 2012). Prior probabilities on the ancestral state of the root node were defined as equal for each of the four possible states. The mapping was repeated 1,000 times and averaged results of all simulations were conserved.

In order to have the most comprehensive analysis, ecological data were also gathered for delphinoid species not included in our morphological dataset. The following species were then added to our dataset for the stochastic mapping: the hourglass dolphin (*Lagenorhynchus cruciger*), the southern right whale dolphin (*Lissodelphis peronii*), the tucuxi (*Sotalia fluviatilis*), and the vaquita (*Phocoena sinus*). The stochastic mapping was calculated based on Steeman's timetree (Steeman *et al.*, 2009). However, due to their recent and rapid diversification, the phylogenetic relationships within the Delphinidae family are still ambiguous. While most phylogenies recover three monophyletic delphinid subfamilies: Lissodelphininae (piebald dolphins), Delphininae (bottlenosed-like dolphins)

and Globicephalinae (blunt-headed dolphins), the relationships between and within these clades differ among phylogenetic trees. Some phylogenies place Globicephalinae as the sister group of both Lissodelphininae and Delphininae (Agnarsson and May-Collado, 2008; Slater *et al.*, 2010; Steeman *et al.*, 2009) while other consider that Globicephalinae and Delphininae form a monophyletic group sister to Lissodelphininae (Banguera-Hinestroza *et al.*, 2014; McGowen, 2011; McGowen *et al.*, 2009; Murakami *et al.*, 2014). Within the Lissodelphininae family, the exclusively coastal *Cephalorhynchus* genus is either considered as monophyletic (Agnarsson and May-Collado, 2008; Harlin-Cognato and Honeycutt, 2006; Pichler *et al.*, 2001; Slater *et al.*, 2010) or paraphyletic with some pelagic and coastal *Lagenorhynchus* species nested in the *Cephalorhynchus* group (Banguera-Hinestroza *et al.*, 2014; McGowen, 2011; McGowen *et al.*, 2009; Murakami *et al.*, 2014; Steeman *et al.*, 2009). Similarly, there is still some uncertainty on the relationships between *Stenella*, *Tursiops* and *Delphinus* genera in the Delphininae subfamily which also comprises both coastal and offshore species. Therefore, the stochastic mapping was also calculated based on two other phylogenetic trees with different topologies from Steeman's tree: the time-tree published by Slater in 2010 and the time calibrated tree published by McGowen in 2009 (McGowen *et al.*, 2009; Slater *et al.*, 2010).

2.5. Vertebral shape trajectories

Finally, an analysis of phenotypic trajectory (PTA) was used to compare the morphological trajectories of Delphinidae, Phocoenidae and *Tursiops truncatus* along the ecological categories (Collyer and Adams, 2013). This analysis allows testing whether habitat-related morphological modification patterns are similar between families and at inter- and intraspecific levels in terms of direction and magnitude. The PTA was performed with the *trajectory.analysis* function (*geomorph* R-package). Similarly to LDA, specimens from the mixed habitat category and common bottlenose dolphin with unknown or intermediate ecotype were excluded from this analysis in order to include only species and specimens with clearly defined ecologies. Prior to analysis, all specimens' size-corrected measurements were scaled and centred. The main PTA was calculated on the three habitat categories (rivers and bays, coasts, offshore) and specimens were divided into two phylogenetic groups: Delphinidae and Phocoenidae. To investigate the phenotypic trajectory at the intraspecific level, *Tursiops truncatus* specimens were considered as a distinct phylogenetic group and were therefore not included in the Delphinidae group. PTA requires that every phylogenetic group

possesses the same ecological categories. Given that *Tursiops truncatus* specimens do not possess a riverine ecotype, this group was not included in the first PTA. However, two ecological pairwise PTAs were also calculated (rivers *vs.* coastal and coastal *vs.* offshore). Common bottlenose dolphins were then included as a third phylogenetic group in the PTA comparing the transition from a coastal to an offshore habitat. The significance of the results of each PTA was calculated from 10,000 simulations and with a RRPP procedure.

3. Results

3.1. Morphospace of vertebrae

In the morphospace including all specimens, the two first principal components (PCs) account together for 52% of the total variance (Figure 3.1). High values on PC1 correspond to more discoidal vertebral centra, narrower vertebral processes and shorter lumbar metapophyses. Positive PC2 values are associated to longer neural spines, neural arches and metapophyses (Figure S 3.1). Specimens' distribution on the morphospace follows an ecological gradient from the lower left corner to the upper right one with a transition from riverine, to coastal and then to offshore morphotype. Specimens with a mixed ecology are mainly found on the extreme left part of PC1 (killer whales, belugas and narwhals) or at the extreme right limit of coastal morphotype overlapping with offshore morphotype.

Interestingly this ecomorphogical gradient across PC1 and PC2 can be observed at different taxonomic levels. Species of dolphins and porpoises that inhabit rivers and bays have similar vertebral morphologies and species of both families living in offshore waters all possess craniocaudally shortened vertebrae. Moreover, this tendency is can also be observed at the intraspecific level. *Tursiops truncatus* specimens from the coastal ecotype tend to have lower PC1 values than offshore ones and intermediate specimens have PC1 value falling between those of coastal and offshore ecotypes. MANOVAs investigating the effect of habitat on vertebral shape further supports these observations as all tests indicate a significant effect of habitat (Table 3.1). Based on the coefficients of determination, the effect is the strongest in the porpoise family ($R^2 = 0.55$). Despite the high *P*-value in *T. trucatus*, the effect is also relatively important (*P*-value = 0.0225, $R^2 = 0.40$).

The visual exploration of the morphospace also revealed few overlap between the three delphinoids families. Only false killer whale specimens (*Pseudorca crassidens*) generate an overlap between Delphinidae and Phocoenidae (dotted lines on Figure 3.1). This single species also enlarges the area of overlap between coastal and offshore Delphinidae. MANOVA on vertebral shape highlighted a significant effect of the phylogenetic group (i.e., Delphinidae, Phocoenidae and *T. truncatus*) (*P*-value = 0.0001, R^2 = 0.22) (Table 3.1). It also found a significant difference of vertebral shape between delphinids and phocoenids (*P*-value = 0.0001, R^2 = 0.13).

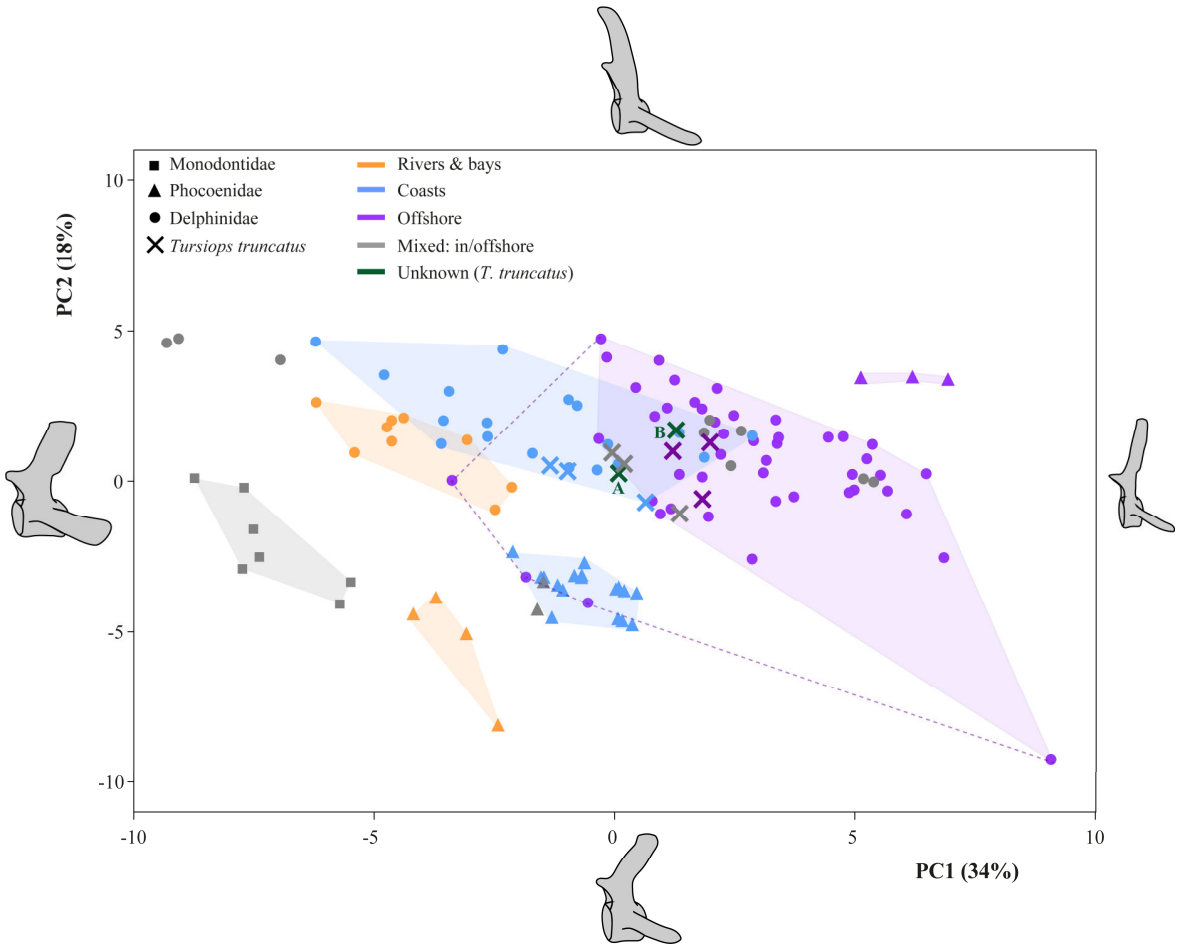

Figure 3.1. Morphospace of vertebral shape. Scatter plot of the two first principal components (PC1 and PC2) of the PCA calculated for 126 delphinoid. Each point corresponds to one specimen. PC1 explains 34% of the total variance and is correlated to shorter vertebral centra and lumbar metapophyses and narrower vertebral processes. PC2 explains 18% of the total variance and is associated with higher neural spines, neural arches and metapophyses. Symbol shapes correspond to delphinoid families and *Tursiops truncatus* specimens are represented by crosses. Symbol colours correspond to habitat categories. Coloured convex hulls represent the area occupied by each habitat category of each family. Letters indicate each *T. truncatus* specimen of unknown ecotype: *A*: NWA specimen (USNM 572831), *B*: Adriatic Sea specimen (SAM ZM35678). Dotted purple lines represent the extension of the area occupied by offshore Delphinidae if *Pseudorca crassidens* specimens are included. Typical vertebral shapes corresponding to each axe extremity are shown along the axes.

Table 3.1. Effect of habitat and family on vertebral shape. Results of MANOVAs applied on specimens to test the effect of habitat (*Ecology*) and family (*Phylogenetic group*) on vertebral shape for all delphinoids and for several clades within delphinoids. Significant values are indicated in bold.

	Ecology		**Phylogenetic group**	
	P-value	R^2	*P*-value	R^2
All specimens	**0.0001**	0.21	**0.0001**	0.22
Delphinidae & Phocoenidae	**0.0001**	0.22	**0.0001**	0.13
Delphinidae	**0.0001**	0.24	/	/
Phocoenidae	**0.0001**	0.55	/	/
Tursiops truncatus	**0.0225**	0.40	/	/

3.2. Discriminant analysis and variables significance

All pairwise Hotelling's T-squared tests found a significant difference of distribution between habitat categories (all *P*-values < 0.001). The linear discriminant model was able to accurately predict the ecological group of 91% of specimens with the cross-validation procedure. Based on Wilks' lambda, 12 variables out of 42 were retained to build the model (Table 3.2and Table S 3.2). The first linear discriminant (LD1) explains 70% of the total between-groups variance and separates riverine and estuarine from coastal and offshore ones (Figure 3.2*a*). The second linear discriminant (LD2) explains the remaining 30% of total variance and differentiates coastal specimens from offshore ones. Although the LDA completely separates riverine specimens from all the others, some overlap persists between coastal and offshore specimens. Accordingly, misclassified specimens in the cross-validation procedure were only coastal or offshore specimens (4 coastal specimens classified as offshore and 5 offshore classified as coastal) (Figure S 3.2). All porpoises were accurately classified. Solely one NWA bottlenose dolphin was misclassified (offshore specimen classified as coastal). However, two other NWA bottlenose dolphins (a specimen of each ecotype) had almost equal probabilities of belonging to coastal or offshore habitats.

Based on structure coefficients and specimens LDA scores (Figure 3.2*a, b* and Table 3.2), species living in rivers and bays have wider caudal transverse processes (WtpC), wider and shorter neural spines (WnpL and HnpL) and wider neural arches (WaL) in the lumbar region, larger metapophyses (WmT and LmT), shorter transverse processes (LtpT) and more posteriorly oriented neural spines (InpT) in the thoracic region than coastal and offshore species. The distinction between coastal and offshore species is more subtle and is due to the cumulative effect of several small

contributions but three variables have higher contributions than the rest. Coastal species diverge from offshore ones by having more posteriorly oriented caudal transverse processes and, to a lesser extent, neural spines (ItpC and InpC), wider neural spines and neural arches in the lumbar region (WnpL and WaL) and lower metapophyses (HmL). The LDA calculated on all variables instead of Wilks variables highlighted the same variables as main discriminators between the three ecological groups. Their equivalents in other backbone regions were also identified as main discriminators showing that morphological modifications are not restricted to a peculiar region of the backbone (Table S 3.2).

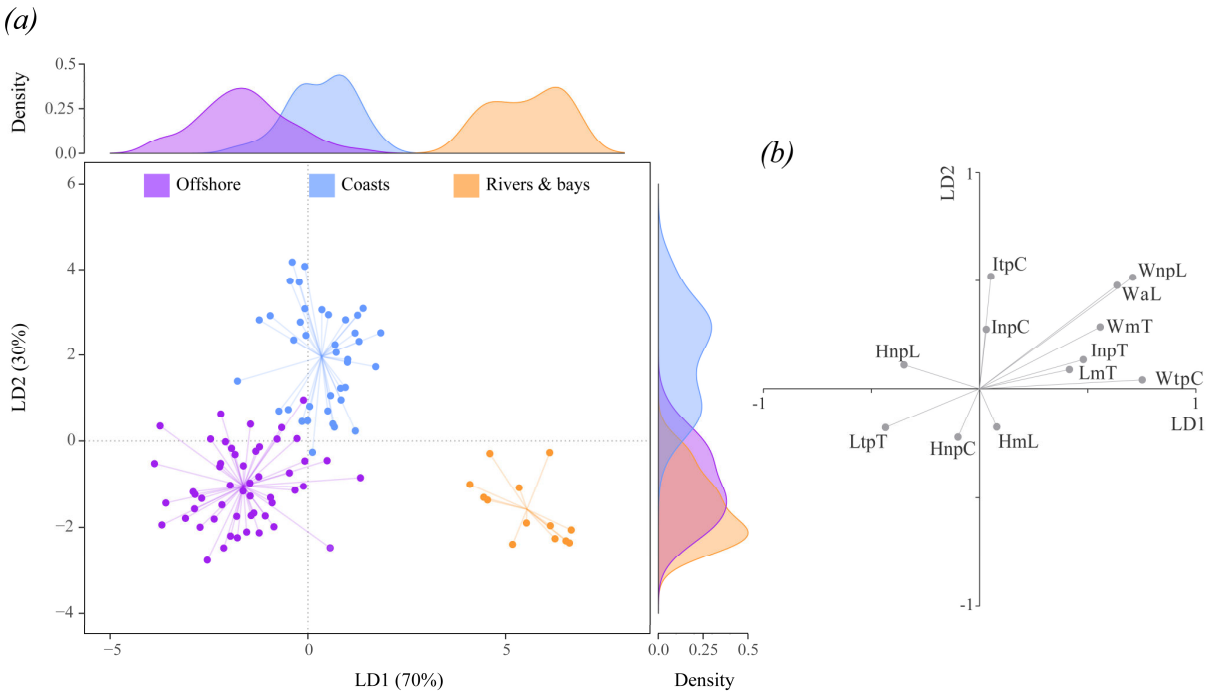

Figure 3.2. Linear discriminant analysis. *(a)* Scatter plot of specimens scores on the two linear discriminant functions (LD1 and LD2). Each point corresponds to a specimen. The densities of each group on each discriminant function are shown on the top and right sides of the scatter plot. LD1 accounts for 70% of the total between-groups variance and mainly separates the rivers & bays group from the two other groups. LD2 accounts for the remaining 30% of variance and separates coastal specimens from other specimens. *(b)* Biplot of structure coefficients on LD1 and LD2 showing variables contribution to each discriminant function. Higher LD1 values correspond to shorter and wider vertebral processes, larger metapophyses and more posteriorly oriented neural spines. Higher LD2 values correspond to wider neural spines and arches, slightly shorter caudal neural spines, lower metapophyses and more posteriorly oriented caudal neural spines and transverse processes. *WnpL*: lumbar neural spines width, *ItpC*: caudal transverse processes posterior orientation, *WtpC*: caudal transverse processes width, *HnpL*: lumbar neural spine height, *HnpC*: caudal neural spine height, *WmT*: thoracic metapophyses width, *InpT*: thoracic neural spine posterior orientation, *WaL*: lumbar neural arch width, *InpC*: caudal neural spine posterior orientation, *LtpT*: thoracic transverse processes length, *LmT*: thoracic metapophyses length, *HmL*: lumbar metapophyses height position on neural spine.

The LDA accuracy rapidly increases with the number of variables until it reaches its maximum around 10 variables (Figure S 3.3*a*). Adding more variables does not substantially improve the model and retaining more than 30 variables impairs the model's accuracy. Hence, the number of variables retained based on Wilks' lambda (12) is a good balance between model accuracy and model complexity. The accuracy test on the number of individuals shows that the maximum accuracy rate is achieved from 40 individuals and then remains stable (Figure S 3.3*b*).

The two bottlenose dolphin specimens of unknown ecotype were classified as pelagic by the LDA model. The Adriatic Sea specimen had a 94% probability of belonging to the offshore category which is congruent with its position in the morphospace as it is grouped with other pelagic *T. truncatus* specimens (Figure 3.1). The NWA specimen had a 75% probability of being pelagic despite its position close to coastal and intermediate bottlenose dolphin ecotypes on the morphospace.

Table 3.2. Variables contribution to linear discriminant functions based on variables selected according to Wilks' lambda criterion. General Wilks' lambda (λ) and associated *P*-value of each variable retained to build the LDA model. Standardised coefficients (*Stand.*), structure coefficients (r) and squared structure coefficients (r^2) of each variable retained for each discriminant function. *LD1*: first discriminant function; *LD2*: second discriminant function. *WnpL*: lumbar neural spines width, *ItpC*: caudal transverse processes posterior orientation, *WtpC*: caudal transverse processes width, *HnpL*: lumbar neural spine height, *HnpC*: caudal neural spine height, *WmT*: thoracic metapophyses width, *InpT*: thoracic neural spine posterior orientation, *WaL*: lumbar neural arch width, *InpC*: caudal neural spine posterior orientation, *LtpT*: thoracic transverse processes length, *LmT*: thoracic metapophyses length, *HmL*: lumbar metapophyses height position on neural spine. Variables with $r^2 \geq 0.15$ are shown in bold.

Var.	λ	*P*-value	LD1			LD2		
			Stand.	r	r^2	Stand.	r	r^2
WnpL	0.391	<0.0001	0.288	**0.708**	**0.501**	0.520	**0.515**	**0.266**
ItpC	0.284	<0.0001	0.453	0.052	0.003	0.722	**0.520**	**0.270**
WtpC	0.207	<0.0001	1.184	**0.752**	**0.565**	-0.452	0.041	0.002
HnpL	0.162	<0.0001	-1.525	-0.350	0.122	1.598	0.110	0.012
HnpC	0.109	<0.0001	0.798	-0.100	0.010	-1.553	-0.223	0.050
WmT	0.086	<0.0001	0.492	**0.558**	**0.312**	0.138	0.286	0.082
InpT	0.075	0.0016	0.410	**-0.480**	**0.230**	-0.295	0.134	0.018
WaL	0.066	0.0021	-0.684	**0.636**	**0.405**	0.602	**0.478**	**0.228**
InpC	0.060	0.0113	-0.185	0.031	0.001	0.438	0.275	0.076
LtpT	0.055	0.0317	-0.644	**-0.435**	**0.189**	0.130	-0.179	0.032
LmT	0.051	0.0255	0.403	**0.416**	**0.173**	-0.353	0.088	0.008
HmL	0.047	0.0196	0.501	0.080	0.006	0.047	-0.177	0.031

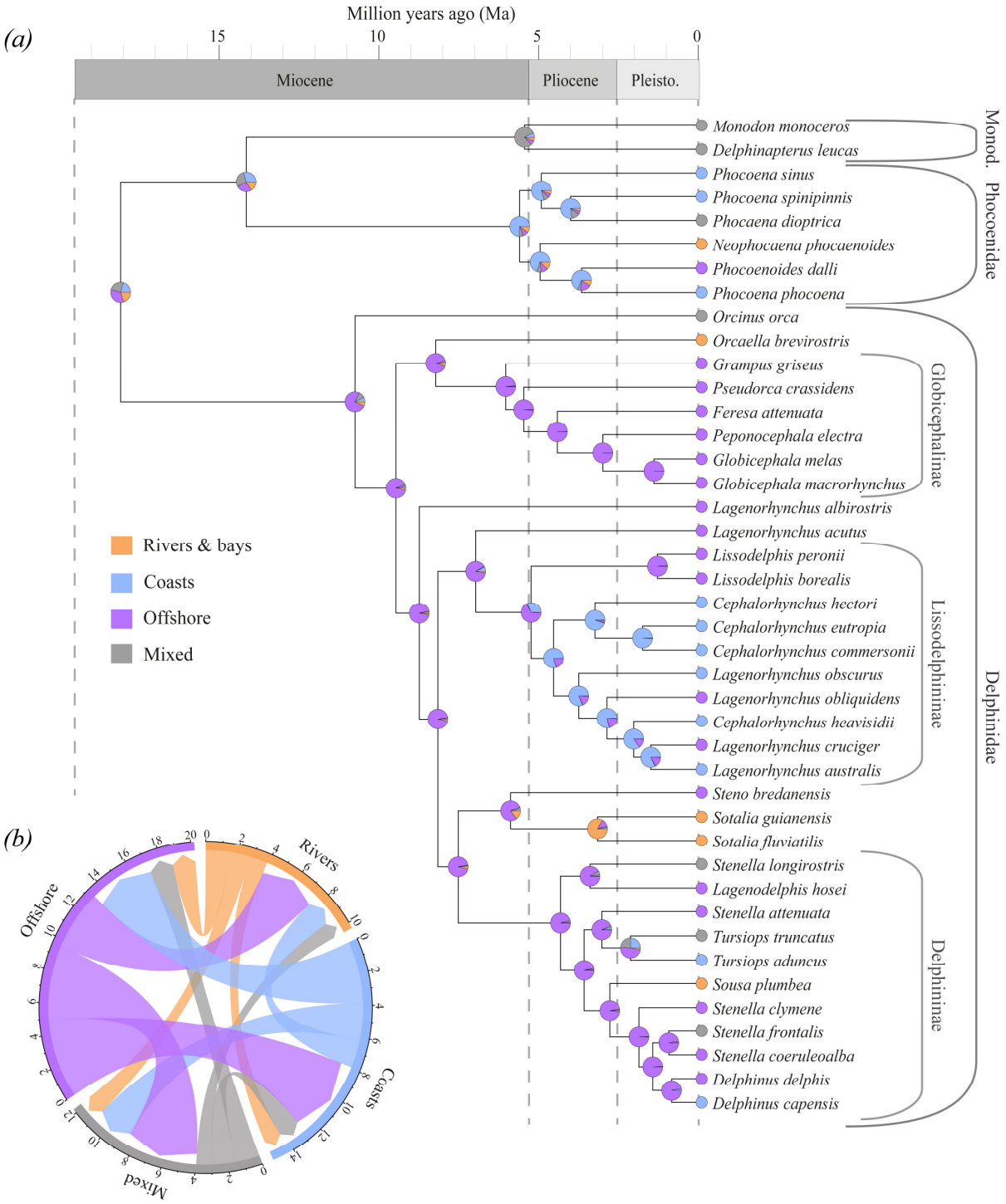

Figure 3.3. Ecological ancestral states and transitions. *(a)* Results of the equal rates (ER) stochastic mapping of ecological categories for the Delphinoid family based on Steeman's phylogenetic tree. Coloured circles at tips represent the actual ecology of extant species. Pie charts on internal nodes show the posterior probability of being in each habitat category based on 1,000 simulations. The three main delphinoid families and delphinid subfamilies are indicated by brackets on the right side. The time scale (in million years) and the geological time scale are shown at the top of the tree. *(b)* Estimated number of ecological transitions from each habitat (part of the arrows in contact with the external ring) to other habitats (tip of arrows, not in contact with external ring). Graduations on external ring and arrow width correspond to the number of transitions for each type of ecological transition.

3.3. Habitat shifts during delphinoid evolution

Despite the phylogenetic uncertainty within the clade of delphinoids, the ancestral state estimates obtained from the three different phylogenies were congruent (Table 3.3). Results obtained from Steeman's phylogenetic tree are presented in the Figure 3.3, results obtained from Slater's and McGowen's tree are presented in the Figure S 3.4. For all phylogenetic tree used for the discrete trait mapping, the equal rates model (ER) was the best model (weighted AICc: Steeman's tree = 0.97, Slater's tree = 0.99, McGowen's tree = 0.97). The most probable ancestral state for the Delphinoidea class was the offshore habitat (approximately 30%). However coastal and mixed ecologies were almost as probable (approximately 23% and 25%, respectively).

On average, there were 30 habitat shifts within the Delphinoidea tree (Figure 3.3*b* and Table 3.3). The most frequent changes were from offshore to coasts (Steeman's tree = 17%), from offshore to mixed (Steeman's tree = 16%), from offshore to rivers (Steeman's tree = 13%), from coasts to offshore (Steeman's tree = 13%) and from coasts to mixed habitats (Steeman's tree = 8%). Thus, almost half of all habitat shifts were from offshore to another habitat.

In overall, 6 habitat transitions occurred in the Phocoenidae family and almost half of them were from coasts to another habitat. A coastal ecology was the most probable ancestral for the family (Steeman's tree = 72%, Slater's tree = 50%, McGowen's tree = 48%). In Delphinidae, an average of 19 changes occurred and more than half of them were from offshore to another habitat. The common ancestor of the family was most probably pelagic habitat (Steeman's tree = 75%, Slater's tree = 79%, McGowen's tree = 76%). Finally, the estimated ancestral state for the ancestor of extant Monodontidae was a mixed habitat (Steeman's tree = 80%, Slater's tree = 69%, McGowen's tree = 68%).

3.4. Phenotypic trajectories

The phenotypic trajectories of Delphinidae and Phocoenidae along the three habitat categories (rivers, coasts, offshore) were significantly different (Table 3.4). Although the shape of trajectory did not differ (P-value = 0.065), the trajectory length and direction were significantly different between the two families (P-value $_{length}$ = 0.0007, P-value $_{direction}$ = 0.003). The pairwise TDAs (Figure 3.4*b, c*) showed that trajectory directions between dolphins and porpoises differ both in the rivers-coasts and the coasts-offshore transitions (P-value $_{rivers\text{-}coasts}$ = 0.0001, P-value $_{coasts\text{-}offshore}$ = 0.0028). However, the

trajectory length difference is only caused by the coasts-offshore transition with porpoises having a path more than twice longer (P-value $_{\text{rivers-coasts}}$ = 0.99, P-value $_{\text{coasts-offshore}}$ = 0.0001).

While, dolphins and porpoises have relatively similar PC1 scores both for riverine and coastal species, the two families are separated from each other on PC2 axis (Figure 3.4*a*). This segregation on PC2 shows that riverine and coastal dolphins tend to have higher/longer vertebral processes (transverse processes, neural arches and neural spines), higher metapophyses on neural spines and transverse processes more anteriorly oriented than porpoises in the same habitats (Table S 3.3). On the contrary, offshore species of both families tend to have similar PC2 scores but they diverge along PC1. This corresponds to dolphins having longer vertebral centra, wider vertebral processes (transverse processes, neural arches and neural spines), larger metapophyses but shorter neural spines than offshore porpoises. Along the coasts-offshore transition, neither the length nor the direction of the *Tursiops truncatus* trajectory differed from the Delphinidae one (P-value $_{\text{length}}$ = 0.41, P-value $_{\text{direction}}$ = 0.13) (Table 3.4). The path length of bottlenose dolphins was significantly different from the path length of porpoises (P-value = 0.0001) but their trajectory directions did not differ (P-value = 0.23).

Table 3.3. Habitats transitions during delphinoid evolution. Number and proportion (%) of transitions between each habitat pair for the entire Delphinoidea clade obtained from the discrete trait stochastic mapping. Results are reported for three different phylogenetic with different topologies (McGowen *et al.*, 2009; Slater *et al.*, 2010; Steeman *et al.*, 2009). Numbers of shifts are averaged from 1,000 repeated stochastic mapping for each tree.

	Steeman's tree		**Slater's tree**		**McGowen's tree**	
Total number of shifts	29.06		31.01		31.46	
	Number	%	Number	%	Number	%
Rivers & bays → Coasts	1.12	3.8	1.36	4.4	1.32	4.2
Rivers & bays → Mixed	1.25	4.3	1.64	5.3	1.46	4.7
Rivers & bays → Offshore	1.52	5.2	1.71	5.5	1.87	5.9
Coasts → Rivers & bays	1.72	5.9	1.70	5.5	1.64	5.2
Coasts → Mixed	2.35	8.1	2.34	7.5	2.39	7.6
Coasts → Offshore	3.85	13.2	3.94	12.7	4.12	13.1
Mixed → Rivers & bays	1.03	3.5	1.53	4.9	1.34	4.2
Mixed → Coasts	1.39	4.8	1.51	4.9	1.73	5.5
Mixed → Offshore	1.54	5.3	1.92	6.2	2.00	6.4
Offshore → Rivers & bays	3.72	12.8	3.44	11.1	3.79	12.0
Offshore → Coasts	4.90	16.9	5.20	16.8	4.93	15.7
Offshore → Mixed	4.67	16.1	4.72	15.2	4.88	15.5

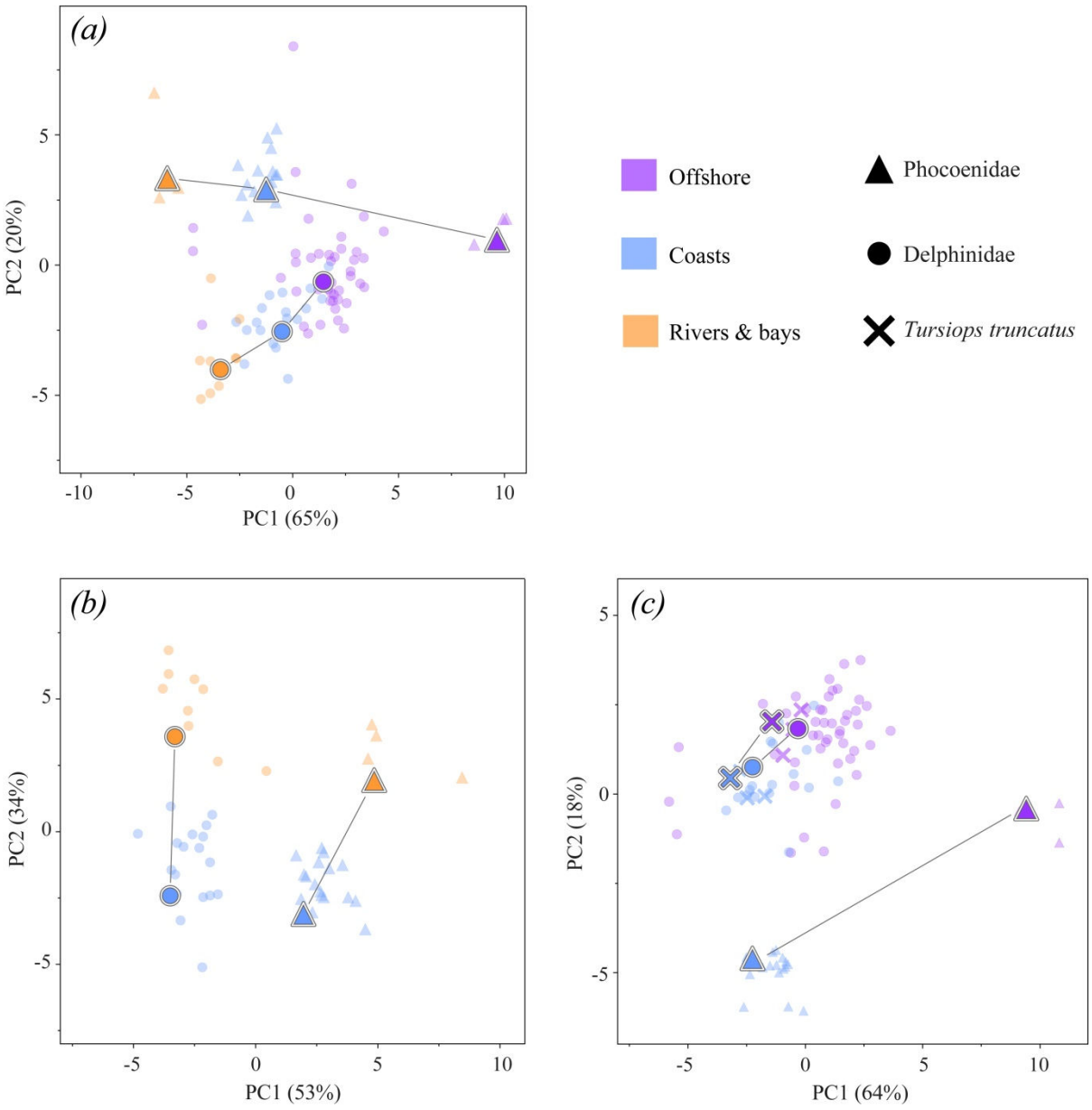

Figure 3.4. Phenotypic trajectory analysis. Scatter plots of the two first principal components (PC1 and PC2) of the phenotypic trajectory analysis. *(a)* Transitions for Delphinidae and Phocoenidae along the rivers-coasts-offshore gradient. *(b)* Transitions for Delphinidae and Phocoenidae along the rivers-coasts gradient. *(c)* Transitions for Delphinidae, Phocoenidae and *Tursiops truncatus* along the coasts-offshore gradient. For each panel, symbol shapes correspond to the phylogenetic group and symbol colours correspond to the habitat categories. Large symbols connected by lines represent the mean coordinates for each habitat category of each phylogenetic group. Each small semi-transparent point corresponds to one specimen.

Table 3.4. Phenotypic trajectory analyses results. PTAs pairwise comparisons of phylogenetic groups along three ecological gradients: from riverine to coastal to offshore habitats, from rivers to coastal habitats and from coastal to offshore habitats. Absolute differences (*Diff.*), effect size (*E.S.*) and associated *P*-value (*P*) between pairwise phylogenetic groups are shown for the size of the path (*Length*), its direction (*Angles*, in degrees) and its shape (*Shape*). Path shape was not calculated for PTAs with only two habitats as their path is just a vector.

	Length			**Angles**			**Shape**		
	Diff.	E.S.	*P*	Diff.	E.S.	*P*	Diff.	E.S.	*P*
Rivers - Coasts - Offshore									
Delphinidae × Phocoenidae	7.073	4.90	**0.0007**	61.53	4.25	**0.0030**	0.277	1.68	0.0645
Rivers - Coasts									
Delphinidae × Phocoenidae	0.001	-1.35	0.9994	67.51	5.15	**0.0001**	/	/	/
Coasts - Offshore									
Delphinidae × Phocoenidae	7.111	5.94	**0.0001**	71.03	3.70	**0.0028**	/	/	/
Delphinidae × *T. truncatus*	1.668	0.01	0.4147	55.08	1.12	0.1296	/	/	/
Phocoenidae × *T. truncatus*	8.779	5.62	**0.0001**	57.14	0.64	0.2333	/	/	/

4. Discussion

Our results showed that several habitat shifts occurred during the evolutionary history of delphinoids (Figure 3.3 and Figure S 3.4). These ecological changes are supported by morphological modifications of their axial skeleton. The main direction of vertebral modifications follows a gradient from riverine to coastal and then to offshore habitats (Figure 3.1). However, patterns of vertebral modifications along this ecological gradient differ between Delphinidae and Phocoenidae (Figure 3.4). Nonetheless, vertebral shape characteristics allow the automatic classification of specimens in one of the three ecological categories (Figure 3.2).

4.1. Vertebral shape modifications in Delphinoidea

Delphinoids living in rivers, estuaries and bays have a morphology perfectly differentiated from other species (Figure 3.2). These species have more elongated vertebrae providing a higher flexibility to the backbone (Buchholtz, 2001b; Long *et al.*, 1997). Moreover, their transverse processes are shorter which might permit larger bending angles between successive vertebrae. These species also possess wider neural spines, neural arches and transverse processes which probably provides larger areas of origin and insertion for axial muscles implied in backbone oscillations during swimming (Pabst, 1990; Parry, 1949; Slijper, 1936). Finally, they also exhibit enlarged metapophyses which are the main surface of insertion of the *m. multifidus*, one of the two main dorsal muscles implied in

dorsal bending of the axial skeleton during swimming (Pabst, 1990; Parry, 1949; Slijper, 1936). Larger metapophyses suggest that a greater muscular force is applied on each metapophyses. If the power output of the *m. multifidus* is similar between riverine, coastal and offshore species, the force applied on each vertebra would hence be more important in species with fewer vertebrae. These vertebral characteristics correspond to increased backbone flexibility both dorsoventrally and laterally which is coherent with higher manoeuvrability capacities needed in shallow and complex habitats. Conversely, offshore species have shorter vertebral centra, narrower vertebral processes and longer neural processes and transverse processes enhancing backbone rigidity (Buchholtz, 2001b; Long *et al.*, 1997). Coastal delphinoids tend to have an intermediate morphology between pelagic and riverine species but more similar to offshore than riverine morphology.

4.2. Interfamily variability

During their evolutionary history, delphinoids seem to have experienced numerous habitat transitions (Figure 3.3, Figure S 3.4 and Table 3.3). However, patterns are different between phocoenids and delphinids. Based on our results, the ancestor of crown porpoises had most probably a coastal ecology. On the contrary, the common ancestor of Delphinidae and all ancestors of early delphinids (i.e., all deep nodes in the delphinid family) were estimated as pelagic lineages. Assuming that a pelagic way of life promotes long distance travels, these results would be consistent with the hypothesis of early dispersal of delphinids (Banguera-Hinestroza *et al.*, 2014).

Delphinids and phocoenids possess clearly distinct vertebral morphologies since both families do not overlap on the morphospace. However, the false killer whales (*Pseudorca crassidens*) surprisingly cluster with coastal porpoises. The position of false killer whales in the delphinoid morphospace might be related to its large body size since this feature can also influence vertebral morphology (chapter 2; Gillet *et al.*, 2019). In addition to distinct vertebral shapes, the phenotypic trajectories along the ecological gradient also differ between delphinids and phocoenids. Coastal and riverine porpoises differ from dolphins by having shorter neural arches and lower metapophyses. This implies that the lever arm of the *m. multifidus* is smaller in porpoises and probably impacts their swimming movements. In addition to the general elongation on vertebral centra and widening of apophyses along the coastal-river transition observed in both families, riverine porpoise have an even more important shortening of neural arches and lowering of metapophyses. Conversely, offshore

species of both families tend to have similar, intermediate neural arches length and metapophyses height. However, the vertebral centra shortening and apophyses narrowing, and neural spines elongation along the coastal-offshore transition are largely greater in the offshore Dall's porpoises than in any dolphins. In fact, Dall's porpoises (*Phocoenoides dalli*) have a remarkably specialised vertebral column as it possesses the highest vertebral count of any cetaceans (97 vertebrae, see Buchholtz *et al.*, 2005; Gillet *et al.*, 2019; chapter 2) and, consequently, has extremely shortened vertebrae. This morphology could reflect the acute adaptation of this species in the exploitation of a specialised niche.

Given that the common ancestor of delphinids was probably pelagic while the ancestor of porpoises was possibly a coastal lineage, the morphological distinctions between the two families could be the result of the different evolutionary history of the two clades. Both families diversified in similar habitats following equivalent global morphological trend (i.e., vertebral shortening in deeper waters) but starting from different ecomorphological states which resulted in slightly different strategies. Alternatively, it could reflect different strategies of fine scale habitat use for species living in sympatry (Bearzi, 2005; Parra, 2006; Spitz *et al.*, 2006).

Despite Phocoenidae and Delphinidae both diversified in similar habitats following the same kind of morphological trend (i.e., vertebral shortening in deeper waters), fine analysis of the backbone shows differences that are probably related to the evolution from a different ancestral state. The common ancestor of delphinids was probably pelagic while the ancestor of porpoises was probably a coastal lineage, supporting anatomical differences. Environmental constraints drive the global direction of morphological adaptation but ancestral state constrains the fine-scale orientation of these modifications. Delphinidae and Phocoenidae being two closely related clades, these similar ecomorphological trends possibly reflect parallel evolution of these families.

4.3. Micro- and macroevolutionary processes

The vertebral morphology of NWA bottlenose dolphins clearly differs between coastal and offshore ecotypes as highlighted by the MANOVA (Table 3.1) and the PCA (Figure 3.1). Moreover the position of coastal and pelagic ecotypes felt within the area of morphospace occupied by coastal and offshore delphinids, respectively. The discriminant model also performed relatively well on these

specimens (Figure S 3.2) suggesting that NWA bottlenose dolphin vertebral morphology differs between ecotypes in a similar way than do coastal and offshore delphinid species. This is further supported by the similarity of the phenotypic trajectory directions between *Tursiops truncatus* and Delphinidae along the coastal-offshore transition (Figure 3.4). Hence, offshore NWA bottlenose dolphins have more discoidal centra and narrower apophyses than coastal individuals. These substantial vertebral modifications are coherent with previous studies that showed divergences between NWA ecotypes based on genetics, ecology, as well as external and skull morphology (Hoelzel *et al.*, 1998; Mead and Potter, 1995; Moura *et al.*, 2013; Natoli *et al.*, 2004; Torres *et al.*, 2003). Surprisingly, the length of the phenotypic trajectory in the morphospace of *T. truncatus* and delphinids are also equivalent. This implies that morphological modifications at the population level are as important as at the family level supporting the previous hypothesis of an incipient speciation between the two NWA ecotypes (Hoelzel *et al.*, 1998; Moura *et al.*, 2013). Although these results are based on a restricted number of specimens, they are coherent with vertebral shape modifications identified between pelagic and coastal ecotypes from the Southwestern Atlantic population based on 35 specimens (Costa *et al.*, 2016).

Similar distinction between coastal and offshore ecotypes has been described in various bottlenose dolphin populations worldwide, including in the North Eastern Atlantic Ocean (NEA) and Mediterranean Sea (Caballero *et al.*, 2012; Gaspari *et al.*, 2015; Louis *et al.*, 2014a, 2014b; Segura-García *et al.*, 2018). The discriminant analysis model classified the Adriatic bottlenose dolphin specimen (SAM ZM35678) in the offshore group (Figure S 3.2), which is coherent with its position in the morphospace (Figure 3.1). These results are nonetheless in opposition with previous studies that considered the Adriatic population as a coastal population (Gaspari *et al.*, 2015). However, habitat specialisations in the NEA and Mediterranean populations are more recent than in the NWA and gene flow is still detected between the two ecotypes with offshore specimens acting as a source for coastal populations (Gaspari *et al.*, 2015; Louis *et al.*, 2014b; Moura *et al.*, 2013). Moreover, there is no external morphological differences between the two NEA ecotypes unlike what has been observed for NWA ecotypes (Louis *et al.*, 2014a). Hence, it seems likely that specimens from coastal NEA and Mediterranean populations (i.e., Adriatic sea) still possess a vertebral morphology similar to offshore ecotypes given the shorter divergence time and incomplete genetic separation. However, our study

only includes one specimen from the Mediterranean Sea and further morphological works including a large sample of NEA and Mediterranean specimens would be needed to test this hypothesis.

The process of colonisation of shallower habitat from the open sea seems to be iterative in several Delphinidae taxa. Segregation between coastal and pelagic habitats has indeed been proposed as the main ecological driver of speciation between *Tursiops truncatus* and *T. aduncus* (Moura *et al.*, 2013). Similar population partitioning based on habitat preference has also been reported for other delphinids (e.g., *Delphinus* spp., *Stenella longirostris*, *Stenella attenuata*) (Amaral *et al.*, 2012; Andrews *et al.*, 2013; Leslie and Morin, 2018; Natoli *et al.*, 2006; Perrin *et al.*, 1999; Segura-García *et al.*, 2016). For bottlenose and common (*Delphinus* spp.) dolphins at least, coastal populations are thought to have emerged from multiple independent founder events. Some individuals from the more widely distributed pelagic populations specialised in the occupation of shallower habitat further leading to genetic and morphological differences between coastal and offshore ecotypes. Specialisation from pelagic to coastal ecology hence seems to be an important factor of population partitioning in the Delphininae subfamily. In the Lissodelphininae subfamily, speciation through ecological adaptation for more coastal or more pelagic habitat has also been proposed for two pairs of *Lagenorhynchus* species living in sympatry (Banguera-Hinestroza *et al.*, 2014; Galatius and Goodall, 2016).

At a broader phylogenetic scale, our stochastic mapping retrieved numerous ecological changes during the evolutionary history of Delphinoidea. Speciation through ecological specialisation between coastal and offshore waters has also been recently proposed for Phocoenidae. Each of the two sister species of porpoises inhabiting the North Atlantic and Pacific oceans share the oceanic space: the harbour porpoise (*Phocoena phocoena*) lives on the continental shelf while the Dall's porpoise (*Phocoenoides dalli*) lives in offshore waters. This pattern is also mirrored by the sister species living in the Southern Hemisphere: the Brumeister's porpoises (*Phocoena spinipinnis*) living in coastal waters and the spectacled porpoises (*Phocoena dioptrica*) inhabiting offshore and continental waters (Chehida *et al.*, 2019). This suggests that habitat specialisation also played a substantial role in the diversification history of the whole delphinoid clade. As patterns of vertebral shape modifications and ecological specialisation are similar at inter- and intraspecific levels, microevolutionary diversifications might reflect the macroevolutionary history of delphinoids.

5. Conclusion

During their evolutionary history, delphinoid species experienced several transitions between pelagic, coastal and riverine habitats. At the level of the delphinoid clade, these ecological transitions are strongly associated with vertebral shape modifications corresponding to a general vertebral craniocaudal shortening along the transitions from shallow to deep waters. However, vertebral morphology and phenotypic trajectories along this ecological gradient differ between Phocoenidae and Delphinidae. Several extant delphinid species exhibit population differentiations that have been linked to offshore-inshore transitions (Andrews *et al.*, 2013; Leslie and Morin, 2018; Moura *et al.*, 2013; Segura-García *et al.*, 2016). Within the common bottlenose dolphin (*T. truncatus*), vertebral modifications between coastal and offshore ecotypes are exactly similar to those observed between coastal and offshore delphinid species, further supporting the hypothesis that coastal and offshore ecotypes described in several species might reflect ongoing ecological speciation processes. We therefore suggest that coastal-pelagic population segregations observed in some extant dolphin species might reflect the general pattern of delphinoid diversification. It supports our hypothesis that diversification patterns are similar at the micro and macroevolutionary scales in delphinoids.

Supplementary materials

Contents:

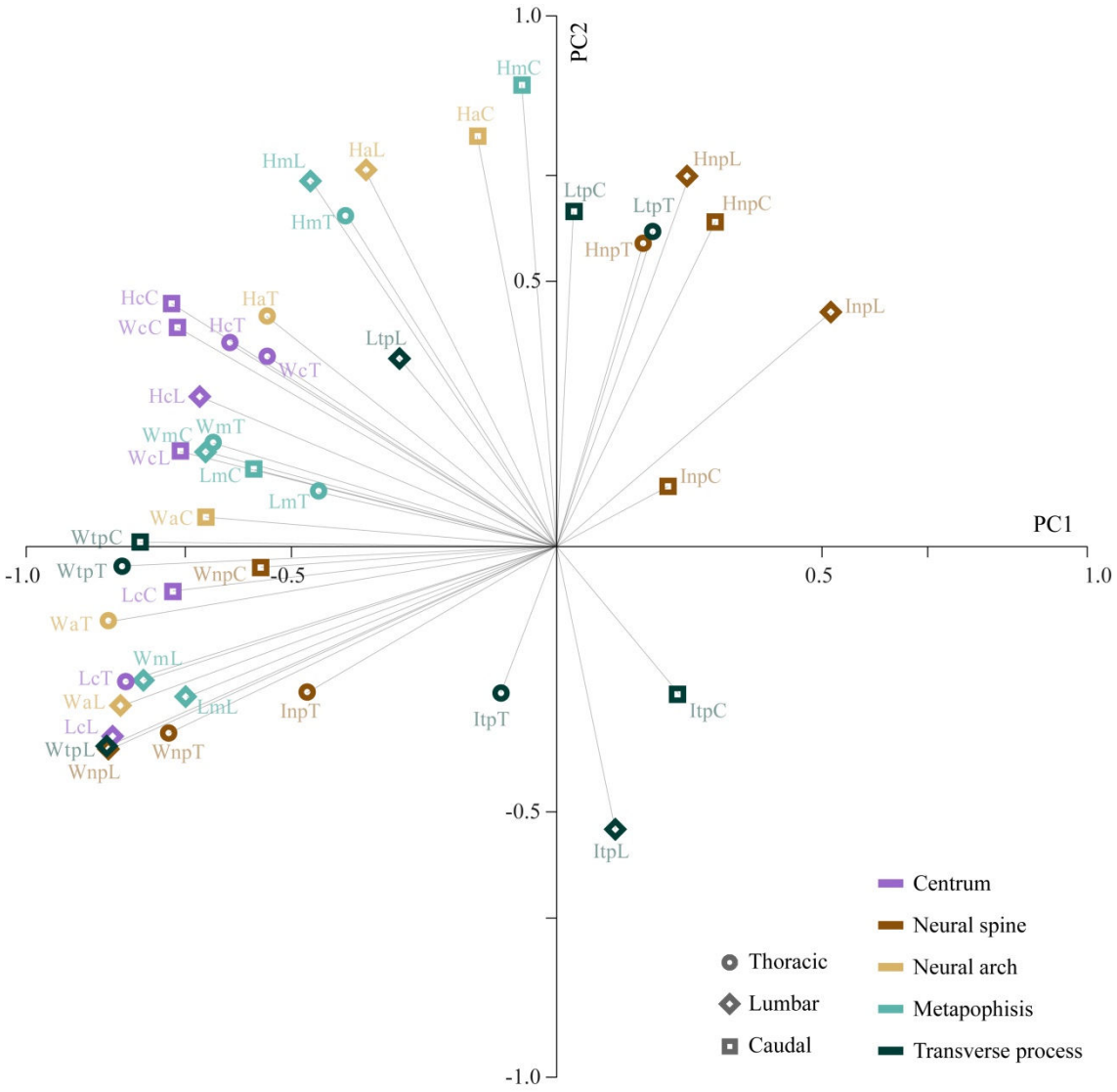

Figure S 3.1. Variables contribution to morphospace. Variables loadings on the two first principal components (PC1 and PC2) of the morphospace. Symbol shapes correspond to the regions of the vertebral column. Each colour corresponds to a different part of the vertebra. Variables names are coded as follow: the first capitalized letter is the measurement type (*L*: length, *H*: height, *W*: width, *I*: inclination); the following lowercased letters are the vertebral part (*c*: centrum, *tp*: transverse process, *np*: neural spine, *a*: neural arch, *m*: metapophyses) and the last capitalized letter is the backbone region (*T*: thoracic, *L*: lumbar, *C*: caudal).

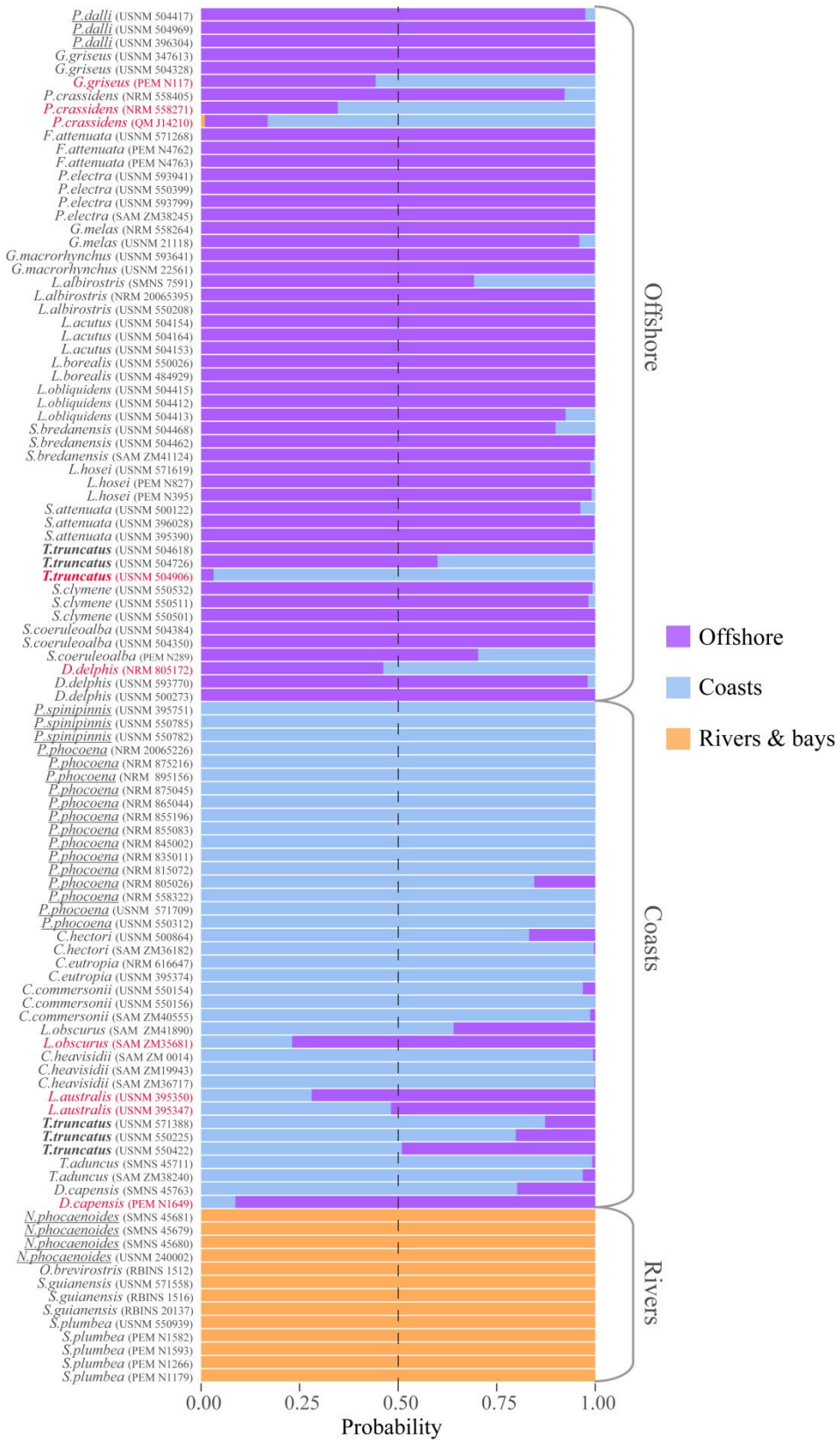

Figure S 3.2. Posterior probabilities of specimens' classification. Probabilities of habitat group membership of each specimen. Probabilities were obtained with a leave-one-out cross-validation procedure. Brackets on the right part of the graph indicate the true habitat category of each specimen. Names of specimens from the family of Phocoenidae are underlined and NWA bottlenose dolphins are in bold. Misclassified specimens appear in red.

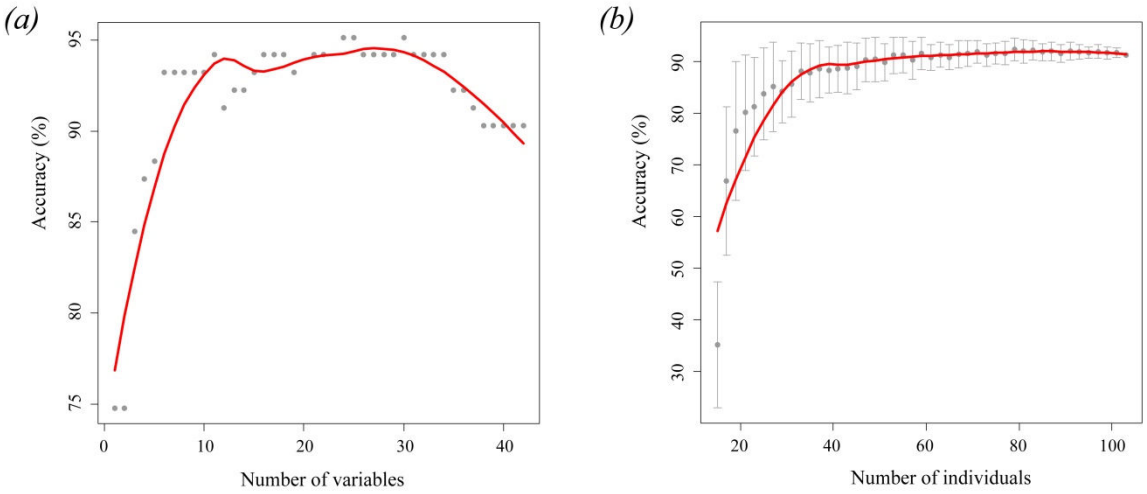

Figure S 3.3. Accuracy of LDA model. *(a)* Accuracy of the model according to the number of variables retained when tested on all specimens. The number of variables retained based on the Wilks' lambda criterion (i.e., 12 variables) lies just after the curve's inflexion point. Adding more variables does not substantially improve the model. Retaining to many variables (i.e., more than 30) impairs the model's accuracy. *(b)* Accuracy of the model according to the number of individuals used to build the model on the 12 Wilks variables. Points correspond to the average accuracy from 50 random samplings of specimens and bars correspond to the standard deviation. From 40 individuals and beyond, the accuracy remains stable around 90%.

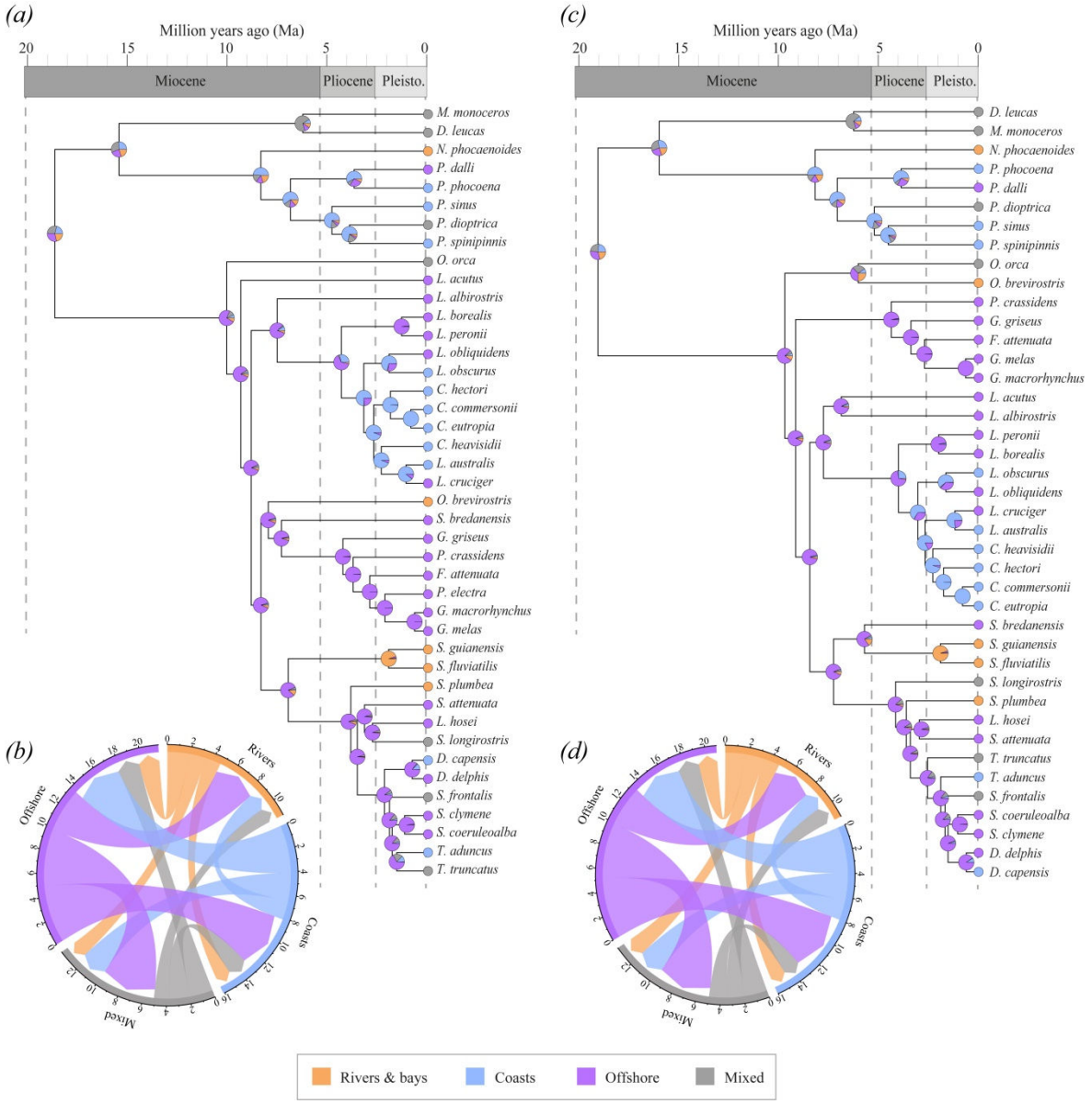

Figure S 3.4. Ancestral state estimates of habitat categories. Results of the equal rates (ER) stochastic mapping of ecological categories for the Delphinoid family based on *(a)* McGowen's phylogenetic tree and *(b)* *(b)* Slater's tree. Coloured circles at tips represent the actual ecology of extant species. Pie charts on internal nodes show the posterior probability of being in each habitat category based on 1,000 simulations. The time scale (in million years) and the geological time scale are shown at the bottom.

Table S 3.1. List of specimens used in this study. Collection numbers of specimens from nine different museums. Museums abbreviations are as follow: *AMNH*: the American Museum of Natural History, New York; *MNHN*: the French National Museum of Natural History, Paris; *NRM*: the Swedish Royal Museum of Natural History, Stockholm; *PEM*: the Bayworld Port Elizabeth Museum, Port Elizabeth; *QM*: the Queensland Museum, Brisbane; *RBINS*: the Royal Belgian Institute of Natural Sciences, Brussels; *SAM*: the Iziko South African Museum, Cape Town; *SMNS*: the State Museum of Natural History, Stuttgart; *USNM*: the National Museum of Natural History, Washington D.C.. Tursiops truncatus ecotypes are indicated by superscript letters beside collection number: *U*: unknown, *C*: coasts, *O*: offshore, *I*: intermediate.

Monodontidae	
Delphinapterus leucas	MNHN A3246
	NRM 558404
	RBINS 1508
	USNM 571021
Monodon monoceros	MNHN A3235
	NRM 558407
	USNM 594407
Phocoenidae	
Neophocaena phocaenoides	SMNS 45679
	SMNS 45680
	SMNS 45681
	USNM 240002
Phocoena dioptrica	USNM 571485
	USNM 571486
Phocoena phocoena	NRM 895156
	NRM 20065226
	NRM 558322
	NRM 805026
	NRM 815072
	NRM 835011
	NRM 845002
	NRM 855083
	NRM 855196
	NRM 865039
	NRM 865044
	NRM 875045
	NRM 875216
	NRM 875358
Phocoena spinipinnis	USNM 395751
	USNM 550782
	USNM 550785
Phocoenoides dalli	USNM 396304
	USNM 504417
	USNM 504969
Delphinidae	
Cephalorhynchus commersonii	SAM ZM40555
	USNM 550154
	USNM 550156
Cephalorhynchus eutropia	NRM 616647
	USNM 395374
Cephalorhynchus heavisidii	SAM ZM 0014
	SAM ZM19943
	SAM ZM36717
Cephalorhynchus hectori	SAM ZM36182
	USNM 500864
Delphinus capensis	PEM N1649
	SMNS 45763
Delphinus delphis	NRM 805172
	USNM 500273
	USNM 593770
Feresa attenuata	PEM N4762
	PEM N4763
	USNM 571268
Globicephala macrorhynchus	USNM 22561
	USNM 593641
Globicephala melas	NRM 558264
	USNM 21118
Grampus griseus	PEM N117
	USNM 347613
	USNM 504328
Lagenodelphis hosei	PEM N395
	PEM N827
	USNM 571619
Lagenorhynchus acutus	USNM 504153
	USNM 504154
	USNM 504164
Lagenorhynchus albirostris	NRM 20065395
	SMNS 7591
	USNM 550208
Lagenorhynchus australis	USNM 395347
	USNM 395350
Lagenorhynchus obliquidens	USNM 504412
	USNM 504413
	USNM 504415
Lagenorhynchus obscurus	SAM ZM41890
	SAM ZM35681
Lissodelphis borealis	USNM 484929
	USNM 550026
Orcaella brevirostris	RBINS 1512
Orcinus orca	NRM 558250
	NRM 558251
	NRM 558401
Peponocephala electra	SAM ZM38245
	USNM 550399
	USNM 593799
	USNM 593941

Pseudorca crassidens	NRM 558271		*Stenella longirostris*	PEM N1278	
	NRM 558405			USNM 395414	
	QM J14210			USNM 500017	
Sotalia guianensis	RBINS 20137		*Steno bredanensis*	SAM ZM41124	
	RBINS 1516			USNM 504462	
	USNM 571558			USNM 504468	
Sousa plumbea	PEM N1179		*Tursiops aduncus*	SAM ZM38240	
	PEM N1266			SMNS 45711	
	PEM N1582		*Tursiops truncatus*	SAM ZM35678	U
	PEM N1593			USNM 484529	I
	USNM 550939			USNM 504618	O
Stenella attenuata	USNM 395390			USNM 504726	O
	USNM 396028			USNM 504906	O
	USNM 500122			USNM 550225	C
Stenella clymene	USNM 550501			USNM 550364	I
	USNM 550511			USNM 550422	C
	USNM 550532			USNM 550852	I
Stenella coeruleoalba	PEM N289			USNM 571388	C
	USNM 504350			USNM 572831	U
	USNM 504384				
Stenella frontalis	USNM 21915				
	USNM 22017				
	USNM 504321				

Table S 3.2. Variables contribution to the linear discriminant analysis based on all variables. General Wilks' lambda (λ) and associated *P*-value of each variable retained to build the LDA model. Standardised coefficients (*Stand.*), structure coefficients (*r*) and squared structure coefficients (r^2) of each variable retained for each discriminant function. *LD1*: first discriminant function; *LD2*: second discriminant function. Variables names are coded as follow: the first capitalized letter is the measurement type (*L*: length, *H*: height, *W*: width, *I*: inclination); the following lowercased letters are the vertebral part (*c*: centrum, *tp*: transverse process, *np*: neural spine, *a*: neural arch, *m*: metapophyses) and the last capitalized letter is the backbone region (*T*: thoracic, *L*: lumbar, *C*: caudal). Variables with $r^2 \geq 0.2$ are shown in bold.

Var.	λ	*P*-value	LD1			LD2		
			Stand.	r	r^2	Stand.	r	r^2
WnpL	0.391	<0.0001	0.464	**0.708**	**0.502**	-0.030	0.434	0.189
ItpC	0.284	<0.0001	0.858	0.077	0.006	0.617	**0.476**	**0.227**
WtpC	0.207	<0.0001	1.374	**0.727**	**0.528**	-1.225	-0.006	0.000
HnpL	0.162	<0.0001	-3.198	-0.332	0.110	2.022	0.121	0.015
HnpC	0.109	<0.0001	1.252	-0.107	0.012	-1.131	-0.200	0.040
WmT	0.086	<0.0001	0.227	**0.553**	**0.305**	0.037	0.231	0.053
InpT	0.075	0.0016	0.331	**0.469**	**0.220**	-0.559	0.096	0.009
WaL	0.066	0.0021	-0.273	**0.637**	**0.406**	0.366	0.404	0.163
InpC	0.060	0.0113	-0.292	0.044	0.002	0.233	0.252	0.063
LtpT	0.055	0.0317	-0.783	-0.429	0.184	-0.062	-0.140	0.020
LmT	0.051	0.0255	0.479	0.405	0.164	-0.770	0.057	0.003
HmL	0.047	0.0196	0.171	0.068	0.005	0.130	-0.168	0.028
HnpT	0.044	0.0527	1.155	-0.157	0.025	-0.237	0.257	0.066
LcT	0.042	0.1259	0.454	**0.665**	**0.443**	0.010	0.200	0.040
WcL	0.038	0.0145	0.275	0.249	0.062	2.245	**0.517**	**0.267**
WcT	0.034	0.0202	1.469	0.147	0.022	-1.646	0.195	0.038
HcT	0.032	0.0556	-1.268	0.158	0.025	0.802	0.323	0.105
ItpL	0.030	0.0842	-0.552	0.083	0.007	-0.073	0.275	0.075
HcC	0.029	0.1174	0.100	0.300	0.090	-1.805	0.303	0.092
HaL	0.027	0.1610	1.002	0.100	0.010	1.305	-0.067	0.004
LtpL	0.026	0.1464	0.072	0.201	0.040	-1.073	0.212	0.045
WmL	0.025	0.1776	0.868	**0.597**	**0.357**	0.106	0.178	0.032
WtpL	0.024	0.1419	-0.855	**0.727**	**0.529**	0.105	0.303	0.092
LmL	0.023	0.2080	-0.476	**0.548**	**0.300**	-0.070	0.050	0.002
HaT	0.022	0.4103	-0.106	0.045	0.002	-0.671	0.045	0.002
HaC	0.022	0.4663	-0.229	0.044	0.002	-0.718	-0.361	0.130
LtpC	0.021	0.2033	-0.331	0.220	0.048	1.142	-0.327	0.107
HmC	0.020	0.3858	0.796	-0.044	0.002	-0.702	-0.340	0.115
LcC	0.020	0.3789	-0.188	**0.654**	**0.427**	0.852	0.118	0.014
WtpT	0.019	0.3376	0.311	**0.589**	**0.347**	0.362	0.337	0.114
LmC	0.019	0.5729	-0.639	0.391	0.153	0.318	-0.217	0.047
WaC	0.019	0.4701	-0.121	**0.620**	**0.385**	-0.735	0.086	0.007
InpL	0.018	0.5394	-0.047	-0.366	0.134	0.289	0.120	0.015
WnpC	0.018	0.6951	0.249	**0.616**	**0.380**	0.372	0.229	0.053
WmC	0.018	0.6251	0.491	**0.529**	**0.280**	-0.001	-0.096	0.009
HmT	0.017	0.6000	-0.414	-0.017	0.000	0.163	-0.112	0.012
ItpT	0.017	0.7730	0.132	0.124	0.015	-0.181	0.034	0.001
WaT	0.017	0.7096	-0.159	**0.664**	**0.441**	0.301	0.318	0.101
HcL	0.017	0.8025	-0.432	0.219	0.048	0.344	0.412	0.170
WcC	0.017	0.7970	-0.421	0.308	0.095	0.411	0.327	0.107
LcL	0.017	0.8927	0.056	**0.687**	**0.472**	0.467	0.268	0.072
WnpT	0.017	0.9772	0.034	**0.590**	**0.348**	0.087	**0.535**	**0.287**

Table S 3.3. Variables contribution to PCA axes of phenotypic trajectories. Variable loadings for the two first principal components (PC1 and PC2) of each phenotypic trajectory. Variables names are coded as follow: the first capitalized letter is the measurement type (*L*: length, *H*: height, *W*: width, *I*: inclination); the following lowercased letters are the vertebral part (*c*: centrum, *tp*: transverse process, *np*: neural spine, *a*: neural arch, *m*: metapophyses) and the last capitalized letter is the backbone region (*T*: thoracic, *L*: lumbar, *C*: caudal). Absolute values > 0.65 are in bold.

	Rivers - Coasts - Offshore		Rivers - Coasts		Coasts - Offshore	
	PC1	**PC2**	**PC1**	**PC2**	**PC1**	**PC2**
LcT	**-0.881**	-0.163	-0.129	**0.787**	**-0.895**	-0.306
WcT	-0.110	-0.256	-0.170	-0.064	-0.007	-0.131
HcT	-0.205	-0.330	-0.342	-0.089	-0.182	-0.202
HnpT	0.468	-0.337	**-0.655**	-0.207	0.426	-0.074
WnpT	-0.563	0.197	0.602	-0.015	-0.380	**-0.858**
InpT	-0.196	0.186	0.401	0.267	0.130	-0.648
HaT	0.056	-0.623	**-0.698**	0.190	0.020	0.270
WaT	**-0.670**	-0.062	0.327	0.451	-0.491	-0.488
LmT	-0.325	-0.189	-0.181	0.393	-0.203	-0.059
WmT	-0.418	-0.315	-0.491	0.414	-0.240	-0.240
HmT	-0.010	**-0.815**	**-0.881**	0.317	-0.173	0.625
LtpT	0.259	-0.460	**-0.737**	-0.151	0.004	0.610
WtpT	-0.643	-0.259	-0.268	0.594	-0.584	-0.354
ItpT	-0.051	0.255	0.399	-0.110	0.161	-0.286
LcL	**-0.840**	-0.035	0.325	**0.657**	**-0.763**	-0.526
WcL	-0.222	-0.093	-0.028	-0.298	-0.155	-0.428
HcL	-0.216	-0.227	-0.229	-0.187	-0.156	-0.312
HnpL	0.601	-0.526	**-0.747**	-0.149	0.518	0.255
WnpL	**-0.774**	0.077	0.564	0.349	-0.629	**-0.733**
InpL	0.581	-0.313	-0.500	-0.261	0.436	0.185
HaL	0.188	**-0.780**	**-0.915**	0.346	0.236	0.409
WaL	**-0.775**	0.036	0.558	0.362	**-0.665**	-0.631
LmL	**-0.776**	-0.069	0.105	0.553	**-0.720**	-0.191
WmL	**-0.794**	-0.097	0.120	0.554	**-0.723**	-0.329
HmL	0.051	**-0.899**	**-0.888**	0.386	-0.021	0.643
LtpL	0.139	-0.240	-0.141	0.032	0.262	-0.183
WtpL	**-0.835**	0.029	0.481	0.576	**-0.712**	-0.619
ItpL	0.019	**0.639**	**0.745**	-0.367	0.109	**-0.661**
LcC	**-0.717**	-0.316	-0.394	**0.844**	**-0.684**	-0.241
WcC	-0.224	-0.401	-0.411	0.072	-0.125	-0.197
HcC	-0.227	-0.473	-0.529	0.108	-0.159	-0.173
HnpC	0.539	-0.459	-0.605	0.368	0.601	0.325
WnpC	-0.473	-0.223	-0.281	0.672	-0.326	-0.357
InpC	0.179	-0.026	-0.048	-0.242	0.194	-0.163
HaC	0.215	**-0.784**	**-0.801**	0.540	0.304	0.632
WaC	**-0.662**	-0.393	-0.402	**0.798**	-0.618	-0.140
LmC	-0.554	-0.517	-0.482	**0.714**	-0.515	0.411
WmC	**-0.680**	-0.551	-0.491	**0.800**	-0.645	0.242
HmC	0.215	**-0.886**	**-0.910**	0.437	0.183	**0.799**
LtpC	0.145	**-0.615**	-0.546	**0.658**	0.346	0.473
WtpC	**-0.691**	-0.438	-0.323	0.908	-0.619	-0.189
ItpC	0.118	0.445	0.571	**-0.693**	0.136	-0.432

Chapter 4 :
Linking vertebral morphology to backbone biomechanics and swimming kinematics

Abstract

Cetacean vertebral morphology substantially varies in accordance with their habitat. Changes in vertebral morphology are though to impact the backbone stiffness and therefore the swimming movements. However explicit relation between vertebral morphology, backbone stiffness and swimming movements remains unclear. Here, we propose the first study to analyse morphological data, backbone biomechanics and swimming kinematics of cetaceans in a quantitative and comparative framework. We used vertebral shape data collected on CT-scanned and museum specimens to model the backbone stiffness and bending abilities based on engineer's beam theory. In addition, swimming movements of four different species of dolphins were analysed based on high speed videos using regular kinematic parameters as well as geometric morphometric motion analyses. We demonstrate that craniocaudal vertebral shortening associated with high vertebral count in offshore small-sized cetaceans results in increased backbone stiffness, especially in the anterior and mid-body regions. This increased stiffness restricts movements in the anterior part of the body, providing enhanced stability during swimming. It also allows small species to use higher tailbeat frequencies and therefore swim faster in an energy efficient manner.

1. Introduction

During their evolutionary history, cetaceans have acquired a fusiform streamlined body shape adapted to their aquatic environment (Fordyce *et al.*, 1994; Thewissen *et al.*, 2009). Other morphological adaptations to a fully aquatic lifestyle notably include the loss of hindlimbs and the acquisition of a swimming mode based on dorso-ventral oscillations of their tail and backbone (Fish, 2016; Thewissen and Fish, 1997). In fishes, variability of the vertebral morphology impacts the stiffness and biomechanics properties of the spine which, in turn, affects swimming movements. Precise mechanisms linking vertebral stiffness and swimming efficiency remain however unclear (Hebrank, 1982; Long, 1992; Long *et al.*, 2011; Nowroozi and Brainerd, 2014). For instance, vertebrae and intervertebral joints with a larger diameter result in stiffer segments with a lower range of motion in the striped bass (*Morone saxatillis*) (Nowroozi *et al.*, 2012; Nowroozi and Brainerd, 2012). In the blue marlin (*Makaira nigricans*), segment stiffness decreases with increasing length of the corresponding vertebra (Long, 1992). However, kinematic analysis of five galeomorph shark species produced contradictory results as increases in body curvature during turning manoeuvres were associated with decreases in vertebral centrum length and increases in vertebral centrum diameter (Porter *et al.*, 2009).

In cetaceans, *in-vitro* biomechanical tests of eight different segments along the backbone in the common dolphin (*Delphinus delphis*) have demonstrated variability in segment stiffness. Stiffness slightly increases from the anterior thoracic region up to the lumbo-caudal transition where the column is the stiffest and then decreases progressively in the caudal region with a drastic drop in rigidity at the fluke insertion (Long *et al.*, 1997). This study found that increases in stiffness were significantly associated with more flattened intervertebral disks and shorter vertebral centrum. Based on these results, the combination of data from the vertebral morphology of numerous modern and extinct cetaceans, and qualitative analysis of swimming movements in four different species, Buchholtz (2001) identified three different swimming patterns according to the region of the body in which most of the undulatory movement occurred. The first group is characterised by uniformly elongated vertebrae along the backbone and swim through undulation of their entire body length. The second group still possess elongated vertebrae in the anterior torso but mid-torso vertebrae are anteroposteriorly shortened resulting in important curvature of the anterior torso during swimming

movements. Finally, the last group present an important shortening of all torso vertebrae but elongated tail stock vertebrae producing oscillatory movements restricted to the posterior region of the body. Numerous kinematic studies focusing on swimming speed, fluke amplitude, pitch angle and tailbeat frequency have highlighted differences among cetaceans (Curren *et al.*, 1994; Fish, 1998; Rohr and Fish, 2004; Videler and Kamermans, 1985). These variations result in different swimming performances in relation to species behavioural ecology (i.e., shallow-water slow swimmers or offshore fast swimmers) and external morphology such as body fineness ratio, fins aspect ratio and sweep angle (Bose *et al.*, 1990; Curren *et al.*, 1994; Fish, 1998; Fish and Rohr, 1999). For instance, belugas (*Delphinatperus leucas*) can be encountered in very shallow waters. They are slow swimmers using low tailbeat frequencies but can perform thigh turns at low speed. They also possess broad pectoral fins assisting in precise manoeuvers. Conversely, Pacific white-sided dolphins (*Lagenorhynchus obliquidens*) are fast swimmers, using high tailbeat frequencies and taking large turns but at higher speed (Fish, 1998; Fish and Rohr, 1999; Rohr and Fish, 2004).

Previous works have highlighted the tremendous variability of vertebral morphology among cetaceans (Buchholtz, 2001b; Buchholtz *et al.*, 2005; Gillet *et al.*, 2019; Marchesi *et al.*, 2018; Viglino *et al.*, 2014). This variation should be related to changes in vertebral column stiffness and swimming performances but interactions between these features remain unclear. In this chapter, we aim to investigate the relatedness between vertebral morphology, backbone biomechanics and swimming kinematics in a quantitative and comparative context. Similarly to Buchholtz (2001), we hypothesise that high count of craniocaudally shortened vertebrae should provide a stiffer vertebral column whereas few but elongated vertebrae would result in a more flexible backbone. To this purpose, we used the engineer's beam theory to predict backbone stiffness and curvature in different cetacean species. The beam theory allows calculating the bending properties of a beam depending the loading applied and based on its shape and the intrinsic elastic properties of its material. In addition, swimming movements of four species were videotaped and analysed using regular kinematic parameters and geometric morphometric analysis of motion (Martinez *et al.*, 2018). By comparing predicted biomechanical and kinematic data, we demonstrate that vertebral stiffness of delphinoids increases along the ecological gradient rivers-coasts-offshore. We also suggest that increased backbone stiffness might limit body deformation during a swimming cycle and also increase tailbeat frequency without requiring higher muscular force input.

2. Materials and methods

2.1. Data sampling

2.1.1. Scanned and dissected specimens

In order to measure the size of intervertebral disks and characterise muscle morphology, several specimens were scanned, dissected and/or cross-sectioned. All animals used for scans, dissection and cross-section stranded on the Belgian or northern French coasts and were provided by the Veterinary Faculty of the University of Liège which is in charge of cetacean necropsies. Two harbour porpoises (*Phocoena phocoena*) and one white-beaked dolphin (*Lagenorhynchus albirostris*) were CT-scanned with a Siemens Somatom Sensation 16 Slice CT-scanner at the Veterinary Faculty of the University of Liège. To prevent artefacts due to tissue decomposition, we used fresh individuals with a condition code of 2 or 3 (Jauniaux *et al.*, 2002).

These two delphinoid species possess different vertebral morphologies and ecologies. The harbour porpoise is a species usually encountered on the continental shelf in the North Atlantic and North Pacific. It possesses an average of 65 vertebrae. The white-beaked dolphin is mainly found in offshore waters of the North Atlantic and possesses 91 vertebrae.

The first harbour porpoise (female, juvenile, body length = 123.5 cm, weight = 23 kg) was frozen at -20 °C after stranding. It was then CT-scanned and cross-sectioned in 15 mm-thick slices using a band saw. Faces of each slice were photographed in high resolution (7360 x 4912 pixels). The muscular cross-sectional area (CSA), i.e., the surface of a muscle in transverse section, of the entire epaxial complex was measured on each picture with ImageJ software (Schneider *et al.*, 2012). As we focus on dorsal extension, hypaxial complex CSA was not measured here. The surface of each independent epaxial muscle (*m. longissimus* and *m. multifidus*) was measured on the slice having the highest CSA in order to calculate the proportional surface of each muscle.

The second harbour porpoise (female, adult, body length = 146 cm, weight = 42 kg) and the white-beaked dolphin (female, adult, body length = 236 cm, weight = 175 kg) were scanned 24 hours after stranding and dissected afterwards. CT-scan voxel sizes were 0.85 x 0.85 x 1 mm for the harbour porpoise and 0.98 x 0.98 x 1 mm for the white-beaked dolphin. Morphological data necessary to predict spinal flexibility were collected on the CT-scan of these two individuals. Measurements were

taken on DICOM images with Amira software (v.6.1) (FEI, Thermo Fischer Scientific, USA). The following data were collected (Figure 4.1 *a, b*): vertebral centra length (*Lc*) and height (*Hc*), intervertebral disks length (*Ld*), length between the dorsal tip of neural spines and the centre of the corresponding vertebral centra (*Hcnp*), length between the dorsal part of the neural arches and the centre of the corresponding vertebral centra (*Hcna*), length between the metapophyses tip and the centre of the corresponding vertebral centra (*Hcm*), length from the distal tip of the transverse process to the centre of the corresponding vertebral centra (*Lctp*), distance between the tips of two consecutive neural spines (*Dnp*) and distance between two consecutive neural arches (*Dna*). These data were taken on each thoracic, lumbar, caudal and fluke vertebra. Due to vertebral ankylosis in cetacean necks, cervical vertebrae were indistinguishable from each other on scan images. Hence, only the total length of the cervical region was measured as the distance between the anterior face of the atlas to the anterior face of the vertebral centrum of first thoracic vertebra. The total centrum length (TCL) was calculated as the sum of the vertebral centrum of all vertebrae (Buchholtz *et al.*, 2005). The total disk length (TDL) was calculated in a similar manner and the total length of the backbone was calculated as the sum of TCL and TDL. The maximal length of the skull was measured. The maximal CSA for the entire epaxial complex was also measured on both specimens.

2.1.2. Museum specimens

Several specimens from the museum specimens used in Chapter 2 (see material and methods, p.36) were selected to investigate backbone flexibility. Only specimens with a fully complete axial skeleton (skull and all vertebrae) for which the total body length of the animal was available in the museum database were selected, resulting in 60 specimens from 41 species (Table S 4.1). The following vertebral measurements taken on each vertebra were used (Figure 4.1 *c, d*): vertebral centrum length (*Lc*), width (*Wc*) and height (*Hc*), neural arch height (*Hna*) and width (*Wna*), neural process height (*Hnp*) and width (*Wnp*), metapophyses height on the vertebra (*Hm*), transverse process length (*Ltp*). The maximal length of the skull (*Lskull*) was measured and the total centrum length (TCL) was calculated for each specimen. The type of insertion of each rib was also recorded (single-headed or double-headed rib).

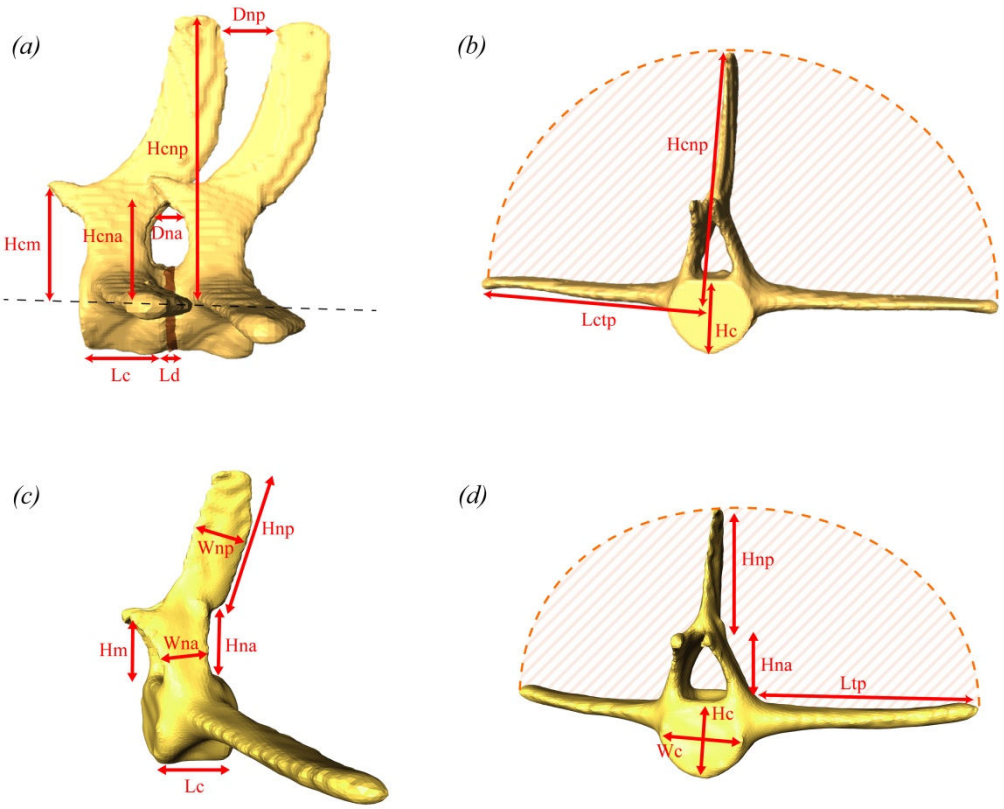

Figure 4.1. Vertebral measurements taken on scanned specimens. 3D model of the last thoracic and first lumbar vertebrae of a harbour porpoise in lateral view (*a, c*) and frontal view (*b, d*). Red arrows show measurements taken on vertebrae and disks. (*a-b*) Measurements taken on scanned specimens. (*c-d*) Measurements taken on museum specimens. Hatched surface corresponds to the CSA calculated from vertebral measurements (CSA_{vert}; Equations 15 and 16). Measurement abbreviations are detailed in the text.

2.1.3. Live animals

In order to quantify and analyse real functional data, underwater videos of swimming animals were recorded in five zoos and aquariums: the Moorea Dolphin Centre (French Polynesia), the Boudewijn Seapark (Belgium), the Ecomare center (the Netherlands), the Duisburg Zoo (Germany) and the Shedd Aquarium (USA). Videos were recorded on 15 specimens belonging to 4 different species with different ecologies and vertebral morphologies (Figure 4.2). The Amazon River dolphin, *Inia geoffrensis* (n = 1), is a riverine species measuring between 1.8 and 2.6 meters and having 42 elongated vertebrae. The harbour porpoise, *Phocoena phocoena* (n = 2), is a coastal species possessing 65 vertebrae and usually measures between 1.3 and 1.8 meters. The common bottlenose dolphin, *Tursiops truncatus* (n = 6), can be encountered both in coastal and offshore waters, possesses between 60 and 65 vertebrae and has a body length varying between 2.5 and 3.8 meters. The Pacific white-sided

dolphin, *Lagenorhynchus obliquidens* (n = 5), is an offshore species measuring between 1.7 and 2.5 meters and having 75 vertebrae (Berta, 2015; Perrin *et al.*, 2009).

Videos were recorded with a GoPro 6 camera at 100 frames per second with a resolution of 2704 x 1520 pixels. The camera was fixed on a tripod that was either positioned at the bottom of the pool or was held from the surface of the water. In all configurations, the camera was stationary and deep enough to prevent animals from swimming at the surface. Animals were asked by trainers to swim at a normal average speed in a straight line in front of the camera in order to record dorso-ventral oscillations in lateral view. Only sequences in which animals swam actively (at least one complete dorso-ventral oscillation) were conserved for analysis.

Figure 4.2. Skeletons of species recorded on videos. Pictures show the vertebral morphology of the four species filmed in aquariums. From top to bottom: Amazon River dolphin (*Inia geoffrensis*) (USNM 49582), harbour porpoise (*Phocoena phocoena*) (NRM 895156), bottlenose dolphin (*Tursiops truncatus*) (USNM 484529) and Pacific white-sided dolphin (*Lagenorhynchus obliquidens*) (USNM 504413).

2.2. Backbone biomechanics modelling

2.2.1. Building the model

In order to model the flexibility of the backbone in extension for different species, we built a mathematical model in the R environment based on the Euler-Bernoulli beam theory (R Core Team, 2017). In this model, the backbone is considered as a beam where vertebrae are stiff and non-deformable elements while intervertebral disks are elastic elements where bending occurs. Vertebrae are numbered from the first to the last one and the disk preceding each vertebra is its corresponding disk. Hence, the first vertebra has no disk (Figure 4.3). The compliance (i.e., flexibility) (C_i) of a single intervertebral disk is proportional to its shape and its Young's modulus (E):

$$C_i = \frac{Ld_i}{E \,.\, I_i} \quad \textbf{(1)}$$

where Ld is the intervertebral disk length (from its anterior to its posterior face) and I is the area moment of inertia of the intervertebral disk. We considered that all disks have a circular cross-sectional area. Hence, the area moment of inertia of a single disk is:

$$I_i = \frac{\pi \,.\, Hd^4}{64} \quad \textbf{(2)}$$

where Hd is the disk height. As our model aims at evaluating backbone flexibility only in the dorso-ventral plane, we retained the intervertebral disk height as circle diameter to calculate I. Therefore, equation (1) becomes:

$$C_i = \frac{64 \,.\, Ld_i}{E \,.\, \pi \,.\, Hd_i^4} \quad \textbf{(3)}$$

In opposition to the compliance, the stiffness (k_i) of a disk reflects its resistance to deformation and is the reciprocal of the compliance:

$$k_i = \frac{1}{C_i} = \frac{E.\pi.Hd_i^4}{64 \,.\, Ld_i} \quad \textbf{(4)}$$

As disks are arranged in series along the vertebral column, the total compliance (C) of the backbone is equal to the sum of the compliance of each disk and the total stiffness (k) is the reciprocal of the total compliance:

$$C = \sum_{i=1}^{Nd} \frac{64 \,.\, Ld_i}{E \,.\, \pi \,.\, Hd_i^4} \tag{5}$$

$$k = \frac{1}{C} = \frac{1}{\sum_{i=1}^{Nd} \frac{64 \,.\, Ld_i}{E \,.\, \pi \,.\, Hd_i^4}} \tag{6}$$

where Nd is the total number of disks in the backbone.

The Young's modulus, or elastic modulus (E), is a constant reflecting the elastic properties of a given material. Currently, no value has been directly reported for the intervertebral disk of cetaceans. However, relationships between the backbone stiffness and vertebral morphology have previously been experimentally investigated in the common dolphin (*Delphinus delphis*) (Long *et al.*, 1997). Authors reported values of stiffness in extension and flexion (k_i) as well as intervertebral disk length (Ld_i) and height (Hd_i) for six different intervertebral segments along the backbone. Using equation (4) we thus calculated the Young's modulus (E) of each intervertebral disk used in that study based on reported values of stiffness in extension and on morphological measurements. The mean value of the six segments (2.21 MPa) was used as the elastic modulus constant in our model.

Besides calculating the compliance and stiffness of the vertebral column, we also aimed to model its bending angle and vertical movement amplitude in dorsal extension. These parameters depend on the compliance of each disk and the bending moment applied to each vertebrae. For a single disk, the bending angle (θ_{di}) is:

$$\theta_{di} = C_i \,.\, M_i = C_i \,.\, F_i \,.\, r_i \tag{7}$$

where M_i is the bending moment applied on the vertebra following the disk of interest and is proportional to the force applied to the vertebrae (F_i) and to the distance at which it is applied (r_i). In the backbone model, F_i corresponds to the force applied by epaxial muscles on the vertebra and r_i corresponds to the distance between the muscle insertion on the vertebra and the centre of rotation, in

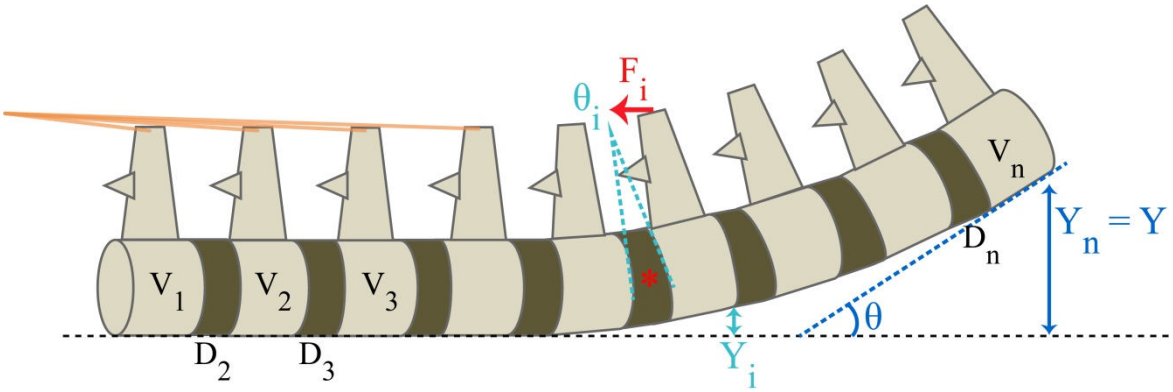

Figure 4.3. Schematic vertebral column and parameters used in the model. Simplified vertebrae are represented in beige and intervertebral disks in brown. Vertebrae and disks are numbered in black (*V* and *B* respectively). Orange lines represent epaxial muscles fibres and show their insertion point on the vertebra (neural spine). The red arrow shows the force applied by muscles on the i^{th} vertebrae (F_i) and the red asterisk shows its rotational centre. The resulting disk bending angle (θ_i) and vertical displacement (Y_i) are shown in light blue. The total angle of curvature of the backbone (θ) and the total vertical displacement (Y) are indicated in dark blue.

other words, the leverage. For this model, we considered that the centre of rotation is at mid-height of the intervertebral disk and that the force direction is parallel to the longitudinal axe of the backbone. We also considered that the first vertebra is fixed and backbone bending can only start from the disk following the first vertebra.

The disk bending angle (θ_{di}) only depends on morphological and physical properties of the disk itself. However, neural processes might limit dorsal bending if two consecutive processes touch each other during backbone extension. Therefore, we calculated the maximal bending angle allowed by neural spines (θ_{npi}) and by neural arches (θ_{nai}):

$$\theta_{npi} = 2 \,.\, arcsin \frac{Dnp_i}{2 \,.\, \overline{Hcnp_i}} \quad \textbf{(8)}$$

$$\theta_{nai} = 2 \,.\, arcsin \frac{Dna_i}{2 \,.\, \overline{Hcna_i}} \quad \textbf{(9)}$$

where Dnp_i is the distances between neural processes of vertebrae *i-1* and *i* and $\overline{Hcnp_i}$ is the mean value of the distance between the rotational centre and the tip of the neural process of vertebrae *i-1* and *i*. Dna_i and $\overline{Hcna_i}$ are parameters equivalent to Dnp_i and $\overline{Hcnp_i}$ for neural arches. The disk (θ_{di}), neural processes (θ_{npi}) and neural arches (θ_{nai}) angles were compared and the smallest one (θ_i) was conserved in order to account for potential contact between neural spines or neural arches during

bending. The total angle of curvature (θ) of the backbone is the sum of the bending angles (θ_i) of all vertebral segments.

The cumulative vertical displacement (i.e., amplitude) of the posterior face of a vertebra (Y_i) is:

$$Y_i = Y_{i-1} + (Ld_i + Lc_i) \,.\, sin\,(\sum_{j=1}^{i} \theta_j) \quad \textbf{(10)}$$

where Lc_i is the length of the vertebral centrum and Y_{i-1} is the cumulative vertical displacement of the vertebra preceding the vertebra of interest. The angle used in equation (10) corresponds to the orientation of the vertebra and is the sum of the bending angles of all preceding disks. The total vertical displacement of the backbone (Y) is then the vertical displacement of the last vertebra (Y_n).

The vertical displacement and bending angle both depend on the muscular force applied on the vertebrae. We used the muscle cross-sectional area (CSA) to predict the theoretical muscular force output (F):

$$F = CSA \,.\, MS \quad \textbf{(11)}$$

where MS is the muscle stress value which reflects the intrinsic contractile properties of the muscle. The muscle stress value commonly used for mammals in 300 kPa (Pabst, 1993; Wells, 1965). Calculating the force output based on this value implies that the entire contractile force of the muscle is dedicated to bend the vertebral column alone which is unlikely. Indeed, to bend the body of the animal, muscles have to counteract the backbone stiffness but also the stiffness of all surrounding tissues such as ligaments, muscles, internal organs, the blubber layer and the skin as well as the external pressure and drag of water. Using whole body force outputs reported for swimming bottlenose dolphins (*Tursiops truncatus*), Arthur *et al.* (2015) calculated "nominal" stress values which reflect the proportion of muscle stress resulting in the production of the necessary force to swim. They obtained a maximal "nominal" MS value of 61 kPa and a suboptimal value of 15 kPa. All three values of muscle stress were used to calibrate our model (see section 2.2.3, this chapter).

For all the vertebral columns tested in our model (theoretical, scanned and museum specimens), we postulated that the total muscle force was equally distributed on all the vertebrae on which it has an insertion. Hence, the muscular force applied on a single vertebra (F_i) is:

$$F_i = \frac{F}{Nv_m} \quad (12)$$

where Nv_m is the number of vertebrae on which the muscle inserts.

2.2.2. *Theoretical backbones*

In order to understand the effect of morphological changes of each vertebral process on the flexibility of the backbone, several theoretical backbones were created and their stiffness and curvature angles were calculated. Morphological characteristics of all theoretical backbones were chosen to correspond to the range of values observed in small cetaceans (Table 4.1). For all models, the total body length of the theoretical specimen was 2 meters. Its skull measured 0.35 meters and its backbone measured 1.65 meters. Based on values measured on CT-scanned specimens, we postulated that the TCL corresponded to 80% of the total length of the backbone and hence the TDL accounted for 20% of the backbone length for all models.

Based on these criteria, we conceived a basic theoretical backbone made of 40 similar vertebrae (the lowest vertebral count for cetaceans is 42) and therefore 39 intervertebral disks. Vertebral centrum length and height were 3.45 and 3 centimetres, respectively, resulting in a centrum length/height ratio (*Lc/Hc*) of 1.15 which is comparable to ratios of some non-delphinoid riverine dolphins (*Lipotes vexillifer* and *P. blainvillei*). Intervertebral disk height was equal to centrum height

Table 4.1. Average morphological parameters of small cetaceans by ecological group. Mean values and standard deviation of vertebral count (*Vertebrae*), centrum length/height ratio (*Lc/Hc*), neural process height/centrum length ratio (*Hnp/Lc*) and neural process width/centrum length ratio (*Wnp/Lc*) for small delphinoids according to their habitat and for riverine non-delphinoids.

	Vertebrae	Lc/Hc	Hnp/Lc	Wnp/Lc
Rivers & bays (non-delphinoid)	44 (± 3)	1.07 (± 0.14)	1.60 (± 0.32)	0.73 (± 0.11)
Rivers & bays	58 (± 5)	0.91 (± 0.10)	2.03 (± 0.34)	0.58 (± 0.04)
Coasts	67 (± 4)	0.69 (± 0.09)	2.93 (± 0.37)	0.62 (± 0.05)
Offshore	75 (± 13)	0.71 (± 0.16)	3.17 (± 1.27)	0.56 (± 0.08)
Mixed	62 (± 10)	0.84 (± 0.16)	2.28 (± 0.81)	0.60 (± 0.08)

and disk length was 0.69 centimetres resulting in a disk length/height ratio (*Ld/Hd*) equal to 0.23 (Figure 4.4). As we did not include transverse processes in our theoretical backbones, it was not possible to measure the muscle CSA. Hence an alternative equation for muscular force prediction was used for these theoretical models. This equation allows the prediction of muscular force based on body length. It was developed by Arthur *et al.* (2015) based on their 61 kPa nominal muscle stress for epaxial muscles of cetaceans:

$$F = 0.401 \, . \, BL^{1.56} \tag{13}$$

where *BL* is the total body length of the specimen. Hence, the total force of epaxial muscles for our 2 meters long model is 1.182 kN. For all theoretical models, except model MHnp2 which accounted for the effect of neural processes height (see below), we considered that muscles inserted on the dorsal surface of vertebral centra. Thus, the leverage corresponded to half the centrum height (1.5 cm). For model MHnp2, the point of muscular insertion was the dorsal tip of neural processes which corresponds to the insertion point of the *m. longissimus* in cetaceans.

The first model (MNvLd) investigated the effect of the increase of the vertebral count and the associated shortening of vertebrae and intervertebral disks (Figure 4.4). Several theoretical backbones with a gradually increasing number of vertebrae starting from the original theoretical backbones were created. The number of vertebrae gradually increases in order to decrease the *Lc/Hc* ratio by 0.05 (starting from 1.15 up to 0.45) between each successive theoretical backbone. The backbone with the highest vertebral count had 102 vertebrae, an *Lc/Hc* ratio of 0.45 and 0.27 cm long disks. These morphological characteristics are close to those of small oceanic delphinoids having the highest vertebral count: the white-beaked dolphin (*L. albirostris*, 91 vertebrae, *Lc/Hc* = 0.45) and the Dall's porpoise (*P. dalli*, 97 vertebrae, *Lc/Hc* = 0.47).

In the first model, two parameters influencing the backbone curvature vary together: the number of vertebrae and the length of the disks. Changing the disk length will impact the stiffness (equations (4) and (6)) and thus the bending angle (equation (7)). The number of vertebrae will influence de force applied on each vertebra (equation (12)) and thus the bending angle (equation (7)). To assess the effect of vertebral and disk shortening without the effect of the number of vertebrae, the backbones of the second model (MLd) have the same variation in disk length as the first model (from

0.69 to 0.27 cm) but all possess 40 vertebrae (Figure 4.4). Hence, each model has a slightly different total body length (gradually decreasing from 2 m to 1.83 m).

The third model investigated the effect of centrum height (MHc). Similar to the first model (MNvLd), *Lc/Hc* ratios varied from 1.15 to 0.45 but this variation was due to changes in centrum and disk height instead of length. Height varied from 3 cm to 7.67 cm. As the leverage increase with centrum height, we build two version of this model. In the first one (MHc1), the leverage was fixed to 1.5cm for all models while in the second one (MHc2), the leverage varied with the centrum height (Figure 4.4).

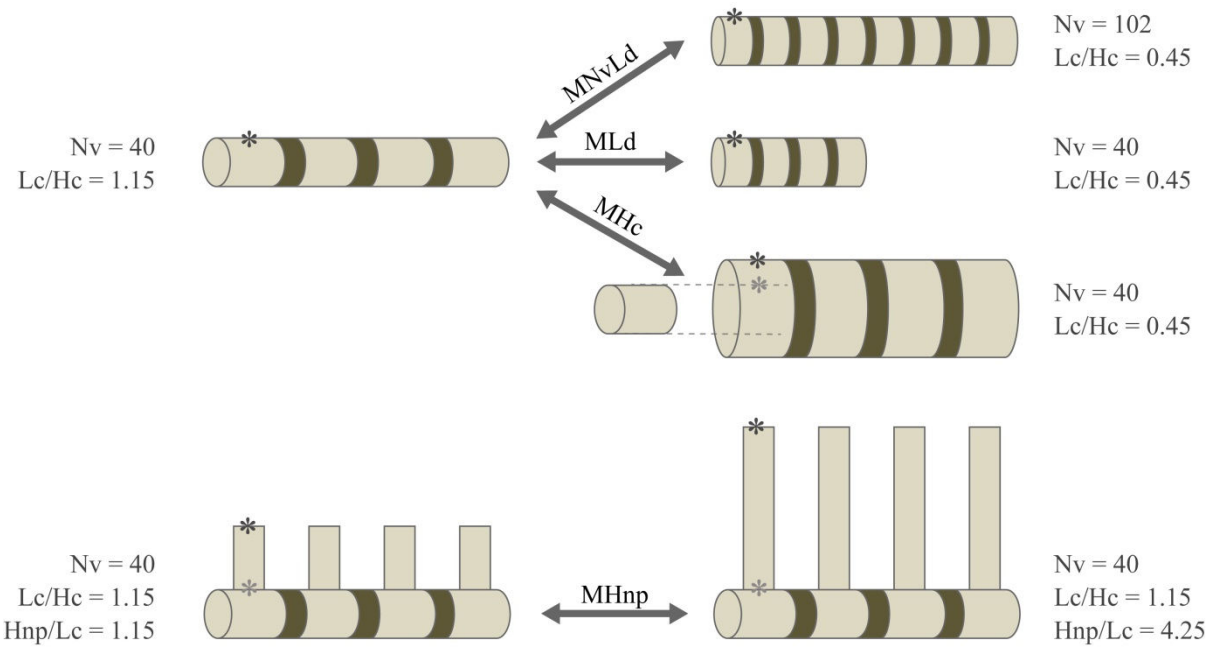

Figure 4.4. Schematic representation of theoretical backbones. Several theoretical backbone models (names indicated on arrows) were used to investigate the effect of vertebral morphology on stiffness and bending. In each model, we gradually modified one of the vertebral features of the original model (left made of 40 vertebrae (*Nv*) with a centrum length-height ratio (*Lc/Hc*) of 1.15 and a neural process height-centrum length ratio (*Hnp/Lc*) of 1.15. Asterisks show the point of insertion of muscles on a single vertebra. For MHc models, light grey asterisk represents insertion for model MHc1 and dark grey asterisk for MHc2. Similarly, for MHnp models, light grey asterisk shows insertion for MHnp1 and dark grey asterisk for MHnp2.

The last model investigated the effect of neural process height (MHnp). Neural processes with varying height were added to the original theoretical backbone (40 vertebrae, *Lc/Hc* = 1.15, *Ld* = 0.69 cm). Neural processes height varied from 3.97 cm to 14.66 cm corresponding to neural process height/centrum length (*Hnp/Lc*) ratio of 1.15 to 4.25 and fall within the range of most small cetaceans (Figure 4.4). For instance, the non-delphinoid estuarine Franciscana (*Pontoporia blainvillei*) has an *Hnp/Lc* ratio of 1.17 and the pelagic white-beaked dolphin (*Lagenorhynchus albirostris*) has a ratio of 4.29. Neural processes width was fixed for all backbones and corresponded to 60% of centrum length as it is for most delphinoids (Table 4.1). Similar to centrum height, neural processes impact backbone bending through the maximal angle allowed by neural spines (equation (8)) and through the leverage if muscles insert on the dorsal tip of neural processes (equation (7)) as observed on dissected specimens and reported in the literature for the *m. longissimus*. Hence, two different models were created. In MHnp1, we consider that muscles insert on the dorsal surface of the vertebral centra. The leverage is then fixed to 1.5 cm. In MHnp2, muscles insert on the tip of neural processes and leverage value varies with process height. Calculating the maximal angle allowed by neural spines require to know the distance between two successive neural processes. We considered that neural processes were centred on their respective vertebral centrum. The distance between two neural processes (Dnp_i) was then equal to:

$$Dnp_i = 0.5\,(Lc_{i-1} - Wnp_{i-1}) + 0.5\,(Lc_i - Wnp_i) + Ld_i \quad \textbf{(14)}$$

where *Wnp* is the neural process width.

2.2.3. Scanned specimens

The compliance, stiffness, curvature angle and vertical displacement were calculated for two scanned specimens: the adult harbour porpoise and the white-beaked dolphin. Morphological measurements from CT-scans were used in the model (see section 2.1.1, this chapter). Their muscular force was estimated using equation (11) which is based on the CSA and muscle stress values.

Several values of muscle stress have been reported for mammals and cetaceans. The model was thus calibrated to select the best muscle stress value. As functional data (videos) have also been collected on harbour porpoises, this species was used as the model species for calibration. Muscle force was calculated using three different muscle stress values (300, 61 and 15 kPa). The theoretical

vertical displacement of the backbone of the CT-scanned harbour porpoise was calculated using the three different muscle force values. The maximal dorsal amplitude of swimming harbour porpoise was obtained from videos. Both the vertical displacement and the amplitude were scaled according to body length of the specimen. The muscle stress value of 15 kPa yielded the closest vertical displacement to the amplitude measured on videos and was conserved for subsequent modelling of scanned and museum specimens.

The force was also estimated based on two different CSA values. The first CSA was the CSA directly measured on the scan (CSA_{scan}). The second CSA was calculated from vertebral shape (CSA_{vert}) (Figure 4.1 *b*). As demonstrated by Arthur *et al.* (2015), epaxial muscles cross-sectional shape is similar to a semi-ellipse with neural and transverse processes as radius and the CSA can then be calculated based on the formula to calculate the area of an ellipse. Hence, the CSA of each vertebra can be calculated as follow:

$$CSA_{vert\ i} = \frac{1}{2}\ \pi\ Hcnp_i\ Lctp_i \quad \textbf{(15)}$$

where $Hcnp_i$ is the distance between the dorsal tip of the neural process and the centre of the corresponding vertebra and $Lctp_i$ is the distance between the distal tip of one of the transverse process and the centre of the corresponding vertebra (Figure 4.1). Both CSA were used to predict the force output of each specimen.

The epaxial musculature responsible for dorsal extension is composed of two muscles, the *m. multifidus* and the *m. longissimus* (Pabst, 1990; Parry, 1949; Slijper, 1936) (Figure S 4.1). Based on CSA measurements of the cross-sectioned harbour porpoise specimen, the CSA of the *m. multifidus* corresponds approximately to 20% of the maximal CSA. The remaining 80% correspond to the *m. longissimus*. These proportions are coherent with muscle weight values reported by Pabst for a bottlenose dolphin (Pabst, 1993). These proportions were thus used for scanned and museum specimens in order to calculate the CSA and total force output of both muscles. Given the highly complex architecture of cetacean epaxial musculature that would be extremely difficult to model, we decided to solely retain main points of muscular insertion of each muscle, mainly based on Parry's description (Parry, 1949) and our observations during dissections. The *m. multifidus* inserts on vertebral metapophyses. The distance between the vertebral centre of rotation and the corresponding

metapophysis was then used as the leverage value for this muscle. The *m. longissimus* inserts on the dorsal tip of the neural processes. Hence, the distance between the rotational centre and the neural process tip was used as leverage value to calculate the bending moment applied by this muscle on each vertebra. The total bending moment applied on each vertebra corresponds to the sum of the bending moment of each muscle. As the *m. multifidus* does not insert on the fluke vertebrae, only the bending moment of the *m. longissimus* was used on fluke vertebrae.

The few first pairs of ribs are double-headed, implying that they insert on two successive vertebrae. Hence, the two successive vertebrae on which a single bicipital rib inserts are connected by bone. The effect of these bicipital ribs was also included in the model to predict body curvature and vertical displacement by using a Young's modulus of 17 GPa, which corresponds to the modulus of cortical bone, for thoracic vertebrae connected by bicipital ribs (Reilly *et al.*, 1974). In cetaceans, fluke vertebrae are extremely small and spaced by long intervertebral disks. Hence, based on our model, this terminal portion of the backbone appears as extremely flexible (see results). However, fluke vertebrae are embedded in the stiff fibrous tissue forming the flukes and there mobility is reduced. This implies that our model overestimates bending amplitude in the flukes. Therefore, we report bending angles including and excluding fluke vertebrae for each specimen.

2.2.4. Museum specimens

As disk lengths (Figure 4.1) are not available on museum specimens, these values were predicted based on scanned specimens. Long *et al.* (1997) found correlations between disk length and some vertebral measurements (vertebra height and transverse processes width). We did not find similar correlations based on our scanned specimens (*P. phocoena* and *L. albirostris*) but the ratio (*Ld/Lc* ratio) between the disk length (Ld_i) and the mean length of the two vertebrae adjacent to the disk (Lc_{i-1} and Lc_i) followed the same pattern along body length (represented by the TCL) for these two specimens (Figure 4.9). Several polynomial curves from order 2 to 16 were fitted on these data using the *lm* function in the built-in R-package *stats*. The model with the lowest Bayesian information criterion (BIC) and for which all coefficients were significant was retained to predict the length of each disk along the backbone of museum specimens. For each museum specimen, several prediction curves were fitted within the prediction interval (from 0% to 99.5% with increments of 0.5%). To avoid biologically improbable predictions, curves having a ratio lower than 0.05 (corresponding to a

1 mm long disk for a 2 cm long vertebra) for at least one of the segments along the backbone were not conserved. The predicted total body length was then calculated for each curve by summing the specimen TCL and skull length to the sum of predicted disk lengths. The curve with the predicted body length closest to the real total body length retrieved from the museum database was then conserved to predict disk length of the specimen. Effect of body size on vertebral centrum and intervertebral disk height and length and on their second moment of area were investigated with a phylogenetic linear regression on log-transformed mean values per species using the *procD.pgls* function from the *geomorph* R-package (v.3.0.7) (Adams *et al.*, 2018).

The CSA of each vertebra was calculated based on vertebral measurements and based on equation (15). The distance between the dorsal tip of the neural process and the centre of the corresponding vertebra ($Hcnp_i$) corresponds to the sum of the transverse process length (Ltp_i) and half the vertebral centrum width (Wc_i) and the distance between the distal tip of one of the transverse process and the centre of the corresponding vertebra ($Lctp_i$) is equal to the sum of the neural process height (Hnp_i), neural arch height (Hna_i) and half the vertebral centrum height (Hc_i) (Figure 4.1 *d*). Hence the CSA of a vertebra is:

$$CSA_{vert\ i} = \frac{1}{2}\,\pi\,\left(Ltp_i + \tfrac{1}{2}Wc_i\right)\left(Hnp_i + Hna_i + \tfrac{1}{2}Hc_i\right) \quad \textbf{(16)}$$

The largest CSA for each specimen was conserved for bending modelling. As we found a 25% difference between CSA_{scan} and CSA_{vert} for *L. albirostris* (see section 3.1.2, this chapter), CSA values for *L. albirostris* museum specimens (NRM 2006653951 and USNM 550208) were increased by 25%. Arthur *et al.* (2015) also investigated the differences between the real CSA and the CSA_{vert} (equation (15)) in eight cetacean species from four different families (*Megaptera novaeangliae*, *Balaenoptera physalus, Mesoplodon europaeus, Mesoplodon mirus, Delphinus delphis, Stenella frontalis, Tursiops truncatus* and *Kogia sima*). *K. sima* was the only investigated species for which the calculated CSA underestimated the true CSA by 40%. Hence, we applied a 40% correction to CSA_{vert} for kogiids (*K. sima* and *K. breviceps*). The CSA_{scan} and CSA_{vert} of CT-scanned *P. phocoena* specimen were similar and Long *et al.* did not find differences between real CSA and CSA_{vert} in species they investigated apart from (Kogiidae). Hence, CSA_{vert} was not corrected for other species included in our model.

Similarly to scanned specimens, we assumed that the *m. multifidus* accounted for 20% of the CSA and the *m. longissimus* for 80% in each species. We considered that the force of each muscle was equally distributed between vertebrae on which it has an insertion. The effect of double-headed ribs was also considered to calculate bending and vertical displacement. We computed the ratio between the CSA and squared body length (CSA/BL^2) to compare CSA, and hence associated muscular force, among species in a body size-standardised manner. We also compared the muscle lever arm between specimens by calculating the ratio between mean neural process height and body length (*Hnp/BL*) and between mean metapophyses height and body length (*Hm/BL*).

The mean vertebral stiffness ($\bar{k}$), total bending angle (θ) and total vertical displacement (Y) of the entire body and of each vertebral region (thoracic, lumbar and caudal) were computed for each specimen. We investigated the effect of body size on these parameters using a linear regression on log-transformed data without and with phylogenetic correction using the functions *lm* from the *stats* R-base package (v.3.5.1) and the *procD.pgls* from the *geomorph* R-package, respectively. For parameters significantly related to body length, phylogenetic residuals of each specimen were computed using the function *phyl.resid.intra* (López-Fernández *et al.*, 2014). Phylogenetic residuals (for parameters related to body size) or raw data (for parameters unrelated to body size) were used to compare species according to habitat (rivers, coasts, offshore, mixed) and phylogenetic group (delphinoids, non-delphinoids). Given the low sample size for riverine specimens, the effect of habitat and phylogeny were not statistically tested. Relationships between parameters or residuals with the vertebral count were also investigated with phylogenetic linear regressions (pgls). Finally, curves of stiffness and vertical displacement along body length were also generated for each specimen. Stiffness curves were body-size corrected using the phylogenetic linear regression used to standardise mean parameters (function *phyl.resid.intra*). Mean curves per habitat for delphinoids were computed with the *ggplot2* R-package (v.3.2.1), using a generalized additive model (GAM) (Wickham, 2016). Due to large morphological variability within non-delphinoids, mean stiffness and displacement curves were computed for each family rather than for each ecological category. All phylogenetic analyses were conducted based on the time-calibrated tree of cetaceans published by Steeman *et al.* (2009) and linear regression were calculated on species mean values.

In order to link results of the predicted backbone flexibility and swimming movements, modelled backbone flexibility parameters of specimens belonging to species recorded on videos were compared. The backbone flexibility was modelled for three of the four species for which swimming videos were recorded: *L. obliquidens* (n = 1), *P. phocoena* (n = 3) and *T. truncatus* (n = 4). No *I. geoffresnsis* specimen was included in the model as their total body length were not available. However, two *Pontoporia blainvillei* specimens were included in the model (Table S 4.1). As this species also belong to the phylogenetic group of 'river dolphins' and has a vertebral morphology similar to *I. geoffresnsis*, it was used for comparison with the three other species recorded on videos.

2.3. Swimming kinematics

In order to quantify swimming kinematics in each species, we used regular kinematic data (e.g., amplitude, frequency) and geometric morphometric methods to analyse video data. The latter method requires the comparison of homologous anatomical points. However, the external morphology of cetaceans does not possess many homologous points that can be easily identified. Particularly, there is no useful landmark in the peduncle region, between the posterior margin of the dorsal fin and the insertion of the flukes. This region of the body plays however a key role for oscillatory movements and its shape changes should be quantified. We hence used the midline of the body, defined as the line at mid-height between the dorsal and ventral sides of the animal, as a curve with sliding landmarks for geometric morphometric analyses.

2.3.1. Video processing

For each video sequence, frames corresponding to a complete swimming cycle (entire upstroke and downstroke) were extracted using the publicly-available VirtualDub software. Each frame was segmented in Amira (v.6.1) to extract the body outline of the animal from the background resulting in binary images with the background in black and foreground (dolphin) in white. The dorsal and pectoral fins were not included in the extracted body outline. The fluke's surface was also not included and only the leading edge facing the camera was outlined (Figure 4.5).

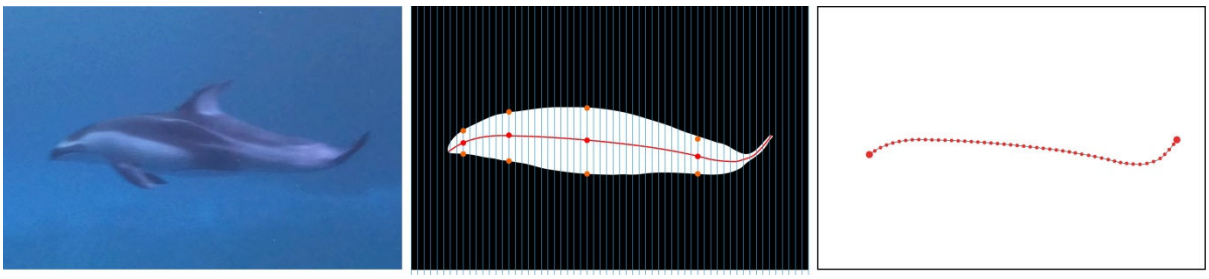

Figure 4.5. Methodology for midlines extraction from videos. Example of midline extraction on a single frame for a Pacific white-sided dolphin (*L. obliquidens*). *(a-b)* For each frame of each sequence, the body outline of the specimen is trimmed manually to obtain a black and white binary image. The margin of the flukes is conserved but not the pectoral and dorsal fins. *(b)* For each pixel row (represented by light blue vertical lines), the custom analysis identify the two points at the transition between fore- and background (orange dots) and calculate the position of the point between these two points (red dots). *(c)* Afterwards, 50 equidistant points are subsampled on the midline. The first and last points (large red dots) being considered as landmarks and the 48 remaining (small red dots) considered as gliding semi-landmarks.

A custom analysis was developed in R to automatically extract the body midline on each frame. For each pixel column of an image, the analysis retains the coordinates (x, y) of the two points at the transition between fore- and background (transition from white to black pixels and vice versa). The position of the point at mid-height between these two points on the pixel column is calculated and its coordinates retained. The resulting midline is defined by coordinates of numerous points, each of them corresponding to a pixel of the image. As the number of pixels of midline varied between videos, depending on the animal body size and the distance between the animal and the camera, 50 points were subsampled along the curve for each frame and each specimen. The first and last points corresponding to the tip of the rostrum and the tip of the fluke were conserved and 48 equidistant points along the curve were subsampled between these two extremities. As animals were not always swimming in a perfect horizontal plane, curves were rotated so that the *x* axis corresponded to the direction of linear displacement of the animal (Mauguit *et al.*, 2010). For each video sequence, the resulting dataset consisted in a group of matrices, each matrix corresponding to a frame of the sequence and containing x and y coordinates of the 50 landmarks.

2.3.2. Data analysis

Amplitude of each point along the body length was calculated from the midlines of each video sequence. As specimens had different body sizes, amplitude was expressed in percent of their body length (%BL). Note that, for backbone flexibility models, the amplitude (or vertical displacement)

measured corresponded to the peak amplitude, i.e., the vertical distance between the horizontal (resting) position and the highest position in dorsal extension. In contrast, the amplitude measured in video analysis is the peak-to-peak amplitude, i.e., the distance between the lowest point in ventral flexion and the highest point in dorsal extension, and is then the double of the peak amplitude. Fluke oscillation frequency was also retrieved from videos by recording the time necessary to complete an entire swimming cycle. As tailbeat frequency decreases with increasing body weight in secondarily aquatic vertebrates, mean species frequencies were body size-corrected using residuals from the equation previously reported ($frequency = 3.56\ mass^{-0.29}$) (Sato *et al.*, 2007).

The shape change occurring during the cycle can be considered as a trajectory in the morphospace where each frame corresponds to a step of the trajectory and the amount of morphological change along the trajectory can be quantified (Adams and Cerney, 2007). To this purpose, we used geometric morphometric methods to quantify shape change during a swimming cycle in each species. As the number of frames constituting a cycle varied depending on the speed of the animal, ten upstroke and ten downstroke frames were subsampled in each sequence, resulting in a group of twenty frames per sequence. The landmarks of all frames were aligned with a generalized Procrustes analysis using the function *gpagen* from the *geomorph* R-package. Among the 50 points of each midline, the first and the last one were considered as landmarks and the remaining 48 equidistant points in-between were considered as sliding semi-landmarks. Standardised shapes are then projected in the tangent space along the two first principal components using the *plotTangentSpace* function from the *geomorph* R-package.

Shape change along the swimming cycle was quantified with three different metrics. The first metric, the kinesis, quantifies the total amount of shape change along the trajectory by summing the linear distance between two consecutive steps for each landmark (frames) (Martinez *et al.*, 2018). In order to describe the type of shape change during a cycle, the quantity of shape modification on the two first principal components (PC1 and PC2) was also quantified by measuring the distance between the minimal and maximal coordinates of a sequence on each axis. All values were averaged by specimen and by species.

3. Results

3.1. Backbone biomechanics modelling

3.1.1. Theoretical backbones

The theoretical models show that increasing the number of vertebrae and therefore decreasing the vertebral centrum and disk length (*Lc, Ld*) (model MNvLd) increases the stiffness of each segment (k_i) and therefore reduces their bending angle (θ_i) (Figure 4.6 *a, b, c*). Although the total stiffness of the backbone (k) remains more or less constant, the total curvature of the backbone (θ) still decreases with increasing vertebral count and decreasing disk length (Figure 4.6 *e, f, g*). When using the same disk length values as model MNvLd but keeping the number of vertebrae fixed to 40 (model MLd), the stiffness for a single segment and the total bending of the backbone are similar to models where the number of vertebrae varies (Figure 4.6 *a, b, g*) but the total stiffness of the backbone increases with decreasing disk length (Figure 4.6 *e, f*). At equivalent disk lengths, the bending angle of a single segment is higher if the number of vertebrae is fixed to 40 than if it increases (Figure 4.6*c*).

In models having the same disk length/height ratio (*Ld/Hd*) than models MNvLd and MLd but where the disk height (*Hd*) is the varying parameters instead of vertebral count and disk length (models MHc1 and MHc2), the segment and backbone stiffness increase dramatically with decreasing ratio (Figure 4.6 *a, e*). The resulting bending angles are also smaller (Figure 4.6 *c, g*). The curvature is slightly higher in the model accounting for the effect of increasing leverage with increasing centrum height (MHc2) than in the model with fixed leverage (MHc1).

Finally, for the model investigating the effect of neural processes height (models MHnp1 and MHnp2), the stiffness is not affected and is thus constant (segment stiffness = 12.73, backbone stiffness = 0.33). The maximal bending angle allowed by neural processes (θ_{np}) decreases with increasing processes height (brown line on Figure 4.6 *d, h*). In the model that does not account for increased leverage (MHnp1), the bending angle remains lower than the maximal possible angle and thus neural process height (*Hnp*) does not impact the resulting bending angle. However, when accounting for the effect of increasing leverage due to higher processes height (model MHnp2), the bending angle increases with process height but, at some point, it becomes higher than the maximal allowed angle and the movement is then restricted by the contact of two successive neural processes.

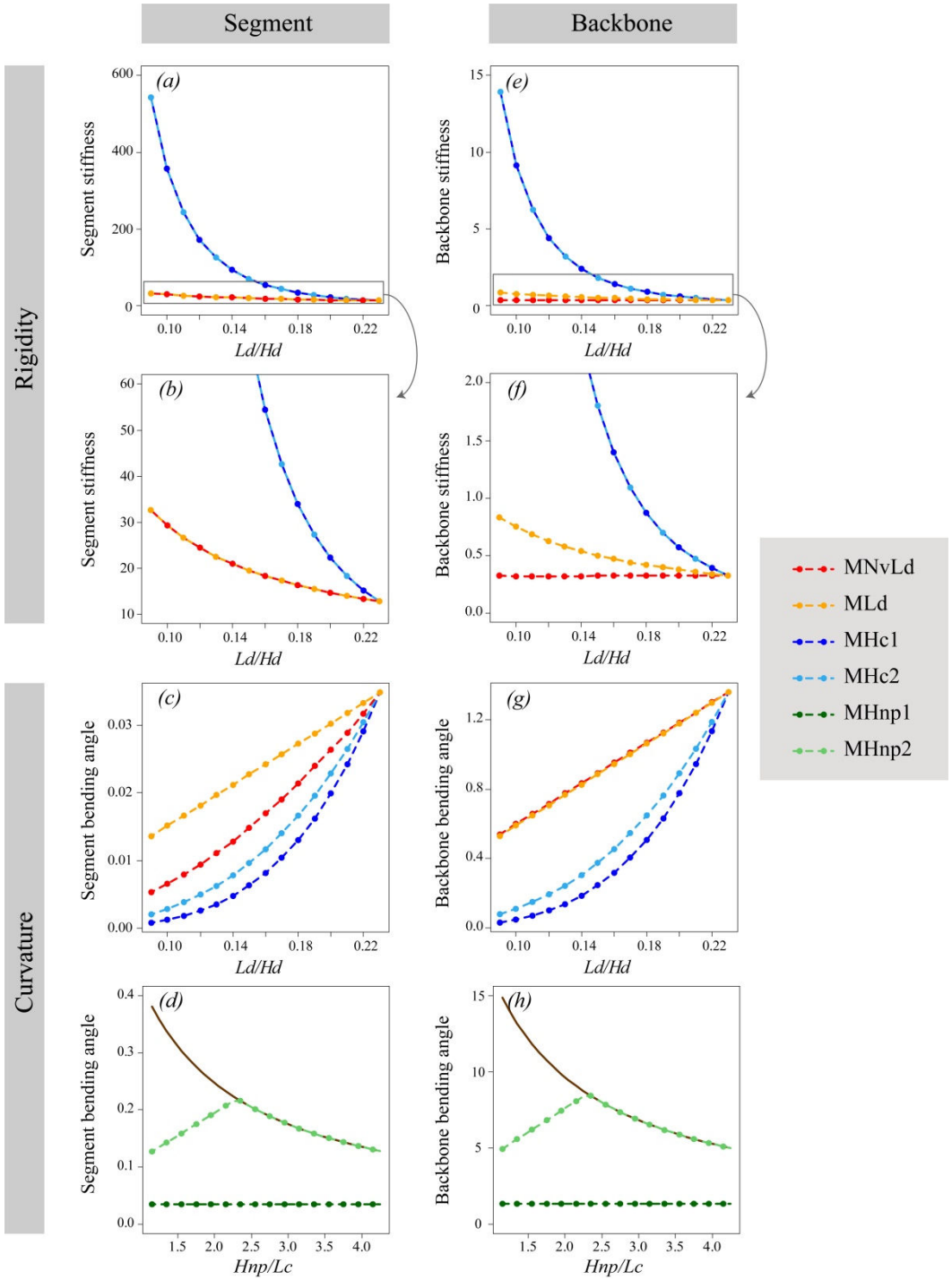

Figure 4.6. Stiffness and bending of theoretical backbones. *(a-d)* Stiffness and curvature for a single segment (one disk and the two surrounding vertebrae) along the backbone, *(e-h)* stiffness and curvature for the entire backbone. *(b)* and *(f)* Expanded portion represented by the grey frame in *(a)* and *(e)* respectively. Each coloured line corresponds to a theoretical backbone: for MNvLd (red) the number of vertebrae increases (from 40 to 102) which reduces the centrum and disk length (*Ld*) relative to their height (*Hd*), in the remaining models, the number of vertebrae in constant (40), in MLd (orange) only the disk length decreases, for MHc the centrum and disk height increase and leverage is either constant (MHc1, dark blue) or varies with centrum height (MHc2, light blue), for MHnp only the neural processes height (*Hnp*) varies in proportion to vertebral length (*Lc*) and the leverage is either constant (MHnp1, dark green) or varies with *Hnp* (MHnp2, light green). The brown line in *(d)* and *(h)* shows the maximal angle allowed by neural processes height (θ_{np}).

3.1.2. Scanned specimens

Intervertebral disks of *L. albirostris* (mean disk stiffness = 66.19 N/m) are, in average, stiffer than those of *P. phocoena* (mean disk stiffness = 10.05 N/m) (Figure 4.7 *a*). Both species presents same stiffness trend along their body length (detailed hereafter). The thoracic and anterior lumbar regions are relatively flexible; however, the effect of bicipital ribs is not included here. The stiffest point is at approximately 60% of the body length. It falls just at the lumbo-caudal transition in *L. albirostris* and in the posterior portion of the lumbar region in *P. phocoena*. After that point, stiffness decreases in two steps. It first decreases in the anterior part of the caudal region, and then stabilizes in the mid-caudal region at approximately 85% of body length before decreasing dramatically in the posterior caudal region and at the fluke insertion.

The CSA directly measured on scan (CSA_{scan}) and modelled from vertebral shape (CSA_{vert}) only differed by 5% for *P. phocoena*. However, the CSA_{vert} only accounted for 75% of the CSA_{scan} for *L. albirostris* because epaxial musculature extends beyond transverse and neural processes in this species. Hence, we expect to obtain different bending angles and vertical displacements for *L. albirostris* depending on the CSA used.

Similarly to stiffness, the average bending angle of each disk is lower for *L. albirostris* (mean θ_d = 0.92°; mean θ_d without fluke disks = 0.50°) than for *P. phocoena* (mean θ_d = 1.52°; mean θ_d without fluke disks = 0.70°) when using CSA_{scan} (Figure 4.7 *b*). With CSA_{vert}, the mean bending angle of *P. phocoena* is similar (mean θ_d = 1.62°; mean θ_d without fluke disks = 0.74°) but the mean bending angle of *L. albirostris* changes (mean θ_d = 0.68°; mean θ_d without fluke disks = 0.37°). Angles in the posterior caudal region are similar in both species. In the most anterior part of the thoracic region, bending angles are close to 0° due to the effect of bicipital ribs that limit movements between successive vertebrae in that region. Due to drastic decrease in stiffness of the few last disks, bending angles are extremely high in the fluke. For both species, bending angles are largely lower than angles allowed by neural spines (mean θ_{np} *L. albirostris* = 4.31°; mean θ_{np} *P. phocoena* = 8.20°) or by neural arches (mean θ_{na} *L. albirostris* = 5.23°; mean θ_{na} *P. phocoena* = 11.23°).

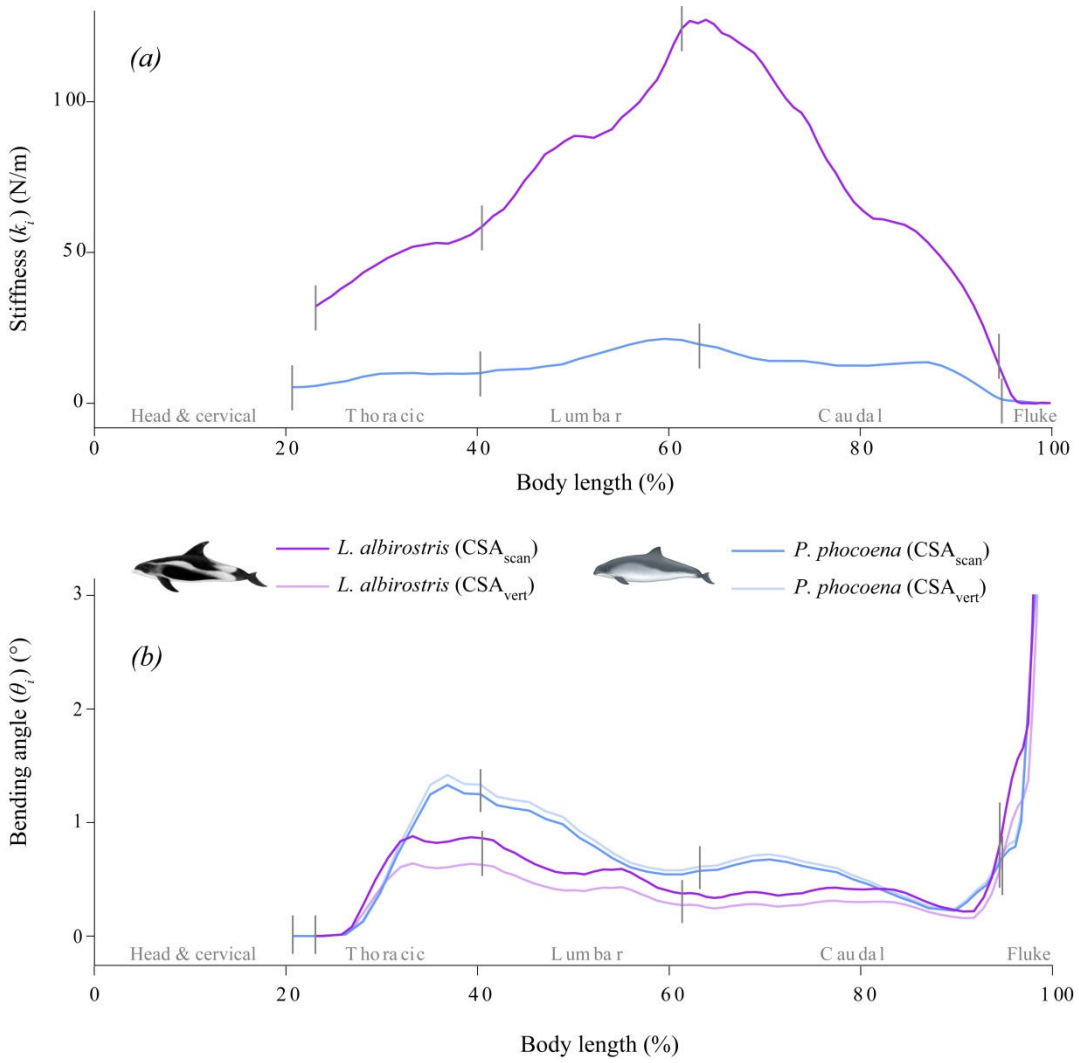

Figure 4.7. Individual disk stiffness and bending angle along body length. (*a*) Stiffness and (*b*) bending angle of each disk along the body length for two CT-scanned species: the white-beaked dolphin (*L. albirostris*) represented by purple lines and the harbour porpoise (*P. phocoena*) represented by blue lines. Dark purple and blue lines in (*b*) correspond to bending obtained with the muscle cross-sectional area (CSA) measured on CT-scans (CSA_{scan}) and lighter coloured lines correspond to bending obtained with the CSA modelled from vertebral shape (CSA_{vert}). Vertical grey lines indicate the transitions between two vertebral regions for each specimen.

Cumulated bending and cumulated vertical displacement also varied depending on the CSA used. With CSA_{scan}, *L. albirostris* has a body curvature ($\theta = 70.47°$; θ without fluke = 33.23°) and vertical displacement ($Y = 24.83\%$ body length) slightly higher than *P. phocoena* ($\theta = 73.34°$; θ without fluke = 27.50°; $Y = 21.07\%$ body length) despite its stiffer backbone (Figure 4.8). However, with CSA_{vert}, its body curvature and vertical displacement ($\theta = 51.56°$; θ without fluke = 24.06°; $Y = 18.57\%$ body length) are lower than *P. phocoena* ($\theta = 77.92°$; θ without fluke = 29.79°; $Y = 22.34\%$ body length). Whereas the total bending sharply increases in the fluke, this pattern is not

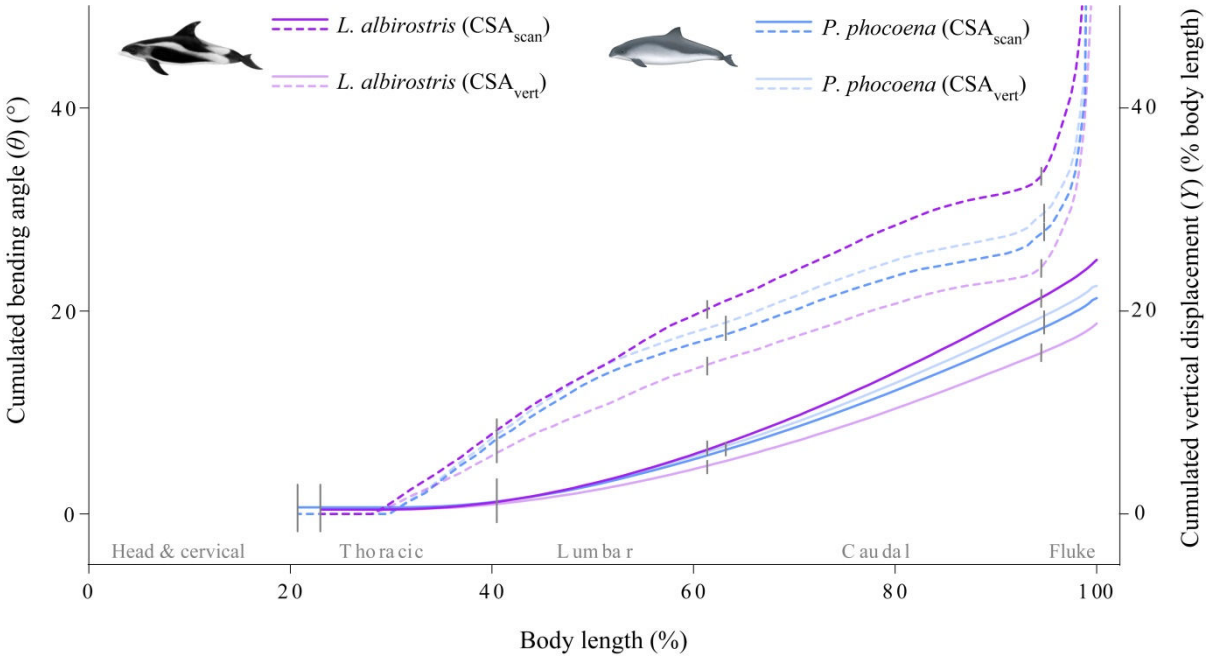

Figure 4.8. Cumulated bending angle and vertical displacement along body length. Dotted lines show the cumulated bending angles and solid lines show the vertical displacement along the body length of the white-beaked dolphin (*L. albirostris*) (purple) and the harbour porpoise (*P. phocoena*) (blue). Darker colour lines correspond to bending obtained with the muscle cross-sectional area (CSA) measured on CT-scans (CSA_{scan}) and lighter colour lines correspond to bending obtained with the CSA modelled from vertebral shape (CSA_{vert}). Vertical grey lines indicate the transitions between two vertebral regions for each specimen.

observed for the cumulated vertical displacement. For both species, the cumulated displacement at the thoraco-lumbar transition is extremely limited and inferior to 2% of body length. At the lumbo-caudal transition, the cumulated vertical displacement is close to 6% of body length. Overall, *L. albirostris* has stiffer intervertebral disks than *P. phocoena*. However, due to its enlarged CSA, it has a larger cumulated bending angle and vertical displacement of the backbone.

3.1.3. Museum specimens

The best fit polynomial retained to predict disk lengths of museum species was an order 9 polynomial ($R^2 = 0.85$) (Figure 4.9). The difference between body length obtained based on predicted disk lengths and real body length was always smaller than 8% (mean difference = 2.38%) except for *M. densirostris* (USNM 550741) for which the difference was 9.42% (Table S 4.1). Vertebral centra length and height as well as intervertebral disk length and second moment of area significantly increase with body size (Figure S 4.2). Disk and centrum height significantly increases with body size (PGLS: *P*-value = 0.001, $R^2 = 0.92$, slope = 0.94) at a lower rate than their respective length (PGLS disk

length: *P*-value = 0.001, R^2 = 0.71, slope = 1.24; PGLS centrum length: *P*-value = 0.001, R^2 = 0.76, slope = 1.14). On the contrary, the second moment of area of intervertebral disks increases with body size at a much higher rate (PGLS: *P*-value = 0.001, R^2 = 0.92, slope = 3.76).

Body size had a significant effect on CSA (PGLS: *P*-value = 0.001, R^2 = 0.89, slope = 1.68), neural spine height (PGLS: *P*-value = 0.001, R^2 = 0.86, slope = 0.94) and metapophyses height (PGLS: *P*-value = 0.001, R^2 = 0.94, slope = 0.91). Therefore, these variables were size-corrected to make comparison among species. Several species such as the Franciscana dolphin (*Pontoporia blainvillei*), the Northern right whale dolphin (*Lissodelphis borealis*), the pantropical spotted dolphin (*Stenella attenuata*) and blackfishes (*Globicephala macrohrynchus, Peponocephala electra* and *Feresa attenuata*) have a CSA lower than most species (Figure S 4.3). Among these species, *L. borealis* and *P. blainvillei* also possess lower lever arms for the *m. multifidus* and *m. longissimus*. On the contrary, other species have an increased muscular CSA, in particular Kogiidae (*K. sima* and *K. breviceps*), the white-beaked dolphin (*L. albirostris*) and the Dall's porpoise (*Phocoenoides dalli*). The latter, as well as beaked whales (*Mesoplodon* spp., *Ziphius cavirostris* and *Tasmacetus shepherdi*), have extremely developed neural spines resulting in a large leverage for the *m. longissimus*.

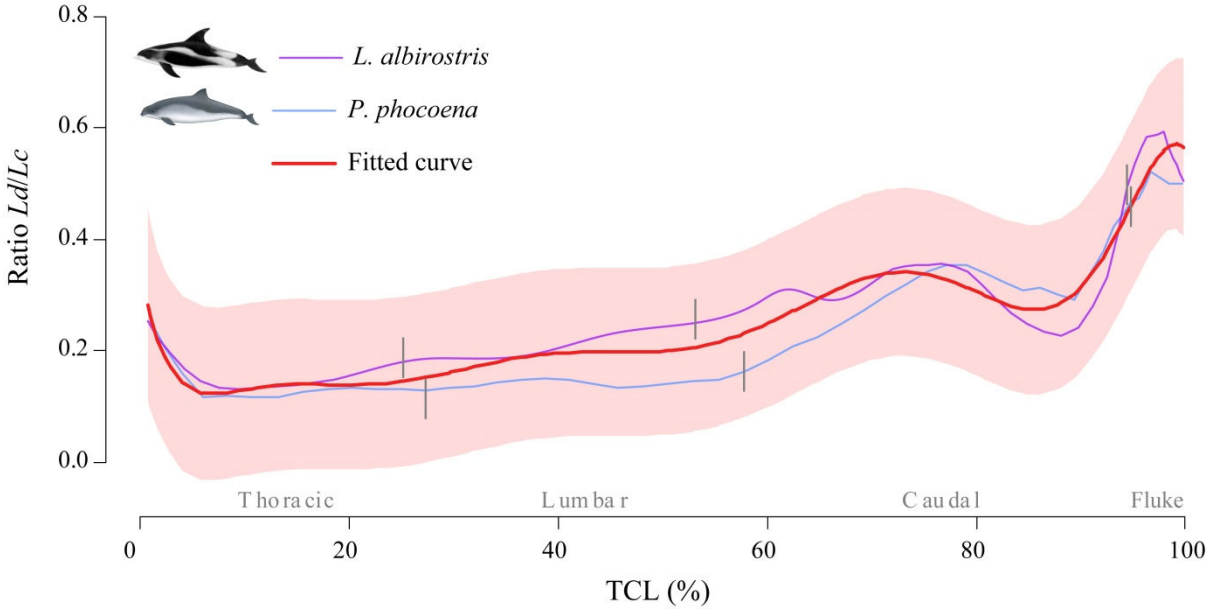

Figure 4.9. Evolution of the *Ld/Lc* ratio along body length of scanned specimens. Ratio between the disk length and the mean centrum length of the two adjacent vertebrae (*Ld/Lc* ratio) along the total centrum length (TCL) of scanned specimens: *L. albirostris* (purple line) and *P. phocoena* (blue line). Both species have similar ration patterns along their body length. The best fit polynomial for the two species is represented by the red line. The light red area corresponds to the 99% prediction interval. Vertical grey lines show transitions between vertebral regions for each specimen.

As body size has a strong impact on the mean stiffness of the entire body (PGLS: *P*-value = 0.001, R^2 = 0.83, slope = 2.61) (Figure S 4.4) and in each vertebral region (thoracic: *P*-value = 0.001, R^2 = 0.81; lumbar: *P*-value = 0.001, R^2 = 0.81; caudal: *P*-value < 0.001, R^2 = 0.82) (Table S 4.2), stiffness was size-corrected to allow comparison between species with different body sizes. Mean body stiffness significantly increases with the number of vertebrae (PGLS: *P*-value = 0.001, R^2 = 0.54, slope = 0.020) (Table S 4.2). Coastal, mixed and offshore delphinoids have higher mean body stiffness than riverine delphinoids and all non-delphinoids except the unique coastal non-delphinoid from our dataset (the North Atlantic right whale, *Eubalaena glacialis*) (Figure 4.10). These differences are particularly apparent in the lumbar region. In the thoracic region, most non-riverine delphinoids are stiffer than non-delphinoids but there is some overlap. In the caudal region non-delphinoids and riverine delphinoids completely overlap with other delphinoids except for some extremely stiff delphinoids. Curves of segment stiffness along the backbone show that offshore, coastal and mixed delphinoids have an increased stiffness at approximately 60% of their body length, which corresponds to the lumbo-caudal transition. This pattern is not observed in riverine delphinoids (Figure 4.11).

Total bending angle and vertical displacement (expressed in percentage of body length) are significantly but poorly related to body length (PGLS θ: *P*-value = 0.027, R^2 = 0.114, slope = -0.069; PGLS *Y*: *P*-value = 0.030, R^2 = 0.11, slope = -0.078) and thus, were not size-corrected (Table S 4.3). The mean bending angle significantly decreases with increasing vertebral count for all regions of the body, the effect being the greatest in the lumbar region (PGLS body: *P*-value = 0.004, R^2 = 0.24, slope = -0.022; PGLS lumbar: *P*-value = 0.001, R^2 = 0.58, slope = -0.041). Species with higher vertebral count have significantly lower cumulated bending in the thoracic (*P*-value = 0.049, R^2 = 0.10, slope = -0.019) and lumbar regions (*P*-value = 0.012, R^2 = 0.16, slope = -0.019) and lower cumulated displacement in the thoracic region (*P*-value = 0.005, R^2 = 0.21, slope = -0.009) but effect are relatively small (Table S 4.3). Within delphinoids, the cumulated bending angle tends to be higher for riverine species than for other species, except in the caudal region (Figure 4.10). The same trend is also observed for the cumulated vertical displacement in the thoracic region. In offshore delphinoids, *L. albirostris* is the stiffest species (k = 1.37) and *P. dalli* is the fourth stiffest (k = 0.75). However, *P. dalli* has the second highest amplitude (Y = 21.7% body length) and has an amplitude comparable to more

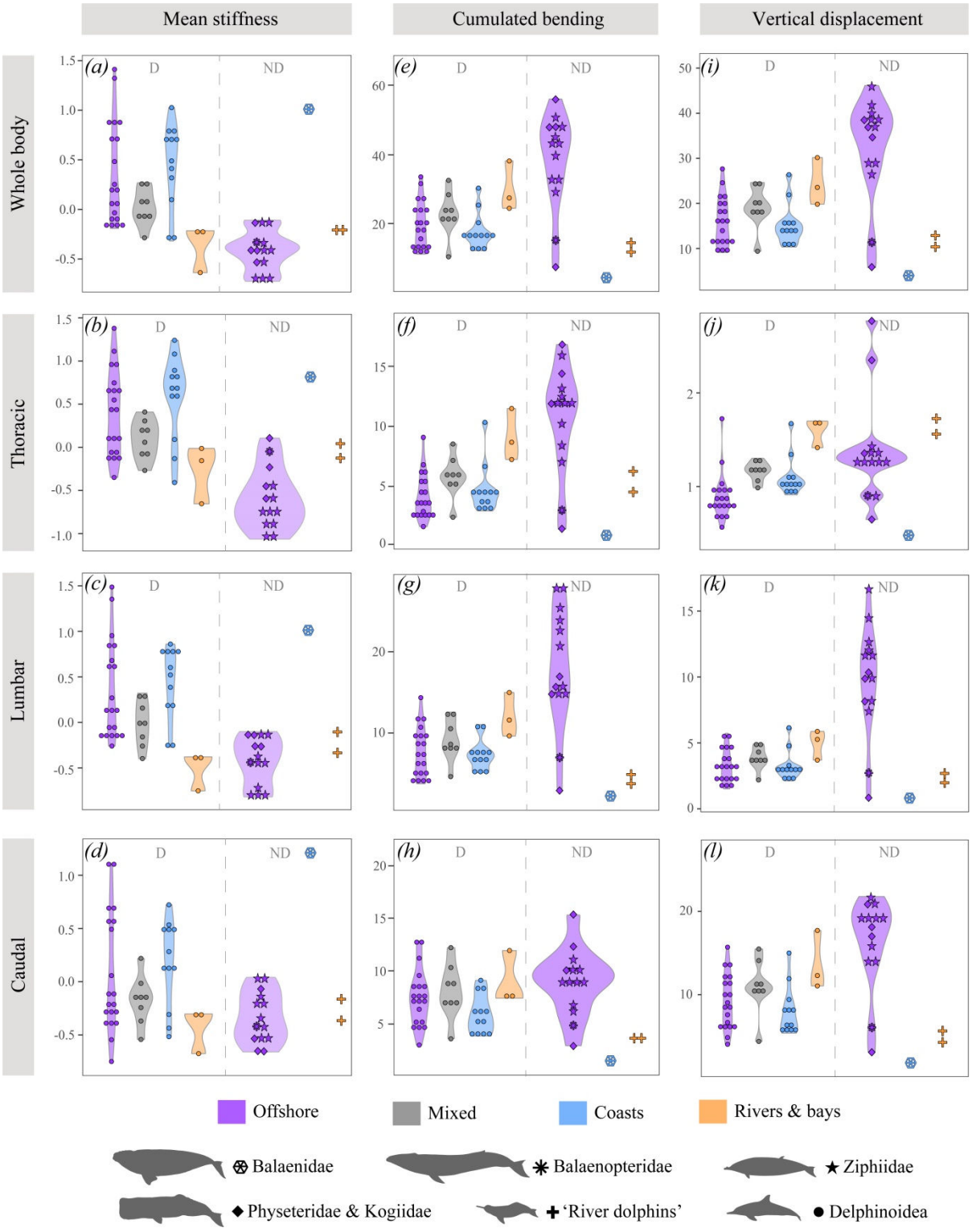

Figure 4.10. Relationship between backbone biomechanics, phylogeny and habitat. Violin plots of (*a-d*) standardised mean stiffness, (*e-h*) cumulated bending angle (in degrees) and (*i-l*) cumulated vertical displacement (in body length %) for (*a, e, i*) the entire backbone, (*b, f, j*) the thoracic region, (*c, g, k*) the lumbar region and (*d, h, l*) the caudal region. Delphinoids are on the left side of each graph (*D*) and non-delphinoids on the right side (*ND*). Habitats are represented by different colours. Each point on the graphs corresponds to a specimen.

flexible species (e.g., *Stenella clymene*, k = -0.12, Y = 24.5% body length), whereas *L. albirostris* has the lowest amplitude (Y = 10.1% body length). On the contrary, *L. borealis* is the most flexible offshore delphinoid (k = -0.19) but has a low amplitude similar to *L. albirostris* (Y = 10.1%). Most offshore non-delphinoids (except the sperm whale, *Physeter macrocephalus* and the blue whale, *Balaenoptera musculus*) have a cumulated vertebral bending higher than offshore or coastal delphinoids for the whole body and in the thoracic and lumbar regions but not in the caudal region. Similarly, they also tend to have a higher vertical displacement than offshore delphinoids, mainly in the lumbar region. Despite their more flexible backbone, riverine non-delphinoids do not have a higher bending angle or vertical displacement than coastal and offshore delphinoids, excepted in the thoracic region where their vertical displacement is comparable to riverine delphinoids. *E. glacialis* always has the lowest bending angle and vertical displacement of specimens included in our analyses.

Regarding species recorded on videos for kinematic anaylses, *L. obliquidens* has the stiffest backbone both for mean and cumulated stiffness (mean size-corrected stiffness = 0.86; cumulated size-corrected stiffness = 0.36). For mean stiffness, *P. phocoena* is the second stiffest (0.19 ± 0.39), followed by *T. truncatus* (0.04 ± 0.15) and *P. blainvillei* (-0.21 ± 0.01). However, for cumulated stiffness, *P. blainvillei* (0.12 ± 0.04) is surprinsingly stiffer than *P. phocoena* (-0.09 ± 0.29) and *T. truncatus* (-0.17 ± 0.11). Similarly, mean bending, total bending and displacement are always lower for *L. obliquidens* (mean θ = 0.24°; θ = 13.57°; Y = 11.4 %BL) than for *P. phocoena* (mean θ = 0.41 ± 0.14°; θ = 18.98 ± 6.17°; Y = 15.1 ± 5.33 %BL) and then *T. truncatus* (mean θ = 0.54 ± 0.09°; θ = 23.65 ± 3.65°; Y = 20.24 ± 2.76 %BL). *P blainvillei* has a high mean bending, comparable to *T. truncatus*but a low cumulated bending and displacement, similar to *L. obliquidens* (mean θ = 0.53 ± 0.07°; θ = 13.52 ± 1.93°; Y = 11.61 ± 1.65 %BL). Nonetheless, *P. blainvillei* always has the highest predicted flexibility, bending and displacement in the thoracic region (see Table S 4.4 for values detailled for each vertebral region).

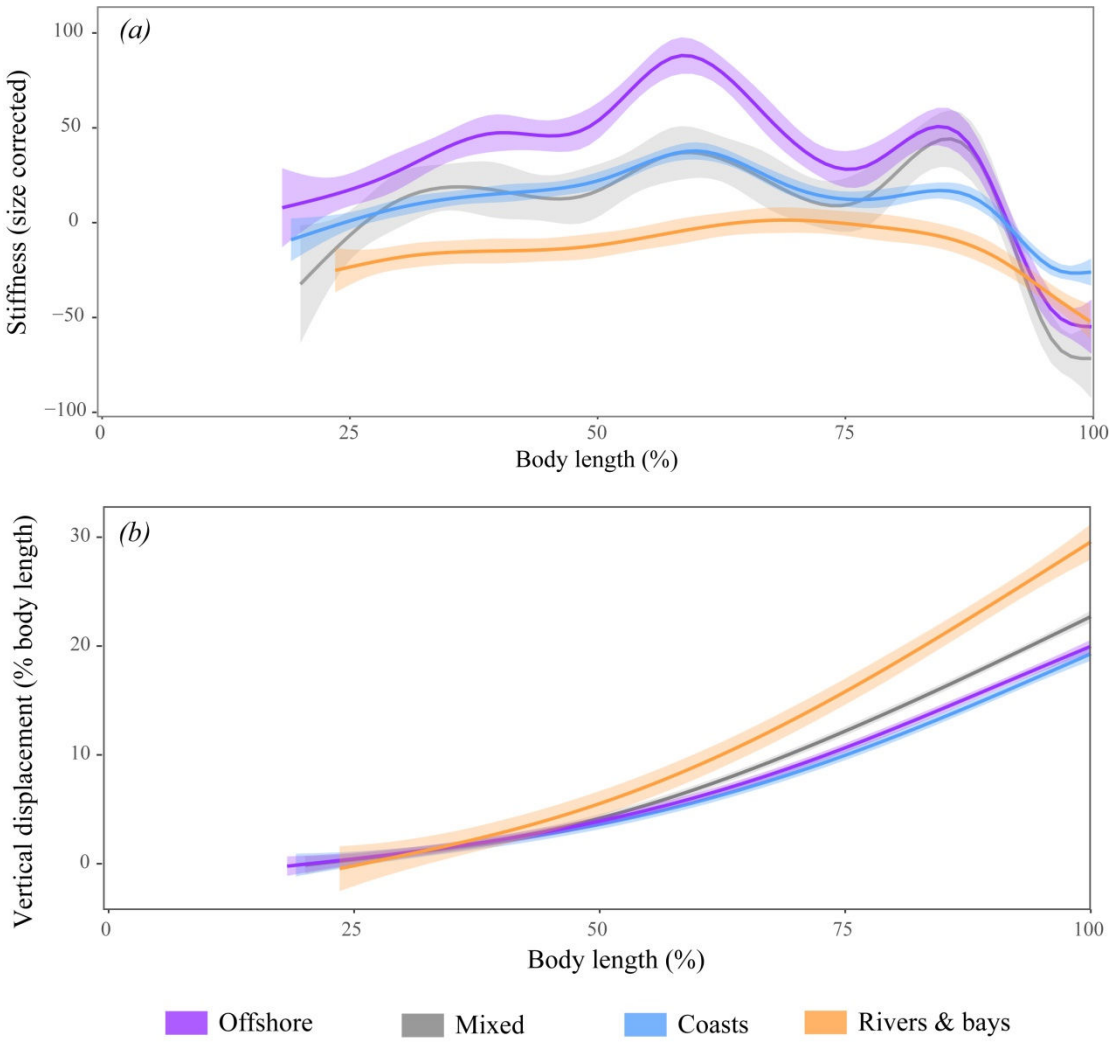

Figure 4.11. Stiffness and amplitude along body length of Delphinoids. *(a)* Size-corrected stiffness and *(b)* vertical displacement along body length per habitat category for delphinoids. Each curves correspond to the mean per habitat with its 95% confidence interval.

3.2. Swimming kinematics

Maximal fluke amplitude is always comprised between 20 and 30 % of the body length (%BL) (Figure 4.12*a*). In average the total amplitude of *I. geoffrensis* is slightly higher (28.2 %BL) than other species. Total amplitude (mean ± S.D.) also gradually decreases from *P. phocoena* (25.19 ± 2.13), to *T. truncatus* (22.76 ± 3.92), and to *L. obliquidens* (21.47 ± 3.11). However differences are low and there is a large overlap between standard deviations for all species. *I. geoffrensis* has higher movement amplitude than other species along its body length and especially in the anterior region of the body (Figure 4.12*b*).

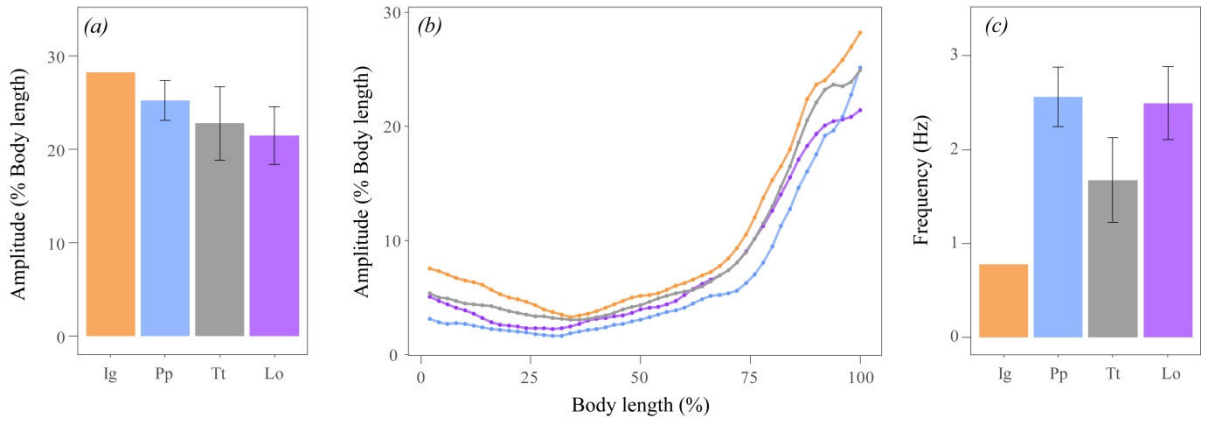

Figure 4.12. Amplitude and frequency of each species. *(a)* Mean maximal amplitude, *(b)* mean amplitude (in body length percent) along body length, *(c)* stroke frequency for each species. Standard deviations are represented by vertical lines and correspond to the variability between individuals of the same species. *Ig: Inia geoffrensis* (orange), *Pp: Phocoena phocoena* (blue), *Tt: Tursiops truncatus* (grey), *Lo: Lagenorhynchus obliquidens* (purple).

Differences in tailbeat frequency are more important. *I. geoffrensis* has the lowest frequency (mean = 0.79 Hz; body size corrected = -0.15), *P. phocoena* (mean ± S.D. = 2.56 ± 0.31 Hz; body size-corrected = 1.36 ± 0.31) and *L. obliquidens* (2.49 ± 0.39 Hz; body size-corrected = 1.53 ± 0.35) have the highest frequency and *T. truncatus* (1.68 ± 0.45 Hz; body size-corrected = 0.91 ± 0.44) has an intermediate frequency (Figure 4.12*c*).

The two first principal components (PC1 and PC2) of the geometric morphometric analysis of midline shapes explain 90.66% of the total variance (Figure 4.13*a*). PC1 accounts for 77.10% of total variance and corresponds to the curvature movements of the peduncle. PC2 corresponds to 13.56% of total variance and is associated with curvature of the anterior part of the body and the oscillations of the flukes on the peduncle. *I. geoffrensis* tends to have the highest shape change on PC1 (0.229), on PC2 (0.089) and the highest kinesis (0.638) (Figure 4.13*b, c, d*). On the contrary, *L. obliquidens* had the lowest kinetic shape deformation on PC1 (0.181 ± 0.022), PC2 (0.068 ± 0.012) and also the lowest kinesis (0.484 ± 0.069). The amounts of shape variation of *P. phocoena* (PC1 = 0.182 ± 0.016; PC2 = 0.087 ± 0.001; kinesis = 0.546 ± 0.002) and *T. truncatus* (PC1 = 0.207 ± 0.026; PC2 = 0.082 ± 0.012; kinesis = 0.569 ± 0.078) are intermediate between *I. geoffrensis* and *L. obliquidens* for the three different metrics.

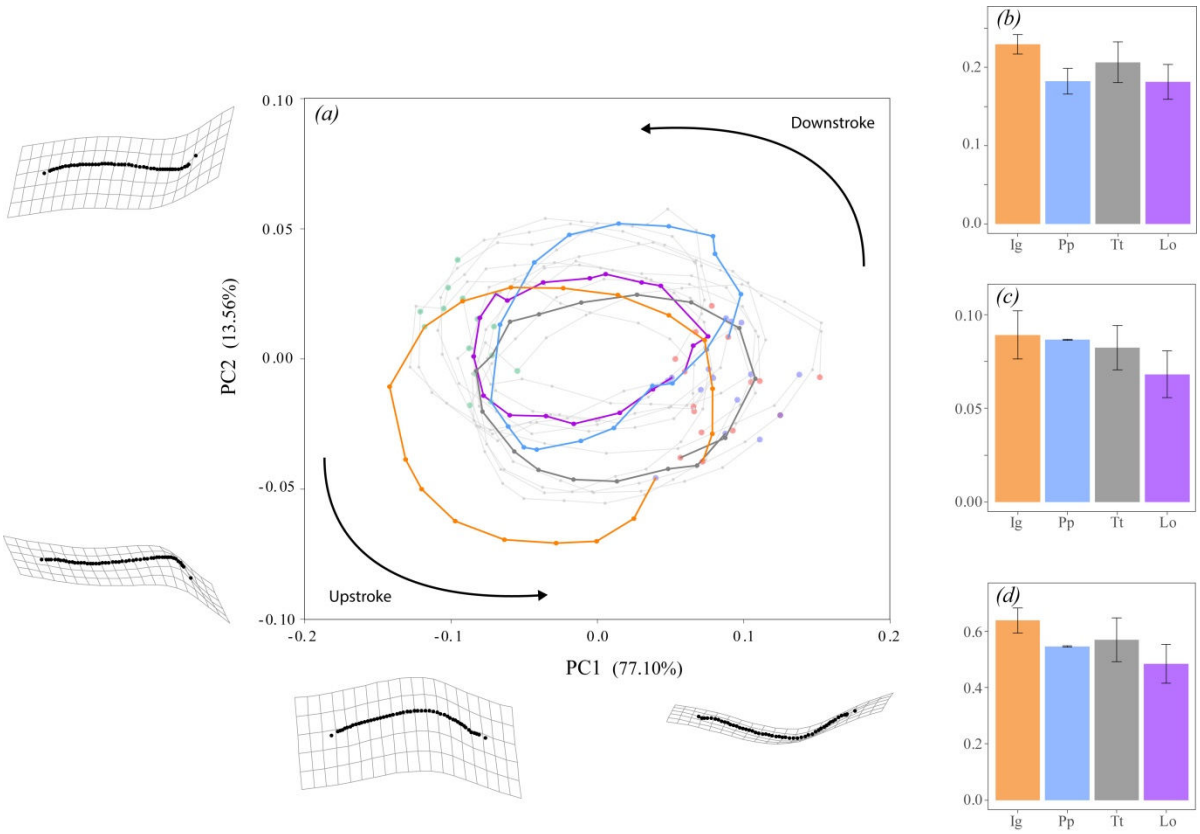

Figure 4.13. Geometric morphometric analysis of swimming movements. *(a)* Scatter plot of the two first principal components of the geometric morphometric analysis of swimming movements. Deformation grids show midline shape modification along each axis (animal head on the left side of the grids). PC1 (77.10%) is associated with peduncle curvature while PC2 (13.56%) corresponds to changes in curvature of the anterior region of the body and to the fluke oscillations. Each point on the graph corresponds to a frame. All frames belonging to the same cycle are connected by lines. A representative cycle is shown in colour for each species. Red dots correspond to the first frame of the sequence (maximal dorsal extension), green dots to the 10th frame of the sequence (maximal ventral bending) and blue dots to the last frame of the sequence (back in maximal dorsal extension). *(b-c)* Maximal shape change on PC1 *(b)* and PC2 *(c)* during a cycle. *(d)* Total kinesis during a cycle. Error bars correspond to the variability between specimens. Each colour corresponds to a species: *I. geoffrensis* (orange); *P. phocoena* (blue); *T. truncatus* (grey); *L. obliquidens* (purple).

4. Discussion

By using vertebral morphology and beam theory to model backbone biomechanics of several cetacean species, we showed that variation in intervertebral disks shape, vertebral morphology, and body size have a significant impact on the stiffness and maximum curvature of the backbone in dorsal extension. Our predictions show that mean stiffness tend to increase in coastal and offshore delphinoids compared to non-delphinoids and riverine delphinoids. Moreover, kinematic data from videos of four cetacean species suggest that stiffer species exhibit slightly reduced body deformation during a swimming cycle and tend to oscillate their fluke at higher frequencies.

4.1. Parameters influencing backbone stiffness and motion

Based on our model, the main parameter influencing backbone stiffness is the ratio between intervertebral disk height and length (*Ld/Hd*) (equation (4)). For a given body length, an increase in the number of vertebrae corresponds to a shortening of each vertebrae and intervertebral disk, hence reducing the *Ld/Hd* ratio. This implies that the stiffness of each individual disk should increase with increasing vertebral count. However, our model suggests that the total (cumulated) stiffness of the entire backbone remains approximately constant with increasing vertebral count. Thus, a backbone with a few flexible segments has a cumulated stiffness equivalent to a backbone with numerous stiff segments (Figure 4.10). This trend is also visible in species included in this study as we did not find a significant relationship between backbone stiffness and vertebral count (Table S 4.2). Nonetheless, the total backbone curvature is lower in specimens with numerous stiff segments. The total curvature of the theoretical backbone with decreasing disk length but constant vertebral count (MLd) decreases with decreasing *Ld/Hd* ratio in the same manner as the backbone with increasing vertebral count (MNvLd). This suggests that the lower backbone curvature observed in backbones with higher vertebral count is not due to the distribution of total muscular force on a higher number of vertebrae but to the increased stiffness of each segment.

Predicted stiffness and bending of theoretical backbones also highlight the dual role of neural spines. For a given vertebral centrum and disk morphology, higher neural spines should reduce the potential maximal angle between two successive vertebrae before apophyses overlap each other and should consequently reduce curvature in the backbone. On the other hand, higher neural spines also increase the leverage for the *m. longissimus* providing higher bending angle. It seems however that neural spines only have an effect on backbone movements through leverage increase as the bending angle of each disk resulting from stiffness and bending moment was always smaller than the maximal angle permitted by neural spines. Based on experimental testing of backbone stiffness in a common dolphin, Long *et al.* (1997) predicted that a typical stiff vertebral segment in dolphins would be characterised by short intervertebral disks with a large diameter and short vertebral centra which in agreement with our results. The positive correlation between centrum height and joint stiffness has also been reported for crocodilians by experimentally testing intervertebral disks stiffness and mobility (Molnar *et al.*, 2014). In sharks, intervertebral disk width is also correlated to the animal bending ability in lateral flexion, although, in that precise case, the bending abilities increased with

increasing vertebral width (i.e., stiffness) (Porter *et al.*, 2009). Long *et al.* (1997) also predicted that a stiff segment would have high neural spines as it would increase the second moment of area of interspinous ligaments that reduce segment flexibility in ventral flexion and dorsal extension. Including the effect of these ligaments on backbone stiffness in future works could improve the model and provide better stiffness prediction. Furthermore, higher neural spines result in a larger body diameter and can hence contribute to increase body stiffness.

Finally, body size also has an important effect on backbone stiffness; larger species having stiffer intervertebral disks (Table S 4.2). Increasing stiffness with body size has been documented in several terrestrial mammalian clade and helps counteracting the increasing effect of gravity with increasing body mass (Gál, 1993a; Halpert *et al.*, 1987; Jones, 2015; Smeathers, 1981). However, pinnipeds appear to follow a different trend, probably related to their aquatic lifestyle, as morphological data suggest that the backbone of large species would instead be more flexible than smaller species (Jones and Pierce, 2016). This conclusion was based, in part, on the fact that larger pinniped species have more spool-shaped vertebrae than smaller ones. Our results show a similar trend as centrum and disk height increases with body size at a lower rate than their respective length (Figure S 4.2). However, stiffness is proportional to the second moment of area which is related to disk height in an exponential way rather than in a linear one (equation (4)). This implies that the second moment of area of a disk increases at a higher rate than its length (Figure S 4.2), leading to increased stiffness in larger species. We assume that a similar trend should be found in pinnipeds if stiffness is expressed proportionally to the vertebral second moment of area. We however expect that the rate of rigidity increase with body size would be lower for pinnipeds and cetaceans than for terrestrial mammals, still reflecting a change in constraints applied on the backbone associated with the land-to-water transition as proposed by Jones and Pierce (2016).

4.2. Backbone stiffness, swimming movements and ecology

Results of stiffness modelling show that delphinoids, except riverine species, tend to have the stiffest intervertebral joints, especially in the thoracic and lumbar regions (Figure 4.10). Due to intervertebral disk shortening, mean joint stiffness also significantly increases with vertebral count (Table S 4.2). A similar ecological gradient is also visible for bending curvature and vertical displacement only in delphinoids, with offshore species having lower bending and displacement than

inshore species. For all cetaceans, bending and displacement significantly decrease with increasing vertebral count only in the thoracic and/or lumbar regions which could reflect a stabilisation of the anterior body part in stiffer species (Table S 4.3).

Surprisingly, riverine non-delphinoids have lower body curvature and vertical displacement than riverine delphinoids despite their similar backbone stiffness. This could be due to their shorter neural spines resulting in a lower muscular cross-sectional area and lower leverage for the *m. longissimus*. In offshore delphinoids, muscular force also highly impacts the predicted body curvature. For example, due to their high vertebral counts, *P. dalli* and *L. albirostris* have extremely stiff intervertebral disks, but, due to its extremely large neural spines, *P. dalli* has the highest vertical displacement of offshore delphinoids (21 % body length in average) while *L. albirostris* still has the lowest vertical displacement (approximately 10 % body length). Similarly, data on scanned specimens show that the increased muscular cross-sectional area (CSA) of *L. albirostris* due to an extension of muscles beyond vertebral apophyses allow this species to achieve higher body curvature than the more flexible *P. phocoena*.

Predicted backbone curvature and displacement are however relatively variable for offshore and coastal non-delphinoids. The model predicted that the three largest species of our dataset, the blue whale (*B. musculus*), the sperm whale (*P. macrocephalus*) and the North Atlantic right whale (*E. glacialis*), would have extremely low body curvature and vertical displacement because body size has an important effect on backbone stiffness. Hence, these large species have absolute stiffness value higher than other smaller cetaceans. Muscle CSA and leverage also increase with body length but at a lower rate (regression slope: stiffness = 2.83, CSA = 1.68, neural spine height = 0.94, metapophyses height = 0.91). The low body curvature predicted for these large specimens could thus be explained by a lower bending moment relative to the stiffness of their backbone. On the other hand, the remaining offshore non-delphinoids have a higher curvature and vertical displacement than delphinoids. These specimens belong to two different families: beaked whales (Ziphiidae) and pygmy and dwarf sperm whales (Kogiidae). Species belonging to both families are specialised deep-divers and possess peculiar morphologies that could be related to their ecology. Due to the extension of epaxial muscle beyond vertebral apophyses, Kogiidae have large CSA for their body size compared to other cetaceans (Arthur *et al.*, 2015). In our model, this larger CSA results in a higher bending moment and could explain the

high predicted body curvature of pygmy and dwarf sperm whales. As a large portion of oxygen storage is located in skeletal muscles in marine mammals, the increased CSA of small-sized Kogiidae could increase their aerobic diving limit and permit prolonged deep-dives (Kielhorn *et al.*, 2013; Kooyman and Ponganis, 2017). Compared to most species, beaked whales do not have a particularly large muscular CSA for their body size but their neural spines are extremely well developed. This creates a large leverage for the *m. longissimus* which is the largest epaxial muscle. Recent swimming kinematic obtained from accelerometers and magnetometers placed on free-ranging beaked whale have shown that these species use a peculiar swimming gait undocumented in other cetaceans. These so-called B-strokes are characterised by faster and higher amplitude fluke movements than regular strokes and are followed by brief gliding phases. As this specialised gait is only used during the ascending phase of deep dives, it has been suggested that B-strokes could be produced by the numerous anaerobic fast-twitch muscular fibres reported in beaked whales, replacing slow aerobic fibres contraction when the animal reaches its aerobic diving limit and hence, permitting longer dives (Martín López *et al.*, 2015). While the high proportion of fast-twitch fibres could be related to the production of faster strokes, the extremely high neural spines of beaked whales could explain their ability to generate high amplitude strokes as it would generate a high muscular leverage.

In the four species corresponding to species recorded on videos, mean joint stiffness also varies according to habitat, with the riverine species (*P. blainvillei*) having the most flexible joints, followed by the species having a mixed ecology (*T. truncatus*), then the coastal species (*P. phocoena*) and, finally, the offshore species (*L. obliquidens*). However, when comparing cumulated stiffness instead of mean stiffness, this gradient is only observed in the thoracic region as *P. phocoena* and *T. truncatus* are more flexible than *P. blainvillei* when considering the entire body. Similarly, *P. blainvillei* has the highest bending and vertical displacement only in the thoracic region. This is coherent with the results obtained from videos showing that the riverine species, *I. geoffrensis*, appears to have higher movement amplitudes than other species in the anterior body part. Our model also predicts that *P. blainvillei* has a low curvature and amplitude for the entire body but, conversely, kinematic data show that *I. geoffrensis* has a higher fluke amplitude and experiences larger body deformation during a swimming cycle. In accordance with our hypothesis, *L. obliquidens* has the lowest stroke amplitude and body movements compared to other species, which is coherent with its increased backbone stiffness. Reducing body movements and fluke amplitude result in a more efficient swimming style

and would be beneficial for fast swimming species. Lower levels of body deformations during a swimming cycle in stiffer species are congruent with previous studies that qualitatively investigated swimming patterns in four cetacean species and concluded that *I. geoffrensis* exhibit a higher body curvature than *P. phocoena* and *Lagenorhynchus acutus* (Buchholtz, 2001b). However, previous analyses of swimming kinematics of several delphinoid species showed that fluke amplitude is relatively constant among species (varying approximately between 15 and 30 % body length) (Fish, 2002; Rohr and Fish, 2004). As observed differences in swimming amplitude are relatively small and standard deviations large, a larger dataset of kinematic data would be necessary to determine if differences in fluke amplitude observed in our dataset between species are significant or not.

While swimming amplitude and body deformation slightly differed among species, kinematic data highlighted large differences in fluke oscillation frequencies with the most flexible species having the lowest frequencies (*I. geoffrensis* and *T. truncatus*) and the stiffest species having the highest frequencies (*P. phocoena* and *L. obliquidens*). Previously reported tailbeat frequencies of small and medium sized cetaceans also support these results. For example, the finless porpoise (*Neophocaena phocaenoides*), the Guiana dolphin (*Sotalia guianensis*) and the beluga (*Delphinapterus leucas*) that are considered as flexible and slow swimming species have frequencies between 0.5 and 1.5 Hz while the fast swimming Pacific white-sided dolphin (*L. obliquidens*) and the Atlantic spotted dolphin (*Stenella frontalis*) have higher oscillating frequencies varying between 1.5 and 4.5 Hz (Rohr and Fish, 2004; Sato *et al.*, 2007; Videler and Kamermans, 1985). An approximate tailbeat frequency of 2 Hz has also been reported for harbour porpoises (Smith *et al.*, 1976). Furthermore, cruising swimming speed is usually increased by increasing fluke oscillation frequency in cetaceans and fishes (Bainbridge, 1958; Fish, 1998; Rohr and Fish, 2004; Steinhausen *et al.*, 2005). In mechanical engineering, the natural frequency of a uniform beam increases with increasing stiffness (Géradin and Rixen, 2015). Long and Nipper (1996) showed that, for a given bending amplitude, the bending moment required to dynamically bend the intervertebral disk of a blue marlin (*Makaira nigricans*) is the lowest at oscillating frequencies close to the natural frequency of the disk. This would imply that the optimal tailbeat frequency, i.e., the frequency at which minimal mechanical force is required to bend the backbone, would be higher in species having a stiffer backbone. However, data reported by Long and Nipper (1996) are for a single intervertebral disk and would need to be tested on the entire backbone. In another study, Long *et al.* (1996) showed that experimentally decreasing body stiffness of longnose

gar (*Lepisosteus osseus*) results in a decrease in tailbeat frequency. While our results show an increase in single disk stiffness with increasing vertebral count, the cumulated stiffness of the entire backbone do not appear to follow the same pattern. In addition, the relationship between stiffness and natural frequency used here is for a uniform object (beam). The backbone is a highly complex structure with alternating flexible (intervertebral disks) and rigid (vertebrae) sections. The calculation of its total stiffness and its natural frequency could be more complicated and further works should aim at experimentally testing the relationship between stiffness and oscillating frequency in the entire backbone of cetaceans with various morphologies.

4.3. Model validity and limitations

Our model is based on several simplifications and assumptions that most probably do not meet all features of biological samples. Moreover, previous works have demonstrated that vertebral morphology cannot completely predict vertebral stiffness/mobility (Long *et al.*, 1997; Molnar *et al.*, 2014; Porter *et al.*, 2009). Hence, predictions of vertebral stiffness and mobility from morphological data should be approached with caution. Our model uses a constant value for the Young's modulus of intervertebral disk. This value could however differ along body length in a specimen but also among species. Mammalian intervertebral disk is composed of a gel-like central part (the nucleus pulposus) and a surrounding fibrous part (the annulus fibrosus) (Bray and Burbidge, 1998). Variation in proportion and/or position of each component in the disk has been reported along the backbone of cats and dogs and between several mammalian clades such as felids, canids, pinnipeds and primates (Butler, 1989; Gál, 1993b). Although variation in disk morphology could also affect the Young's modulus, our model is in agreements with the pattern described along the backbone of the common dolphin (*Delphinus delphis*) based on experimental testing if individual segments stiffness (Long *et al.*, 1997): the backbone stiffness increases in the anterior part of the body and decreases in the posterior part (Figure 4.7 and Figure 4.11).

The model is a static model, meaning that it does not account for dynamic effects due to swimming oscillatory movements although mechanical properties are likely to change during a cycle (e.g., Long, 1992; Long and Nipper, 1996). In dolphins, the experimental set-up used by Long *et al.* (1997) demonstrated that disk stiffness is not impacted by oscillating frequency but increases with bending amplitude implying that a higher bending moment will be required to bend the backbone at

higher angles. Similarly, we considered that epaxial muscles were parallel to the longitudinal axis of the animal and inserted perpendicularly on the neural spines and metapophyses. However, as the curvature of the backbone increases and induces vertebral rotation, the angle of insertion of muscles on apophyses might change, which would affect the bending moment transmitted to the vertebrae. Furthermore, our model did not consider the elastic limits of the disk. In other words, we did not define a maximal angle at which high stress and strain could result in lesions in the disk. To the best of our knowledge, such effect has not been tested in cetacean intervertebral disk.

We used kinematic data from harbour porpoises recorded on videos to calibrate our model and define the proportion of muscular force necessary to bend the body at biological realistic angles. We used a muscle stress value of 15 kPa which corresponds to 5% of the 300 kPa value commonly used for mammals (Arthur *et al.*, 2015; Pabst, 1993; Wells, 1965). Our model likely underestimates body stiffness and the force required to bend it at a given angle as it does not account for the effect of surrounding tissues such as ligaments, tendons, muscles, blubber and skin (Long *et al.*, 1996; Molnar *et al.*, 2015; Valentin *et al.*, 2012). Similarly, predicted bending angles in the flukes are biologically unlikely high as the model does not include the effect of the dense connective tissue surrounding fluke vertebrae (Sun *et al.*, 2010). In addition, cetaceans also need to overcome water pressure and drag during tail oscillations. It is then probable that cetaceans use more than 5% of their total theoretical muscular force to bend their backbone although they probably only use a portion of their muscular force. For example, fishes rely mainly on red muscular fibres contractions during steady swimming (Jayne and Lauder, 1994). The proportion of red fibres varies between species but it usually corresponds to less than 15% of the total muscular volume (He, 1986; Stevens *et al.*, 1974; Videler, 1985). Similarly, mammals recruit different types of fibres depending on the effort required (Armstrong and Laughlin, 1985). Different fibre types have also been reported in several cetacean species which supports the hypothesis that they might only use a portion of their muscle volume during steady swimming (Kielhorn *et al.*, 2013; Ponganis and Pierce, 1978; Rivero, 2018; Velten *et al.*, 2013). It is also important to note that we used the same muscle stress value for both epaxial muscles, implying that their force is directly proportional to their physical cross-sectional area. However, Pabst (1993) predicted that the small *m. multifidus* of the bottlenose dolphin would produce a force equivalent to the larger *m. longissimus* due to its higher muscular fibre pinnation angle. Our model might be improved by using different muscle stress values for each muscle to account for their

different pinnation angles but, to our knowledge, similar data are not available for other cetacean species and we cannot be certain that angles are similar among all cetaceans.

Our predicted vertical displacement values along the backbone did not allow us to identify regions of increased curvature as observable in swimming animals (Figure 4.11 andFigure 4.13). This might be due to the fact that we simplified epaxial musculature insertion patterns and considered that muscular force was uniformly distributed among vertebrae on which it inserts (Pabst, 1990; Slijper, 1936). For example, metapophyses (on which *m. multifidus* inserts) do not have uniform shape and size along the backbone and tend to be less developed in the mid and posterior lumbar regions than in the anterior thoracic and caudal regions (see *T. truncatus* and *L. obliquidens* in Figure 4.2). This variation could reflect changes in the force applied on apophyses and reveal non-uniform distribution of muscular forces (Lloyd *et al.*, 2014; Sharir *et al.*, 2011). In the same way, we did not account for the effect of neural spines inclination (on which *m. longissimus* inserts) but it varies along the backbone and could impact the bending moment applied on the vertebrae.

Finally, our predictive model of disk length in museum specimen is based only on morphological data of two delphinoid species. We are aware that the *Ld/Lc* ratio pattern along body length described in these two species might not be applicable to all cetaceans, especially to non-delphinoids. The increased percentage error between body length predicted by the model and true body length of beaked whales might for example indicate that disk length does not follow the same pattern in this family. However, currently, there is no available data on intervertebral disk in large non-delphinoids to confirm or infirm our disk length pattern.

Future works investigating backbone stiffness should aim at including most of the aforementioned parameters and combine prediction to experimental measurements on various species to calibrate and validate the model. This would however require extensive data collection on entire, fresh and undamaged specimens from numerous different species which can be challenging, especially for larger specimens. Despite these limitations, amplitudes values reported by our model are coherent with values measured on videos with peak-to-peak amplitude measured on videos varying between 20 and 30 % body length (up to 35 % body length for fast swimming bottlenose dolphin) and predicted peak amplitude (i.e., half peak-to-peak amplitude) varying between 11 and 20 % body length for these four species. While Pabst (1993) predicted mean joint bending angle in the

bottlenose dolphin (approximately 2°) higher than those predicted with our model (0.5° in average), our values are in agreement with intervertebral disk bending reported for steady swimming in fish (0.6 – 0.9°) (Jayne and Lauder, 1995). We are therefore convinced that this relatively simple model can provide good estimations of backbone rigidity patterns, at least in delphinoids.

5. Conclusion

This study is the first to develop a mathematical model based on beam theory and vertebral morphology to predict stiffness and curvature of cetacean backbone and combine these predictions with quantitative analysis of swimming movements of several species. Our model suggests that mean joint stiffness increases with vertebral count and body size in cetaceans. In small cetaceans, mean joint stiffness increases along an ecological gradient from rivers to offshore habitats. Based on kinematic analysis of video recorded for four cetacean species, we propose that joint stiffness plays a dual role in swimming kinematics. Increased stiffness slightly reduces body deformation during fluke and peduncle oscillations providing enhanced hydrodynamics and stability and it allows animals to use higher tailbeat frequencies without requiring higher muscular work. As swimming speed increases with tailbeat frequency, small, stiff oceanic species should reach higher swimming speed at a reduced energetic cost.

Supplementary materials

Contents:

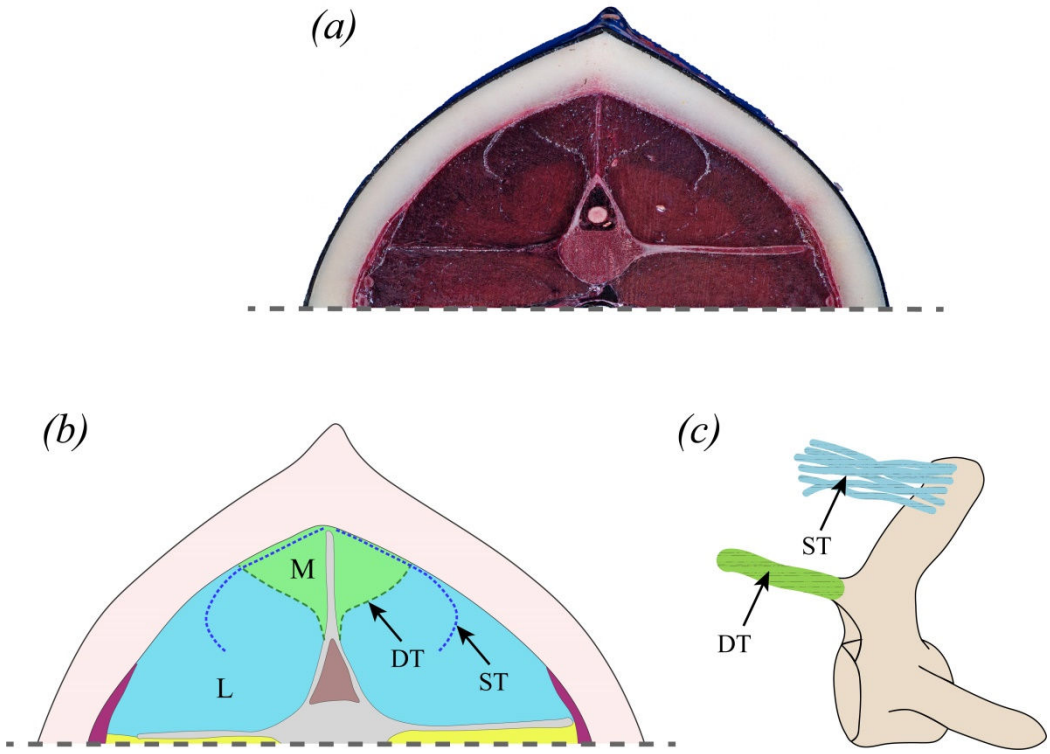

Figure S 4.1. Anatomy of epaxial musculature and vertebral insertions. (*a*) Picture of cross-section in a harbour porpoise (*P. phocoena*) in the anterior lumbar region. (*b*) Schematic representation of cross-section in (*a*). (*c*) Schematic vertebrae showing insertion points of the two main epaxial muscles. *M*: *m. multifidus*; *L*: *m. longissimus*; *DT*: deep tendon of the *m. multifidus* inserting on vertebral metapophyses; *ST*: superficial tendon of the *m. longissimus* inserting on dorsal tip of neural processes (Schematic cross-section by Marion Grimaud).

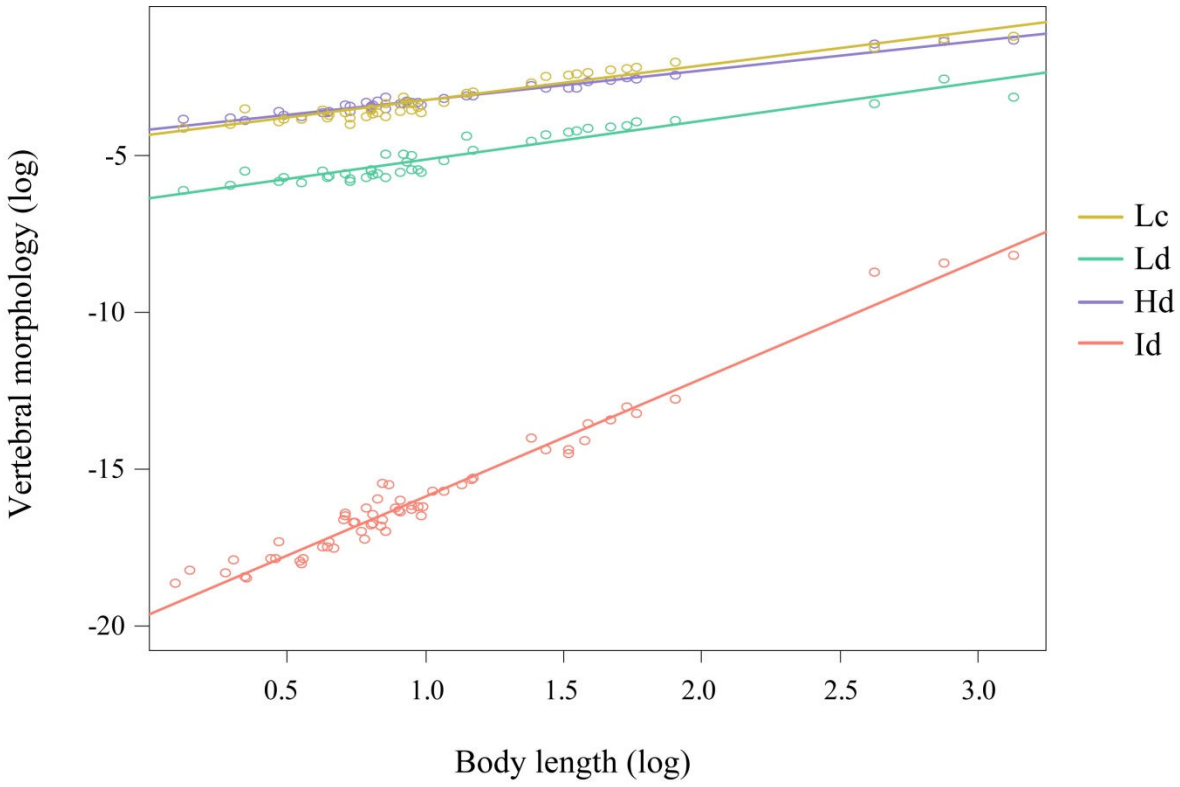

Figure S 4.2. Relationship between vertebral morphology and body size. Scatterplot showing results of phylogenetically-corrected linear regressions between log-transformed vertebral centrum length (*Lc*), intervertebral disk length (*Ld*), height (*Hd*) and second moment of area (*Id*) and log-transformed body length. Each point corresponds to a cetacean species. Note that disk and vertebral centrum height increases with body size at a lower rate (slope = 0.94) than disk length (slope = 1.24) and centrum length (slope = 1.14) but that the second moment of area of intervertebral disk increases at a higher rate (slope = 3.76).

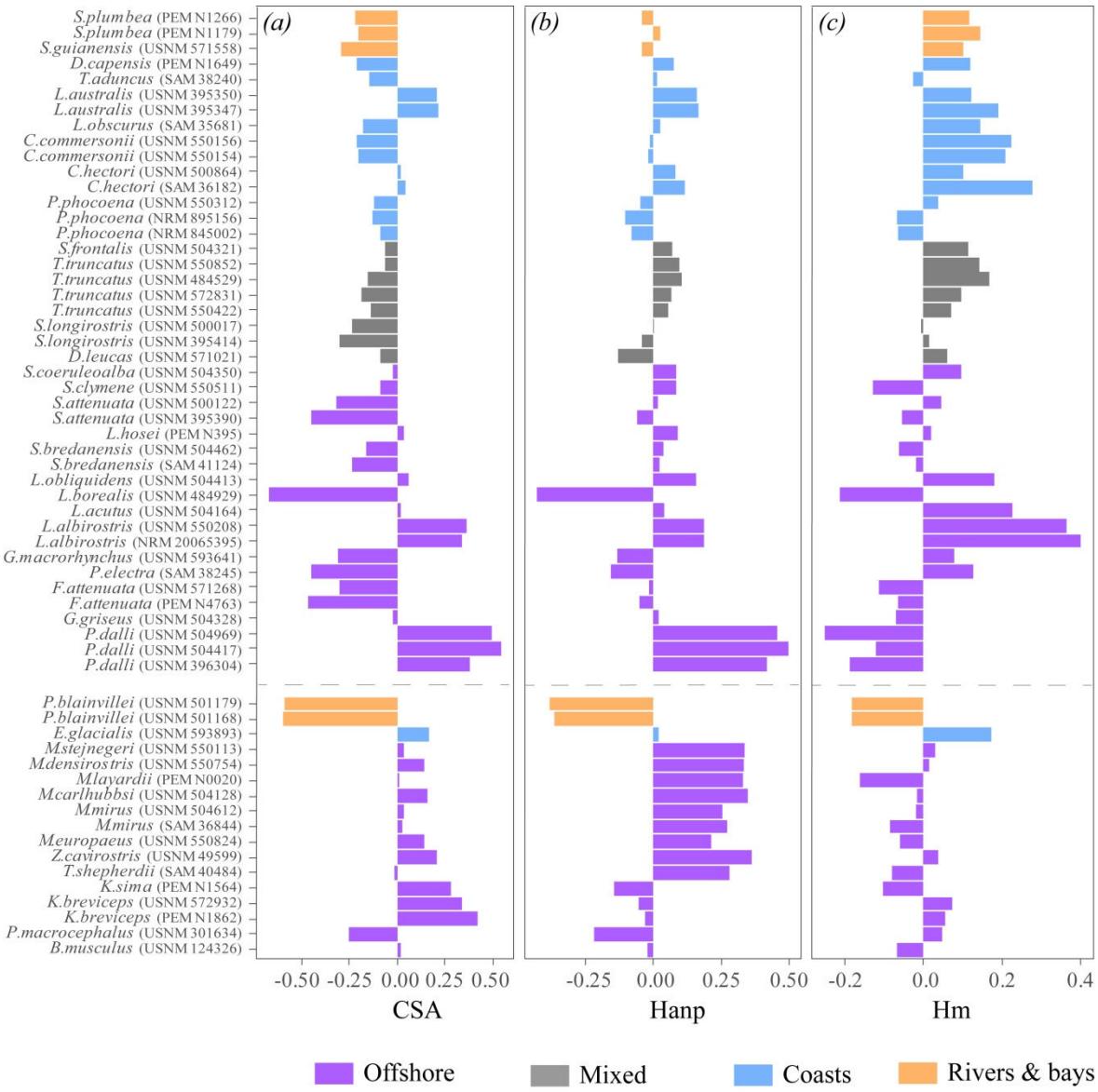

Figure S 4.3. Relative muscle surface and lever arm. Bar plot showing the size-corrected (*a*) muscular cross-sectional area (*CSA*), (*b*) lever arm of the *m. longissimus* (*Hanp*) and (*c*) lever arm of the *m. multifidus* (*Hm*) of each specimen.

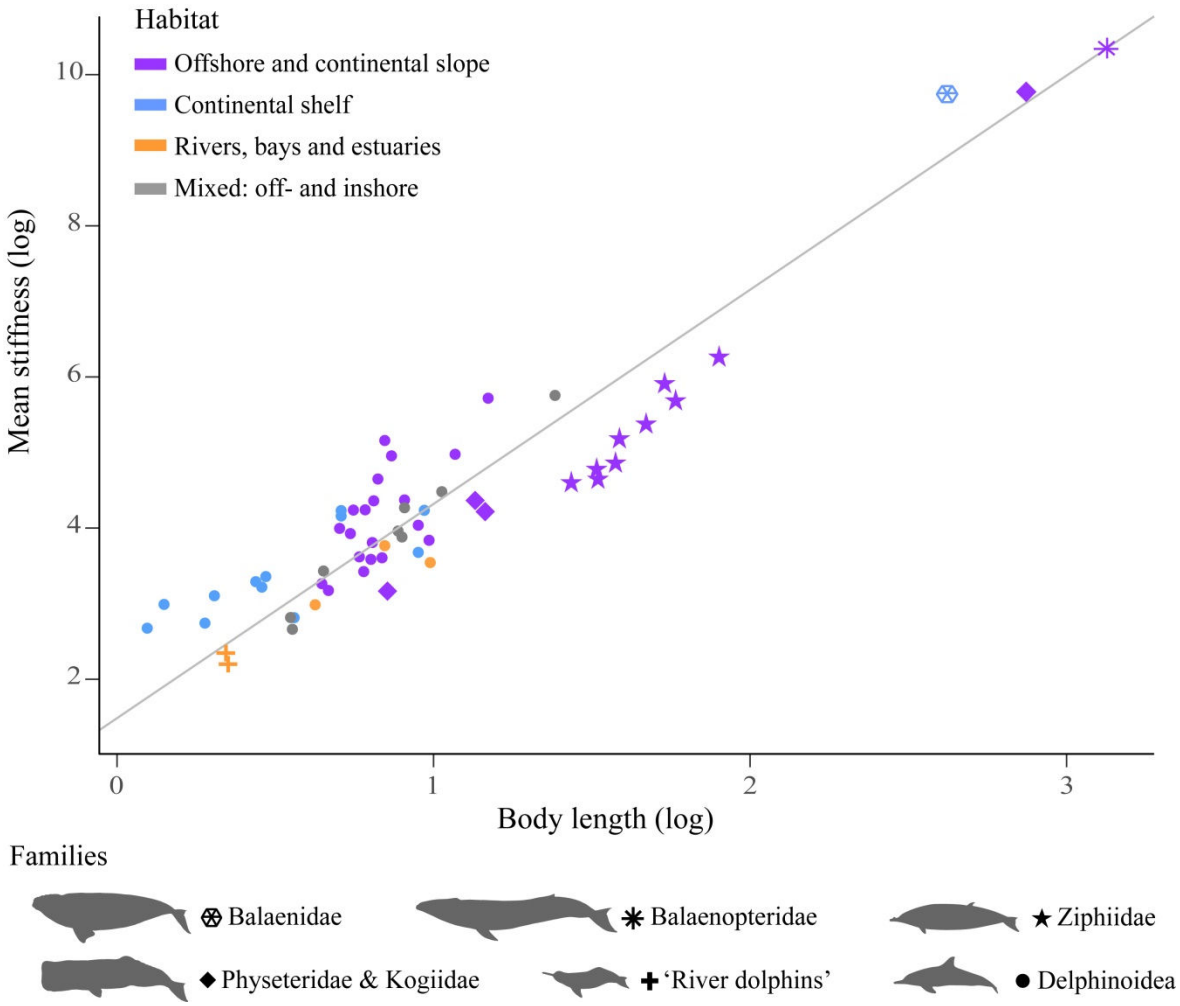

Figure S 4.4. Relationship between mean disk stiffness and body size. The log-transformed mean stiffness of the whole body is significantly related to the log-transformed body size of specimens. The significant liner regression is represented by the grey line. Symbol shapes represent phylogenetic groups, colours represent habitat.

Table S 4.1. List of museum specimens used for backbone flexibility modelling. Museum species and specimens for which backbone flexibility was modelled. *N*: number of specimens per species; *Phy*: phylogenetic group of the species: non-delphinoid (*ND*) or delphinoid (*D*); *Eco*: habitat category of the species: offshore (*Off*), coasts (*Coa*), rivers & bays (*Riv*) or mixed off- and inshore (*Mix*); *Spec. number*: museum abbreviation and collection number of each specimen; *Nv*: vertebral count of each specimen; *Rib*: number of double-headed ribs ; *BL*: total body length (in meters); *Lskull*: skull length (in meters); *TCL*: total centrum length (in meters); *δBL*: difference (in %) between predicted and real body length. Museum abbreviations: *NRM*: the Swedish Royal Museum of Natural History, Stockholm; *PEM*: the Bayworld Port Elizabeth Museum, Port Elizabeth; *SAM*: the Iziko South African Museum, Cape Town; *USNM*: the National Museum of Natural History, Washington D.C.

Species	**N**	**Phy**	**Eco**	**Spec. number**	**Nv**	**Rib**	**BL**	**Lskull**	**TCL**	**δBL**
B. musculus	1	ND	Off	USNM124326	65	5	22.76	5.54	13.8958	0.01
C. commersonii	2	D	Coa	USNM550154	65	7	1.32	0.294	0.8722	2.23
				USNM550156	64	7	1.36	0.307	0.8982	2.65
C. hectori	2	D	Coa	SAM36182	62	5	1.16	0.28	0.7361	1.36
				USNM500864	64	6	1.1	0.2815	0.7223	5.65
D. capensis	1	D	Coa	PEMN1649	73	5	2.64	0.54	1.7186	1.14
D. leucas	1	D	Mix	USNM571021	50	7	3.99	0.609	2.7601	1.17
E. glacialis	1	ND	Coa	USNM593893	56	12	13.78	3.983	7.7365	< 0.01
F .attenuata	2	D	Off	PEMN4763	67	6	2.24	0.361	1.5443	0.02
				USNM571268	69	6	2.23	0.354	1.5532	0.01
G. griseus	1	D	Off	USNM504328	69	6	2.91	0.477	2.1193	3.46
G. macrorhynchus	1	D	Off	USNM593641	57	6	3.23	0.561	2.3369	4.24
K. breviceps	2	ND	Off	PEMN1862	50	7	3.2	0.416	2.117	0.01
				USNM572932	53	7	3.1	0.458	2.0597	< 0.01
K. sima	1	ND	Off	PEMN1564	56	9	2.35	0.265	1.6994	0.01
L. acutus	1	D	Off	USNM504164	82	6	2.19	0.396	1.5221	1.68
L. albirostris	2	D	Off	NRM20065395	89	6	2.33	0.44	1.6017	2.23
				USNM550208	91	6	2.38	0.425	1.6677	2.51
L. australis	2	D	Coa	USNM395347	68	7	2.03	0.397	1.3867	2.01
				USNM395350	67	6	2.03	0.371	1.4103	2.21
L. borealis	1	D	Off	USNM484929	91	4	2.68	0.422	1.9669	4.82
L. hosei	1	D	Off	PEMN395	79	7	2.59	0.435	1.7977	0.01
L. obliquidens	1	D	Off	USNM504413	75	6	2.28	0.432	1.5533	1.41
L. obscurus	1	D	Coa	SAM35681	70	6	1.6	0.336	1.0264	< 0.01
M. carlhubbsi	1	ND	Off	USNM504128	46	7	5.32	0.921	3.9393	6.42
M. densirostris	1	ND	Off	USNM550754	47	7	4.2	0.772	3.1779	9.42
M. europaeus	1	ND	Off	USNM550824	47	7	4.57	0.745	3.4097	5.76
M. layardii	1	ND	Off	PEMN0020	44	7	5.84	1.15	3.797	< 0.01

Table S 4.1. (Continued)

Species	N	Phy	Eco	Spec. number	Nv	Rib	BL	Lskull	TCL	δBL
M. mirus	2	ND	Off	SAM36844	47	7	4.55	0.727	3.4797	7.87
				USNM504612	47	7	4.83	0.806	3.5333	4.84
M. stejnegeri	1	ND	Off	USNM550113	46	7	4.89	0.756	3.6952	6.58
P. blainvillei	2	ND	Riv	USNM501168	42	5	1.41	0.353	0.9078	2.44
				USNM501179	43	4	1.42	0.382	0.8817	4.06
P. dalli	3	D	Off	USNM396304	95	13	2.02	0.358	1.3531	0.01
				USNM504417	97	11	2.09	0.338	1.4242	0.01
				USNM504969	97	13	2.11	0.338	1.4827	0.03
P. electra	1	D	Off	SAM38245	81	6	2.48	0.471	1.7838	5.73
P. macrocephalus	1	ND	Off	USNM301634	50	8	17.68	5.185	8.6878	0.03
P. phocoena	3	D	Coa	NRM845002	67	7	1.55	0.269	1.0666	0.01
				NRM895156	66	7	1.75	0.281	1.1849	2.26
				USNM550312	65	7	1.58	0.28	1.1127	0.51
S. attenuata	2	D	Off	USNM395390	81	5	2.18	0.405	1.4874	0.51
				USNM500122	79	5	1.95	0.42	1.3469	4.94
S. bredanensis	2	D	Off	SAM41124	64	6	2.31	0.526	1.4914	0.92
				USNM504462	65	6	2.15	0.526	1.3855	2.23
S. clymene	1	D	Off	USNM550511	73	4	1.91	0.409	1.2362	0.01
S. coeruleoalba	1	D	Off	USNM504350	80	5	2.25	0.444	1.5711	4.00
S. frontalis	1	D	Mix	USNM504321	71	6	1.92	0.406	1.3297	4.54
S. guianensis	1	D	Riv	USNM571558	56	4	1.87	0.388	1.2239	0.40
S. longirostris	2	D	Mix	USNM395414	76	7	1.73	0.404	1.1705	4.55
				USNM500017	73	6	1.74	0.405	1.1653	3.73
S. plumbea	2	D	Riv	PEMN1179	49	7	2.69	0.54	1.7285	< 0.01
				PEMN1266	51	6	2.33	0.5	1.5083	0.72
T. aduncus	1	D	Coa	SAM38240	60	5	2.59	0.476	1.6803	0.01
T. shepherdi	1	ND	Off	SAM40484	44	7	6.7	1.164	4.617	0.10
T. truncatus	4	D	Mix	USNM550422	61	4	2.79	0.487	2.0012	4.06
				USNM572831	60	5	2.46	0.474	1.6571	0.70
				USNM484529	60	4	2.43	0.451	1.6156	0.02
				USNM550852	61	4	2.48	0.451	1.7206	1.71
Z.cavirostris	1	ND	Off	USNM49599	46	6	5.64	0.897	4.0815	3.19

Table S 4.2. Effect of body size and vertebral count on backbone stiffness. The table summarizes statistical results of linear regressions between backbone stiffness and body length (*BL*) or vertebral count (*Nv*). Regressions were tested with and without phylogenetic correction. For body length regression, data were log-transformed prior to analysis (*log*). If the regression between stiffness and body length was significant, residuals from this regression were used to test the effect of vertebral count (*res*). Each regression was tested on values of the entire body and for each backbone region. Fluke vertebrae were not included in total stiffness of the entire body. Significant values are indicated in bold.

	Without phylogenetic correction			**With phylogenetic correction**		
	P-value	**R^2**	**Slope**	**P-value**	**R^2**	**Slope**
Mean stiffness (log) *vs* BL (log)	**< 0.001**	0.92	2.609	**0.001**	0.83	2.605
Mean stiffness thoracic (log) *vs* BL (log)	**< 0.001**	0.89	2.603	**0.001**	0.81	2.603
Mean stiffness lumbar (log) *vs* BL (log)	**< 0.001**	0.91	2.531	**0.001**	0.81	2.531
Mean stiffness caudal (log) *vs* BL (log)	**< 0.001**	0.93	2.664	**0.001**	0.82	2.664
Mean stiffness (res) *vs* Nv	**< 0.001**	0.38	0.0205	**0.001**	0.54	0.020
Mean stiffness thoracic (res) *vs* Nv	**< 0.001**	0.35	0.023	**0.001**	0.37	0.023
Mean stiffness lumbar (res) *vs* Nv	**< 0.001**	0.39	0.021	**0.001**	0.48	0.021
Mean stiffness caudal (res) *vs* Nv	**0.008**	0.14	0.012	**0.001**	0.44	0.012
Total stiffness (log) *vs* BL (log)	**< 0.001**	0.94	2.747	**0.001**	0.83	2.747
Total stiffness thoracic (log) *vs* BL (log)	**< 0.001**	0.92	2.704	**0.001**	0.81	2.704
Total stiffness lumbar (log) *vs* BL (log)	**< 0.001**	0.94	2.722	**0.001**	0.81	2.722
Total stiffness caudal (log) *vs* BL (log)	**< 0.001**	0.93	2.843	**0.001**	0.79	2.843
Total stiffness (res) *vs* Nv	0.962	-0.03	-0.001	0.370	0.02	-0.001
Total stiffness thoracic (res) *vs* Nv	**0.009**	0.14	0.013	**0.004**	0.17	0.013
Total stiffness lumbar (res) *vs* Nv	0.624	-0.02	-0.002	0.529	0.01	-0.002
Total stiffness caudal (res) *vs* Nv	**0.01**	0.14	-0.013	0.458	0.02	-0.013

Table S 4.3. Effect of body size and vertebral count on backbone bending and vertical displacement. The table summarizes statistical results of linear regressions between backbone bending angles or vertical displacement and body length (*BL*) or vertebral count (*Nv*). Regressions were tested with and without phylogenetic correction. Data log-transformed prior to analysis are indicated (*log*). Each regression was tested on values of the entire body and for each backbone region. Fluke vertebrae were not included in mean bending and total bending of the entire body. Significant values are indicated in bold.

	Without phylogenetic correction			**With phylogenetic correction**		
	P-value	**R^2**	**Slope**	**P-value**	**R^2**	**Slope**
Mean bending (log) *vs* BL (log)	0.54	-0.02	0.105	0.081	0.08	0.105
Mean bending thoracic (log) *vs* BL (log)	0.821	-0.02	-0.042	**0.017**	0.13	-0.042
Mean bending lumbar (log) *vs* BL (log)	0.21	0.02	0.235	0.132	0.06	0.235
Mean bending caudal (log) *vs* BL (log)	0.802	-0.02	0.036	0.126	0.06	0.036
Mean bending (log) *vs* Nv	**< 0.001**	0.45	-0.033	**0.001**	0.48	-0.033
Mean bending thoracic (log) *vs* Nv	**< 0.001**	0.31	-0.030	**0.001**	0.28	-0.030
Mean bending lumbar (log) *vs* Nv	**< 0.001**	0.58	-0.041	**0.001**	0.58	-0.041
Mean bending caudal (log) *vs* Nv	**< 0.001**	0.34	-0.024	**0.001**	0.41	-0.024
Total bending (log) *vs* BL (log)	0.603	-0.02	-0.069	**0.027**	0.11	-0.069
Total bending thoracic (log) *vs* BL (log)	0.433	-0.01	-0.129	**0.009**	0.15	-0.129
Total bending lumbar (log) *vs* BL (log)	0.757	-0.02	0.045	0.115	0.06	0.045
Total bending caudal (log) *vs* BL (log)	0.099	0.05	-0.185	**0.046**	0.10	-0.185
Total bending (log) *vs* Nv	**0.022**	0.11	-0.013	0.094	0.07	-0.013
Total bending thoracic (log) *vs* Nv	**0.007**	0.15	-0.019	**0.049**	0.10	-0.019
Total bending lumbar (log) *vs* Nv	**0.002**	0.19	-0.019	**0.012**	0.16	-0.019
Total bending caudal (log) *vs* Nv	0.887	-0.06	-0.001	0.851	0.01	-0.001
Total displacement (log) *vs* BL (log)	0.561	-0.02	-0.078	**0.030**	0.11	-0.078
Total displacement thoracic (log) *vs* BL (log)	0.145	0.03	-0.114	0.057	0.08	-0.114
Total displacement lumbar (log) *vs* BL (log)	0.913	-0.03	0.019	0.103	0.06	0.019
Total displacement caudal (log) *vs* BL (log)	0.495	-0.01	-0.094	0.056	0.09	-0.094
Total displacement (log) *vs* Nv	**0.015**	0.12	-0.014	0.064	0.09	-0.014
Total displacement thoracic (log) *vs* Nv	**0.008**	0.15	-0.009	**0.005**	0.21	-0.009
Total displacement lumbar (log) *vs* Nv	**0.004**	0.17	-0.021	0.088	0.08	-0.021
Total displacement caudal (log) *vs* Nv	0.056	0.07	-0.012	0.127	0.06	-0.012

Table S 4.4. Predicted backbone flexibility and movements of species recorded on videos. The table summarizes results of backbone movements modelling (mean ± S.D.) for specimens belonging to three species recorded on videos and for *P. blainvillei* specimens which have a vertebral morphology similar to *I. geoffrensis*. Parameters are reported for the entire body and for each vertebral region. Stiffness values are size-corrected values, bending is in degrees and displacement in body length percent. Fluke vertebrae were not included to calculate total stiffness, mean bending and total bending of the entire body.

	P. blainvillei	***P. phocoena***	***T. truncatus***	***L. obliquidens***
Mean stiffness	-0.208 ± 0.007	0.185 ± 0.388	0.037 ± 0.150	0.862
Mean stiffness thoracic	-0.041 ± 0.119	0.378 ± 0.447	0.122 ± 0.156	0.932
Mean stiffness lumbar	-0.221 ± 0.161	0.189 ± 0.417	-0.044 ± 0.222	0.856
Mean stiffness caudal	-0.265 ± 0.142	-0.066 ± 0.321	-0.127 ± 0.093	0.562
Total stiffness	0.122 ± 0.042	-0.086 ± 0.288	-0.168 ± 0.106	0.355
Total stiffness thoracic	0.084 ± 0.060	0.280 ± 0.339	0.121 ± 0.133	0.768
Total stiffness lumbar	0.226 ± 0.112	-0.173 ± 0.301	-0.395 ± 0.170	0.099
Total stiffness caudal	0.171 ± 0.038	-0.398 ± 0.265	-0.332 ± 0.092	0.107
Mean bending	0.529 ± 0.061	0.410 ± 0.137	0.538 ± 0.086	0.238
Mean bending thoracic	0.544 ± 0.127	0.346 ± 0.148	0.496 ± 0.079	0.208
Mean bending lumbar	0.753 ± 0.118	0.592 ± 0.221	0.722 ± 0.148	0.288
Mean bending caudal	0.375 ± 0.033	0.329 ± 0.082	0.419 ± 0.048	0.210
Total bending	13.52 ± 1.93	18.98 ± 6.17	23.65 ± 3.65	13.57
Total bending thoracic	5.45 ± 1.27	4.49 ± 1.93	5.96 ± 0.95	2.90
Total bending lumbar	4.52 ± 0.71	8.01 ± 2.67	10.26 ± 1.90	6.05
Total bending caudal	3.55 ± 0.05	6.48 ± 1.68	7.44 ± 0.92	4.62
Total displacement	11.62 ± 1.65	15.10 ± 5.33	20.24 ± 2.76	11.40
Total displacement thoracic	1.65 ± 0.12	1.10 ± 0.22	1.19 ± 0.05	0.84
Total displacement lumbar	2.33 ± 0.46	3.43 ± 1.20	4.17 ± 0.58	2.42
Total displacement caudal	4.91 ± 0.94	8.51 ± 3.15	11.60 ± 1.69	6.38

Chapter 5 :
General discussion and conclusion

Investigating ecomorphology in an evolutionary context can highlight the major factors that promoted or hindered diversification processes. Cetaceans represent the most successful clade of extant marine mammals and exhibit a wide morphological and ecological diversity, making them an interesting group for ecomorphological studies. Most ecomorphological studies have investigated the variation of their body, fins or skull shape in relation to the ecology (e.g., McCurry *et al.*, 2017; Slater *et al.*, 2010; Woodward *et al.*, 2006) and few have documented the vertebral disparity of whales and dolphins (Buchholtz and Gee, 2017; Buchholtz and Schur, 2004; Marchesi *et al.*, 2019, 2018; Viglino *et al.*, 2014). These studies however could not satisfactorily explain vertebral shape variation among cetaceans in a phylogenetic and ecologic framework.

The main objective of this work was then to precisely understand cetacean backbone morphological variability by combining morphological, functional, ecological and phylogenetic data on a wide variety of species. To this purpose, I thoroughly quantified the vertebral morphology of 80 % of extant cetacean species and analysed its variability according to habitat using recently developed phylogenetic comparative methods. I also investigated the functional consequences of such variability by modelling backbone biomechanics and analysing dolphin swimming kinematics. Hereafter, I summarise the main factors associated with variability of the vertebral morphology and I discuss how morphological changes are related to functional novelties and the evolutionary history of cetaceans.

1. Ecomorphology of the backbone and evolutionary patterns

The overall results of the present study demonstrate that cetacean vertebral morphology is shaped by the combination of multiple factors such as phylogeny, habitat and body size. Although the habitat was the only ecological factor that we studied in this work, our result show that cetacean backbone morphology could also likely be related to other ecological parameters such as foraging and feeding strategies (e.g., bulk-feeding *versus* single-prey targeting).

1.1. Phylogenetic impacts

1.1.1. Delphinoids and non-delphinoids

Analyses of the tempo and mode of vertebral evolution highlighted the co-existence of two well-defined groups that followed distinct phenotypic evolutionary patterns: delphinoids (Delphinidae, Phocoenidae, and Monodontidae) and non-delphinoids (mysticetes, sperm whales, beaked whales, and 'river dolphins') (chapter 2, figure 2.7). Non-delphinoids retained ancestral morphological characteristics comparable to terrestrial mammals with a low vertebral count, relatively elongated vertebrae and large variation in body size. However, contrarily to other mammals, the number of vertebra increases with body size in this group (see section 1.3 below). The vertebral morphology of delphinoids is clearly different from the morphology of non-delphinoids and evolved under a novel pattern. Delphinoids differ from the remaining cetacean families by retaining a small body size but having an extremely high vertebral count paralleled by a shortening of all vertebrae. In this group, the vertebral count is only poorly influenced by body size but is related to the habitat (see section 1.2 hereafter).

1.1.2. Delphinidae and Phocoenidae

Within the delphinoid clade, there is also a clear distinction of the vertebral morphology between the two most speciose families: Delphinidae (oceanic dolphins) and Phocoenidae (porpoises) (chapter 3, figure 3.1). Although both families diversified in similar habitats (rivers, coastal waters, offshore) following the general morphological pattern of delphinoids (i.e., numerous shortened vertebrae in offshore environments), each family followed a slightly different evolutionary trajectory, resulting in distinct morphologies. Riverine and coastal phocoenids are characterised by shorter and lower vertebral processes (neural arches, metapophyses, neural spines and transverse processes) than riverine and coastal delphinids whereas offshore phocoenids have more discoidal vertebra than their delphinid counterparts.

Several non-mutually exclusive factors might be associated to this morphological distinction between both families. All porpoise species are considered as paedomorphic (Barnes, 1985a; Galatius *et al.*, 2006, 2011) suggesting that shorter vertebral apophyses of porpoises compared to delphinids, especially in riverine and coastal species, could be the result of their uncompleted morphological development. Alternatively, several species of porpoises are known to live in sympatry with delphinids

such as the finless porpoise, *Neophocaena phocoena*, with the humpback dolphin, *Sousa chinensis*, and the Irrawaddy dolphin, *Orcaella brevirostris*, or the harbour porpoise, *Phocoena phocoena*, with the bottlenose dolphin, *Tursiops truncatus* (Jutapruet *et al.*, 2017; Spitz *et al.*, 2006). Differences in vertebral morphology could also reflect different functional abilities and, hence, small-scale niche partitioning to avoid competition (Bearzi, 2005; Jutapruet *et al.*, 2017; Parra, 2006). Interestingly, the sole fully offshore porpoise species, the Dall's porpoise (*Phocoenoides dalli*) possesses an extreme vertebral morphology (97 highly flattened vertebrae with extremely long neural spine) different from any other delphinoid. As delphinid extensively diversified in the offshore environment, the distinct morphology of *P. dalli* might reflect a distinct ecomorphological strategy with a high specialisation in a peculiar ecological niche, hence avoiding competition with offshore delphinids (figures 2.4 and 3.1). Finally, our ancestral state reconstruction for ecological trait of delphinoid revealed that both families have different evolutionary history. The common ancestor of delphinids was most likely an offshore species, whereas the ancestor of porpoises probably lived in coastal waters. Both families have diversified in a variety of habitats starting from different ecological and, potentially, morphological states which could also explain the morphological differences observed between the two clades.

1.2. Ecological signal and functional implications

Besides anatomical differences between phylogenetic groups, vertebral morphology is also strongly associated to the habitat (i.e., rivers, coasts or offshore waters). Vertebral shape is indeed related to the ecology both in non-delphinoids and delphinoids but in different ways. Habitat has an effect on vertebral count in delphinoids only.

1.2.1. Non-delphinoids

In non-delphinoids, riverine species are characterised by more elongated vertebrae than coastal and offshore species. Riverine non-delphinoids are also characterised by a small body size, while most coastal and offshore non-delphinoids have larger body length. From a functional point of view, longer vertebrae provide a greater flexibility of the backbone which is related to shallow waters where habitat complexity requires manoeuvre abilities. Differences between coastal and offshore non-delphinoids correspond to an increased vertebral diameter and larger metapophyses in coastal species. The wider vertebral centra in coastal non-delphinoids imply an increased rigidity compared to offshore species.

This seems counter-intuitive since swimming in shallower waters should require more manoeuvrability (especially in large species) while swimming in the open ocean does not require *a priori* high agility. Due to their large body size and/or deep diving ecology, kinematic data on coastal and offshore non-delphinoids remain scarce which prevents us to precisely infer how vertebral morphology correlates to swimming movements. Manoeuvre abilities might also be related to feeding strategies rather than habitat. For instance, a recent kinematic analysis of blue whales (*Balaenoptera musculus*), which is an offshore species, highlighted that body flexibility plays an important role in gulp feeding manoeuvers (Segre *et al.*, 2019). Despite their wider vertebral centra, humpback whales (*Megaptera novaeangliae*), which are considered as coastal species, also rely on gulp feeding and have high manoeuvring abilities (Woodward *et al.*, 2006).

These considerations clearly indicate that habitat is not the only factor affecting backbone morphology and other ecological constrains might also shape the vertebral anatomy. Non-delphinoids include specialised deep-diving species mainly relying on suction feeding (sperm whales, beaked whales), mysticetes relying on bulk-feeding (most balaenopterids), and mysticetes relying on skim-feeding (balaenids). These ecological features most probably require different swimming abilities suggesting that ecomorphological investigations of non-delphinoids (or the entire cetacean clade) should include more detailed ecological parameters. Finally, contrarily to delphinoids that form a monophyletic clade, non-delphinoids are a paraphyletic group. It is hence likely that the different non-delphinoid families evolved under different constraints and patterns, implying that this group should probably be considered as several subgroups rather than a unique one.

1.2.2. Delphinoids

Contrarily to non-delphinoids, habitat has an important effect on vertebral count in delphinoids with an increasing number of vertebrae along the rivers-coasts-offshore gradient. The mean vertebral count in non-Delphinoidea is close to 50 and never exceeds 65, which is comparable to other mammalian clades. In contrast, the average number of vertebrae in Delphinoidea is 67 and the species with the highest count has 97 vertebrae. This increase in vertebral count is associated with a craniocaudal shortening of vertebral centra and apophyses. This ecomorphological pattern is observed both in phocoenids and delphinids although they have slightly different morphologies and follow distinct evolutionary trajectories as discussed above. Furthermore, the effect of habitat on the

vertebral morphology is so strong that backbone modifications, similar to those observed in the whole Delphinidae family, are also present between coastal and offshore ecotypes in the Northwest Atlantic Ocean bottlenose dolphin (*Tursiops truncatus*) population. The remarkable morphological, ecological and genetic partitioning between coastal and offshore ecotypes in several delphinid species (e.g., bottlenose dolphins, *T. truncatus*, spotted dolphins, *Stenella attenuata*, and common dolphins, *Delphinus* spp.) most probably reflects incipient speciation processes through ecological specialisation (Hoelzel *et al.*, 1998; Moura *et al.*, 2013; Segura-García *et al.*, 2016). This suggests that similar evolutionary patterns act at the macroevolutionary and microevolutionary levels in delphinids. A recent phylogeographic work on porpoises also suggested that ecological specialisation between coastal and offshore environments is an important pattern in this family both at the intra- and interspecific level, further supporting the possible continuity between micro- and macroevolutionary processes in delphinoids (Chehida *et al.*, 2019).

The increased vertebral count and vertebral shortening of coastal and particularly offshore small-sized delphinoids result in an increased stiffness of each intervertebral joint. This, in turn, reduces the theoretically predicted mobility (i.e., maximal curvature) of the backbone. However kinematic data of several cetacean species with different vertebral morphologies showed that fluke oscillation amplitude is similar among species (this study; Fish *et al.*, 2003; Rohr and Fish, 2004). Similarly, the amount of movements in the rostral region remains low for all species although anterior movements appear slightly higher in more flexible species. Reduced rostral movements provide higher stability adapted for steady high speed swimming over long distances (Fish *et al.*, 2003; Fish and Rohr, 1999). More importantly, species with increased backbone rigidity swim with higher tailbeat frequencies. Based on mechanical vibration properties, a stiffer backbone should have a higher natural frequency and the force necessary to create oscillations are lower when the material oscillates at a frequency close to its natural frequency (Géradin and Rixen, 2015; Long and Nipper, 1996). Species with a stiffer backbone could therefore use higher tailbeat frequencies without increasing the energetic cost. As swimming speed increases with fluke oscillation frequency, it allows small, stiff species to swim at higher speed and cover long distances in offshore environments.

1.3. Effect of body size

Besides correlation between phylogeny, ecology and vertebral morphology, body size also has an effect on vertebral count in non-delphinoids and, to a lesser extent, in delphinoids.

1.3.1. Non-delphinoids

Large non-delphinoids, especially mysticetes, reach body lengths unparalleled in terrestrial mammals. In this group, the vertebral count is not correlated to habitat but to body size with eight additional vertebrae per ten meters increase in body length. This phenomenon, termed pleomerism, is known to occur in fishes or snakes but has never been previously reported for mammals that rather increase their body size by increasing vertebral size (Lindell, 1994; Lindsey, 1975; Muller *et al.*, 2010). Body size increase through extreme vertebral elongation is only observed in archaeocetes of the genus *Basilosaurus* but not in other cetaceans which might reflect structural and/or developmental constraints related to their gigantism (Buchholtz, 2001b; Gingerich *et al.*, 1990). Alternatively, if vertebrae keep a relatively spool-shaped morphology, adding a few vertebrae might provide more flexibility to the body. For example, the elongated neck of giraffes and camels composed of 7 vertebrae is less flexible than the neck of ostriches which have 18 cervical vertebrae (Dzemski and Christian, 2007). As mentioned above, blue whales (*B. musculus*) partly rely on body flexibility to execute manoeuvres, notably during foraging (Segre *et al.*, 2019). Pleomerism in large cetaceans might then provide the flexibility necessary for prey capture during bulk-feeding.

1.3.2. Delphinoids

Among delphinoids, vertebral morphology is mainly associated to habitat. However, the vertebral count is significantly but poorly related to body size as large delphinoids tend to have fewer vertebrae. Killer whales (*Orcinus orca*), false killer whales (*Pseudorca crassidens*), and pilot whales (*Globicephala macrorhynchus* and *G. melas*) are the largest delphinids, reaching body size close to or higher than 5 meters, but have low vertebral count (53, 48, 57, and 60 vertebrae, respectively) despite their offshore ecology (or mixed inshore-offshore ecology for *O. orca*). Similarly, monodontids, belugas (*Delphinapterus leucas*) and narwhals (*Monodon monoceros*), reach body size higher than most delphinoids (between 3 and 5 meters) and have a low vertebral count (50 and 53 vertebrae, respectively). Although our results cannot provide a clear explanation to this pattern, several factors might be considered.

Because backbone rigidity increases at a higher rate with increasing vertebral disk diameter than with decreasing disk length, larger species have a stiffer backbone. Hence, larger species might not need to further increase their spine rigidity by shortening their vertebrae and intervertebral disks. In aquatic tetrapods such as seabirds, pinnipeds and cetaceans, swimming speed is independent of body size but fins oscillatory frequency significantly decreases with increasing body size (Sato *et al.*, 2007). At equivalent tailbeat frequencies, larger species should be able to cover a given distance faster than smaller species. Therefore, larger species might not need to use high tailbeat frequencies to reach swimming speeds comparable to those of small, stiff species. Increasing vertebral count and stiffness to use higher tailbeat frequencies might then not be necessary for larger offshore delphinoids.

Besides their relatively large body size, monodontids also have peculiar ecologies. Both species live in Artic and sub-Artic environment sometimes close to ice-caps, are found both in deep and shallow waters and feed, at least partly, on benthic preys (Berta, 2015; Laidre *et al.*, 2004; Richard *et al.*, 2001). These behaviours probably require high manoeuvring abilities associated to low vertebral count. The low vertebral count of killer whales might also be associated with their ecology rather than body size. Indeed they feed on a large variety of prey depending on the population and can also be encountered in various habitats both in deep and shallow waters which might require good manoeuvring performances (Berta, 2015; de Bruyn *et al.*, 2013). Moreover, they possess extremely large and rounded pectoral fins allowing precise manoeuvres (Fish and Rohr, 1999; Weber *et al.*, 2009). This suggests that killer whales might require good turning performances and therefore a relatively flexible body. Hence, the vertebral morphology of narwhals, belugas and killer whales might be related to their ecology and/or to an effect of body size.

2. Delphinoid backbone modification as key innovation

Albeit some aspects about the definition of key innovation are still debated, it is generally accepted that these key novelties are defined as: (1) the appearance of a new morphological trait in a lineage, (2) this trait supports new functional abilities, and (3) these new performances allow the colonization of a new adaptive zone (Hunter, 1998; Miller, 1949; Stroud and Losos, 2016). In this work, we also decided to consider that the acquisition of a key innovation should result in an increase

in species richness as the lineage can diversify within the new adaptive zone (Alfaro, 2013; Rabosky, 2017).

In this study, we demonstrated that delphinoids acquired a distinctive vertebral morphology characterised by numerous discoidal vertebrae. These characteristics are unique among cetaceans and even among mammals. Indeed, the mammalian vertebral count is highly conserved due to functional and/or developmental constraints and never exceeds 70 vertebrae while delphinoids can have up to 97 vertebrae (Galis *et al.*, 2014; Narita and Kuratani, 2005). Based on biomechanical model of the backbone and swimming kinematic analyses we showed that vertebral count increase in small-sized species increased the backbone stiffness. This would permit to increase the body stability but, particularly, to use higher tailbeat frequencies and hence higher swimming speed in an energy efficient manner.

Delphinoids, and especially delphinids and phocoenids, are the only extant oceanic small-sized cetaceans relying on single-prey targeting in the epipelagic and, to a lesser extent, mesopelagic zones. Other cetaceans either rely on bulk-feeding close to the surface and reach gigantic body sizes (e.g., rorquals and right whales), hunt single preys in the bathyal zone and possess medium to large body length (e.g., sperm whales and beaked whales), or are small-sized and rely on single-prey targeting but live in rivers or shallow bays close to the shore ('rivers dolphins'). Productive areas are more scattered in offshore environments (Bainbridge, 1957; Jacobs *et al.*, 2004), requiring long-distance travels between food sources. The large body size of mysticetes allow them to cover long distances and to support long duration fasting and is then adapted to patchy distributed feeding resources (Lindstedt and Boyce, 1985; Millar and Hickling, 1990; Slater *et al.*, 2017). On the contrary, delphinoids are less resilient to fasting because of their small size (Kastelein *et al.*, 1997; Lindstedt and Boyce, 1985; Millar and Hickling, 1990) but their increased swimming speed allows them to cover long distances in a short period. In addition, despite the increased body stability of delphinoids, their small body size provides higher turning performances compared to larger mysticetes (Fish, 1997), allowing them to rely in single-prey targeting rather than bulk-feeding. Hence, their small body size combined to increased backbone stiffness, due to the acquisition of numerous shortened vertebrae, allows delphinoids to exploit resources in a different manner than other cetaceans in offshore environment.

The delphinoid clade groups 46 species out of 89 living cetaceans and thus represents the most diverse taxon of extant cetaceans (Committee on Taxonomy, 2019). Previous studies have highlighted an increase in diversification rate in delphinids and, to a lesser extent, in phocoenids, indicating that they rapidly diversified in new ecological niches (Morlon *et al.*, 2011; Rabosky, 2014; Slater *et al.*, 2010; Steeman *et al.*, 2009). An increase in diversification rate is not a necessary condition to identify a key innovation as evolutionary turnover can blur the signal but it can provide additional support for the key novelty hypothesis (Rabosky, 2017). Delphinoids are a relatively recent group which emerged during the Early Miocene (approximately 20 Ma) (McGowen *et al.*, 2019), suggesting that species turnover might not have been sufficient yet to completely prevent the detection of a diversification rate increase. In this work we identified a shift in tempo and mode of vertebral morphology evolution occur at the same position on the cetacean phylogenetic tree. Moreover, we found a significant correlation between diversification rate and vertebral morphology (both count and shape), suggesting that changes in vertebral morphology are associated to the explosive radiation of dolphins and porpoises.

Overall, we demonstrated that (1) the acquisition of numerous discoidal vertebrae in delphinoids is a morphological novelty, (2) this new morphology allowed small-sized species to acquire an efficient high speed swimming style relying on greater frequency tailbeat, (3) their newly acquired swimming abilities allowed them to exploit feeding resources in epipelagic environments in a new manner, and (4) the acquisition of these new morpho-functional traits resulted in an increase in species richness and an explosive radiation, with delphinoids representing half of the extant cetacean diversity. All these arguments hence support the idea that the dramatic morphological changes observed in delphinoid backbone acted as a key innovation, contributing to the species richness of oceanic dolphins and porpoises.

3. Clues and leads about the evolutionary history of delphinoids

The rise of delphinoids approximately co-occurred with the extinction of several groups of archaic small sized odontocetes related to the Platanistoidea superfamily during the Middle or Late Miocene (approximately 15-10 Ma) (Fordyce and de Muizon, 2001; Marx *et al.*, 2016). Given their morphology including elongated snout and flexible neck comparable to extant river dolphin, it is

considered that both clades probably had distinct ecologies. This suggests that Platanistoidea decline was not driven by competition with delphinoids but possibly by climatic and environmental changes such as general cooling and marine regression (Cassens *et al.*, 2000; Fordyce and de Muizon, 2001). Based on this, Marx *et al.* (2016) suggested that extinct Platanistoidea might have been characterised by a shallow-water ecology and that their extinction could be linked to major climatic changes that occurred during the mid-Miocene and would have negatively impacted shallow-water habitats. If these hypotheses are correct, it suggests that early delphinoids were already adapted to deep-water habitats, which is coherent with our offshore ancestral state estimates and the vertebral morphology of some stem delphinoids such as *Albireo whistleri*. The extreme vertebral modifications of small sized delphinoids allowed them to exploit scattered food resources in offshore environments whereas Platanistoidea might not have been able to adapt to the environmental changes during the Miocene. Early delphinoids might have then diversified in oceanic waters and, later on, colonize shallower habitats.

The Delphinidae family experienced two major events of diversity increase: one during the Late Miocene (approximately 7 – 10 Ma) and another during the Late Pliocene-Pleistocene (around 1 – 4 Ma) (Bianucci, 2013). The first radiation might correspond to events of early dispersal of delphinids which would have been promoted by their offshore ecology and morphology, resulting in the establishment of the main extant subfamilies (i.e., Lissodelphininae, Globicephalinae, and Delphininae) (Banguera-Hinestroza *et al.*, 2014). The second radiation event corresponds to the rapid apparition of most extant species within each subfamily, implying that most Miocene and Pliocene delphinids are extinct now. Our stochastic mapping identified that most transitions to shallower habitats also occurred during the Late Pliocene and Pleistocene. Hence, this second diversification event could have been promoted, at least in part, by several independent recolonizations of shallower habitat (i.e., coasts, bays, rivers) by pelagic species, especially in Lissodelphininae and Delphininae subfamilies. This phenomenon is however unlikely for extant species with antitropical distribution for which dispersal and vicariance effects are more plausible (do Amaral *et al.*, 2016; Banguera-Hinestroza *et al.*, 2014; Steeman *et al.*, 2009). The offshore-onshore transitions have been accompanied by modifications of the vertebral morphology, suggesting some plasticity of the backbone. Colonisation of shallower habitats both at the population and family level could have been supported by cyclic sea-level fluctuations that occurred from the Late Pliocene to the present and

probably impacted shallow habitats, as previously suggested (do Amaral *et al.*, 2016; Bianucci, 2013; Miller *et al.*, 2005; Moura *et al.*, 2013; Segura-García *et al.*, 2016, 2018; Steeman *et al.*, 2009). Similarly, ecological specialisations between coastal and offshore environments are thought to have played a central role in the diversification of extant porpoises (Chehida *et al.*, 2019). Therefore, the current diversity of Delphinidae and, to a larger extent, Delphinoidea probably results from a combination of dispersal events, ecological preferences, phenotypic plasticity and abiotic factors.

4. Vertebral count and developmental constraints

Due to developmental and biomechanical constraints related to the presence of the sacrum, the vertebral count is highly conserved in mammals, especially in the pre-sacral region (ten Broek *et al.*, 2012; Galis *et al.*, 2014; Muller *et al.*, 2010; Narita and Kuratani, 2005). Indeed, modifications of the vertebral count in the trunk region imply homeotic transformations in the pre-caudal region. Such modifications usually result in the occurrence of a transitional lumbosacral vertebra that can hinder locomotor abilities in terrestrial mammals (ten Broek *et al.*, 2012; Galis *et al.*, 2014). Previous works have already suggested that the reduction and the loss of locomotor function of the pelvic girdle in cetaceans and other limbless tetrapods released functional constraints allowing modifications of the pre-sacral vertebral count (Buchholtz and Gee, 2017; Caldwell, 2003; Cohn and Tickle, 1999; Thewissen *et al.*, 2006; Woltering, 2012). However, this would imply that all cetaceans rather than only Delphinoidea could have experienced an extreme vertebral count increase.

In pantropical spotted dolphin (*Stenella attenuata*) embryos, hindlimb buds are present during the first developmental stages but then they gradually degenerate from the fifth gestational week due to the lack of expression of the signalling factor *Sonic hedgehog* (*Shh*) (Thewissen *et al.*, 2006). Only a vestigial pelvis remains in adult dolphins. As the hindlimb of archaeocetes became gradually more reduced, it is likely that the loss of expression of *Shh* was not sudden but rather gradual (Bejder and Hall, 2002; Thewissen *et al.*, 2006). Currently, the expression of *Shh* has not been investigated in any other cetacean species, however, embryonic hindlimb buds persist longer in humpback whales (*Megaptera novaeangliae*) than in odontocetes (Bejder and Hall, 2002). Therefore, we cannot exclude the hypothesis that *Shh* expression in the hindlimbs gradually decreased during crown cetacean evolution until it totally disappeared in Delphinoidea.

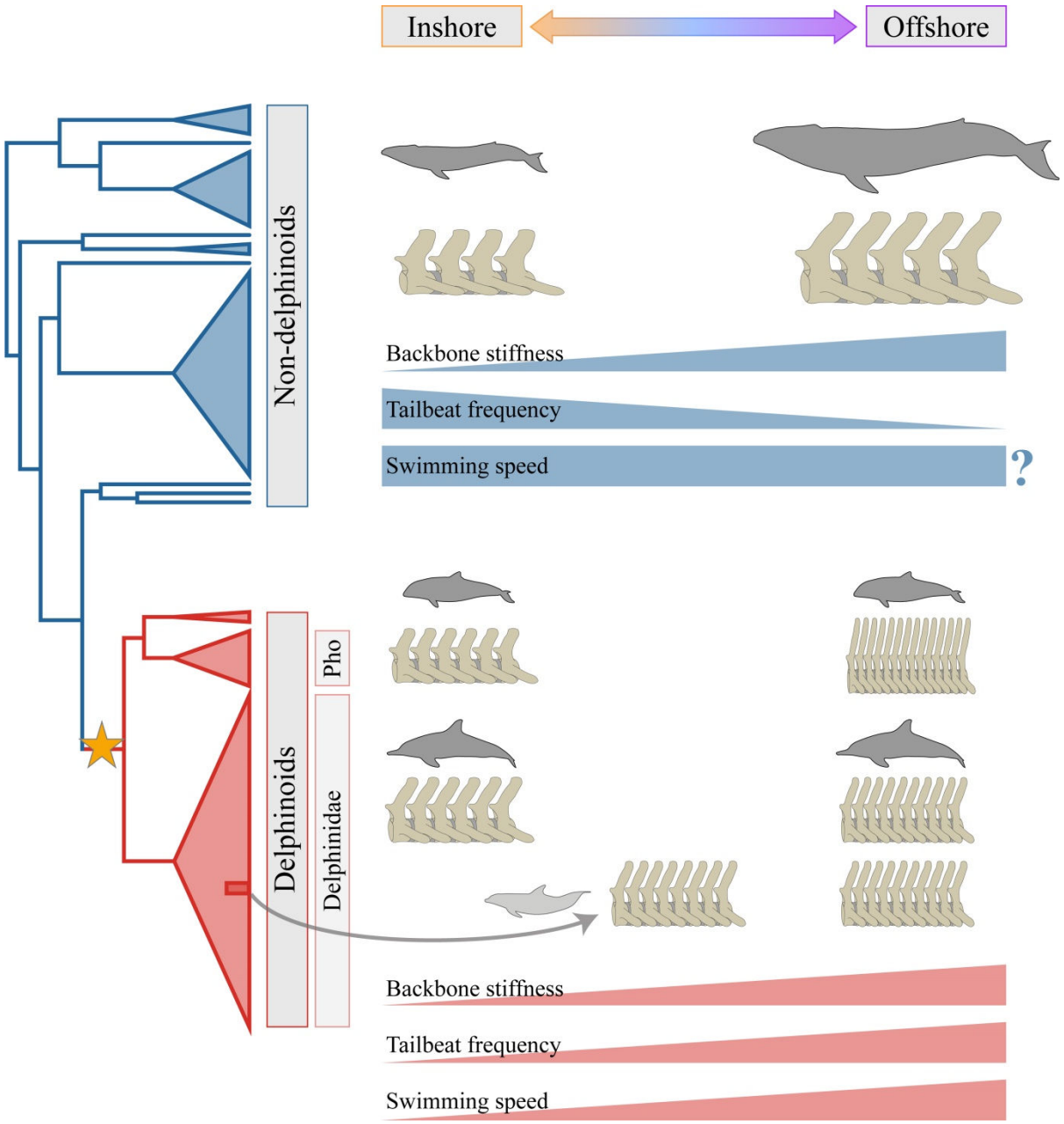

Figure 5.1. Summary of cetacean backbone evolution and biomechanical impacts. The tempo and mode of cetacean backbone evolution experienced a shift (shown by orange star) and followed two distinct patterns: non-delphinoids and delphinoids. Non-delphinoids (mysticetes, sperm whales, beaked whales, and 'river dolphins') retained a low vertebral count and elongated vertebrae. Offshore species are larger than inshore species and have a few more vertebrae (pleomerism). Backbone stiffness increases and tailbeat frequency decreases (Sato *et al.*, 2007) with increasing body size. Body size corrected swimming speed is probably relatively constant but further work is needed to confirm or infirm this trend. Delphinoids (belugas, narwhals, porpoises, and oceanic dolphins) have an extremely modified vertebral morphology defined by numerous discoidal vertebrae while retaining a small body size. In this group, offshore species have a higher vertebral count than inshore species. The two most species-rich delphinoid families, Phocoenidae and Delphinidae, followed slightly different pattern along the habitat gradient and offshore porpoises exhibit vertebral count increase more pronounced than delphinids. Vertebral shape modifications associated to habitat are also found at the intraspecific level between coastal and offshore ecotypes of *Tursiops truncatus* (light grey silhouette). The vertebral anatomy of offshore delphinoids increases their backbone stiffness and tailbeat frequency, resulting in higher swimming speed. It allowed them to colonize a new adaptive zone and acted as key innovations supporting their explosive radiation.

The dramatic change in vertebral counts observed in delphinoids might also result from an increased frequency in the somitogenesis clock during embryogenesis (Bejder and Hall, 2002; Buchholtz and Gee, 2017). However, additional vertebrae are not evenly distributed between the different regions of the backbone. Buchholtz and Gee (2017) thus suggested the existence of a region-specific somitogenesis rate in odontocetes to explain their variation in vertebral counts implying some interaction between somitogenesis and axial patterning. Somitogenesis process and *Shh* expression both interact, at least partially, with *Hox* genes (ten Broek *et al.*, 2012; Thewissen *et al.*, 2006; Woltering, 2012; Zákány *et al.*, 2001, 2004). Consequently, modifications in *Hox* genes expression level could have led to the highly reduced hindlimbs of dolphins and the extreme modification of the vertebral count and shape in Delphinoidea. Further ontogenetic and genetic studies are clearly needed to better understand the evolutionary variation in vertebral counts among cetaceans.

5. Conclusion

The main aim of this study was to identify the relation between vertebral morphology; backbone biomechanics, swimming kinematics, ecology and evolutionary history of cetaceans. Our results clearly demonstrate that both ecological and phylogenetic factors are related to their vertebral morphology and we identified two distinct phenotypic evolutionary patterns (Figure 5.1).

All non-delphinoids (mysticetes, sperm whales, beaked whales and 'river dolphins') are characterised by a relatively low vertebral count comparable to other mammals, spool-shaped vertebrae and a large variability in body size. Within this group, vertebral shape is correlated to habitat but vertebral count is rather correlated to body size. Riverine and estuarine non-delphinoids are small sized and have elongated vertebrae assuring high manoeuvring performances necessary in shallow and complex habitats. Coastal and offshore non-delphinoids retained a low vertebral count, similar to terrestrial mammals, but have medium-to-large body size providing advantages for deep diving or bulk-feeding and long-distances migration.

Delphinoids experienced a sudden and drastic change in vertebral morphology. Most delphinoids retained a small body size but show extreme increase in vertebral count, associated with a shortening of all vertebrae. In this group, the vertebral shape and count are correlated to habitat but not to body size. Riverine species possess few elongated vertebrae while offshore species exhibit an

exceptionally high number of discoidal vertebrae. This peculiar morphology increases backbone stiffness, allowing delphinoids to use higher tailbeat frequencies and therefore higher swimming speed in an energy efficient way. This functional novelty permitted small cetaceans to exploit oceanic resources in a novel way, relying on single-prey targeting in the epipelagic zone, compared to non-delphinoids which rely on bulk-feeding in the epipelagic zone or on single-prey targeting at high depths. The evolutionary history of delphinoids is characterised by numerous ecological transitions between offshore, coastal and riverine habitats both at the inter- and intraspecific levels. This suggests that the combination of a small body size with a modified vertebral morphology provide them some ecological plasticity. Hence, the exceptional vertebral morphology of delphinoids can be considered as a key innovation that supported their explosive radiation and ecological success.

6. Perspectives

A condition to efficiently identify key innovations would be to test if the independent appearance of the trait in several lineages always leads to a shift in adaptive zone and an increase in species richness (Alfaro, 2013; Wainwright and Price, 2016). This point of view is nonetheless arguable as diversification most probably relies on the combination of numerous other intrinsic of extrinsic factors. For example, the acquisition of a key trait might trigger an adaptive radiation in a few clades but not in others because the adaptive zone might already be occupied or because developmental of functional constraints might restrict the ability of the clade to diversify (Alfaro, 2013; Stroud and Losos, 2016). Besides this concern, this methodology might be challenging in practice as numerous key innovations only occurred once. In cetaceans, the shift in vertebral morphology is only observed in Delphinoidea and prevented us to use such an approach. However, several other vertebrate clades such as ichthyosaurs, mosasaurs or plesiosaurs, secondarily adapted to a fully aquatic ecology in the past (Kelley and Pyenson, 2015; Lindgren *et al.*, 2010). Previous studies have demonstrated that Early Triassic ichthyosaurs had more elongated vertebrae and morphology similar to bottom-dwelling sharks while Late Triassic and Cretaceous species, especially the highly diverse Parvipelvians, had a deep body and discoidal vertebrae similar to pelagic lamnid sharks (Buchholtz, 2001a; Motani, 2005; Motani *et al.*, 1996). Similarly, derived mosasaurs exhibit shortened vertebrae compared to more basal species. This shortening is believed to be associated with a transition from anguilliform swimming in shallow environment to efficient carangiform swimming in

pelagic habitat (Lindgren *et al.*, 2011). Investigating the vertebral disparity and species richness of extinct secondarily aquatic vertebrates in an evolutionary context might be useful to further test the key innovation hypothesis of our work. However, ecomorphological and evolutionary investigations on extinct clade are challenging and might be impaired by the preservation state of the specimens.

In this work, we considered the backbone as a whole, investigating the impact of ecology on all vertebral region together. However, ecomorphological analyses of the backbone of felids and mammals in general have demonstrated that the lumbar region is indeed correlated to habitat and locomotor modes (fossorial, terrestrial, scansorial, arboreal, and semi-aquatic) while a weak or even no correlation at all is found in the thoracic region (Jones *et al.*, 2018a; Randau *et al.*, 2016). This suggests that vertebral regions are impacted by different functional constraints. Testing the effect of ecology for each vertebral region independently might provide further information on the ecomorphological and evolutionary patterns of the cetacean backbone.

In our analyses of cetacean vertebral shape (chapter 2), beaked whales (Ziphiidae) occupy a restricted and distinct area of the morphospace. They are characterised by elongated vertebrae with a low diameter, low metapophyses and extremely long neural spines. Interestingly, an evolutionary shift corresponding to a decrease in evolutionary rate of the vertebral shape was also detected in Ziphiidae (especially when using non-phylogenetically corrected measurements). Beaked whales represent the second largest family of extant cetaceans, are all specialised deep divers, and use a peculiar swimming gait, termed B-strokes (Martín López *et al.*, 2015). Their peculiar and conserved vertebral morphology might be associated with these eco-functional characteristics but further work focusing on beaked whales and, to a larger extent, deep-divers would be needed.

Finally, our results regarding the biomechanics of the backbone provide important information about the effect of vertebral shortening in delphinoids. However, these results rely on modelling and numerous simplifications of the musculo-skeletal anatomy. Moreover, the sole experimental study that tested the biomechanics of dolphins intervertebral disk did it on a few single vertebral segments in one species (Long *et al.*, 1997). Hence, it remains unsure if the increased vertebral count of delphinoids corresponds to an increased stiffness of the entire backbone and not just of each individual segment. Further work experimentally testing the entire backbone biomechanics would greatly improve the understanding the impact of morphological change on functional abilities.

References

Adams D.C. and Cerney M.M. (2007) Quantifying biomechanical motion using Procrustes motion analysis. *Journal of Biomechanics*, **40**(2): 437–444.

Adams D.C., Collyer M.L. and Kaliontzopoulou A. (2018) Geomorph: Software for geometric morphometric analyses. *R package version 3.0.6*.

Agnarsson I. and May-Collado L.J. (2008) The phylogeny of Cetartiodactyla: the importance of dense taxon sampling, missing data, and the remarkable promise of cytochrome b to provide reliable species-level phylogenies. *Molecular Phylogenetics and Evolution*, **48**(3): 964–985.

Aguirre-Fernández G. and Fordyce R.E. (2014) *Papahu taitapu*, gen. et sp. nov., an early Miocene stem odontocete (Cetacea) from New Zealand. *Journal of Vertebrate Paleontology*, **34**(1): 195–210.

Alfaro M.E. (2013) Key evolutionary innovations. In *The Princeton Guide to Evolution* (ed. Losos J.B.), pp.592–598. Princeton: Princeton University Press.

Amaral A.R., Beheregaray L.B., Bilgmann K., Freitas L., Robertson K.M., Sequeira M., Stockin K.A., Coelho M.M. and Möller L.M. (2012) Influences of past climatic changes on historical population structure and demography of a cosmopolitan marine predator, the common dolphin (genus *Delphinus*). *Molecular Ecology*, **21**(19): 4854–4871.

Andrews K.R., Perrin W.F., Oremus M., Karczmarski L., Bowen B.W., Puritz J.B. and Toonen R.J. (2013) The evolving male: spinner dolphin (*Stenella longirostris*) ecotypes are divergent at Y chromosome but not mtDNA or autosomal markers. *Molecular Ecology*, **22**(9): 2408–2423.

Armstrong R.B. and Laughlin M.H. (1985) Metabolic indicators of fibre recruitment in mammalian muscles during locomotion. *Journal of Experimental Biology*, **115**(1): 201–213.

Arnold S.J. (1983) Morphology, performance and fitness. *Integrative and Comparative Biology*, **23**(2): 347–361.

Arnold S.J., Pfrender M.E. and Jones A.G. (2001) The adaptive landscape as a conceptual bridge between micro- and macroevolution. *Genetica*, **112–113**(1): 9–32.

Arthur L.H., McLellan W.A., Piscitelli M.A., Rommel S.A., Woodward B.L., Winn J.P., Potter C.W. and Pabst D.A. (2015) Estimating maximal force output of cetaceans using axial locomotor muscle morphology. *Marine Mammal Science*, **31**(4): 1401–1426.

Asher R.J. and Helgen K.M. (2010) Nomenclature and placental mammal phylogeny. *BMC Evolutionary Biology*, **10**: 102.

Bainbridge R. (1957) The size, shape and density of marine phytoplankton concentrations. *Biological Reviews*, **32**(1): 91–115.

Bainbridge R. (1958) The speed of swimming of fish as related to size and to the frequency and amplitude of the tail beat. *Journal of Experimental Biology*, **35**(1): 109–133.

Banguera-Hinestroza E., Hayano A., Crespo E. and Hoelzel A.R. (2014) Delphinid systematics and biogeography with a focus on the current genus *Lagenorhynchus*: Multiple pathways for antitropical and trans-oceanic radiation. *Molecular Phylogenetics and Evolution*, **80**: 217–230.

Bannister J.L. (2009) Baleen whales (mysticetes). In *Encyclopedia of Marine Mammals*, 2nd edn (eds Perrin W.F., Würsig B.G., and Thewissen J.G.M.), pp.80–89. San Diego: Academic Press.

Barnes L.G. (1985a) Evolution, taxonomy and antitropical distributions of the porpoises (Phocoenidae, Mammalia). *Marine Mammal Science*, **1**(2): 149–165.

Barnes L.G. (1985b) The late Miocene dolphin *Pithanodelphis* Abel, 1905 (Cetacea: Kentriodontidae) from California. *Contributions in Science*, **367**: 1–27.

Barnes L.G. (2008) Miocene and Pliocene Albireonidae (Cetacea, Odontoceti), rare and unusual fossil dolphins from the eastern North Pacific Ocean. *Natural History Museum of Los Angeles County Science Series*, **41**: 99–152.

Bearzi M. (2005) Dolphin sympatric ecology. *Marine Biology Research*, **1**(3): 165–175.

Bejder L. and Hall B.K. (2002) Limbs in whales and limblessness in other vertebrates: mechanism of evolutionary and developmental transformation and loss. *Evolution and Development*, **4**(6): 445–458.

Bell A. and Chiappe L.M. (2011) Statistical approach for inferring ecology of Mesozoic birds. *Journal of Systematic Palaeontology*, **9**(1): 119–133.

Bellwood D.R. (2003) Origins and escalation of herbivory in fishes: a functional perspective. *Paleobiology*, **29**(1): 71–83.

Berta A. (2015) *Whales, dolphins and porpoises: A natural history and species guide*. East Sussex: Ivy Press.

Berta A., Sumich J. and Kovacs K. (2006) Cetacean evolution and systematics. In *Marine mammals*, 2nd edn, pp.51–87. San Diego: Academic Press.

Bianucci G. (2013) *Septidelphis morii*, n. gen. et sp., from the Pliocene of Italy: new evidence of the explosive radiation of true dolphins (Odontoceti, Delphinidae). *Journal of Vertebrate Paleontology*, **33**(3): 722–740.

Bininda-Emonds O.R.P., Cardillo M., Jones K.E., MacPhee R.D.E., Beck R.M.D., Grenyer R., Price S.A., Vos R.A., Gittleman J.L. and Purvis A. (2007) The delayed rise of present-day mammals. *Nature*, **446**(7135): 507–513.

Bisconti M. and Varola A. (2006) The oldest eschrichtiid mysticete and a new morphological diagnosis of Eschrichtiidae (gray whales). *Rivista Italiana di Paleontologia e Stratigrafia*, **112**(3): 447–457.

Bloodworth B.E. and Marshall C.D. (2007) A functional comparison of the hyolingual complex in pygmy and dwarf sperm whales (*Kogia breviceps* and *K. sima*), and bottlenose dolphins (*Tursiops truncatus*). *Journal of Anatomy*, **211**(1): 78–91.

Bock W.J. (1990) From biologische anatomie to ecomorphology. *Netherlands Journal of Zoology*, **40**(1–2): 254–277.

Bose N., Lien J. and Ahia J. (1990) Measurements of the bodies and flukes of several cetacean species. *Proceedings of the Royal Society B: Biological Sciences*, **242**(1305): 163–173.

Boyden A. and Gemeroy D. (1950) The relative position of the Cetacea among the orders of Mammalia as indicated by precipitin tests. *Zoologica*, **35**(11): 145–151.

Bray J.P. and Burbidge H.M. (1998) The canine intervertebral disk: part one: structure and function. *Journal of the American Animal Hospital Association*, **34**(1): 55–63.

de Bruyn P.J.N., Tosh C.A. and Terauds A. (2013) Killer whale ecotypes: is there a global model? *Biological Reviews*, **88**(1): 62–80.

Buchholtz E.A. (2001a) Swimming styles in Jurassic ichthyosaurs. *Journal of Vertebrate Paleontology*, **21**(1): 61–73.

Buchholtz E.A. (2001b) Vertebral osteology and swimming style in living and fossil whales (Order: Cetacea). *Journal of Zoology*, **253**(2): 175–190.

Buchholtz E.A. (2007) Modular evolution of the cetacean vertebral column. *Evolution and Development*, **9**(3): 278–289.

Buchholtz E.A. (2011) Vertebral and rib anatomy in *Caperea marginata*: Implications for evolutionary patterning of the mammalian vertebral column. *Marine Mammal Science*, **27**(2): 382–397.

Buchholtz E.A. and Gee J.K. (2017) Finding sacral: Developmental evolution of the axial skeleton of odontocetes (Cetacea). *Evolution and Development*, **19**(4–5): 190–204.

Buchholtz E.A. and Schur S.A. (2004) Vertebral osteology in Delphinidae (Cetacea). *Zoological Journal of the Linnean Society*, **140**(3): 383–401.

Buchholtz E.A., Wolkovich E.M. and Cleary R.J. (2005) Vertebral osteology and complexity in *Lagenorhynchus acutus* (Delphinidae) with comparison to other delphinoid genera. *Marine Mammal Science*, **21**(3): 411–428.

Butler W.F. (1989) Comparative anatomy and development of the mammalian disc. In *The Biology of the Intervertebral Disc* (ed. Ghosh P.), pp.84–108. Boca Raton: CRC Press.

Caballero S., Islas-Vilanueva V., Tezanos-Pinto G., Duchene S., Delgado-Estrella A., Sanchez-Okrucky R. and Mignucci-Giannoni A.A. (2012) Phylogeography, genetic diversity and population structure of common bottlenose dolphins in the Wider Caribbean inferred from analyses of mitochondrial DNA control region sequences and microsatellite loci: conservation and management implications. *Animal Conservation*, **15**(1): 95–112.

Caldwell M.W. (2003) 'Without a leg to stand on': on the evolution and development of axial elongation and limblessness in tetrapods. *Canadian Journal of Earth Sciences*, **40**(3): 573–588.

Cassens I., Vicario S., Waddell V.G., Balchowsky H., Van Belle D., Ding W., Fan C., Mohan R.S.L., Simões-Lopes P.C., Bastida R., Meyer A., Stanhope M.J. and Milinkovitch M.C. (2000) Independent adaptation to riverine habitats allowed survival of ancient cetacean lineages. *Proceedings of the National Academy of Sciences*, **91**(21): 11343–11347.

Chehida Y.B., Thumloup J., Schumacher C., Harkins T., Aguilar A., Borrell A., Ferreira M., Rojas-Bracho L., Robertson K.M., Taylor B.L., Víkingsson G.A., Weyna A., Romiguier J., Morin P.A. and Fontaine M.C. (2019) Evolutionary history of the porpoises (Phocoenidae) across the speciation continuum: a mitogenome phylogeographic perspective. *bioRxiv*, doi: 10/1101/851469.

Chen M. and Wilson G.P. (2014) A multivariate approach to infer locomotor modes in Mesozoic mammals. *Paleobiology*, **41**(2): 280–312.

Chen X., Milne N. and O'Higgins P. (2005) Morphological variation of the thoracolumbar vertebrae in Macropodidae and its functional relevance. *Journal of Morphology*, **266**(2): 167–181.

Clausen J. (1951) *Stages in the evolution of plant species*. Ithaca, NY: Cornell University Press.

Clauset A. (2013) How large should whales be? *PLoS one*, **8**(1): e53967.

Clementz M.T., Goswami A., Gingerich P.D. and Koch P.L. (2006) Isotopic records from early whales and sea cows: contrasting patterns of ecological transition. *Journal of Vertebrate Paleontology*, **26**(2): 355–370.

Cohn M.J. and Tickle C. (1999) Developmental basis of limblessness and axial patterning in snakes. *Nature*, **399**(6735): 474–479.

Collyer M.L. and Adams D.A. (2013) Phenotypic trajectory analysis: comparison of shape change patterns in evolution and ecology. *Hystrix, the Italian Journal of Mammalogy*, **24**(1): 75–83.

Committee on Taxonomy (2019) List of marine mammal species and subspecies. *Society for Marine Mammalogy*.

Costa A.P.B., Rosel P.E., Daura-Jorge F.G. and Simões-Lopes P.C. (2016) Offshore and coastal common bottlenose dolphins of the western South Atlantic face-to-face: what the skull and the spine can tell us. *Marine Mammal Science*, **32**(4): 1433–1457.

Costa A.P.B., Fruet P.F., Secchi E.R., Daura-Jorge F.G., Simões-Lopes P.C., Di Tullio J.C. and Rosel P.E. (2019) Ecological divergence and speciation in common bottlenose dolphins in the western South Atlantic. *Journal of Evolutionary Biology*, 13575.

Cracraft J. (1986) The origin and early diversification of birds. *Paleobiology*, **12**(4): 383–399.

Cracraft J. (1990) The origin of evolutionary novelties: pattern and process at different hierarchical levels. In *Evolutionary innovations* (ed. Nitecki M.), pp.21–44. Chicago: University of California Press.

Cranford T.W. (1999) The sperm whale's nose: sexual selection on a grand scale? *Marine Mammal Science*, **15**(4): 1133–1157.

Crespo E.A., Pedraza S.N., Grandi M.F., Dans S.L. and Garaffo G. V. (2010) Abundance and distribution of endangered Franciscana dolphins in Argentine waters and conservation implications. *Marine Mammal Science*, **26**(1): 17–35.

Curran J. (2018) Hotelling: Hotelling's T^2 and variants. *R package version 1.0-5*.

Curren K., Bose N. and Lien J. (1994) Swimming kinematics of a harbor porpoise (*Phocoena phocoena*) and an Atlantic white-sided dolphin (*Lagenorhynchus acutus*). *Marine Mammal Science*, **10**(4): 485–492.

Dahlheim M.E., Schulman-Janiger A., Black N., Ternullo R., Ellifrit D. and Balcomb K.C.I. (2008) Eastern temperate North Pacific offshore killer whales (*Orcinus orca*): occurrence, movements, and insights into feeding ecology. *Marine Mammal Science*, **24**(3): 719–729.

DeSmet W.M.A. (1977) The regions of the cetacean vertebral column. In *Functional anatomy of marine mammals, Vol 3* (ed. Harrison J.), pp.58–80. New York: Academic Press.

do Amaral K.B., Amaral A.R., Ewan Fordyce R. and Moreno I.B. (2016) Historical biogeography of delphininae dolphins and related taxa (Artiodactyla: Delphinidae). *Journal of Mammalian Evolution*, **25**(2): 241–259.

Dobzhansky T. (1951) *Genetics and the origin of species*. 3rd edn. New York: Columbia University Press.

Drummond C.S., Eastwood R.J., Miotto S.T.S. and Hughes C.E. (2012) Multiple continental radiations and correlates of diversification in *Lupinus* (Leguminosae): testing for key innovation with incomplete taxon sampling. *Systematic Biology*, **61**(3): 443–460.

Dzemski G. and Christian A. (2007) Flexibility along the neck of the ostrich (*Struthio camelus*) and consequences for the reconstruction of dinosaurs with extreme neck length. *Journal of Morphology*, **268**(8): 701–714.

Emlong D. (1966) A new archaic cetacean from the Oligocene of northwest Oregon. *Bulletin of the Museum of Natural History of the University of Oregon*, **3**: 1–51.

Fish F.E. (1993) Power output and propulsive efficiency of swimming bottlenose dolphins (*Tursiops truncatus*). *Journal of Experimental Biology*, **185**(1): 179–193.

Fish F.E. (1997) Biological designs for enhanced maneuvrability: analysis of marine mammal performance. In *Proceedings of the Tenth International Symposium on Unmanned Untethered Submersible Technology: Proceedings of the special session on bioengineering research related to autonomous underwater vehicles*, pp.109–117. Lee, New Hampshire.

Fish F.E. (1998) Comparative kinematics and hydrodynamics of odontocete cetaceans: morphological and ecological correlates with swimming performance. *Journal of Experimental Biology*, **201**(20): 2867–2877.

Fish F.E. (2002) Balancing requirements for stability and maneuverability in cetaceans. *Integrative and Comparative Biology*, **42**(1): 85–93.

Fish F.E. (2016) Secondary evolution of aquatic propulsion in higher vertebrates : validation and prospect. *Integrative and Comparative Biology*, **56**(6): 1285–1297.

Fish F.E., Peacock J.E. and Rohr J.J. (2003) Stabilization mechanism in swimming odontocete cetaceans by phased movements. *Marine Mammal Science*, **19**(3): 515–528.

Fish F.E. and Rohr J.J. (1999) *Review of dolphin hydrodynamics and swimming performance*. San Diego: SSC San Diego.

Fitch W.J. and Beintema J.J. (1990) Correcting parsimonious tress for unseen nucleotide substitutions: the effect of dense branching as exemplified by ribonuclease. *Molecular Biology and Evolution*, **7**(5): 438–443.

Flower W.H. (1883) On whales, past and present, and their probable origin. *Nature*, **28**(713): 199–202.

Flower W.H. (1885) *An introduction to the osteology of the Mammalia*. 3rd edn. London: Macmillan.

Fontaine M.C., Roland K., Calves I., Austerlitz F., Palstra F.P., Tolley K.A., Ryan S., Ferreira M., Jauniaux T., Llavona A., *et al.* (2014) Postglacial climate changes and rise of three ecotypes of harbour porpoises, *Phocoena phocoena*, in western Palearctic waters. *Molecular Ecology*, **23**(13): 3306–3321.

Foote M. (1997) The evolution of morphological diversity. *Annual Review of Ecology, Evolution, and Systematics*, **28**: 129–152.

Fordyce E. and de Muizon C. (2001) Evolutionary history of cetaceans: a review. In *Secondary Adaptation of Tetrapods to Life in Water* (eds Mazin J.-M. and de Buffrénil V.), pp.169–233. München: Verlag Dr. Friedrich Pfeil.

Fordyce R.E., Barnes L.G. and Miyazaki N. (1994) General aspects of the evolutionary history of whales and dolphins. *Island Arc*, **3**(4): 373–391.

Fordyce R.E. and Marx F.G. (2013) The pygmy right whale *Caperea marginata*: the last of the cetotheres. *Proceedings of the Royal Society B: Biological Sciences*, **280**(1753): 20122645.

Frédérich B., Marramà G., Carnevale G. and Santini F. (2016) Non-reef environments impact the diversification of extant jacks, remoras and allies (Carangoidei, Percomorpha). *Proceedings of the Royal Society B: Biological Sciences*, **283**(1842): 20161556.

Gál J.M. (1993a) Mammalian spinal biomechanics: I. Static and dynamic mechanical properties of intact intervertebral joints. *Journal of Experimental Biology*, **174**(1): 247–280.

Gál J.M. (1993b) Mammalian spinal biomechanics: II. Intervertebral lesion experiments and mechanisms of bending resistance. *Journal of Experimental Biology*, **174**(1): 281–297.

Galatius A., Andersen M.E.R., Haugan B., Langhoff H.E. and Jespersen Å. (2006) Timing of epiphyseal development in the flipper skeleton of the harbour porpoise (*Phocoena phocoena*) as an indicator of paedomorphosis. *Acta Zoologica*, **87**(1): 77–82.

Galatius A., Berta A., Frandsen M.S. and Goodall R.N.P. (2011) Interspecific variation of ontogeny and skull shape among porpoises (Phocoenidae). *Journal of Morphology*, **272**(2): 136–148.

Galatius A. and Goodall R.N.P. (2016) Skull shapes of the Lissodelphininae: radiation, adaptation and asymmetry. *Journal of Morphology*, **277**(6): 776–785.

Galis F., Carrier D.R., van Alphen J., van der Mije S.D., Van Dooren T.J.M., Metz J.A.J. and ten Broek C.M.A. (2014) Fast running restricts evolutionary change of the vertebral column in mammals. *Proceedings of the National Academy of Sciences*, **111**(31): 11401–11406.

Garland T.J. and Losos J.B. (1994) Ecological morphology of locomotor performance in squamate reptiles. In *Ecological morphology: Integrative organismal biology* (eds Wainwright P.C. and Reilly S.M.), pp.240–302. Chicago: University of Chicago Press.

Gaspari S., Scheinin A., Holcer D., Fortuna C., Natali C., Genov T., Frantzis A., Chelazzi G. and Moura A.E. (2015) Drivers of population structure of the bottlenose dolphin (*Tursiops truncatus*) in the Eastern Mediterranean Sea. *Evolutionary Biology*, **42**(2): 177–190.

Gatesy J. (1998) Molecular evidence for the phylogenetic affinities of Cetacea. In *The Emergence of Whales*, pp.63–112. New York: Plenum Press.

Gatesy J., Geisler J.H., Chang J., Buell C., Berta A., Meredith R.W., Springer M.S. and McGowen M.R. (2013) A phylogenetic blueprint for a modern whale. *Molecular Phylogenetics and Evolution*, **66**(2): 479–506.

Geisler J., McGowen M., Yang G. and Gatesy J. (2011) A supermatrix analysis of genomic, morphological, and paleontological data from crown Cetacea. *BMC Evolutionary Biology*, **11**: 112.

Geisler J.H. (2018) Neoceti. In *Encyclopedia of Marine Mammals*, 3rd edn (eds Würsig B.G., Thewissen J.G.M., and Kovacs K.M.), pp.631–632. San Diego: Academic Press.

Geisler J.H., Godfrey S.J. and Lambert O. (2012) A new genus and species of late Miocene inioid (Cetacea , Odontoceti) from the Meherrin River, North Carolina, USA. *Journal of Vertebrate Paleontology*, **32**(1): 198–211.

Geisler J.H. and Theodor J.M. (2009) Hippopotamus and whale phylogeny. *Nature*, **458**(7236): E1-4.

Géradin M. and Rixen D.J. (2015) *Mechanical vibrations: Theory and application to structural dynamics*. 3rd edn. Chichester: Wiley.

Gillet A., Frédérich B. and Parmentier E. (2019) Divergent evolutionary morphology of the axial skeleton as a potential key innovation in modern cetaceans. *Proceedings of the Royal Society B: Biological Sciences*, **286**(1916): 20191771.

Gingerich P.D., ul Haq H., Zalmout I.S., Khan I.H. and Malkani M.S. (2001) Origin of whales from early artiodactyls: hands and feet of eocene Protocetidae from Pakistan. *Science*, **293**(5538): 2239–2242.

Gingerich P.D., Arif M. and Clyde W.C. (1995) New archaeocetes (Mammalia, Cetacea) from the Middle Eocene Domanda Formation of the Sulaiman Range, Punjeb (Pakistan). *Contributions from the Museum of Paleontology*, **29**(11): 291–330.

Gingerich P.D., Smith B.H. and Simons E.L. (1990) Hind limbs of Eocene *Basilosaurus*: evidence of feet in whales. *Science*, **249**(4965): 154–157.

Goodman M., Czelusniak J. and Beeber J.E. (1985) Phylogeny of primates and other eutherian orders: a cladistic analysis using amino acid and nucleotide sequence data. *Cladistics*, **1**(2): 171–185.

Gough W.T., Segre P.S., Bierlich K.C., Cade D.E., Potvin J., Fish F.E., Dale J., di Clemente J., Friedlaender A.S., Johnston D.W., *et al.* (2019) Scaling of swimming performance in baleen whales. *Journal of Experimental Biology*, **222**(20): jeb204172.

Granatosky M.C., Miller C.E., Boyer D.M. and Schmitt D. (2014) Lumbar vertebral morphology of flying, gliding, and suspensory mammals: implications for the locomotor behavior of the subfossil lemurs *Palaeopropithecus* and *Babakotia*. *Journal of Human Evolution*, **75**: 40–52.

Grant P.R. (2013) Adaptive radiation. In *The Princeton Guide to Evolution* (ed. Losos J.B.), pp.559–566. Princeton: Princeton University Press.

Grant P.R. and Grant B.R. (2008) *How and why species multiply: The radiation of Darwin's finches*. Princeton: Princeton University Press.

Grantham T. (2007) Is macroevolution more than successive rounds of microevolution? *Palaeontology*, **50**(1): 75–85.

Gutstein C.S., Figueroa-Bravo C.P., Pyenson N.D., Yury-Yañez R.E., Cozzuol M.A. and Canals M. (2014) High frequency echolocation, ear morphology, and the marine-freshwater transition: a comparative study of extant and extinct toothed whales. *Palaeogeography, Palaeoclimatology, Palaeoecology*, **400**: 62–74.

Halpert A.P., Jenkins F.A. and Franks H. (1987) Structure and scaling of the lumbar vertebrae in African bovids (Mammalia: Artiodactyla). *Journal of Zoology*, **211**(2): 239–258.

Harima Y., Takashima Y., Ueda Y., Ohtsuka T. and Kageyama R. (2013) Accelerating the tempo of the segmentation clock by reducing the number of introns in the *Hes7* gene. *Cell Reports*, **3**(1): 1–7.

Harlin-Cognato A.D. and Honeycutt R.L. (2006) Multi-locus phylogeny of dolphins in the subfamily Lissodelphininae: character synergy improves phylogenetic resolution. *BMC Evolutionary Biology*, **6**: 87.

Harmon L.J., Weir J.T., Brock C.D., Glor R.E. and Challenger W. (2008) GEIGER: investigating evolutionary radiations. *Bioinformatics*, **24**(1): 129–131.

Harper C.J., Mclellan W.A., Rommel S.A., Gay D.M., Dillaman R.M. and Pabst D.A. (2008) Morphology of the melon and its tendinous connections to the facial muscles in bottlenose dolphins (*Tursiops truncatus*). *Journal of Morphology*, **269**(7): 820–839.

Harvey M.G. and Rabosky D.L. (2018) Continuous traits and speciation rates: alternatives to state-dependent diversification models. *Methods in Ecology and Evolution*, **9**(4): 984–993.

Hassanin A., Delsuc F., Ropiquet A., Hammer C., Jansen Van Vuuren B., Matthee C., Ruiz-Garcia M., Catzeflis F., Areskoug V., Nguyen T.T. and Couloux A. (2012) Pattern and timing of diversification of Cetartiodactyla (Mammalia, Laurasiatheria), as revealed by a comprehensive analysis of mitochondrial genomes. *Comptes Rendus Biologies*, **335**(1): 32–50.

He P. (1986) *Swimming performance of three species of marine fish and some aspects of swimming in fishing gears*. PhD Thesis. University of Aberdeen.

Heard S.B. and Hauser D.L. (1995) Key evolutionary innovations and their ecological mechanisms. *Historical Biology*, **10**(2): 151–173.

Hebrank M.R. (1982) Mechanical properties of fish backbones in lateral bending and in tension. *Journal of Biomechanics*, **15**(2): 85–89.

Herrel A., Vanhooydonck B., Porck J. and Irschick D.J. (2008) Anatomical basis of differences in locomotor behavior in *Anolis* lizards: a comparison between two ecomorphs. *Bulletin of the Museum of Comparative Zoology*, **159**(4): 213–238.

Hersh S.L. and Duffield D.A. (1990) Distinction between Northwest Atlantic offshore and coastal bottlenose dolphins based on hemoglobin profile and morphometry. In *The Bottlenose Dolphin* (eds Leatherwood S. and Reeves R.R.), pp.129–139. New York: Academic Press.

Hodges S.A. and Arnold M.L. (1995) Spurring plant diversification: are floral nectar spurs a key innovation? *Proceedings of the Royal Society B: Biological Sciences*, **262**(1365): 343–348.

Hoelzel A.R., Potter C.W. and Best P.B. (1998) Genetic differentiation between parapatric 'nearshore' and 'offshore' populations of the bottlenose dolphin. *Proceedings of the Royal Society B: Biological Sciences*, **265**(1402): 1177–1184.

Hooker S.K. (2009) Toothed whales, overview. In *Encyclopedia of Marine Mammals*, 2nd edn (eds Perrin W.F., Würsig B.G., and Thewissen J.G.M.), pp.1173–1179. San Diego: Academic Press.

Hufthammer A.K., Arntsen L., Kitchener A.C. and Buckley M. (2018) Grey whale (*Eschrichtius robustus*) in Norwegian waters 2000 years ago. *Palaeogeography, Palaeoclimatology, Palaeoecology*, **495**: 42–47.

Hulsey C.D., García de León F.J. and Rodiles-Hernández R. (2006) Micro- and macroevolutionary decoupling in cichlid jaws: a test of Liem's key innovation hypothesis. *Evolution*, **60**(10): 2096–2109.

Hunter J.P. (1998) Key innovations and the ecology of macroevolution. *Trends in Ecology and Evolution*, **13**(1995): 31–36.

Irschick D.J. and Losos J.B. (1998) A comparative analysis of the ecological significance of maximal locomotor performance in Caribbean *Anolis* lizards. *Evolution*, **52**(1): 219.

Irwin D.M., Kocher T.D. and Wilson A.C. (1991) Evolution of the cytochrome *b* gene of mammals. *Journal of Molecular Evolution*, **32**(2): 128–144.

IUCN (2017) The IUCN Red List of Threatened Species. *Version 2017-3*.

Jacobs D.K., Haney T.A. and Louie K.D. (2004) Genes, diversity, and geologic process on the Pacific coast. *Annual Review of Earth and Planetary Sciences*, **32**(1): 601–652.

Jauniaux T., Garcia Hartmann M., Haelters J., Tavernier J. and Coignoul F. (2002) Echouage de mammifères marins: guide d'intervention et procédures d'autopsie. *Annales de Medecine Veterinaire*, **146**(5): 261–276.

Jayne B.C. and Lauder G. V. (1994) How swimming fish use slow and fast muscle fibers: implications for models of vertebrate muscle recruitment. *Journal of Comparative Physiology A*, **175**(1): 123–131.

Jayne B.C. and Lauder G. V (1995) Speed effects on midline kinematics during steady undulatory swimming of largemouth bass, *Micropterus salmoides*. *Journal of Experimental Biology*, **198**(2): 585–602.

Jones K.E., Bielby J., Cardillo M., Fritz S.A., O'Dell J., Orme C.D.L., Safi K., Sechrest W., Boakes E.H., Carbone C., *et al.* (2009) PanTHERIA: a species-level database of life history, ecology, and geography of extant and recently extinct mammals. *Ecology*, **90**(9): 2648–2648.

Jones K.E. (2015) Evolutionary allometry of the thoracolumbar centra in felids and bovids. *Journal of Morphology*, **276**(7): 818–831.

Jones K.E., Benitez L., Angielczyk K.D. and Pierce S.E. (2018a) Adaptation and constraint in the evolution of the mammalian backbone. *BMC Evolutionary Biology*, **18**: 172.

Jones K.E., Angielczyk K.D., Polly P.D., Head J.J., Fernandez V., Lungmus J.K., Tulga S. and Pierce S.E. (2018b) Fossils reveal the complex evolutionary history of the mammalian regionalized spine. *Science*, **361**(6408): 1249–1252.

Jones K.E. and Pierce S.E. (2016) Axial allometry in a neutrally buoyant environment: effects of the terrestrial-aquatic transition on vertebral scaling. *Journal of evolutionary biology*, **29**(3): 594–601.

Jones M. Lou and Swartz S.L. (2009) Gray whale. In *Encyclopedia of Marine Mammals*, 2nd edn (eds Perrin W.F., Würsig B.G., and Thewissen J.G.M.), pp.503–511. San Diego: Academic Press.

Jutapruet S., Intongcome A., Wang X., Kittiwattanawong K. and Huang S.L. (2017) Distribution of three sympatric cetacean species off the coast of the central-western Gulf of Thailand. *Aquatic Mammals*, **43**(5): 465–473.

Kastelein R.A., van der Sijs S.J., Staal C. and Nieuwstraten S.H. (1997) Blubber thickness in harbour porpoises (*Phocoena phocoena*). In *The biology of the harbour porpoise* (eds Read A.J., Wiepkema P.R., and Nachtigall P.E.), pp.179–199. Woerden: De Spil.

Kelley N.P. and Pyenson N.D. (2015) Evolutionary innovation and ecology in marine tetrapods from the Triassic to the Anthropocene. *Science*, **348**(6232): aaa3716.

Kellogg R. (1924) A fossil porpoise from the Calvert formation of Maryland. *Proceedings of the United States National Museum*, **63**(2482): 1–39.

Kellogg R. (1927) *Kentriodon pernix*, a Miocene porpoise from Maryland. *Proceedings of The United States National Museum*, **69**: 1–55.

Kellogg R. (1936) A review of the archaeoceti. *Carnegie Institution of Washington Publications*, **482**: 1–366.

Kellogg R. (1969) Cetothere skeletons from the Miocene Choptank Formation of Maryland and Virginia. *United States National Museum Bulletin*, **294**: 1–40.

Kemper C.M. (2009) Pygmy right whale. In *Encyclopedia of Marine Mammals*, 2nd edn (eds Perrin W.F., Würsig B.G., and Thewissen J.G.M.), pp.939–941. San Diego: Academic Press.

Kenney R.D. (2009) Right whales. In *Encyclopedia of Marine Mammals*, 2nd edn (eds Perrin W.F., Würsig B.G., and Thewissen J.G.M.), pp.962–972. San Diego: Academic Press.

Kessel M. and Gruss P. (1990) Murine developmental control genes. *Science*, **249**(4967): 374–379.

Kielhorn C.E., Dillaman R.M., Kinsey S.T., McLellan W.A., Gay D.M., Dearolf J.L. and Pabst D.A. (2013) Locomotor muscle profile of a deep (*Kogia breviceps*) versus shallow (*Tursiops truncatus*) diving cetacean. *Journal of Morphology*, **274**(6): 663–675.

Kim S.H., Shimada K. and Rigsby C.K. (2013) Anatomy and evolution of heterocercal tail in lamniform sharks. *The Anatomical Record*, **296**(3): 433–442.

Kooyman G.L. and Ponganis P.J. (2017) Diving physiology. In *Encyclopedia of Marine Mammals*, 3rd edn (eds Würsing B., Thewissen J.G.M., and Kovacs K.), pp.267–271. London: Academic Press.

Kröger B. and Yun-Bai Z. (2009) Pulsed cephalopod diversification during the Ordovician. *Palaeogeography, Palaeoclimatology, Palaeoecology*, **273**(1–2): 174–183.

Laidre K.L., Heide-Jørgensen M.P., Logdson M.L., Hobbs R.C., Heagerty P., Dietz R., Jørgensen O.A. and Treble M.A. (2004) Seasonal narwhal habitat associations in the high Arctic. *Marine Biology*, **145**(4): 821–831.

Lambert O., Martínez-Cáceres M., Bianucci G., Di Celma C., Salas-Gismondi R., Steurbaut E., Urbina M. and de Muizon C. (2017) Earliest mysticete from the Late Eocene of Peru sheds new light on the origin of baleen whales. *Current Biology*, **27**(10): 1535-1541.e2.

LeDuc R. (2009) Delphinids, overview. In *Encyclopedia of Marine Mammals*, 2nd edn (eds Perrin W.F., Würsig B.G., and Thewissen J.G.M.), pp.298–302. San Diego: Academic Press.

Lerner H.R.L., Meyer M., James H.F., Hofreiter M. and Fleischer R.C. (2011) Multilocus resolution of phylogeny and timescale in the extant adaptive radiation of Hawaiian honeycreepers. *Current Biology*, **21**(21): 1838–1844.

Leslie M.S. and Morin P.A. (2018) Structure and phylogeography of two tropical predators, spinner (*Stenella longirostris*) and pantropical spotted (*S. attenuata*) dolphins, from SNP data. *Royal Society Open Science*, **5**(4): 171615.

Liem K.F. (1973) Evolutionary strategies and morphological innovations: cichlid pharyngeal jaws. *Systematic Zoology*, **22**(4): 425–441.

Lindell L.E. (1994) The evolution of vertebral number and body size in snakes. *Functional Ecology*, **8**(6): 708–719.

Lindgren J., Caldwell M.W., Konishi T. and Chiappe L.M. (2010) Convergent evolution in aquatic tetrapods: insights from an exceptional fossil mosasaur. *PLoS one*, **5**(8): e11998.

Lindgren J., Polcyn M.J. and Young B.A. (2011) Landlubbers to leviathans: evolution of swimming in mosasaurine mosasaurs. *Paleobiology*, **37**(3): 445–469.

Lindsey C.C. (1975) Pleomerism, the widespread tendency among related fish species for vertebral number to be correlated with maximum body length. *Journal of the Fisheries Research Board of Canada*, **32**(12): 2453–2469.

Lindstedt S.L. and Boyce M.S. (1985) Seasonality, fasting endurance, and body size in mammals. *American Naturalist*, **125**(6): 873–878.

Lloyd S.A., Lang C.H., Zhang Y., Paul E.M., Laufenberg L.J., Lewis G.S. and Donahue H.J. (2014) Interdependence of muscle atrophy and bone loss induced by mechanical unloading. *Journal of Bone and Mineral Research*, **29**(5): 1118–1130.

Long J.H. (1992) Stiffness and damping forces in the intervertebral joints of blue marlin (*Makaira nigricans*). *Journal of Experimental Biology*, **162**(1): 131–155.

Long J.H., Hale M.E., McHenry M.J. and Westneat M.W. (1996) Functions of fish skin: flexural stiffness and steady swimming of longnose gar *Lepisosteus osseus*. *Journal of Experimental Biology*, **199**(10): 2139–2151.

Long J.H., Pabst D.A., Shepherd W.R. and McLellan W.A. (1997) Locomotor design of dolphin vertebral columns: bending mechanics and morphology of *Delphinus delphis*. *Journal of Experimental Biology*, **200**(1): 65–81.

Long J.H. and Nipper K.S. (1996) The importance of body stiffness in undulatory propulsion. *American Zoologist*, **36**(6): 678–694.

Long J.H.J., Krenitsky N.M., Roberts S.F., Hirokawa J., Leeuw J. De and Porter M.E. (2011) Testing biomimetic structures in bioinspired robots: how vertebrae control the stiffness of the body and the behavior of fish-like swimmers. *Integrative and Comparative Biology*, **51**(1): 158–175.

López-Fernández H., Arbour J., Willis S., Watkins C., Honeycutt R.L. and Winemiller K.O. (2014) Morphology and efficiency of a specialized foraging behavior, sediment sifting, in neotropical cichlid fishes. *PLoS one*, **9**(3): e89832.

Losos J.B. (1990a) Ecomorphology, performance capability, and scaling of West Indian *Anolis* lizards: an evolutionary analysis. *Ecological Monographs*, **60**(3): 369–388.

Losos J.B. (1990b) The evolution of form and function: morphology and locomotor performance in West Indian *Anolis* lizards. *Evolution*, **44**(5): 1189–1203.

Losos J.B. (2010) Adaptive radiation, ecological opportunity, and evolutionary determinism. *The American Naturalist*, **175**(6): 623–639.

Losos J.B. and Miles D.B. (1994) Adaptation, constraint, and the comparative method: phylogenetic issues and methods. In *Ecological morphology: Integrative organismal biology*, pp.60–98.

Louis M., Fontaine M.C., Spitz J., Schlund E., Dabin W., Deaville R., Caurant F., Cherel Y., Guinet C. and Simon-Bouhet B. (2014a) Ecological opportunities and specializations shaped genetic divergence in a highly mobile marine top predator. *Proceedings of the Royal Society B: Biological Sciences*, **281**(1795): 20144558.

Louis M., Viricel A., Lucas T., Peltier H., Alfonsi E., Berrow S., Brownlow A., Covelo P., Dabin W., Deaville R., De Stephanis R., Gally F., Gauffrier P., Penrose R., Silva M.A., Guinet C. and Simon-Bouhet B. (2014b) Habitat-driven population structure of bottlenose dolphins, *Tursiops truncatus*, in the North-East Atlantic. *Molecular Ecology*, **23**(4): 857–874.

Lovette I.J., Bermingham E. and Ricklefs R.E. (2002) Clade-specific morphological diversification and adaptive radiation in Hawaiian songbirds. *Proceedings of the Royal Society B: Biological Sciences*, **269**(1486): 37–42.

Lowry D.B. (2012) Ecotypes and the controversy over stages in the formation of new species. *Biological Journal of the Linnean Society*, **106**(2): 241–257.

Mabuchi K., Miya M., Azuma Y. and Nishida M. (2007) Independent evolution of the specialized pharyngeal jaw apparatus in cichlid and labrid fishes. *BMC Evolutionary Biology*, **7**: 10.

MacLeod C.D., Santos M.B., López A. and Pierce G.J. (2006) Relative prey size consumption in toothed whales: implications for prey selection and level of specialisation. *Marine Ecology Progress Series*, **326**: 295–307.

MacLeod C.D., Santos M.B. and Pierce G.J. (2003) Review of data on diets of beaked whales: evidence of niche separation and geographic segregation. *Journal of the Marine Biological Association of the United Kingdom*, **83**(3): 651–665.

Madar S.I. (2007) The postcranial skeleton of Early Eocene pakicetid cetaceans. *Journal of Paleontology*, **81**(1): 176–200.

Madar S.I., Thewissen J.G.M. and Hussain S.T. (2002) Additional holotype remains of *Ambulocetus natans* (Cetacea , Ambulocetidae), and their implications for locomotion in early whales. *Journal of Vertebrate Paleontology*, **22**(2): 405–422.

Marchesi M.C., Mora M.S., Crespo E.A., Boy C.C., González-José R. and Goodall R.N.P. (2018) Functional subdivision of the vertebral column in four south american dolphins. *Mastozoología Neotropical*, **25**(2): 329–343.

Marchesi M.C., Boy C.C., Dans S.L., Mora M.S. and González-José R. (2019) Morphology of the vertebral centra in dolphins from the southwestern South Atlantic: a 3D morphometric approach and functional implications. *Marine Mammal Science*, 12660.

Martín López L.M., Miller P.J.O., Aguilar de Soto N. and Johnson M. (2015) Gait switches in deep-diving beaked whales: Biomechanical strategies for long-duration dives. *Journal of Experimental Biology*, **218**(9): 1325–1338.

Martínez-Cáceres M., Lambert O. and de Muizon C. (2017) The anatomy and phylogenetic affinities of *Cynthiacetus peruvianus*, a large *Dorudon*-like basilosaurid (Cetacea, Mammalia) from the late Eocene of Peru. *Geodiversitas*, **39**(1): 7–163.

Martinez C.M., Mcgee M.D., Borstein S.R. and Wainwright P.C. (2018) Feeding ecology underlies the evolution of cichlid jaw mobility. *Evolution*, **72**(8): 1645–1655.

Marx F.G. and Fordyce R.E. (2015) Baleen boom and bust: a synthesis of mysticete phylogeny, diversity and disparity. *Royal Society Open Science*, **2**(4): 140434.

Marx F.G., Lambert O. and Uhen M.D. (2016) *Cetacean paleobiology*. Chichester: Wiley Blackwell.

Marx F.G. and Uhen M.D. (2010) Climate, critters, and cetaceans: Cenozoic drivers of the evolution of modern whales. *Science*, **327**(5968): 993–996.

Matschiner M., Hanel R. and Salzburger W. (2011) On the origin and trigger of the notothenioid adaptive radiation. *PLoS one*, **6**(4): e18911.

Mauguit Q., Olivier D., Vandewalle N. and Vandewalle P. (2010) Ontogeny of swimming movements in bronze corydoras (*Corydoras aeneus*). *Canadian Journal of Zoology*, **88**(4): 378–389.

Mayr E. (1947) Ecological factors in speciation. *Evolution*, **1**(4): 263–288.

Mayr E. (1963) *Animal species and evolution*. Cambridge: Harvard University Press.

McAlpine D.F. (2009) Pygmy and dwarf sperm whales. In *Encyclopedia of Marine Mammals*, 2nd edn (eds Perrin W.F., Würsig B.G., and Thewissen J.G.M.), pp.936–938. San Diego: Academic Press.

McCurry M.R., Fitzgerald E.M.G., Evans A.R., Adams J.W. and McHenry C.R. (2017) Skull shape reflects prey size niche in toothed whales. *Biological Journal of the Linnean Society*, **121**(4): 936–946.

McGowen M.R. (2011) Toward the resolution of an explosive radiation - A multilocus phylogeny of oceanic dolphins (Delphinidae). *Molecular Phylogenetics and Evolution*, **60**(3): 345–357.

McGowen M.R., Tsagkogeorga G., Álvarez-Carretero S., Dos Reis M., Struebig M., Deaville R., Jepson P.D., Jarman S., Polanowski A., Morin P.A. and Rossiter S. (2019) Phylogenomic resolution of the cetacean tree of life using target sequence capture. *Systematic Biology*, syz068.

McGowen M.R., Spaulding M. and Gatesy J. (2009) Divergence date estimation and a comprehensive molecular tree of extant cetaceans. *Molecular Phylogenetics and Evolution*, **53**(3): 891–906.

McGuire J.A. and Dudley R. (2011) The biology of gliding in flying lizards (genus *Draco*) and their fossil and extant analogs. *Integrative and Comparative Biology*, **51**(6): 983–990.

McKenna D.D., Sequeira A.S., Marvaldi A.E. and Farrell B.D. (2009) Temporal lags and overlap in the diversification of weevils and flowering plants. *Proceedings of the National Academy of Sciences*, **106**(17): 7083–7088.

Mead J.G. (2009) Beaked whales, overview. In *Encyclopedia of Marine Mammals*, 2nd edn (eds Perrin W.F., Würsig B.G., and Thewissen J.G.M.), pp.94–97. San Diego: Academic Press.

Mead J.G. and Potter C.W. (1995) Recognizing two populations of the bottlenose dolphin (*Tursiops truncatus*) off the Atlantic coast of North America: morphologic and ecologic considerations. *Ibi Reports*, **5**: 31–44.

Meredith R.W., Janečka J.E., Gatesy J., Ryder O.A., Fisher C.A., Teeling E.C., Goodbla A., Eizirik E., Simão T.L.L., Stadler T., *et al.* (2011) Impacts of the Cretaceous terrestrial revolution and KPg extinction on mammal diversification. *Science*, **334**(6055): 521–525.

Millar J.S. and Hickling G.J. (1990) Fasting endurance and the evolution of mammalian body size. *Functional Ecology*, **4**(1): 5–12.

Miller A.H. (1949) Some ecologic and morphologic considerations in the evolution of higher taxonomic categories. In *Ornithologie als biologische wissenschaft* (eds Mayr E. and Schüz E.), pp.84–88. Heidelberg: Carl Winter.

Miller G.S. (1923) The telescoping of the cetacean skull. *Smithsonian Miscellaneous Collections*, **76**(5): 1–70.

Miller K.G., Kominz M.A., Browning J. V, Wright J.D., Mountain G.S., Katz M.E., Sugarman P.J., Cramer B.S., Christie-Blick N. and Pekar S.F. (2005) The Phanerozoic record of global sea-level change. *Science*, **310**(5752): 1293–1298.

Moermond T.C. (1979) Habitat constraints on the behavior, morphology, and community structure of *Anolis* lizards. *Ecology*, **60**(1): 152–164.

Molnar J.L., Pierce S.E., Bhullar B.A.S., Turner A.H. and Hutchinson J.R. (2015) Morphological and functional changes in the vertebral column with increasing aquatic adaptation in crocodylomorphs. *Royal Society Open Science*, **2**(11): 150439.

Molnar J.L., Pierce S.E. and Hutchinson J.R. (2014) An experimental and morphometric test of the relationship between vertebral morphology and joint stiffness in Nile crocodiles (*Crocodylus niloticus*). *Journal of Experimental Biology*, **217**(5): 758–68.

Montgomery S.H., Geisler J.H., Mcgowen M.R., Fox C., Marino L. and Gatesy J. (2013) The evolutionary history of cetacean brain and body size. *Evolution*, **67**(11): 3339–3353.

Morlon H., Parsons T.L. and Plotkin J.B. (2011) Reconciling molecular phylogenies with the fossil record. *Proceedings of the National Academy of Sciences of the United States of America*, **108**(39): 16327–32.

Motani R. (2002) Scaling effects in caudal fin propulsion and the speed of ichthyosaurs. *Nature*, **415**(6869): 309–312.

Motani R. (2005) Evolution of fish-shaped reptiles (Reptilia: Ichthyopterygia) in their physical environments and constraints. *Annual Review of Earth and Planetary Sciences*, **33**: 395–420.

Motani R., You H. and McGowan C. (1996) Eel-like swimming in the earliest ichthyosaurs. *Nature*, **382**(6589): 347–348.

Moura A.E., Nielsen S.C.A., Vilstrup J.T., Moreno-Mayar J.V., Gilbert M.T.P., Gray H.W.I., Natoli A., Möller L. and Hoelzel A.R. (2013) Recent diversification of a marine genus (*Tursiops* spp.) tracks habitat preference and environmental change. *Systematic biology*, **62**(6): 865–877.

de Muizon C. (1984) Les vertébrés fossiles de la Formation Pisco (Pérou). Deuxième partie: les odontocètes (Cetacea, Mammalia) du Pliocène inférieur de Sud-Sacaco. *Travaux de l'Institut Français d'Etudes Andines*, **50**: 1–188.

de Muizon C. (1988) Les vertébrés fossiles de la Formation Pisco (Pérou). Troisième partie: Les Odontocètes (Cetacea, Mammalia) du Miocène. *Travaux de l'Institut Français d'Etudes Andines*, **78**: 1–244.

Muller J., Scheyer T.M., Head J.J., Barrett P.M., Werneburg I., Ericson P.G.P., Pol D. and Sanchez-Villagra M.R. (2010) Homeotic effects, somitogenesis and the evolution of vertebral numbers in recent and fossil amniotes. *Proceedings of the National Academy of Sciences*, **107**(5): 2118–2123.

Murakami M., Shimada C., Hikida Y., Soeda Y. and Hirano H. (2014) *Eodelphis kabatensis*, a new name for the oldest true dolphin *Stenella kabatensis* Horikawa, 1977 (Cetacea , Odontoceti , Delphinidae), from the upper Miocene of Japan, and the phylogeny and paleobiogeography of Delphinoidea. *Journal of Vertebrate Paleontology*, **34**(3): 491–511.

Narita Y. and Kuratani S. (2005) Evolution of the vertebral formulae in mammals: a perspective on developmental constraints. *Journal of Experimental Zoology Part B: Molecular and Developmental Evolution*, **304**(2): 91–106.

Natoli A., Cañadas A., Peddemors V.M., Aguilar A., Vaquero C., Fernández-Piqueras P. and Hoelzel A.R. (2006) Phylogeography and alpha taxonomy of the common dolphin (*Delphinus* sp.). *Journal of Evolutionary Biology*, **19**(3): 943–954.

Natoli A., Peddemors V.M. and Hoelzel A.R. (2004) Population structure and speciation in the genus *Tursiops* based on microsatellite and mitochondrial DNA analyses. *Journal of Evolutionary Biology*, **17**(2): 363–375.

Newsome S.D., Clementz M.T. and Koch P.L. (2010) Using stable isotope biogeochemistry to study marine mammal ecology. *Marine Mammal Science*, **26**(3): 509–572.

Noren S.R. and Williams T.M. (2000) Body size and skeletal muscle myoglobin of cetaceans: adaptations for maximizing dive duration. *Comparative Biochemistry and Physiology - A Molecular and Integrative Physiology*, **126**(2): 181–191.

Nosil P. (2007) Divergent host plant adaptation and reproductive isolation between ecotypes of *Timema cristinae* walking sticks. *The American Naturalist*, **169**(2): 151–162.

Nosil P., Harmon L.J. and Seehausen O. (2009) Ecological explanations for (incomplete) speciation. *Trends in Ecology and Evolution*, **24**(3): 145–156.

Nosil P. and Sandoval C.P. (2008) Ecological niche dimensionality and the evolutionary diversification of stick insects. *PLoS one*, **3**(4): e1907.

Nowroozi B.N., Harper C.J., De Kegel B., Adriaens D. and Brainerd E.L. (2012) Regional variation in morphology of vertebral centra and intervertebral joints in striped bass, *Morone saxatilis*. *Journal of Morphology*, **273**(4): 441–452.

Nowroozi B.N. and Brainerd E.L. (2012) Regional variation in the mechanical properties of the vertebral column during lateral bending in *Morone saxatilis*. *Journal of the Royal Society Interface*, **9**(75): 2667–2679.

Nowroozi B.N. and Brainerd E.L. (2014) Importance of mechanics and kinematics in determining the stiffness contribution of the vertebral column during body-caudal-fin swimming in fishes. *Zoology*, **117**(1): 28–35Elsevier GmbH.

Pabst D.A. (1990) Axial muscles and connective tissues of the bottlenose dolphin. In *The Bottlenose Dolphin* (eds Leatherwood S. and Reeves R.R.), pp.51–67. New York: Academic Press.

Pabst D.A. (1993) Intramuscular morphology and tendon geometry of the epaxial swimming muscles of dolphins. *Journal of Zoology*, **230**(1): 159–176.

Page C.E. and Cooper N. (2017) Morphological convergence in 'river dolphin' skulls. *PeerJ*, **5**: e4090.

Parmentier E., Lanterbecq D. and Eeckhaut I. (2016) From commensalism to parasitism in Carapidae (Ophidiiformes): heterochronic modes of development? *PeerJ*, **4**: e1786.

Parra G.J. (2006) Resource partitioning in sympatric delphinids: space use and habitat preferences of Australian snubfin and Indo-Pacific humpback dolphins. *Journal of Animal Ecology*, **75**(4): 862–874.

Parry D.A. (1949) The anatomical basis of swimming in whales. *Proceedings of the Zoological Society of London*, **119**(1): 49–60.

Pennell M.W., Eastman J.M., Slater G.J., Brown J.W., Uyeda J.C., Fitzjohn R.G., Alfaro M.E. and Harmon L.J. (2014) Geiger v2.0: an expanded suite of methods for fitting macroevolutionary models to phylogenetic trees. *Bioinformatics*, **30**(15): 2216–2218.

Perrin W.F., Thieleking J.L., Walker W.A., Archer F.I. and Robertson K.M. (2011) Common bottlenose dolphins (*Tursiops truncatus*) in California waters: cranial differentiation of coastal and offshore ecotypes. *Marine Mammal Science*, **27**(4): 769–792.

Perrin W.F., Dolar M.L.L. and Robineau D. (1999) Spinner dolphins (*Stenella longirostris*) of the western Pacific and Southeast Asia: pelagic and shallow-water forms. *Marine Mammal Science*, **15**(4): 1029–1053.

Perrin W.F., Wu ̈rsig B.G. and Thewissen J.G.M. (2009) *Encyclopedia of marine mammals*. 2nd edn. San Diego: Academic Press.

Pichler F.B., Robineau D., Goodall R.N.P., Meÿers M.A., Olivarria C. and Baker C.S. (2001) Origin and radiation of southern Hemisphere coastal dolphins (genus *Cephalorhynchus*). *Molecular Ecology*, **10**(9): 2215–2223.

Pinheiro J., Bates D., DebRoy S., Sarkar D. and R Core Team (2017) nlme: linear and nonlinear mixed effects models. *R package version 3.1-131*.

Pivorunas A. (1979) The feeding mechanisms of baleen whales. *American Scientist*, **67**(4): 432–440.

Pointer M.A. and Mundy N.I. (2008) Testing whether macroevolution follows microevolution: are colour differences among swans (*Cygnus*) attributable to variation at the *MC1R* locus? *BMC Evolutionary Biology*, **8**: 249.

Ponganis P.J. and Pierce R.W. (1978) Muscle metabolic profiles and fiber-type composition in some marine mammals. *Comparative Biochemistry and Physiology. B, Comparative Biochemistry*, **59**(2): 99–102.

Porter M.E., Roque C.M. and Long J.H. (2009) Turning maneuvers in sharks: predicting body curvature from axial morphology. *Journal of Morphology*, **270**(8): 954–965.

R Core Team (2017) R: A language and environment for statistical computing. *R Fundation for Statistical Computing*.

Rabosky D.L. (2014) Automatic detection of key innovations, rate shifts, and diversity-dependence on phylogenetic trees. *PLoS one*, **9**(2): e89543.

Rabosky D.L., Grundler M., Anderson C., Title P., Shi J.J., Brown J.W., Huang H. and Larson J.G. (2014) BAMMtools: an R package for the analysis of evolutionary dynamics on phylogenetic trees. *Methods in Ecology and Evolution*, **5**(7): 701–707.

Rabosky D.L. (2017) Phylogenetic tests for evolutionary innovation: the problematic link between key innovations and exceptional diversification. *Philosophical Transactions of the Royal Society B: Biological Sciences*, **372**(1735): 20160417.

Randau M., Goswami A., Hutchinson J.R., Cuff A.R. and Pierce S.E. (2016) Cryptic complexity in felid vertebral evolution: shape differentiation and allometry of the axial skeleton. *Zoological Journal of the Linnean Society*, **178**(1): 183–202.

Read A.J. (2009) Porpoises, overview. In *Encyclopedia of Marine Mammals*, 2nd edn (eds Perrin W.F., Wϋrsig B.G., and Thewissen J.G.M.), pp.920–923. San Diego: Academic Press.

Reilly D.T., Burstein A.H. and Frankel V.H. (1974) The elastic modulus for bone. *Journal of Biomechanics*, **7**(3): 271–275.

Revell L.J. (2012) Phytools: an R package for phylogenetic comparative biology (and other things). *Methods in Ecology and Evolution*, **3**(2): 217–223.

Rice D.W. (2009) Baleen. In *Encyclopedia of Marine Mammals*, 2nd edn (eds Perrin W.F., Würsig B., and Thewissen J.G.M.), pp.78–80. San Diego: Academic Press.

Richard P.R., Heide-Jørgensen M.P., Orr J.R., Dietz R. and Smith T.G. (2001) Summer and autumn movements and habitat use by belugas in the Canadian high Arctic and adjacent areas. *Arctic*, **54**(3): 207–222.

Rivero J.L.L. (2018) Locomotor muscle fibre heterogeneity and metabolism in the fastest large-bodied rorqual: the fin whale (*Balaenoptera physalus*). *Journal of Experimental Biology*, **221**(12): jeb177758.

Rohr J.J. and Fish F.E. (2004) Strouhal numbers and optimization of swimming by odontocete cetaceans. *Journal of Experimental Biology*, **207**(10): 1633–1642.

Rolland J., Silvestro D., Litsios G., Faye L. and Salamin N. (2018) Clownfishes evolution below and above the species level. *Proceedings of the Royal Society B: Biological Sciences*, **285**(1873): 20171796.

Rommel S. (1990) Osteology of the bottlenose dolphin. In *The Bottlenose Dolphin* (eds Leatherwood S. and Reeves R.R.), pp.29–49. New York: Academic Press.

Rommel S. and Reynolds J.E. (2009) Postcranial skeleton. In *Encyclopedia of Marine Mammals*, 2nd edn (eds Perrin W.F., Wϋrsig B.G., and Thewissen J.G.M.), pp.1021–1033. San Diego: Academic Press.

Ross G.J.B., Best P.B. and Donnelly B.G. (1975) New records of the pygmy right whale (*Caperea marginata*) from South Africa, with comments on distribution, migration, appearance, and behavior. *Journal of the Fisheries Research Board of Canada*, **32**(7): 1005–1017.

Rugh D.J. and Shelden K.E. (2009) Bowhead whale. In *Encyclopedia of Marine Mammals*, 2nd edn (eds Perrin W.F., Wϋrsig B.G., and Thewissen J.G.M.), pp.131–133. San Diego: Academic Press.

Sanderson M.J. and Donoghue M.J. (1994) Shifts in diversification rate with the origin of angiosperms. *Science*, **264**(5165): 1590–1593.

Sato K., Watanuki Y., Takahashi A., Miller P.J.O., Tanaka H., Kawabe R., Ponganis P.J., Handrich Y., Akamatsu T., Watanabe Y., Mitani Y., Costa D.P., Bost C.-A., Aoki K., Amano M., Trathan P., Shapiro A. and Naito Y. (2007) Stroke frequency, but not swimming speed, is related to body size in free-ranging seabirds, pinnipeds and cetaceans. *Proceedings of the Royal Society B: Biological Sciences*, **274**(1609): 471–477.

Schenkkan E.J. and Purves P.E. (1973) The comparative anatomy of the nasal tract and the function of the spermaceti organ in the Physeteridae (Mammalia, Odontoceti). *Bijdragen tot de Dierkunde*, **43**(1): 93–112.

Schluter D. (2000) *The ecology of adaptive radiation*. Oxford: Oxford University Press.

Schluter D. (2001) Ecology and the origin of species. *Trends in Ecology and Evolution*, **16**(7): 372–380.

Schneider C.A., Rasband W.S. and Eliceiri K.W. (2012) NIH Image to ImageJ: 25 years of image analysis. *Nature Methods*, **9**(7): 671–675.

Schorr G.S., Falcone E.A., Moretti D.J. and Andrews R.D. (2014) First long-term behavioral records from Cuvier's beaked whales (*Ziphius cavirostris*) reveal record-breaking dives. *PLoS one*, **9**(3): e92633.

Segre P.S., Cade D.E., Calambokidis J., Fish F.E., Friedlaender A.S., Potvin J. and Goldbogen J.A. (2019) Body flexibility enhances maneuverability in the world's largest predator. *Integrative and Comparative Biology*, **59**(1): 48–60.

Segura-García I., Gallo J.P., Chivers S., Díaz-Gamboa R. and Hoelzel A.R. (2016) Post-glacial habitat release and incipient speciation in the genus *Delphinus*. *Heredity*, **117**(6): 400–407.

Segura-García I., Arreola-Rojo L., Rocha-Olivares A., Heckel G., Gallo-Reynoso J.P. and Hoelzel R. (2018) Eco-evolutionary processes generating diversity among bottlenose dolphin, *Tursiops truncatus*, populations off Baja California, Mexico. *Evolutionary Biology*, **45**(2): 223–236.

Sharir A., Stern T., Rot C., Shahar R. and Zelzer E. (2011) Muscle force regulates bone shaping for optimal load-bearing capacity during embryogenesis. *Development*, **138**(15): 3247–3259.

Simons A.M. (2002) The continuity of microevolution and macroevolution. *Journal of Evolutionary Biology*, **15**(5): 688–701.

Simpson G.G. (1953) *The major features of evolution*. New York: Columbia University Press.

Skrovan R.C., Williams T.M., Berry P.S., Moore P.W. and Davis R.W. (1999) The diving physiology of the bottlenose dolphins (*Tursiops truncatus*): II. Biomechanics and changes in buoyancy at depth. *Journal of Experimental Biology*, **202**(20): 2749–2761.

Slater G.J., Price S.A., Santini F. and Alfaro M.E. (2010) Diversity versus disparity and the radiation of modern cetaceans. *Proceedings of the Royal Society B: Biological Sciences*, **277**(1697): 3097–3104.

Slater G.J., Goldbogen J.A. and Pyenson N.D. (2017) Independent evolution of baleen whale gigantism linked to Plio-Pleistocene ocean dynamics. *Proceedings of the Royal Society B: Biological Sciences*, **284**(1855): 20170546.

Slijper E.J. (1936) Die Cetaceen, vergleichend-anatomisch und systematisch. *Capita Zoologica Bd. 6-7*, 1–600.

Smeathers J.E. (1981) *A mechanical analysis of the mammalian lumbar spine*. PhD Thesis. University of Reading.

Smith F.A., Boyer A.G., Brown J.H., Costa D.P., Dayan T., Ernest S.K.M., Evans A.R., Fortelius M., Gittleman J.L., Hamilton M.J., *et al.* (2010) The evolution of maximum body size of terrestrial mammals. *Science*, **330**(6008): 1216–1220.

Smith G.J., Browne K.W. and Gaskin D.E. (1976) Functional myology of the harbour porpoise, *Phocoena phocoena* (L.). *Canadian journal of zoology*, **54**(5): 716–729.

Smith T.D. and Burrows A.M. (2010) Mobility of the axial regions in a captive amazon river dolphin (*Inia geoffrensis*). In *Biology, evolution and conservation of river dolphins within South America and Asia* (eds Ruiz-Garcia M. and Shostell J.), pp.71–81. New York: Nova Science Publishers.

Spaulding M., O'Leary M.A. and Gatesy J. (2009) Relationships of Cetacea (Artiodactyla) among mammals: increased taxon sampling alters interpretations of key fossils and character evolution. *PLoS one*, **4**(9): e7062.

Spitz J., Rousseau Y. and Ridoux V. (2006) Diet overlap between harbour porpoise and bottlenose dolphin: an argument in favour of interference competition for food? *Estuarine, Coastal and Shelf Science*, **70**(1–2): 259–270.

Steeman M.E., Hebsgaard M.B., Fordyce R.E., Ho S.Y.W., Rabosky D.L., Nielsen R., Rahbek C., Glenner H., Sørensen M. V and Willerslev E. (2009) Radiation of extant cetaceans driven by restructuring of the oceans. *Systematic biology*, **58**(6): 573–585.

Steinhausen M.F., Steffensen J.F. and Andersen N.G. (2005) Tail beat frequency as a predictor of swimming speed and oxygen consumption of saithe (*Pollachius virens*) and whiting (*Merlangius merlangus*) during forced swimming. *Marine Biology*, **148**(1): 197–204.

Stevens E.D., Lam H.M. and Kendall J. (1974) Vascular anatomy of the counter current heat exchanger of skipjack tuna. *Journal of Experimental Biology*, **61**(1): 145–153.

Stroud J.T. and Losos J.B. (2016) Ecological opportunity and adaptive radiation. *Annual Review of Ecology, Evolution, and Systematics*, **47**: 507–532.

Sun Q., Morikawa H., Kobayashi S., Ueda K., Miyahara H. and Nakashima M. (2010) Structure and mechanical properties on tail flukes of dolphin. *Journal of Aero Aqua Bio-mechanisms*, **1**(1): 45–50.

ten Broek C.M.A., Bakker A.J., Varela-Lasheras I., Bugiani M., van Dongen S. and Galis F. (2012) Evo-devo of the human vertebral column: on homeotic transformations, pathologies and prenatal selection. *Evolutionary Biology*, **39**(4): 456–471.

Thewissen J.G.M. (1998) *The emergence of whales: Evolutionary patterns in the origin of Cetacea*. New York: Plenum Press.

Thewissen J.G.M., Williams E.M., Roe L.J. and Hussain S.T. (2001) Skeletons of terrestrial cetaceans and the relationship of whales to artiodactyls. *Nature*, **413**(6853): 277–281.

Thewissen J.G.M., Cohn M.J., Stevens L.S., Bajpai S., Heyning J. and Horton W.E. (2006) Developmental basis for hind-limb loss in dolphins and origin of the cetacean bodyplan. *Proceedings of the National Academy of Sciences*, **103**(22): 8414–8418.

Thewissen J.G.M., Cooper L.N., Clementz M.T., Bajpai S. and Tiwari B.N. (2007) Whales originated from aquatic artiodactyls in the Eocene epoch of India. *Nature*, **450**(7173): 1190–1194.

Thewissen J.G.M., Cooper L.N., George J.C. and Bajpai S. (2009) From land to water: the origin of whales, dolphins, and porpoises. *Evolution: Education and Outreach*, **2**: 272–288.

Thewissen J.G.M. and Fish F.E. (1997) Locomotor evolution in the earliest cetaceans: functional model, modern analogues, and paleontological evidence. *Paleobiology*, **23**(4): 482–490.

Thewissen J.G.M., Hussain S.T. and Arif M. (1994) Fossil evidence for the origin of aquatic locomotion in archaeocete whales. *Science*, **263**(5144): 210–212.

Thorne P.M., Ruta M. and Benton M.J. (2011) Resetting the evolution of marine reptiles at the Triassic-Jurassic boundary. *Proceedings of the National Academy of Sciences of the United States of America*, **108**(20): 8339–8344.

Torres L.G., Rosel P.E., D'agrosa C. and Read A.J. (2003) Improving management of overlapping bottlenose dolphin ecotypes through spatial analysis and genetics. *Marine Mammal Science*, **19**(3): 502–514.

Turesson G. (1922) The species and the variety as ecological units. *Hereditas*, **3**(1): 100–113.

Turvey S.T., Pitman R.L., Taylor B.L., Barlow J., Akamatsu T., Barrett L.A., Zhao X., Reeves R.R., Stewart B.S., Wang K., Wei Z., Zhang X., Pusser L.T., Richlen M., Brandon J.R. and Wang D. (2007) First human-caused extinction of a cetacean species? *Biology Letters*, **3**(5): 537–540.

Uhen M.D. (2004) Form, function, and anatomy of *Dorudon atrox* (Mammalia, Cetacea): an archaeocete from the middle to late Eocene of Egypt. *University of Michigan Papers on Paleontology*, **34**: 1–222.

Uhen M.D. (2008) New protocetid whales from Alabama and Mississippi, and a new cetacean clade, Pelagiceti. *Journal of Vertebrate Paleontology*, **28**(3): 589–593.

Uhen M.D. (2009) Evolution of dental morphology. In *Encyclopedia of Marine Mammals*, 2nd edn (eds Perrin W.F., Würsig B.G., and Thewissen J.G.M.), pp.302–307.Academic Press.

Uhen M.D. (2010) The origin(s) of whales. *Annual Review of Earth and Planetary Sciences*, **38**: 189–219.

Uyeda J.C. and Harmon L.J. (2014) A novel Bayesian method for inferring and interpreting the dynamics of adaptive landscapes from phylogenetic comparative data. *Systematic Biology*, **63**(6): 902–918.

Valentin S., Grösel M. and Licka T. (2012) The presence of long spinal muscles increases stiffness and hysteresis of the caprine spine in-vitro. *Journal of Biomechanics*, **45**(15): 2506–2512.

Van Beneden P.J. and Gervais P. (1880) *Ostéographie des cétacés vivants et fossiles, comprenant la description et l'iconographie du squelette et du système dentaire de ces animaux, ainsi que des documents relatifs à leur histoire naturelle*. Paris: Arthus-Bertrand.

Van Valkenburgh B. (1994) Ecomorphological analysis of fossil vertebrates and their paleocommunities. In *Ecological morphology: Integrative organismal biology* (eds Wainwright P.C. and Reilly S.M.), pp.140–166. Chicago: University of Chicago Press.

Velten B.P., Dillaman R.M., Kinsey S.T., McLellan W.A. and Pabst D.A. (2013) Novel locomotor muscle design in extreme deep-diving whales. *Journal of Experimental Biology*, **216**(10): 1862–1871.

Venables W.N. and Ripley B.D. (2002) *Modern Applied Statistics with S*. 4th edn. New York: Springer.

Videler J. and Kamermans P. (1985) Differences between upstroke and downstroke in swimming dolphins. *Journal of Experimental Biology*, **119**(1): 265–74.

Videler J.J. (1985) Fish swimming movements: a study of one element of behaviour. *Netherlands Journal of Zoology*, **35**(1,2): 170–185.

Viglino M., Flores D.A., Ercoli M.D. and Álvarez A. (2014) Patterns of morphological variation of the vertebral column in dolphins. *Journal of Zoology*, **294**(4): 267–277.

Vollmer N.L., Ashe E., Brownell R.L.J., Cipriano F., Mead J.G., Reeves R.R., Soldevilla M.S. and Williams R. (2019) Taxonomic revision of the dolphin genus *Lagenorhynchus*. *Marine Mammal Science*, **35**(3): 957–1057.

Waddell P.J., Okada N. and Hasegawa M. (1999) Towards resolving the interordinal relationships of placental mammals. *Systematic Biology*, **48**(1): 1–5.

Wainwright P.C. (1991) Ecomorphology: experimental functional anatomy for ecological problems. *Integrative and Comparative Biology*, **31**(4): 680–693.

Wainwright P.C., Smith W.L., Price S.A., Tang K.L., Sparks J.S., Ferry L.A., Kuhn K.L., Eytan R.I. and Near T.J. (2012) The evolution of pharyngognathy: a phylogenetic and functional appraisal of the pharyngeal jaw key innovation in labroid fishes and beyond. *Systematic Biology*, **61**(6): 1001–1027.

Wainwright P.C. and Price S.A. (2016) The impact of organismal innovation on functional and ecological diversification. *Integrative and Comparative Biology*, **56**(3): 479–488.

Wainwright P.C. and Reilly S.M. (1994) *Ecological morphology: Integrative organismal biology*. Chicago: University of Chicago Press.

Walker W.A. (1981) *Geographical variation in morphology and biology of bottlenose dolphins (Tursiops) in the Eastern North Pacific*. NOAA/NMFS Administrative Reports , no. LJ-81-03C.

Watson A.G. and Fordyce R.E. (1993) Skeleton of two minke whales, Balaenoptera acutorostrata, stranded on the south-east coas of New Zealand. *New Zealand Natural Sciences*, **20**: 1–14.

Webb P.W. (1975) Hydrodynamics and energetics of fish propulsion. *Bulletin of the Fisheries Research Board of Canada*, **190**: 1–159.

Weber P.W., Howle L.E., Murray M.M. and Fish F.E. (2009) Lift and drag performance of odontocete cetacean flippers. *Journal of Experimental Biology*, **212**(14): 2149–2158.

Weihs C., Ligges U., Luebke K. and Raabe N. (2005) klaR analyzing german business cycles. In *Data analysis and decision support* (eds Baier D., Decker R., and Schmidt-Thieme L.), pp.335–343. Berlin: Springer-Verlag.

Weihs D. (1993) Stability of aquatic animal locomotion. *Contemporary Mathematics*, **141**: 443–461.

Weihs D. (2002) Stability versus maneuverability in aquatic locomotion. *Integrative and Comparative Biology*, **42**(1): 127–134.

Wellik D.M. (2007) *Hox* patterning of the vertebrate axial skeleton. *Developmental Dynamics*, **236**(9): 2454–2463.

Wells J.B. (1965) Comparison of mechanical properties between slow and fast mammalian muscles. *Journal of Physiology*, **178**(2): 252–269.

Werth A.J. (2006) Odontocete suction feeding: experimental analysis of water flow and head shape. *Journal of Morphology*, **267**(12): 1415–1428.

Whitehead H. (2009) Sperm whale. In *Encyclopedia of Marine Mammals*, 2nd edn (eds Perrin W.F., Würsig B.G., and Thewissen J.G.M.), pp.1091–1097. San Diego: Academic Press.

Whitmore F.C. (1994) Neogene climatic change and the emergence of the modern whale fauna of the North Atlantic Ocean. *Proceedings - San Diego Society of Natural History*, **29**: 223–227.

Wickham H. (2016) *Ggplot2: elegent graphics for data analysis*. 2nd edn. New York: Springer-Verlag.

Williams E.E. (1972) The origin of faunas. Evolution of lizard congeners in a complex island fauna: a trial analysis. In *Evolutionary Biology, vol. 6* (eds Dobzhansky T., Hecht M.K., and Steere W.C.), pp.47–89. New York: Springer.

Woltering J.M. (2012) From lizard to snake; behind the evolution of an extreme body plan. *Current Genomics*, **13**(4): 289–299.

Woodward B.L., Winn J.P. and Fish F.E. (2006) Morphological specializations of baleen whales associated with hydrodynamic performance and ecological niche. *Journal of Morphology*, **267**(11): 1284–1294.

Yoder J.B., Clancey E., Des Roches S., Eastman J.M., Gentry L., Godsoe W., Hagey T.J., Jochimsen D., Oswald B.P., Robertson J., Sarver B.A.J., Schenk J.J., Spear S.F. and Harmon L.J. (2010) Ecological opportunity and the origin of adaptive radiations. *Journal of Evolutionary Biology*, **23**(8): 1581–1596.

Zákány J., Kmita M., Alarcon P., de la Pompa J.-L. and Duboule D. (2001) Localized and transient transcription of *Hox* genes suggests a link between patterning and the segmentation clock. *Cell*, **106**(2): 207–217.

Zákány J., Kmita M. and Duboule D. (2004) A dual role for *Hox* genes in limb anterior-posterior asymmetry. *Science*, **304**(5677): 1669–72.

Zerbini A., Secchi E.R., Danilewicz D., Andriolo A., Laake J.L. and Azevedo A. (2010) Abundance and distribution of the franciscana (*Pontoporia blainvillei*) in the Franciscana Management Area II (southeastern and southern Brazil). *International Whaling Commission, Scientific Committee Paper SC/62/SM7*.

Zurano J.P., Magalhães F.M., Asato A.E., Silva G., Bidau C.J., Mesquita D.O. and Costa G.C. (2019) Cetartiodactyla: updating a time-calibrated molecular phylogeny. *Molecular Phylogenetics and Evolution*, **133**: 256–262.